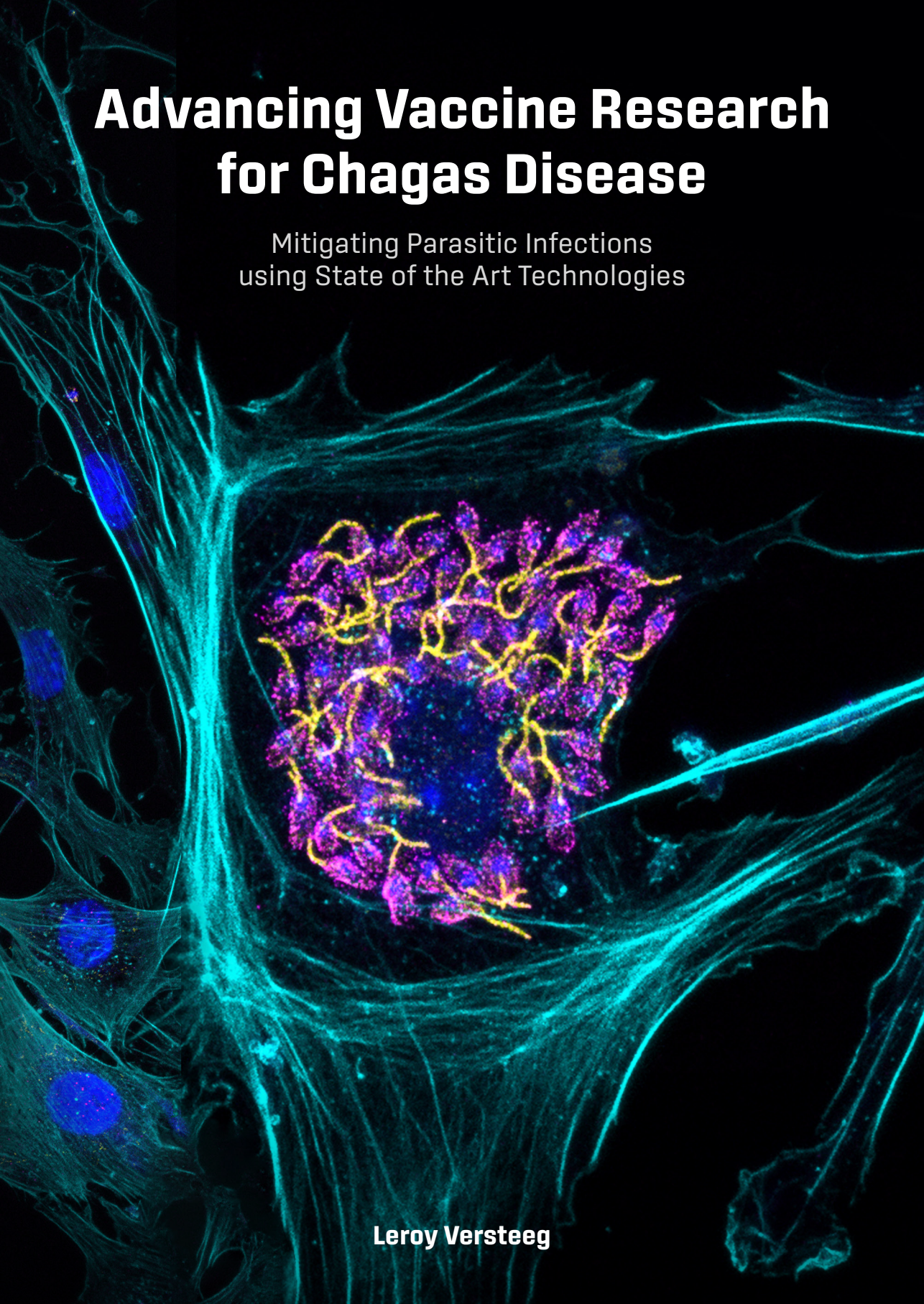


Advancing Vaccine Research for Chagas Disease

Mitigating Parasitic Infections
using State of the Art Technologies



Leroy Versteeg

Propositions

1. The protection against Chagas disease by Tc24 vaccination is not dependent on the antibody-mediated response.
(This thesis)
2. Immunopeptidomics is an effective tool to identify *T. cruzi* vaccine targets for generating cytotoxic T cells.
(This thesis)
3. Personalized medicine benefits from mRNA-based technologies.
4. Incentivizing science communication to the public is a responsibility of academic employers.
5. Human advancements will more likely put mankind on Mars than end the suffering caused by neglected tropical diseases.
6. Social media is to vaccine hesitancy, what *Helicobacter pylori* is to peptic ulcers.
7. The COVID-19 pandemic demonstrated that collective global effort leads to swift development and implementation of medical solutions.

Propositions belonging to the thesis, entitled

Advancing Vaccine Research for Chagas Disease
Mitigating Parasitic Infections using State of the Art Technologies

Leroy Versteeg

Wageningen, 9 October 2024

Advancing Vaccine Research for Chagas Disease

Mitigating Parasitic Infections using State of the Art Technologies

Thesis committee

Promotors

Prof. Dr H.F.J. Savelkoul
Professor of Immune Mechanisms of Allergy
Wageningen University & Research

Prof. Dr M.E. Bottazzi
Professor, Department of Pediatrics, Division of Tropical Medicine
Baylor College of Medicine, Houston, Texas, United States of America

Co-promotors

Dr E.J. Tijhaar
Assistant Professor, Cell Biology and Immunology Group
Wageningen University & Research

Dr J.B. Pollet
Assistant Professor, Department of Pediatrics, Division of Tropical Medicine
Baylor College of Medicine, Houston, Texas, United States of America

Other members

Prof. Dr G.P. Pijlman, Wageningen University & Research
Dr R.H.P. Wilbers, Wageningen University & Research
Dr R. Zonneveld, Amsterdam University Medical Center
Dr R.I. Gálvez, Bernhard-Nocht-Institut für Tropenmedizin, Hamburg, Germany

This research was conducted under the auspices of the Graduate School of Wageningen Institute of Animal Sciences (WIAS).

Advancing Vaccine Research for Chagas Disease

Mitigating Parasitic Infections using State of the Art Technologies

Leroy Versteeg

Thesis

submitted in fulfilment of the requirements for the degree of doctor
at Wageningen University
by the authority of the Rector Magnificus,
Prof. Dr C. Kroeze,
in the presence of the
Thesis Committee appointed by the Academic Board
to be defended in public
on Wednesday 9 October 2024
at 1 p.m. in the Omnia Auditorium.

Leroy Versteeg

Advancing Vaccine Research for Chagas Disease - Mitigating Parasitic Infections using State of the Art Technologies,
212 pages.

PhD thesis, Wageningen University, Wageningen, the Netherlands (2024)
With references, with summary in English and Dutch

ISBN: 978-94-6506-421-5

DOI: <https://doi.org/10.18174/672733>

TABLE OF CONTENTS

Chapter 1	General Introduction	7
Chapter 2	Transferring Luminex Cytokine Assays to a Wall-Less Plate Technology: Validation and Comparison Study with Plasma and Cell Culture Supernatants	31
Chapter 3	Location and Expression Kinetics of Tc24 in Different Life Stages of <i>Trypanosoma Cruzi</i>	53
Chapter 4	Enlisting the mRNA Vaccine Platform to Combat Parasitic Infections	79
Chapter 5	Immunopeptidomic MHC-I Profiling and Immunogenicity Testing Identifies Tcj2 as a New Chagas Disease mRNA Vaccine Candidate	105
Chapter 6	General Discussion	159
Summaries	Summary in English	196
	Samenvatting in het Nederlands	199
Appendices	About the Author	205
	List of Selected Publications	206
	Acknowledgements	208



CHAPTER 1

| General Introduction

Infectious diseases have been a source of consistent suffering throughout human history. Fortunately, thanks to scientific discoveries and medical advancements we have significantly reduced the prevalence, mortality and morbidity associated with many infectious diseases. In 1796, physician Edward Jenner demonstrated that people vaccinated with cowpox virus were protected against smallpox infection (1). This discovery is considered as the start of the field of vaccinology. Smallpox became in 1980 the first infectious disease to be eradicated, mainly by the application of mass vaccination programs (2). From that point, vaccines have played a crucial role in controlling infectious diseases that have posed significant threats to public health globally. It is estimated that vaccination strategies and campaigns prevented over 23 million deaths in 73 countries between 2011 and 2020 (3). In 2021, at the peak of the coronavirus pandemic (COVID-19), worldwide vaccination campaigns prevented at least 14 million deaths (4). Vaccines have also played key roles in preventing other potentially lethal viral infections such as, polio, measles, mumps, and bacterial diseases like Diphtheria and Tetanus (5).

Despite medical advancements and improved public health measures, populations living in low- and middle-income regions are still faced with life-threatening and high-morbidity infectious diseases. Tuberculosis, malaria, and HIV/AIDS, referred to as “The big three”, remain a significant global health burden. In 2018, these diseases together claimed approximately 2.7 million lives (6). In 2021, malaria caused about 247 million cases and 619,000 deaths (7). While much attention is given to “The big three”, less lethal and high-burden tropical diseases present a significantly overlooked health challenge. These neglected tropical diseases (NTDs) affect over a billion people in mainly the poorest regions of the tropics and subtropics (8). In many cases, people are infected with more than one NTD (9,10).

Overall, NTDs account for 19 million disability-adjusted life-years (DALYs) (11). They predominantly affect those in lower socioeconomic groups and are prevalent in both rural and poor urban areas of low- and middle-income countries (LMICs) (12). Of the 20 diseases that are classified as NTDs by the World Health Organization (WHO), many are caused by parasites (13). NTDs contribute significantly to health issues and create a social and economic impact through stigma, malnutrition, delayed cognitive development, and reduced productivity, reinforcing the cycle of poverty (14,15). Notably, NTDs are not exclusive to the tropics; an increase in prevalence has been observed in impoverished areas of wealthier regions, including the USA, Europe, and Australia (16).

NTDs have not gone completely unnoticed. In the early 2000s, the United Nations set forth the Millennium Development Goals (MDGs), including one goal to “combat HIV/AIDS, malaria, and other diseases”. Importantly, this goal had a subgoal to focus on neglected tropical diseases (17). After the start of these MDGs, considerable successes in reducing both the prevalence and effects of malaria and NTDs were achieved, particularly in Africa and Asia (18). However, there appears to be an inequity in the development and availability of NTD vaccines. With the recent exception of malaria (19), the world still lacks effective and approved

vaccines for many of these parasitic and neglected infections, which begs the question as to why there so few vaccines development efforts against these diseases despite their significant global impact.

1.1 CHALLENGES IN VACCINES DEVELOPMENT FOR PARASITIC DISEASES

The development of vaccines for parasitic diseases has been a slow and tedious process, and only a few candidates have made it to clinical trials. Every vaccine candidate requires specialized product and process development to meet the stringent criteria set by the Food and Drug Administration (FDA) for an Investigational New Drug (IND) application, which is necessary before clinical trials can begin (20). The journey from discovery to final licensure is typically lengthy, challenging, and very expensive. One major obstacle is the absence of economic incentives, which discourages multinational organizations from leading the expensive product and clinical development process (21). Another challenge is the lack of suitable animal models; vaccine candidates that are tested in challenge models which do not correlate well with human disease misinform preclinical investigations. This can eventually lead to a higher chance of candidate vaccines failing during costly clinical trials (22). Correlates of protection are often not well-defined, and a more comprehensive understanding is required for effective vaccine candidate design (23). Target communities might also have pre-existing immune responses against parasites from previous infections, which may complicate vaccine-induced immune reactions (20). Furthermore, there is a general lack of awareness and an underestimation of the global impact of these diseases. Most parasitic infections result in chronic illnesses with low mortality rates, and this level of suffering is hard to quantify accurately.

However, the most critical factor to why we have so few vaccines for parasitic disease, lies possibly in the intricate nature and complexity of parasites. This level of complexity presents an immense technical challenge in vaccine development, far greater than that for viruses or bacteria (24). Before the recently developed effective malaria vaccine, over 200 clinical trials testing 40 experimental malaria vaccines, failed to demonstrate significant protection (25). Parasites can have specific life stages that allow it to travel through different organs and tissues in the host, increasing the complexity of a targeted immune response. They can reside intracellularly in host cells, like *Trypanosoma cruzi*, *Toxoplasma gondii* or *Plasmodium spp.*, or extracellularly in the gastrointestinal tract (GI), lungs, and in blood vessels, such as *Ascaris lumbricoides*. Parasites have large genomes with thousands of genes, including multi-gene families that can change expression during different life stages or adapt to various hosts (26). These adaptations, which include complex life cycles and immune evasion strategies, allow parasites to establish chronic infections and resist clearance. For example, *Trypanosoma brucei*, the causative agent of African trypanosomiasis, expresses variant surface glycoproteins on plasma membranes, enabling parasites to evade the humoral immune response (27).

Other immune evasion strategies *T. brucei* applies involve immunomodulation, including the secretion of proteins that either downregulate the innate immune response or inactivate the complement system. Consequently, parasites like *T. brucei* can establish a persistent infection.

For a vaccine to be successful against parasites, the vaccine must either exceed the effectiveness of natural immunity, and/or restore and improve the immune response's functionality during infection (24). Protection against parasitic infections, can be sterilizing immunity in which case the immune system completely eradicates the parasite from the body, or non-sterilizing immunity, in which case life parasites remain present but are kept under control by the immune system and the onset of chronic symptoms is prevented. This, might heavily rely on the cellular branch of the immune response, contrasting most existing vaccines that primarily target the production of antibodies to neutralize crucial pathogenic antigens (28). These difficulties underscore the need for innovative approaches in developing effective vaccines against parasitic diseases.

1.2 CHAGAS DISEASE IS A GLOBAL HEALTH CHALLENGE

Chagas disease, also known as American trypanosomiasis, is a neglected tropical disease caused by infection with the protozoan parasite *Trypanosoma cruzi* (*T. cruzi*). Chagas disease was discovered in 1909 by the medical researcher Carlos Chagas (29). The recently unveiled WHO roadmap, “Ending the neglect to attain the Sustainable Development Goals: A road map for neglected tropical diseases 2021–2030,” identifies Chagas disease as a target for elimination as a public health issue by 2030 (30). Currently, the World Health Organization estimates that 6 to 7 million people are infected globally, causing 10,000 – 50,000 deaths annually (31,32). Another estimated 70 million people are at risk for infection (33). *T. cruzi* exhibits substantial genetic diversity and to date six discrete typing units (DTUs) have been classified, each with a distinct geographic distribution, and some DTUs overlap in certain regions (34). Chagas disease is endemic in 21 countries in Central and South – America and Mexico, predominantly affecting rural and impoverished areas where the Triatominae insect vector facilitates transmission of the disease (35). These insects, commonly referred to as kissing bugs, are endemic in Latin America and defecate on the human skin while taking a blood meal at night. Individuals will scratch the itchy site of the bite, and parasites in the feces can enter through microlesions in the skin (36). Other routes of contracting the disease include consuming *T. cruzi* – infected food or drinks, blood transfusions, organ transplantation, laboratory accidents, or congenital transmission from mother to infant (37). Importantly, congenital transmission has been described as a key transmission route in Mexico and Argentina, with an estimated 5% risk of maternal-fetal transmission (38). Migration patterns and the non-vector transmission methods have caused the geographical spread of Chagas disease, transforming it into a worldwide concern (32). The estimated annual global economic burden of Chagas disease is almost \$7 billion, an estimated annual cost of \$627.46 million in healthcare and more than 806,170 DALYs (39).

There are two successive stages of human infection. The acute phase of Chagas disease is characterized by high parasite levels in the blood, asymptomatic in most cases but symptoms such as fever, swelling at the inoculation site, eyelid swelling on one side (known as Romaña sign, typically when the disease enters through the eye), swollen lymph nodes, and enlarged liver and spleen may present (40). Since these possible symptoms are not specific for Chagas disease, most patients pass the acute stage unnoticed (36). After 4-8 weeks, the acute phase typically subsides and the parasitemia decreases significantly due to the host's natural immune response. While the immune system is often able to control the infection, it typically fails to eliminate the parasites completely, leading to chronic infection. Patients then enter the chronic indeterminate phase, in which 60-70% of patients do not experience symptoms related to Chagas disease (41,42). However, a growing number of patients with indeterminate disease are currently being identified with mild abnormalities due to advancements in diagnostic methods (43,44). About 30-40% of patients may present cardiac, digestive (megacolon or megaesophagus) or neurological symptoms 10-30 years after the acute infection (35,45). Chronic chagasic cardiomyopathy (CCC) is considered the most serious manifestation of Chagas disease. This condition presents with severe symptoms like apical aneurysms, ventricular arrhythmias, dilated cardiomyopathy, and heart failure, which are caused by sustained cardiac inflammation and fibrosis (46). In patients with CCC, sudden death is the primary cause of mortality (47).

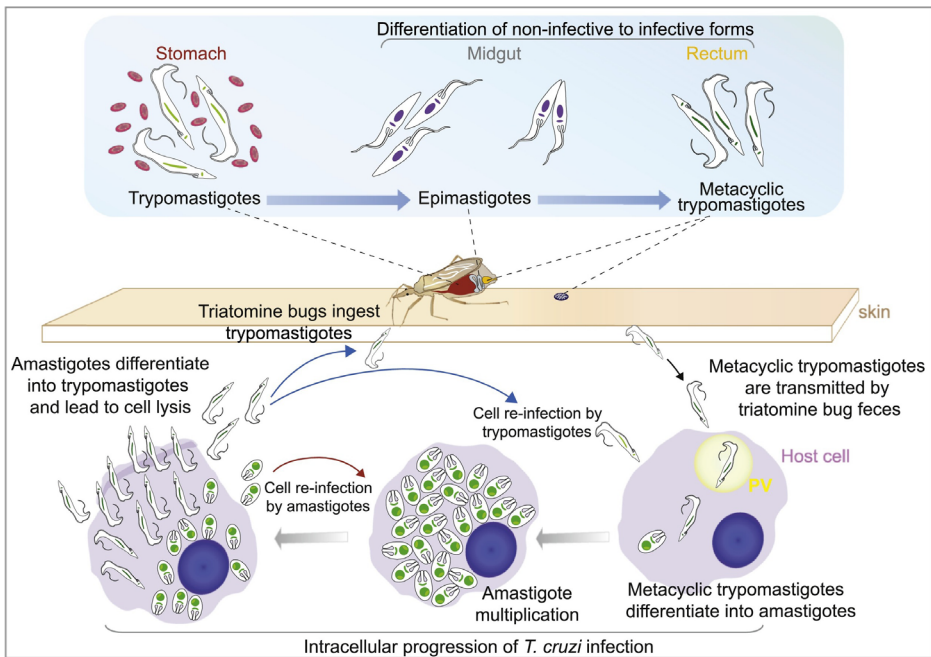
Currently, Chagas disease treatment is restricted to two approved antiparasitic drugs: nifurtimox and benznidazole (BNZ). Nifurtimox has been reported to show high toxicity and parasite resistance development, whereas BNZ offers improved efficacy and safety profile (48,49). When BNZ chemotherapy is initiated during the acute stage of Chagas disease, up to a 100% effectiveness is reported in eliminating blood parasitemia and inducing sero-reversion 18 months post treatment (45). However, acute infections are rarely diagnosed in most cases. In chronic Chagas disease, both nifurtimox and BNZ show only partial success and can cause severe side effects, leading to discontinuation in 10-20% of cases (50). Treatment with BNZ during the chronic phase clears parasitemia in up to 86.7% of individuals after 180 days, but only 15% of these patients seroconvert to become again seronegative. Moreover, In the BENEFIT trial, which involved 3000 patients, there was no significant evidence of halted disease progression in individuals with chronic Chagas cardiomyopathy, indicating the urgent need for improved therapeutic options for Chagas disease (51).

1.3 THE COMPLEXITY OF *T. CRUZI* RESULTS IN PARTIAL IMMUNE PROTECTION

The challenge in developing effective interventions for Chagas disease largely results from the complexity of the *T. cruzi* parasite. *T. cruzi* has a long history of co-evolution with its hosts, equipping it with a variety of mechanisms to resist, escape, or subvert the host's

immune system. This evolutionary process has enabled *T. cruzi* to resist host immunity and establish chronic infections (52).

The complex life cycle of *T. cruzi*, which has multiple parasitic stages, begins with metacyclic trypomastigotes being released in the Triatomine's feces during a blood meal and then entering the host through skin wounds or mucosal surfaces (**Figure 1**). Inside the host, trypomastigotes invade cells and are contained in a structure called a parasitophorous vacuole (PV). *T. cruzi* is capable of invading any nucleated host cell, and can escape the PV after lysosomal fusion to the PV (53,54). The parasites then escape from the PV and multiply in the cytosol of the infected cell. The transformation into amastigotes is initiated in the PV and finished in the cytosol. After multiple replication cycles by binary fission, these amastigotes transform back to trypomastigotes, escape from the ruptured host cell, ready to infect new cells or to be ingested by another insect. Importantly, *T. cruzi* alters the expression of its surface proteins at different life stages, playing a key role in host cell invasion and immune response evasion (55).



Trends in Parasitology

■ **Figure 1. The life cycle of *T. cruzi* simplified.** The top part of this schematic image illustrates the different parasite stages in the kissing bug (Triatomine bug), the bottom part displays the events after human infection, followed by the *in vivo* replication of the parasite together with the trypomastigote and amastigote parasite stages. PV: parasitophorous vacuole. Figure reproduced from (56) with permission from the publisher.

Apart from its complex life cycle, *T. cruzi* utilizes sophisticated immune evasion strategies to evade the immune response and establish a chronic infection. The innate immune system, which serves as the first line of defense against pathogens, plays a vital role in providing immediate nonspecific protection against infections and in initiating the adaptive immune response. *T. cruzi* has developed mechanisms to bypass the innate immune system, particularly by evading the complement system, an integral part of innate immunity. The parasite expresses specific proteins that prevent complement-mediated destruction by inhibiting steps of the classical, alternative, and lectin complement pathway (53). Furthermore, *T. cruzi* is often referred to as a “stealth invader” because it can enter the host without significantly activating pathogen recognition receptors (PRRs) of the innate immune system—crucial for triggering an immune response (56,57). This enables *T. cruzi* to multiply and establish an infection before a substantial immune response is initiated. Activation of the innate immune response is typically delayed till around 4-5 days post-infection, when parasites are released from host cells, along with the release of host cell damage-associated molecular patterns (DAMPs) and *T. cruzi* pathogen-associated molecular patterns (PAMPs). These DAMPs and PAMPs can bind to PRRs on innate immune cells, inducing their activation. This delayed start of the immune response gives *T. cruzi* an advantage in establishing infection (59,60).

The adaptive immune system is known for its specificity and ability to remember infections allowing it to target specific pathogens and respond effectively to subsequent exposures. Within this system, B cells play a role in the humoral immune response by producing and releasing antibodies that are vital for fighting infections. During *T. cruzi* infection, antibodies have a protective effect as evidenced by studies on mutant mice that cannot produce antibodies. These mice, fail to control the infection and ultimately succumb during the acute phase (61). However, despite the generation of *T. cruzi*-specific antibodies the immune response is not completely effective in eradicating the parasite due to immune evasive strategies used by the parasite. *T. cruzi* possesses a range of surface antigens encoded by highly polymorphic multigenic families, such as mucins, trans-sialidases, and mucin-associated membrane proteins (MASPs) (53). This diversity of surface antigens hinders and delays the activation of specific B cell clones. Consequently, the production and maturation of high-affinity antibodies with neutralizing capabilities is delayed as well. Additionally, *T. cruzi* can induce non-specific polyclonal B cell activation triggered by non-specific, T-independent B cell activation, resulting in antibody production that is not specifically targeted against *T. cruzi* (62). This lack of specificity obstructs the immune system’s ability to combat *T. cruzi* infection.

T lymphocytes are master players in the adaptive immune response, in which CD4+ T helper cells play an essential role in orchestrating this response. CD4+ T cells have functions such as activating other immune cells, assisting B cells in antibody production, assisting cytotoxic T cells, secreting cytokines to steer the immune response, and maintaining immune tolerance. In studies in mice, CD4+ T cells have been shown to be important for controlling *T. cruzi* infection and inflammation, although they are not essential for generating and expanding *T. cruzi*-specific CD8+ T cells (63). CD8+ T cells, which recognize infected host cells via major

histocompatibility complex class I (MHC-I), have been studied more extensively since *T. cruzi* is an intracellular replicating parasite. Cytotoxic T cells (CTLs) are activated CD8+ T cells that can recognize and eliminate infected cells using cytotoxic enzymes and cytokines, including perforin, granzyme B, IFN- γ and TNF- α (64). Importantly, when CD8+ T cells were depleted or knocked-out in mice, their vital role in survival during the acute phase of *T. cruzi* infection was shown (65). However, their activation does not always guarantee protection against infection or reinfection. It has been suggested that delayed activation of the innate immune system leads to slow development of adaptive immunity. This is supported by the observation that antigen specific CD8+ T cells appear a few days later post *T. cruzi* infection compared to other viral or bacterial infections (58). Once a robust CD8+ T cell response is triggered, the focus of the response is for a large part on epitopes from the trans-sialidase gene family. This is a phenomenon described as immunodominance (59). While these immunodominant epitopes and proteins play a role in controlling the infection by reducing parasitemia and tissue parasite burdens, they are not sufficient for complete eliminating all parasites and developing immune resistance (66). Consequently, subdominant proteins and epitopes, which are less targeted by the immune response during natural infection, are being investigated for their potential to broaden the immune response and serve as effective targets for eliciting immune protection and cell-mediated immunity (67).

Chronic *T. cruzi* infection results from the host's failure to eliminate the parasite during the acute phase. The combined efforts of the adaptive immune response, and innate immune cells, like natural killer (NK) cells, can clear the majority of parasites from the blood. Nevertheless, residual low-level parasite persistence occurs predominantly within tissue cells (52). During chronic infection, the T cell response is crucial for maintaining low parasitemia (68). Patients with chronic Chagas disease exhibit an increased frequency of circulating activated T cells that secrete both pro-inflammatory and anti-inflammatory cytokines (69). Unfortunately, these T cells often show an impaired proliferative response, with decreased expression of activation receptors upon restimulation *in vitro*. Prolonged exposure to *T. cruzi* and constant antigenic stimulation leads to dysfunctional CD8+ T cell responses, characterized by decreased T cell proliferation and increased expression of inhibitory receptors (70). Additionally, there's a decline in polyfunctional (secreting more than 1 cytokine) memory CD8+ T cells, leading to a predominance of monofunctional cells in advanced stages of the disease (71).

The persistence of the parasite in tissues not only causes damage to cells but also triggers an inflammatory response. Inflammation is a critical determinant in the disease's progression and is characterized by tissue infiltration of CD8+ and CD4+ T cells, macrophages, and, to a lesser extent, B cells. It is important to note that the immune response and the balance between effector and regulatory mechanisms are determining factors in the outcome of the disease (70). Parasite persistence in tissues leads to fibrosis and inflammation, which are the defining features of CCC. A predominant Th1 immune profile in cardiac tissues, characterized by IFN- γ , TNF- α , and IL-6, is associated with the development of CCC (51). In contrast, a balanced immune response encompassing Type 1, Type 2 and Type 3 (Th1, Th2

and Th17, respectively) profiles (with cytokines IFN- γ , IL-17A, and IL-10) may control chronic *T. cruzi* infection without leading to cardiac disease. Therefore, the objective of therapeutic vaccine strategies is to elicit a robust and balanced immune response capable of eliminating *T. cruzi*-infected cells while avoiding aggravation of fibrosis and inflammation.

1.4 THE ADVANCEMENTS OF CHAGAS DISEASE VACCINE DEVELOPMENT

For the development of a Chagas disease vaccine, two primary approaches can be considered. A prophylactic vaccine would be administered to individuals who have not been previously infected, serving as a preventative measure. This strategy would aim for the elimination of the parasite upon exposure. However, for individuals that are already infected with *T. cruzi*, a therapeutic vaccine aims to enhance the existing immune response, reducing parasite load in tissues, and preventing or delaying the onset of clinical manifestations associated with chronic Chagas disease (72). Moreover, in the case of congenital transmission from a *T. cruzi* infected mother to their unborn child, a therapeutic vaccine would aim to prevent maternal-fetal transmission of *T. cruzi* (73).

Various vaccine strategies against Chagas disease have been explored. The first vaccines tested included parasites that were live, attenuated, or killed. Examples include immunization with *Trypanosoma rangeli* or the attenuation of *T. cruzi* through mutation (74). However, these types of vaccines have limitations, including short shelf life, safety concerns due to the possibility of mutations and increase in virulence, as well as variable efficacy. When it became clear that whole parasite vaccines are not essential for protection, the focus shifted to more specific vaccine targets like protein-based (subunit) vaccines and DNA vaccines (74,75). DNA vaccines have gained interest due to their straightforward construction and production, DNA stability, and the potential to boost the immune response by co-delivering genes encoding cytokines (76). DNA vaccines have been effective in inducing specific antibodies, Th1-associated cytokines, and CD8+ T cell responses (74,77). On the other hand, protein-based candidate vaccines involve the administration of recombinant proteins, and are often combined with adjuvants like CpG, Alum, or E6020, to enhance or direct the immune response towards a specific profile (76). More recently, different vaccine strategies have emerged to develop potentially effective vaccine candidates, such as the use glycoproteins and virus-like particles (VLPs) (78). These evolving strategies reflect the ongoing efforts to develop an effective vaccine against Chagas disease.

A range of vaccine targets for *T. cruzi* have been identified and evaluated. In **Table 1** we listed some well-studied vaccine targets which have been tested in animal models. Surface proteins that are highly expressed have been extensively evaluated since these can be recognized by both the cellular as well as the humoral components of the immune system and are typically immunogenic. Examples include trans-sialidases, like amastigote surface

proteins (ASP-1/2), and trypomastigote surface antigen 1 (TSA-1), as well as mucin-associated surface proteins (MASPs) and other membrane proteins such as kinetoplastid membrane protein 11 (KMP-11) (79–81). Another well evaluated vaccine target is cruzipain, a cysteine protease that is both surface-presented and secreted by *T. cruzi* (82). Furthermore, specific intracellular proteins such as paraflagellar rod proteins (PFR1-4), have been identified as vaccine targets since peptides from these antigens are presented on MHC-I of infected host cells and recognized by CD8+ T cells (67). All these vaccine targets have shown promising results when administered as prophylactic and/or therapeutic vaccines in animal models, including controlling *T. cruzi* infection (23,76,83).

■ **Table 1.** *T. cruzi* antigens that are being evaluated as potential vaccine targets. Table adapted from reference (76).

T. cruzi vaccine targets	Antigen names	Description
Cysteine proteases	Cruzipain	Protein present on parasite's surface as well as secreted, involved in host-parasite interactions and metacyclogenesis.
Flagellar Calcium-binding proteins	Tc24 (or FCaBP)	Calcium-sensing protein, located intracellularly and found in <i>T. cruzi</i> 's secretions.
Membrane proteins	KMP-11, MASP	Surface-bound proteins, involved in host cell invasion and immune evasion.
Paraflagellar rod proteins	PFR1, PFR2, PFR3, PFR4	Proteins present in parasite's flagella and involved in flagellar structure.
Trans-sialidases	ASP-1, ASP-2, TSA-1	Proteins present on the surface of <i>T. cruzi</i> , involved in transferring sialic acid from host to parasite, as well as immune evasion.

Abbreviations: Tc24 – Trypanosoma cruzi 24 (kDa sized protein); FCaBP – flagellar calcium-binding protein; KMP-11 – kinetoplastid membrane protein 11; MASP – mucin-associated surface protein; ASP1-2 – amastigote surface protein; TSA-1 – trypomastigote surface antigen 1; PFR1-2-3 – paraflagellar rod protein.

Notably, the vaccine target Tc24, has shown very promising results when administered as DNA vaccine or as protein-based vaccine (84,85). Tc24 is a 24 kDa-sized flagellar calcium-binding protein (FCaBP) in *T. cruzi*, expressed intracellularly as well as secreted. As a recombinant protein vaccine, Tc24 has demonstrated efficacy in various mouse models, particularly through inducing antigen-specific IgG1, IgG2a antibodies, and a Th1-skewed immune response characterized by high levels of IFN- γ (86–88). A modified version of Tc24 was developed, called Tc24-C4, to enhance stability and prevent protein aggregation during manufacturing (89). When recombinant Tc24-C4, together with a TLR-4 agonist adjuvant, was administered to *T. cruzi* infected mice, enhanced control of the infection and reduced tissue inflammation and fibrosis were observed. The observations were attributed to the induction of effector CD8+ T cell responses and a balanced Th1/Th2 cytokine response (86,90). Noteworthy, when the same vaccine formulation was given in combination with BNZ treatment, a four-fold reduced BNZ dose was still effective to decrease parasitemia and tissue parasite burdens. This vaccine-linked chemotherapy approach could help reduce the side-effects that Chagas

disease patients experience during BNZ treatment. Currently, preparations are underway for Phase I clinical trials to evaluate the safety and efficacy of the subunit Tc24-C4 candidate vaccine in humans.

1.5 PROPOSED PROPERTIES OF AN EFFECTIVE VACCINE AGAINST CHAGAS DISEASE

The development of an effective vaccine against Chagas disease, presents several unique challenges and considerations, further complicated by the existence of genetically different strains of the parasite. Based on current knowledge, we believe that an effective Chagas vaccine that can eliminate *T. cruzi* may need to target multiple antigens from *T. cruzi* to diversify the targeted epitopes to increase broadness of protection. Key features defining potential antigens for a multivalent *T. cruzi* vaccine include:

Immunodominant and subdominant antigens and epitopes: Vaccine candidates preferably contain both, antigens and epitopes recognized by the immune system that are dominant during *T. cruzi* infection, such as trans-sialidases, as well as specific subdominant antigens and epitopes that are recognized at a lesser extent during infection (66,67). Since the parasite uses various immune modulation mechanisms, targeting a broad spectrum of proteins, and not just the immunodominant ones, could enhance the vaccine's effectiveness.

Expression of antigens during trypomastigotes and amastigote stages: Vaccine antigens should be accessible to the host's immune system. For the extracellular trypomastigote stage, the focus is therefore on antigens presented on the surface of the plasma membrane, which can be targeted by antibodies. In contrast, amastigotes are intracellular, so antigens shed or secreted from the parasite into the cytoplasm that then become available for antigen processing and presentation on MHC-I to CD8+ T cells are more important. For both *T. cruzi* stages, proteins that remain internal and are not available to the immune system at any given time are not ideal targets for vaccine development. Ideally, targets should be expressed in both trypomastigote and amastigote stages of the parasite (91).

Antigen conserved among *T. cruzi* strains: Antigens should be selected that are conserved between various parasitic strains to ensure the vaccine protects against different *T. cruzi* strains prevalent in different regions of the Americas. Careful consideration should be given to antigens originating from large polymorphic protein families such as trans-sialidases and MASPs because of the genetic variation present within these families across different strains (92,93).

Besides the selection of vaccine targets, the type of immune response that is elicited through vaccination is important, as this determines how effectively the body can defend itself against *T. cruzi*. An effective *T. cruzi* vaccine is believed to elicit specific CD8+ T cell responses

targeting *T. cruzi* antigens, to generate cytotoxic T lymphocytes (CTLs) capable of recognizing and eliminating *T. cruzi*-infected cells (67,94). These CTL are characterized by the production of cytokines IFN- γ and TNF- α , as well as cytotoxic molecules like granzymes and perforins. After vaccination, it is critical that both central memory and effector memory T cells persist for long-term protection. Also, the activation of CD4+ T cells is essential since it helps the development of memory CD8+ T cells and their long term survival (95). Additionally, for prophylactic vaccine strategies, where antibodies have an impact on controlling parasitemia, the vaccination should aim to elicit a B cell response. This response should result in the production of antibodies capable of neutralizing circulating parasites and/or block *T. cruzi* invasion in host cells, ultimately reducing the parasite load and preventing the establishment of chronic or indeterminate phases (53,60). Especially in endemic regions where risk of exposure to *T. cruzi* is high, a robust antibody response elicited by a prophylactic vaccine would reduce the chance of developing chronic Chagas disease (74).

The type of elicited immune response holds critical significance and varies for prophylactic and therapeutic vaccine applications against Chagas disease (96). The immune response can be steered by different factors, such as the vaccine platform, the use of adjuvants, and administration route. For prophylactic applications, a Type 1 response is desired, accompanied by T helper 1 (Th1) cells and CTLs producing pro-inflammatory cytokines including IFN- γ . This type of immune response is very effective against intracellular pathogens, including *T. cruzi*. On the other hand, with therapeutic vaccine applications, the consideration is that *T. cruzi* has already established a persistent infection, and an immune response has already happened. Here, the induction of a strong Type 1 immune response could intensify tissue inflammation and aggravate cardiac disease. Therefore, the objective of therapeutic vaccines is to recalibrate the immune system to target and clear the infection more effectively, while not increasing inflammation. This is particularly crucial for patients with CCC, where the vaccine's aim would be to halt disease progression, lower parasite burden, and mitigate cardiac inflammation and fibrosis, to ultimately improve both survival and cardiac health (45). It is hypothesized that a balanced immune response, with a mix of Type 1 (Th1 with IFN- γ), Type 2 (Th2 with IL-4) and Type 3 (Th17 with IL-17A) responses, is necessary to control the parasite while minimizing tissue inflammation and fibrosis (90).

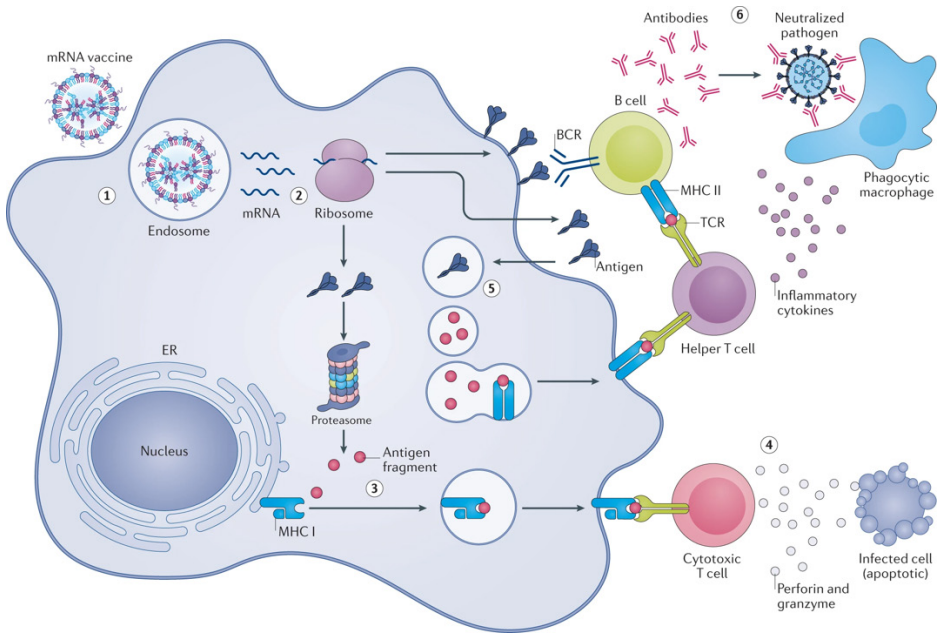
In summary, the development of a Chagas disease vaccine requires a multifaceted approach, carefully selecting *T. cruzi* antigens that are conserved between strains, targeting various stages of the parasite's lifecycle. The desired type of immune response elicited by the vaccine is dependent on the vaccine strategy, where prophylactic vaccines should aim for a Type 1 immune response, and therapeutic vaccines should apply a balanced immune response to avoid aggravation of inflammation.

1.6 MESSENGER RNA VACCINES TO ACCELERATE VACCINE DEVELOPMENT FOR NTDS

Messenger RNA (mRNA) vaccines have emerged as a groundbreaking platform to induce rapid and precise immune responses against infectious diseases. The strategy to make the host produce its own antigens through *in vitro* transcribed mRNA, has proven very successful during the COVID-19 pandemic. Consequently, just in the United States (US) alone, more than 600 million doses of mRNA vaccines have been administered (97). The preference towards the mRNA vaccine platform was initially driven by the incredibly fast development time, which is significantly shorter than that for conventional vaccine platforms (98). One key technology that made the *in vivo* application of mRNA vaccines more effective was the incorporation of modified nucleotides. Pseudouridine, as well as other modifications of uridine, help avoiding host defense responses and significantly increases mRNA translation (99). The discovery and vaccine application of the modified nucleotides resulted in a Nobel Prize in Physiology or Medicine in 2023 (100). A second key development was the advanced formulation within lipid nanoparticles (LNPs), which proficiently facilitates the delivery of mRNA into the host cell cytosol (101). The now widely established safety profile of mRNA vaccinations further bolsters their utilization as a safe and efficient novel vaccine technology. Given that mRNA vaccines are able to elicit strong cellular immunity, are straightforward to develop and manufacture, have fast and scalable production processes, and have the feasibility of creating multi-valent vaccine formulations, make the vaccine platform very promising to overcome the challenges of developing vaccines for parasitic infections (102).

Messenger-RNA vaccines consist of mRNA encoding a target protein, designed to be translated within host cells, aiming to elicit an immune response (**Figure 2**). After immunization, mRNA-loaded LNPs are taken up by antigen-presenting cells (APCs) into endosomes. There, the acidification of the LNPs will disrupt the membrane of the endosome. This process is critical for ensuring that the mRNA reaches the cytosol, where the mRNA can be translated by the host's ribosomes into the target protein (103). Once translated, vaccine antigens undergo processing by the host cell's antigen-presenting machinery. Peptides derived from these antigens are then presented on MHC class I molecules to CD8+ T cells. This MHC class I presentation is crucial for the activation of CTLs, which are crucial in destroying parasite-infected cells (104). Additionally, some of the vaccine antigens can be secreted from the cell or remain bound to the cell's surface. These extracellular antigens may then be re-internalized by APCs and presented on MHC class II molecules to CD4+ T cells (105). This interaction helps stimulate helper T cells, which play an essential role in orchestrating the immune response, including the activation and maturation of B cells. B cells can recognize these secreted or surface-bound proteins and differentiate into plasma cells that produce antibodies specific to the target protein. The role of CD4+ T cells is important in this process as they provide necessary help for B cell activation, class switching, and affinity maturation of antibodies (106). Furthermore, CD4+ T cells help the development of CTLs (95). In summary, mRNA vaccines utilize the host's cellular machinery to produce a specific antigen, which is then presented to both CD8+ and

CD4+ T cell. This stimulates a robust immune response, which includes the generation of memory cells T and B cells, and the production of specific antibodies. All these processes are essential for long-term immunity.



■ **Figure 2. mRNA vaccines induce immune responses by transfecting APCs with mRNA encoding a specific antigen.** After mRNA vaccine enters an APC (1), mRNA escapes the endosome and is translated to proteins by ribosomes (2). The proteins can induce an immune response by being broken down to peptides (3) followed by presentation of MHC-I and CD8+ T cell activation (4), or by exiting the APC where it can be taken up again (5) and presented on MHC-II to CD4+ T cells, further supporting B cells to produce antigen-specific antibodies (6), as well as secreting cytokines which can activate phagocytes and steer the immune response. Figure reproduced from (105) with permission from the publisher.

To date, based on publicly available research data, the application of mRNA for the development of vaccines to parasitic diseases has been limited. In 1988 Tsuji *et al.* published for the first time on mRNA vaccines for parasitic infections, describing a mRNA vaccine targeting a cytotoxic T-cell epitope of the *Plasmodium yoelii* circumsporozoite protein that demonstrated a significant decrease in hepatic parasite burden (107). Since then just a few studies have emerged, mainly addressing malaria and leishmaniasis (108,109). Later, a remarkable achievement was made by Chahal *et al.* They created a dendrimer nanoparticle mRNA vaccine capable of expressing multiple antigens (110). This vaccine provided protection against various pathogens, including Ebola virus, H1N1 influenza, and the parasite *Toxoplasma gondii*. In the case of *T. gondii*, six different antigens were targeted, resulting in 100% protection against a lethal challenge in a mouse model. This vaccine approach illustrates the promising

potential of mRNA vaccines as multivalent vaccines, not just targeting multiple antigens but also multiple diseases. This gives hope for the fight against parasitic diseases.

1.7 AIM AND OUTLINE OF THIS THESIS

The overall goal of this thesis is to advance the development and evaluation of a safe, immunogenic and effective vaccine against Chagas disease. To achieve this goal, the following objectives were aimed for: A) to improve existing techniques to assess vaccine-induced immune responses, B) to advance knowledge on current vaccine targets for Chagas disease, C) to apply alternative approaches to the identification of new vaccine targets that can be targeted by CD8+ T cells, and D) to implement mRNA vaccines as a new vaccine platform for Chagas disease vaccines.

First, in **Chapter 2**, we evaluated DropArray technology to enhance Luminex-based cytokine multiplexing assay to assess vaccine-induced immune responses. While being a powerful tool, Luminex is not extensively used in vaccine research due to cost and volume constraints. By implementing DropArray into the workflows of the commercially available Luminex kits, smaller sample volumes can be used and a reduction in assay cost per sample is achieved.

After assessing DropArray technology for Luminex as a general technique to assess vaccine-induced immune responses, we focused on Chagas disease vaccine candidates. In **Chapter 3**, knowledge on the primary Chagas disease vaccine target Tc24 was expanded. Using in-house produced monoclonal antibodies against Tc24, the protein's location within the *T. cruzi* parasite, and its expression kinetics during trypomastigote and amastigote stages, was determined. These findings shed light on the potential mechanisms of Tc24 induced protection.

Subunit vaccines, like the recombinant Tc24-C4 candidate vaccine, are generally good inducers of antigen specific antibodies and CD4+ T cells, but are typically less effective in inducing MHC-I restricted CD8+ cytotoxic T cells. These cytotoxic T cells are known to play an important role in the protection against *T. cruzi* infection (60). Messenger RNA vaccines are good inducers of cytotoxic T cells (111). Therefore, a literature review on mRNA vaccines was performed (**Chapter 4**), discussing the distinct properties of the mRNA vaccine platform, as well as its design, function, and its potential for preventing parasitic infections. It was concluded that mRNA vaccines could be particularly advantageous for Chagas disease. **Chapter 5** aimed to identify new *T. cruzi* antigens presented on MHC-I molecules of infected host cells, as these will form ideal vaccine candidates for cytotoxic CD8+ T cell-inducing mRNA vaccines. Using a technique known as immunopeptidomics, heat shock protein 40 Tcj2 was identified as a new potential vaccine target for CD8+ cytotoxic T cells. Next, a Tcj2 expressing mRNA vaccine was developed and its immunogenicity evaluated in a mouse model.

Finally, in the general discussion in **Chapter 6**, I integrated the results of the preceding sections, positioning them within a broader context. I discussed the opportunities and limitations for future research unveiled through our studies. These findings are then used to predict the trajectory of vaccine development for Chagas disease, as well as mRNA vaccine development for other NTDs.

Collectively, our aim was to advance Chagas disease vaccine research by expanding our understanding of the parasite, and by integrating novel approaches and research tools into the existing workflows.

1.8 REFERENCES

1. Riedel S. Edward Jenner and the history of smallpox and vaccination. *Proc Bayl Univ Med Cent.* 2005 Jan;18(1):21–5.
2. Strassburg MA. The global eradication of smallpox. *Am J Infect Control.* 1982 May;10(2):53–9.
3. Lee LA, Franzel L, Atwell J, Datta SD, Friberg IK, Goldie SJ, et al. The estimated mortality impact of vaccinations forecast to be administered during 2011–2020 in 73 countries supported by the GAVI Alliance. *Vaccine.* 2013 Apr 18;31 Suppl 2:B61–72.
4. Global impact of the first year of COVID-19 vaccination: a mathematical modelling study - *The Lancet Infectious Diseases* [Internet]. [cited 2023 Oct 28]. Available from: [https://www.thelancet.com/journals/laninf/article/PIIS1473-3099\(22\)00320-6/fulltext](https://www.thelancet.com/journals/laninf/article/PIIS1473-3099(22)00320-6/fulltext)
5. Amanna IJ, Slifka MK. Successful Vaccines. *Curr Top Microbiol Immunol.* 2020;428:1–30.
6. Prudêncio M, Costa JC. Research funding after COVID-19. *Nat Microbiol.* 2020 Aug;5(8):986–986.
7. Fact sheet about malaria [Internet]. [cited 2023 Oct 15]. Available from: <https://www.who.int/news-room/fact-sheets/detail/malaria>
8. Neglected tropical diseases [Internet]. [cited 2023 Nov 12]. Available from: <https://www.who.int/news-room/questions-and-answers/item/neglected-tropical-diseases>
9. Mitchell C. Pan American Health Organization / World Health Organization. 2015 [cited 2023 Nov 12]. PAHO/WHO | More than 100 million people suffer from one or more neglected infectious diseases in the Americas. Available from: https://www3.paho.org/hq/index.php?option=com_content&view=article&id=10440:2015-100-millones-padecen-alguna-enfermedad-infeciosa-desatendida-en-las-americas&Itemid=0&lang=en#gsc.tab=0
10. Winkler AS, Klohe K, Schmidt V, Haavardsson I, Abraham A, Prodjinotho UF, et al. Neglected tropical diseases – the present and the future. *Tidsskr Den Nor Legeforening* [Internet]. 2018 Jan 2 [cited 2023 Nov 12]; Available from: <https://tidsskriftet.no/en/2018/01/global-helse/neglected-tropical-diseases-present-and-future>
11. The Lancet Regional Health – Western Pacific. To end the neglect of neglected tropical diseases. *Lancet Reg Health West Pac.* 2022 Jan 28;18:100388.
12. Hotez PJ. NTDs V.2.0: “blue marble health”--neglected tropical disease control and elimination in a shifting health policy landscape. *PLoS Negl Trop Dis.* 2013 Nov;7(11):e2570.
13. Gyorkos T, Nicholls R, Montresor A, Luciañez A, Casapia M, St-Denis K, et al. Eliminating morbidity caused by neglected tropical diseases by 2030. *Rev Panam Salud Pública.* 2023 Mar 10;47:e16.
14. Mitra AK, Mawson AR. Neglected Tropical Diseases: Epidemiology and Global Burden. *Trop Med Infect Dis.* 2017 Aug 5;2(3):36.
15. Hotez PJ, Fenwick A, Savioli L, Molyneux DH. Rescuing the bottom billion through control of neglected tropical diseases. *The Lancet.* 2009 May 2;373(9674):1570–5.
16. Hotez PJ, Damania A, Naghavi M. Blue Marble Health and the Global Burden of Disease Study 2013. *PLoS Negl Trop Dis.* 2016 Oct 27;10(10):e0004744.
17. Millennium Development Goals (MDGs) [Internet]. [cited 2023 Oct 23]. Available from: [https://www.who.int/news-room/fact-sheets/detail/millennium-development-goals-\(mdgs\)](https://www.who.int/news-room/fact-sheets/detail/millennium-development-goals-(mdgs))
18. Hotez PJ, Fenwick A, Molyneux DH. Collateral Benefits of Preventive Chemotherapy — Expanding the War on Neglected Tropical Diseases. *N Engl J Med.* 2019 Jun 20;380(25):2389–91.

19. WHO recommends R21/Matrix-M vaccine for malaria prevention in updated advice on immunization [Internet]. [cited 2023 Oct 28]. Available from: <https://www.who.int/news/item/02-10-2023-who-recommends-r21-matrix-m-vaccine-for-malaria-prevention-in-updated-advice-on-immunization>
20. Diemert DJ, Bottazzi ME, Plieskatt J, Hotez PJ, Bethony JM. Lessons along the Critical Path: Developing Vaccines against Human Helminths. *Trends Parasitol*. 2018 Sep 1;34(9):747–58.
21. Hotez PJ. The global fight to develop antipoverty vaccines in the anti-vaccine era. *Hum Vaccines Immunother*. 2018;14(9):2128–31.
22. Schwartz L, Brown GV, Genton B, Moorthy VS. A review of malaria vaccine clinical projects based on the WHO rainbow table. *Malar J*. 2012 Jan 9;11(1):11.
23. Dumonteil E, Herrera C. The Case for the Development of a Chagas Disease Vaccine: Why? How? When? *Trop Med Infect Dis*. 2021 Mar;6(1):16.
24. Sacks DL. Vaccines against tropical parasitic diseases: A persisting answer to a persisting problem. *Nat Immunol*. 2014 May;15(5):403–5.
25. Wykes MN. Why haven't we made an efficacious vaccine for malaria? *EMBO Rep*. 2013 Aug;14(8):661.
26. Abath FGC, Montenegro SML, Gomes YM. Vaccines against human parasitic diseases: an overview. *Acta Trop*. 1998 Nov 30;71(3):237–54.
27. Burri C, Chappuis F, Brun R. 45 - Human African Trypanosomiasis. In: Farrar J, Hotez PJ, Junghanss T, Kang G, Lalloo D, White NJ, editors. *Manson's Tropical Infectious Diseases (Twenty-third Edition)* [Internet]. London: W.B. Saunders; 2014 [cited 2022 Oct 3]. p. 606-621.e4. Available from: <https://www.sciencedirect.com/science/article/pii/B9780702051012000467>
28. Pollard AJ, Bijker EM. A guide to vaccinology: from basic principles to new developments. *Nat Rev Immunol*. 2021 Feb;21(2):83–100.
29. Chagas C. Nova tripanozomíaze humana: estudos sobre a morfologia e o ciclo evolutivo do *Schizotrypanum cruzi* n. gen., n. sp., agente etiológico de nova entidade morbida do homem. *Mem Inst Oswaldo Cruz*. 1909 Aug;1:159–218.
30. Heukelbach J, Sousa AS de, Ramos AN. New Contributions to the Elimination of Chagas Disease as a Public Health Problem: Towards the Sustainable Development Goals by 2030. *Trop Med Infect Dis*. 2021 Mar;6(1):23.
31. Chagas disease (American trypanosomiasis) [Internet]. [cited 2023 Oct 15]. Available from: <https://www.who.int/health-topics/chagas-disease>
32. Lidani KCF, Andrade FA, Bavia L, Damasceno FS, Beltrame MH, Messias-Reason IJ, et al. Chagas Disease: From Discovery to a Worldwide Health Problem. *Front Public Health* [Internet]. 2019 [cited 2023 Apr 5];7. Available from: <https://www.frontiersin.org/articles/10.3389/fpubh.2019.00166>
33. Chagas disease - PAHO/WHO | Pan American Health Organization [Internet]. [cited 2023 Oct 15]. Available from: <https://www.paho.org/en/topics/chagas-disease>
34. Brenière SF, Waleckx E, Barnabé C. Over Six Thousand *Trypanosoma cruzi* Strains Classified into Discrete Typing Units (DTUs): Attempt at an Inventory. *PLoS Negl Trop Dis*. 2016 Aug 29;10(8):e0004792.
35. Pérez-Molina JA, Molina I. Chagas disease. *The Lancet*. 2018 Jan 6;391(10115):82–94.
36. Steverding D. The history of Chagas disease. *Parasit Vectors*. 2014 Jul 10;7(1):317.
37. Rassi A, Rassi A, Marin-Neto JA. Chagas disease. *The Lancet*. 2010 Apr 17;375(9723):1388–402.
38. Buekens P, Cafferata ML, Alger J, Althabe F, Belizán JM, Bustamante N, et al. Congenital Transmission of *Trypanosoma cruzi* in Argentina, Honduras, and Mexico: An Observational Prospective Study. *Am J Trop Med Hyg*. 2018 Feb;98(2):478–85.

39. Lee BY, Bacon KM, Bottazzi ME, Hotez PJ. Global economic burden of Chagas disease: a computational simulation model. *Lancet Infect Dis*. 2013 Apr 1;13(4):342–8.
40. Prata A. Clinical and epidemiological aspects of Chagas disease. *Lancet Infect Dis*. 2001 Sep 1;1(2):92–100.
41. Machado FS, Dutra WO, Esper L, Gollob KJ, Teixeira MM, Factor SM, et al. Current understanding of immunity to *Trypanosoma cruzi* infection and pathogenesis of Chagas disease. *Semin Immunopathol*. 2012 Nov 1;34(6):753–70.
42. Rassi A, Rassi A, Marcondes de Rezende J. American trypanosomiasis (Chagas disease). *Infect Dis Clin North Am*. 2012 Jun;26(2):275–91.
43. Viotti RJ, Vigliano C, Laucella S, Lococo B, Petti M, Bertocchi G, et al. Value of echocardiography for diagnosis and prognosis of chronic Chagas disease cardiomyopathy without heart failure. *Heart Br Card Soc*. 2004 Jun;90(6):655–60.
44. Rochitte CE, Oliveira PF, Andrade JM, Ianni BM, Parga JR, Avila LF, et al. Myocardial delayed enhancement by magnetic resonance imaging in patients with Chagas' disease: a marker of disease severity. *J Am Coll Cardiol*. 2005 Oct 18;46(8):1553–8.
45. Jones KM, Poveda C, Versteeg L, Bottazzi ME, Hotez PJ. Preclinical advances and the immunophysiology of a new therapeutic Chagas disease vaccine. *Expert Rev Vaccines*. 2022 Jun 23;0(0):1–19.
46. Ribeiro AL, Nunes MP, Teixeira MM, Rocha MOC. Diagnosis and management of Chagas disease and cardiomyopathy. *Nat Rev Cardiol*. 2012 Oct;9(10):576–89.
47. Rassi A, Rassi SG, Rassi A. Sudden death in Chagas' disease. *Arq Bras Cardiol*. 2001 Jan;76(1):75–96.
48. Coura JR, Castro SL de. A Critical Review on Chagas Disease Chemotherapy. *Mem Inst Oswaldo Cruz*. 2002 Jan;97:3–24.
49. Viotti R, Vigliano C, Lococo B, Alvarez MG, Petti M, Bertocchi G, et al. Side effects of benznidazole as treatment in chronic Chagas disease: fears and realities. *Expert Rev Anti Infect Ther*. 2009 Mar;7(2):157–63.
50. Urbina JA. Recent Clinical Trials for the Etiological Treatment of Chronic Chagas Disease: Advances, Challenges and Perspectives. *J Eukaryot Microbiol*. 2015;62(1):149–56.
51. Rassi A, Marin JA, Rassi A. Chronic Chagas cardiomyopathy: a review of the main pathogenic mechanisms and the efficacy of aetiological treatment following the BENznidazole Evaluation for Interrupting Trypanosomiasis (BENEFIT) trial. *Mem Inst Oswaldo Cruz*. 2017 Feb 16;112:224–35.
52. Acevedo GR, Girard MC, Gómez KA. The Unsolved Jigsaw Puzzle of the Immune Response in Chagas Disease. *Front Immunol*. 2018 Aug 24;9:1929.
53. Cardoso MS, Reis-Cunha JL, Bartholomeu DC. Evasion of the Immune Response by *Trypanosoma cruzi* during Acute Infection. *Front Immunol* [Internet]. 2016 [cited 2018 Mar 22];6. Available from: <https://www.frontiersin.org/articles/10.3389/fimmu.2015.00659/full>
54. Burleigh BA. Host Cell Signaling and *Trypanosoma cruzi* Invasion: Do All Roads Lead to Lysosomes? *Sci STKE*. 2005 Jul 19;2005(293):pe36–pe36.
55. Pech-Canul Á de la C, Monteón V, Solís-Oviedo RL. A Brief View of the Surface Membrane Proteins from *Trypanosoma cruzi*. *J Parasitol Res*. 2017;2017:3751403.
56. Moretti NS, Mortara RA, Schenkman S. *Trypanosoma cruzi*. *Trends Parasitol*. 2020 Apr 1;36(4):404–5.
57. Tarleton RL. Immune system recognition of *Trypanosoma cruzi*. *Curr Opin Immunol*. 2007 Aug;19(4):430–4.

58. Padilla AM, Simpson LJ, Tarleton RL. Insufficient TLR activation contributes to the slow development of CD8+ T cell responses in *Trypanosoma cruzi* infection. *J Immunol Baltim Md* 1950. 2009 Jul 15;183(2):1245–52.
59. Martin DL, Weatherly DB, Laucella SA, Cabinian MA, Crim MT, Sullivan S, et al. CD8+ T-Cell responses to *Trypanosoma cruzi* are highly focused on strain-variant trans-sialidase epitopes. *PLoS Pathog*. 2006 Aug;2(8):e77.
60. Tarleton RL. CD8+ T cells in *Trypanosoma cruzi* infection. *Semin Immunopathol*. 2015 May;37(3):233–8.
61. Kumar S, Tarleton RL. The relative contribution of antibody production and CD8+ T cell function to immune control of *Trypanosoma cruzi*. *Parasite Immunol*. 1998 May;20(5):207–16.
62. Bermejo DA, Amezcua Vesely MC, Khan M, Acosta Rodríguez EV, Montes CL, Merino MC, et al. *Trypanosoma cruzi* infection induces a massive extrafollicular and follicular splenic B-cell response which is a high source of non-parasite-specific antibodies. *Immunology*. 2011 Jan;132(1):123–33.
63. Padilla A, Xu D, Martin D, Tarleton R. Limited Role for CD4+ T-Cell Help in the Initial Priming of *Trypanosoma cruzi*-Specific CD8+ T Cells. *Infect Immun*. 2007 Jan;75(1):231–5.
64. Müller U, Sobek V, Balkow S, Hölscher C, Müllbacher A, Museteanu C, et al. Concerted action of perforin and granzymes is critical for the elimination of *Trypanosoma cruzi* from mouse tissues, but prevention of early host death is in addition dependent on the FasL/Fas pathway. *Eur J Immunol*. 2003;33(1):70–8.
65. Junqueira C, Caetano B, Bartholomeu DC, Melo MB, Ropert C, Rodrigues MM, et al. The endless race between *Trypanosoma cruzi* and host immunity: lessons for and beyond Chagas disease. *Expert Rev Mol Med* [Internet]. 2010 Sep [cited 2021 Oct 31];12. Available from: <https://www.cambridge.org/core/journals/expert-reviews-in-molecular-medicine/article/abs/endless-race-between-trypanosoma-cruzi-and-host-immunity-lessons-for-and-beyond-chagas-disease/BA3C95388A7908FF5D9CE48C9C1916CA>
66. Rosenberg CS, Martin DL, Tarleton RL. CD8+ T cells specific for immunodominant trans-sialidase epitopes contribute to control of *Trypanosoma cruzi* infection but are not required for resistance. *J Immunol Baltim Md* 1950. 2010 Jul 1;185(1):560–8.
67. Kurup SP, Tarleton RL. The *Trypanosoma cruzi* Flagellum Is Discarded via Asymmetric Cell Division following Invasion and Provides Early Targets for Protective CD8+ T Cells. *Cell Host Microbe*. 2014 Oct 8;16(4):439–49.
68. Sartori AMC, Neto JE, Nunes EV, Braz LMA, Caiaffa-Filho HH, Oliveira O da C Jr, et al. *Trypanosoma cruzi* Parasitemia in Chronic Chagas Disease: Comparison between Human Immunodeficiency Virus (HIV)-Positive and HIV-Negative Patients. *J Infect Dis*. 2002 Sep 15;186(6):872–5.
69. Dutra WO, Gollob KJ. Current concepts in immunoregulation and pathology of human Chagas disease. *Curr Opin Infect Dis*. 2008 Jun;21(3):287–92.
70. Puerta CJ, Cuellar A, Lasso P, Mateus J, Gonzalez JM. *Trypanosoma cruzi*-specific CD8+ T cells and other immunological hallmarks in chronic Chagas cardiomyopathy: Two decades of research. *Front Cell Infect Microbiol* [Internet]. 2023 [cited 2023 Dec 3];12. Available from: <https://www.frontiersin.org/articles/10.3389/fcimb.2022.1075717>
71. Lasso P, Mateus J, Pavia P, Rosas F, Roa N, Thomas MC, et al. Inhibitory Receptor Expression on CD8+ T Cells Is Linked to Functional Responses against *Trypanosoma cruzi* Antigens in Chronic Chagasic Patients. *J Immunol*. 2015 Oct 15;195(8):3748–58.

72. Dumonteil E, Bottazzi ME, Zhan B, Heffernan MJ, Jones K, Valenzuela JG, et al. Accelerating the development of a therapeutic vaccine for human Chagas disease: rationale and prospects. *Expert Rev Vaccines*. 2012 Sep 1;11(9):1043–55.
73. Rios L, Campos EE, Menon R, Zago MP, Garg NJ. Epidemiology and pathogenesis of maternal-fetal transmission of *Trypanosoma cruzi* and a case for vaccine development against congenital Chagas disease. *Biochim Biophys Acta Mol Basis Dis*. 2020 Mar 1;1866(3):165591.
74. Rodríguez-Morales O, Monteón-Padilla V, Carrillo-Sánchez SC, Rios-Castro M, Martínez-Cruz M, Carabarin-Lima A, et al. Experimental Vaccines against Chagas Disease: A Journey through History. *J Immunol Res*. 2015;2015:489758.
75. Menezes H. Protective effect of an avirulent (cultivated) strain of *Trypanosoma cruzi* against experimental infection in mice. *Rev Inst Med Trop Sao Paulo*. 1968;10(1):1–4.
76. Rios LE, Vázquez-Chagoyán JC, Pacheco AO, Zago MP, Garg NJ. Immunity and vaccine development efforts against *Trypanosoma cruzi*. *Acta Trop*. 2019 Dec 1;200:105168.
77. Gupta S, Garg NJ. A Two-Component DNA-Prime/Protein-Boost Vaccination Strategy for Eliciting Long-Term, Protective T Cell Immunity against *Trypanosoma cruzi*. *PLoS Pathog*. 2015 May;11(5):e1004828.
78. Maria Vasconcelos Queiroz A, Aleksandrovna Yanshina Y, Thays da Silva Rodrigues E, Luciano Neves Santos F, Alejandra Fiorani Celedon P, Maheshwari S, et al. Antibodies response induced by recombinant virus-like particles from Triatoma virus and chimeric antigens from *Trypanosoma cruzi*. *Vaccine*. 2021 Jul 30;39(33):4723–32.
79. da Costa KM, Marques da Fonseca L, dos Reis JS, Santos MAR da C, Previato JO, Mendonça-Previato L, et al. *Trypanosoma cruzi* trans-Sialidase as a Potential Vaccine Target Against Chagas Disease. *Front Cell Infect Microbiol*. 2021 Oct 26;11:768450.
80. Santos SL dos, Freitas LM, Lobo FP, Rodrigues-Luiz GF, Mendes TA de O, Oliveira ACS, et al. The MASP Family of *Trypanosoma cruzi*: Changes in Gene Expression and Antigenic Profile during the Acute Phase of Experimental Infection. *PLoS Negl Trop Dis*. 2012 Aug 14;6(8):e1779.
81. Diaz-Soto JC, Lasso P, Guzmán F, Forero-Shelton M, Thomas M del C, López MC, et al. Rabbit serum against K1 peptide, an immunogenic epitope of the *Trypanosoma cruzi* KMP-11, decreases parasite invasion to cells. *Acta Trop*. 2012 Sep 1;123(3):224–9.
82. Cerny N, Bivona AE, Sanchez Alberti A, Trinitario SN, Morales C, Cardoso Landaburu A, et al. Cruzipain and Its Physiological Inhibitor, Chagasin, as a DNA-Based Therapeutic Vaccine Against *Trypanosoma cruzi*. *Front Immunol* [Internet]. 2020 [cited 2023 Dec 31];11. Available from: <https://www.frontiersin.org/articles/10.3389/fimmu.2020.565142>
83. Bivona AE, Alberti AS, Cerny N, Trinitario SN, Malchiodi EL. Chagas disease vaccine design: the search for an efficient *Trypanosoma cruzi* immune-mediated control. *Biochim Biophys Acta BBA - Mol Basis Dis*. 2020 May 1;1866(5):165658.
84. Dumonteil E, Escobedo-Ortegon J, Reyes-Rodríguez N, Arjona-Torres A, Ramirez-Sierra MJ. Immunotherapy of *Trypanosoma cruzi* Infection with DNA Vaccines in Mice. *Infect Immun*. 2004 Jan;72(1):46–53.
85. Quijano-Hernandez IA, Bolio-González ME, Rodríguez-Buenfil JC, Ramirez-Sierra MJ, Dumonteil E. Therapeutic DNA vaccine against *Trypanosoma cruzi* infection in dogs. *Ann N Y Acad Sci*. 2008 Dec;1149:343–6.
86. Barry MA, Versteeg L, Wang Q, Pollet J, Zhan B, Gusovsky F, et al. A therapeutic vaccine prototype induces protective immunity and reduces cardiac fibrosis in a mouse model of chronic *Trypanosoma cruzi* infection. *PLoS Negl Trop Dis*. 2019 May 30;13(5):e0007413.

87. Barry MA, Wang Q, Jones KM, Heffernan MJ, Buhaya MH, Beaumier CM, et al. A therapeutic nanoparticle vaccine against *Trypanosoma cruzi* in a BALB/c mouse model of Chagas disease. *Hum Vaccines Immunother.* 2016 02;12(4):976–87.
88. Martinez-Campos V, Martinez-Vega P, Ramirez-Sierra MJ, Rosado-Vallado M, Seid CA, Hudspeth EM, et al. Expression, purification, immunogenicity, and protective efficacy of a recombinant Tc24 antigen as a vaccine against *Trypanosoma cruzi* infection in mice. *Vaccine.* 2015 Aug 26;33(36):4505–12.
89. Seid CA, Jones KM, Pollet J, Keegan B, Hudspeth E, Hammond M, et al. Cysteine mutagenesis improves the production without abrogating antigenicity of a recombinant protein vaccine candidate for human chagas disease. *Hum Vaccines Immunother.* 2016 Oct 13;13(3):621–33.
90. Jones K, Versteeg L, Damania A, Keegan B, Kendricks A, Pollet J, et al. Vaccine-linked chemotherapy improves benznidazole efficacy for acute Chagas disease. *Infect Immun.* 2018 Jan 8;IAI.00876-17.
91. Martín-Escolano J, Marín C, Rosales MJ, Tsaousis AD, Medina-Carmona E, Martín-Escolano R. An Updated View of the *Trypanosoma cruzi* Life Cycle: Intervention Points for an Effective Treatment. *ACS Infect Dis.* 2022 Jun 10;8(6):1107–15.
92. Ricci AD, Bracco L, Salas-Sarduy E, Ramsey JM, Nolan MS, Lynn MK, et al. The *Trypanosoma cruzi* Antigen and Epitope Atlas: antibody specificities in Chagas disease patients across the Americas. *Nat Commun.* 2023 Apr 3;14(1):1850.
93. Wang W, Peng D, Baptista RP, Li Y, Kissinger JC, Tarleton RL. Strain-specific genome evolution in *Trypanosoma cruzi*, the agent of Chagas disease. *PLOS Pathog.* 2021 Jan 28;17(1):e1009254.
94. Dos Santos Virgilio F, Pontes C, Dominguez MR, Ersching J, Rodrigues MM, Vasconcelos JR. CD8(+) T cell-mediated immunity during *Trypanosoma cruzi* infection: a path for vaccine development? *Mediators Inflamm.* 2014;2014:243786.
95. Laidlaw BJ, Craft JE, Kaech SM. The multifaceted role of CD4+ T cells in CD8+ T cell memory. *Nat Rev Immunol.* 2016 Feb;16(2):102–11.
96. Camargo EP, Gazzinelli RT, Morel CM, Precioso AR. Why do we still have not a vaccine against Chagas disease? *Mem Inst Oswaldo Cruz.* 2022 May 9;117:e200314.
97. Statista [Internet]. [cited 2023 Oct 23]. COVID vaccinations administered number by manufacturer U.S. 2023. Available from: <https://www.statista.com/statistics/1198516/covid-19-vaccinations-administered-us-by-company/>
98. Barbier AJ, Jiang AY, Zhang P, Wooster R, Anderson DG. The clinical progress of mRNA vaccines and immunotherapies. *Nat Biotechnol.* 2022 Jun;40(6):840–54.
99. Anderson BR, Muramatsu H, Nallagatla SR, Bevilacqua PC, Sansing LH, Weissman D, et al. Incorporation of pseudouridine into mRNA enhances translation by diminishing PKR activation. *Nucleic Acids Res.* 2010 Sep;38(17):5884–92.
100. Nature [Internet]. 2023 [cited 2023 Dec 27]. Nobel Prize in Physiology or Medicine 2023. Available from: <https://www.nature.com/collections/bieheeeddf>
101. Fang E, Liu X, Li M, Zhang Z, Song L, Zhu B, et al. Advances in COVID-19 mRNA vaccine development. *Signal Transduct Target Ther.* 2022 Mar 23;7(1):1–31.
102. You H, Jones MK, Gordon CA, Arganda AE, Cai P, Al-Wassiti H, et al. The mRNA Vaccine Technology Era and the Future Control of Parasitic Infections. *Clin Microbiol Rev.* 2023 Jan 10;36(1):e00241-21.
103. Aldosari BN, Alfagih IM, Almurshedi AS. Lipid Nanoparticles as Delivery Systems for RNA-Based Vaccines. *Pharmaceutics.* 2021 Feb;13(2):206.
104. Pardi N, Hogan MJ, Porter FW, Weissman D. mRNA vaccines — a new era in vaccinology. *Nat Rev Drug Discov.* 2018 Apr;17(4):261–79.

105. Chaudhary N, Weissman D, Whitehead KA. mRNA vaccines for infectious diseases: principles, delivery and clinical translation. *Nat Rev Drug Discov*. 2021 Nov;20(11):817–38.
106. Charles A Janeway J, Travers P, Walport M, Shlomchik MJ. B-cell activation by armed helper T cells. *Immunobiol Immune Syst Health Dis 5th Ed* [Internet]. 2001 [cited 2019 Aug 19]; Available from: <https://www.ncbi.nlm.nih.gov/books/NBK27142/>
107. Tsuji M, Bergmann CC, Takita-Sonoda Y, Murata KI, Rodrigues EG, Nussenzweig RS, et al. Recombinant Sindbis Viruses Expressing a Cytotoxic T-Lymphocyte Epitope of a Malaria Parasite or of Influenza Virus Elicit Protection against the Corresponding Pathogen in Mice. *J Virol*. 1998 Aug;72(8):6907–10.
108. Baeza Garcia A, Siu E, Sun T, Exler V, Brito L, Hekele A, et al. Neutralization of the Plasmodium-encoded MIF ortholog confers protective immunity against malaria infection. *Nat Commun*. 2018 Jul 13;9(1):2714.
109. Savar NS, Shengjuler D, Doroudian F, Vallet T, Mac Kain A, Arashkia A, et al. An alphavirus-derived self-amplifying mRNA encoding PpSP15-LmSTI1 fusion protein for the design of a vaccine against leishmaniasis. *Parasitol Int*. 2022 Aug 1;89:102577.
110. Chahal JS, Khan OF, Cooper CL, McPartlan JS, Tsosie JK, Tilley LD, et al. Dendrimer-RNA nanoparticles generate protective immunity against lethal Ebola, H1N1 influenza, and *Toxoplasma gondii* challenges with a single dose. *Proc Natl Acad Sci*. 2016 Jul 19;113(29):E4133–42.
111. He Q, Gao H, Tan D, Zhang H, Wang J zhi. mRNA cancer vaccines: Advances, trends and challenges. *Acta Pharm Sin B*. 2022 Jul 1;12(7):2969–89.



CHAPTER 2

Transferring Luminex Cytokine Assays to a Wall-Less Plate Technology: Validation and Comparison Study with Plasma and Cell Culture Supernatants

Leroy Versteeg^{1*}, Xavier Le Guezennec^{2*}, Bin Zhan¹, Zhuyun Liu¹, Minilik Angagaw³, Janice D. Woodhouse³, Subhabrata Biswas³, Coreen Michele Beaumier¹

¹ Texas Children's Hospital Center for Vaccine Development, Baylor College of Medicine 1102 Bates St., Ste. 550, Houston, TX 77030

² Curiox Biosystems, 2 Woodlands Spectrum #03-10, Woodlands Sector I, Singapore 738068

³ Merck Research Laboratories, Merck & Co., Inc., 33 Avenue Louis Pasteur, Boston, MA 02115

* These authors contributed equally to this work

Manuscript published in Journal of Immunological Methods 440, no. Supplement C (January 1, 2017): 74–82.

■ <https://doi.org/10.1016/j.jim.2016.11.003>

ABSTRACT

Luminex® technology provides a powerful methodology for multiplex cytokine detection but remains constrained by high costs and a minimum of 25-50 µL sample volume requirement per assay-well often hindering analysis of limited biological samples. Here we compare the results of Luminex-based cytokine multiplexing assay performed using a conventional 96-well microtiter plates and using a particular 96-well wall-less plate based on Droparray® technology (“DA-Bead”). The application of the DA-Bead plate allows 80% reduction of sample and reagent volume, thus an opportunity for significant Luminex reagents cost savings with no change to the workflow.

To compare the DA-Bead method to the conventional method, two different types of samples were tested with two different commercially available Luminex kits and the results for each method were compared. The first type was splenocyte culture supernatants from murine spleens which were harvested from mice immunized with *Ascaris suum* protein As24 and followed by cell stimulation *ex vivo* at various time points with this same antigen. Cytokine levels in these supernatants were evaluated using a Bio-Plex® T_H1/T_H2 8-plex kit. The second sample type was plasma from mice from an experimental autoimmune encephalomyelitis (EAE) study, and these samples were evaluated using a Milliplex® T_H17 25-plex kit.

The data showed that the DA-Bead method for analysis was comparable to, if not superior to, the conventional method in terms of consistency/precision, accuracy, sensitivity and dynamic range and these results are not specific to sample type, reagents, or commercial vendor.

2.1 INTRODUCTION

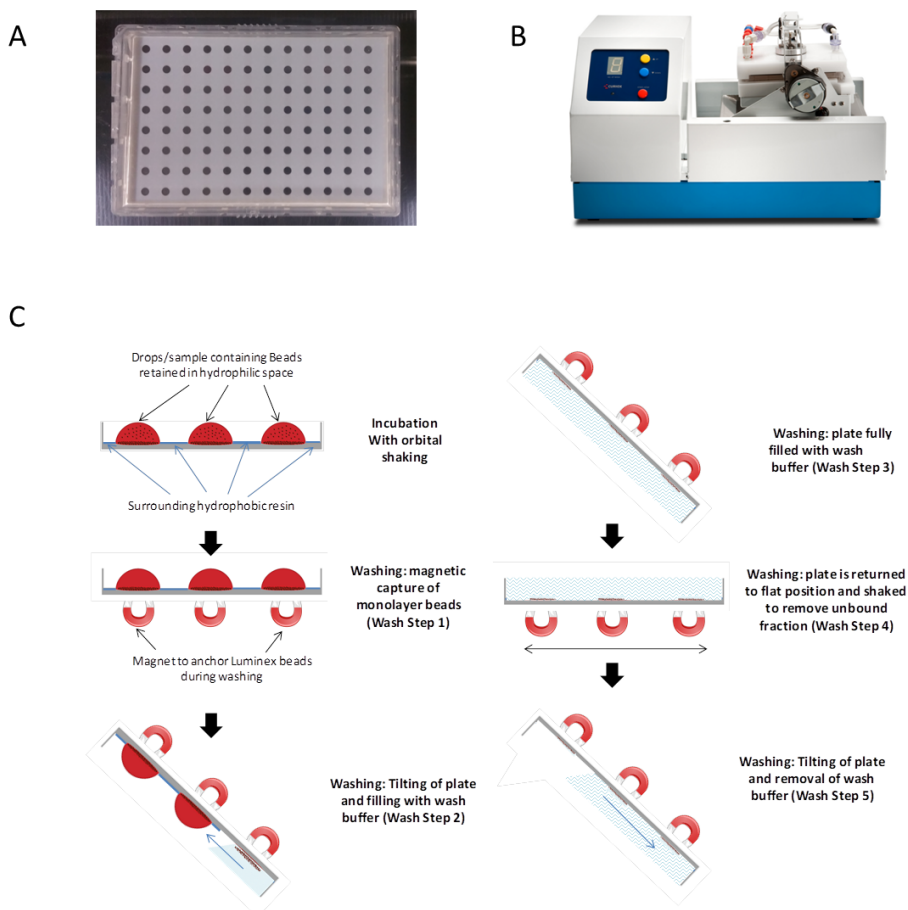
Identification and quantification of biomarkers in biological samples is a key component in research and clinical fields for example, it provides an effective way to make assessment on a new drug efficacy or toxicity and to help in the monitoring of disease progression (Giljohann and Mirkin, 2009). With expansion of diagnostic biomarker panels such as cytokines/chemokines and a growing need to understand more complex physiological processes, integrated molecular profiling solutions with multiplex protein capabilities are increasingly used (Stenken and Poschenrieder, 2015). Although unique protein detection is routinely performed with conventional technologies like enzyme-linked immunosorbent assay (ELISA), multiple protein detection can now be conveniently performed with multiplex capabilities offered by Luminex technology (Houser, 2012). Simply speaking, this method allows the transformation of a solid phase ELISA into a suspension bead ELISA. The unique proprietary color dye coding of Luminex beads can generate up to 500 unique sets of spectral color beads (Lin et al., 2015). Each set of beads with a unique spectral code can be coupled with a specific antibody in a sandwich immunoassay for detection of one specific protein. Multiple sets of different beads can be used together and individually analyzed from a single sample well for convenient multiple protein detection.

Currently, Luminex commercial cytokine panels accommodate a conventional 96-well plate workflow with minimal sample volumes of 25-50 μL per well (Lin et al., 2015). While Luminex is a proven technology for quick identification of compounds of interest, two drawbacks can be identified that limits more widespread use. First, commercial kits are relatively expensive. A Luminex kit is overall more expensive than an ELISA kit, and often multiple Luminex kits are still required for optimization of the particular assay to the individual researcher's system, as with any assay. Additionally, sample volume requirement for the kits using the conventional method may still remain a challenge for many biological samples such as small biopsies, gingival crevicular fluid, tears, mouse cerebrospinal fluid or those that are either generated in limited quantities or that might be required for multiple assays. With precious or limited sample volume, dilution of the sample may also be necessary to meet the minimal volume requirement of the assay and this dilution may lead to difficulties in the detection of analytes that are low in abundance (Staples et al., 2013; Wei et al., 2013; Lomba et al., 2015). Another limitation with Luminex technology is the difficulty in adjusting the standard curve for optimal detection range for the various analytes in samples with minimal instances of out of range (OOR) occurrences (Breen et al., 2015). There is for instance the possibility for users to be left with a sample dataset with many analytes ignored due to undetectable data.

Recent advances have been made to remove the drawbacks of the current Luminex technology and to make the Luminex technology more attractive. Curiox Biosystems developed the DropArray-bead (DA-Bead) method, a Luminex method based on the use of a 96-well wall-less plate capable of a five-fold miniaturized format with regards to sample (5 μL minimum) and Luminex reagents. The fundamental theory behind the feasibility of DA-

Bead method is derived from the working principle of conventional method which uses an excess ~2000 beads/analyte/well when only a minimal satisfactory 50 bead counts is needed to qualify results. In the DA-Bead method, a use of ~400 beads/analyte/well is still sufficiently excessive to meet the 50 bead count requirement. The DA-Bead method also offers the ability to effectively save costs on these commercial Luminex kit reagents by allowing use of these kits up to 5 times as opposed to only once (Le Guezennec et al., 2015) but still maintaining integrity of the data.

The DA-bead method for cytokine multiplexing remains as convenient as the conventional plate format to perform, and workflow utilizes the same set of reagents. Each reaction is individualized in highly confined drops in a wall-less format instead of large volumes in isolated microwells (**Fig. 1A**). Each drop is held firmly in a circular hydrophilic spot and is surrounded by a hydrophobic polytetrafluoroethylene (PTFE) resin coated polymer plastic to prevent movement of the droplet. The drops can be dispensed with a traditional multichannel pipet and can range from 5 μ L to 20 μ L conveniently on each circular well. Magnetic beads from Luminex xMAP format from commercial kits and samples are dispensed together in each well and can be washed using the specially designed LT-MX washer (Curiox) (**Fig. 1B**). The Curiox LT-MX washer generates a laminar-based flow wash with large volumes of wash buffer and works differently from a conventional 96-well plate washer. Information on the general principles of DA-Bead and the Curiox LT-MX washer has been described previously (Kozak et al., 2013; Quinones et al., 2013; Ingle and Scales, 2014; Le Guezennec et al., 2014; Le Guezennec et al., 2015). Briefly, the LT-MX washer allows the wall-less 96-well plate to be inserted and sealed into the washer as a closed chamber (**Fig. 1C**). This complex washing procedure is designed to prevent beads from being lost during the washing process. Also, since the lateral shear force in the washing process is lower compared to conventional washing using a pipetting method, the beads are less prone to aggregation. Overall, this entire process makes it possible to use fewer beads without jeopardizing assay sensitivity. Protocol workflow, addition of Luminex reagents, and incubation time, the DA-Bead method remain highly similar to the conventional workflow, and requires minimal additional training (Supplementary table 1) (Le Guezennec et al., 2015).



■ **Figure 1.** General characteristics of the DA-Bead system used for miniaturization of the Luminex assay: (A) top view of a DA-Bead plate, showing the 96 circular hydrophilic wells which are surrounded by hydrophobic PTFE resin. (B) Front view of the LT-MX washer, used for automated washing of DA-Bead plates. (C) General principle of the washing mechanism of the LT-MX plate washer.

In this study, two different data sets derived from two different commercially available Luminex cytokine assay kits using both the conventional method and the DA-Bead method were generated. Within each study, the data derived from the conventional and DA-Bead methods were systematically compared. Evaluating both methods using a plasma- and supernatant-based set of samples highlighted improvements in sample detectability in the DA-bead method with a reduction in OOR (out of range) occurrences. It was observed that the DA-Bead method provided improved detection of secreted cytokines when stimulating mouse cells *ex vivo* with a protein, As24, compared to the conventional method. Additionally, an analysis of T-helper cell 17 (T_H17) family of cytokine/chemokine profile with DA-Bead method in a mouse model of Experimental Autoimmune Encephalomyelitis (EAE) showed increased levels of detectability of disease-induced cytokines (Constantinescu et al., 2011) as compared

to the conventional method. It was demonstrated that there was a remarkable equivalence of the wall-less plate DA-Bead method compared to the conventional microtiter plate in terms of assay sensitivity, dynamic range, accuracy and precision.

2.2 MATERIALS AND METHOD

Sample Generation

As24 immunization study

All animal studies were approved by the Institutional IACUC at Baylor College of Medicine, Houston, TX (Protocol #AN-6297). For vaccination purposes, 6 to 10 weeks old female BALB/c mice were subcutaneously immunized as previously described (Islam et al., 2005) with either 50 µg of As24 formulated with 400 µg Alhydrogel® or 400 µg Alhydrogel alone. Animals received a booster-immunization with the same formulation as the prime immunization after 3 and 5 weeks. After 7 weeks the animals were sacrificed and spleens were removed aseptically.

In order to prepare a single-cell suspension of the splenocytes, spleens were homogenised through a 70 µm cell strainer and rinsed using RPMI 1640 (Corning, Cat#10-041-CV) culture media, supplemented with 2mM L-Glutamine, Penicillin 10 IU/mL + 10µg/mL streptomycin (Corning, Cat#30-002-Cl), and 10% (v/v) heat-inactivated fetal bovine serum (Hyclone GE, Cat#SH30910.03). Cells were centrifuged for 5 minutes at 300 x g and the pellet was resuspended in 1 mL ACK lysing buffer (Lonza, CAT#10-548E). After 5 minutes of incubation, 5 mL culture media was added and cells were centrifuged as previously described. For restimulation purposes, splenocytes were seeded at 5×10^5 cells in 100 µL/well in a 96 well tissue culture plate (Falcon Corning, Cat#351177) in culture media. Seeded cells received either 2 µg/mL Concanavalin A (Alfa Aesar, Cat#J61221) as a positive control, 25 or 50 µg/mL of recombinant As24 protein, or media alone. Cells were cultured at 37°C, 5% CO₂ in a humidified atmosphere. Collection of the splenocyte culture supernatant was performed after 24 h or 48 h restimulation and was stored at -80°C until usage for Luminex assay.

Experimental Autoimmune Encephalomyelitis (EAE)

All animal studies were approved by the Institutional IACUC (Protocol 200348) and performed at Merck & Co., Inc., Boston, MA USA. EAE was induced in mice via immunization with MOG₃₅₋₅₅ as per the manufacturer recommendations (Hooke Laboratories, Lawrence, MA, USA). Female, 9 to 10 week old C57BL/6 mice (Jackson Laboratory, Bar Harbor, ME, USA) were inoculated by using commercially available ready-to-use inoculum (Hooke Laboratories, Lawrence, MA USA) containing 100 µg of MOG₃₅₋₅₅, 200 µg heat inactivated of *Mycobacterium tuberculosis* in mineral oil in 100 µL of inoculum. Inoculation was done by giving each mouse 2 x 100 µL injections subcutaneously to lower and higher aspect of the back. Intraperitoneal injections of pertussis toxin (4 µg/mL) in 100 µL total volume were given at 2 hours and 24 hours after inoculation with MOG₃₅₋₅₅. EAE induced mice and a naïve control mice group was

orally administered with a vehicle composed of PBS and 0.5% Methylcellulose, 0.25% SDS at a dose volume of 10 mL/kg bodyweight. In the treatment group, mice were orally gavaged with dexamethasone (Sigma, St. Louis, MO) at a dosage of 1 mg/kg bodyweight. Mouse blood was collected at 7 days after injection via cardiac puncture and in EDTA microtainers (Becton, Dickinson and Company, Franklin Lakes, NJ, USA). Centrifugation of microtainers in an Eppendorf® desktop centrifuge was then performed at 350 x g for 15 minutes at 4°C to separate plasma and cells. The supernatant (plasma fraction) was transferred in a fresh tube and stored at -20°C till usage for Luminex assay.

Conventional Bio-Plex and Milliplex Luminex Cytokine Assay Workflow

As24 Study with Bio-Plex Conventional Cytokine Assay

The mouse supernatant samples from the As24 study were assayed using an 8-plex, Bio-Plex® Pro Mouse Cytokine T_H1/T_H2 panel (Cat#M6000003J7, Bio-Rad, Hercules, CA). The conventional 96-well plate-based protocol for the Bio-Plex kit was performed according to the manufacturer's instructions. Bio-Plex kit cytokine standards were reconstituted with cell culture media similar to supernatant samples. Final analysis of the experiments was performed on a Magpix system according to manufacturer's recommendations (Bio-Rad, Hercules, CA).

EAE Study with Milliplex Conventional Cytokine Assay

Mouse plasma samples were tested using a 25-plex Milliplex® MAP Mouse T_H17 Magnetic Bead Panel (Cat#MTH17-MAG-47K, Millipore, Billerica, MA) and the conventional 96-well plate-based protocol was performed according to the manufacturer's instructions, including the recommended manual washing steps. Cytokine standards and cytokine quality control were used with Milliplex provided serum matrix during initial primary incubation. Final analysis of the experiments was performed on a Bio-Plex 200 system according to manufacturer's recommendations (Bio-Rad, Hercules, CA).

DA-Bead Workflow

As24 Study Bio-Plex Kit Workflow with DA-Bead

In order to perform the DA-Bead assay using the wall-less plate and the reagents of the Bio-Plex kit, the protocol of the Bio-Plex kit was slightly adapted. First, the DA-Bead wall-less plate was blocked for 30 min at room temperature with 10 µL 1% Bovine Serum Albumin (BSA) in Phosphate Buffered Saline (PBS). 10 µL of premixed beads were added in each well. Premixed beads were prepared according to the conventional protocol but used only 1/5th of volume and 1/5th of beads. The DA-Bead plate was subsequently washed 1x using the automatic washing station LT-MX (Curiox Biosystems) with 0.1% BSA 0.05% Tween 20 in PBS (wash buffer). Then 10 µL of diluted samples, standards or blank were added in the appropriate wells. The DA-Bead plate was then vortexed for 5-10 sec on an analog microplate Genie Shaker (Scientific Industries Inc, Bohemia, NY) at an intensity scale of 4. The DA-Bead plate was then covered with an anti-evaporation lid and transferred into a Curiox sealed squared container

containing Kimwipes soaked with 100 mL PBS. The container was placed on a 3 mm span orbital shaker (Orbit 300, Labnet, Edison, NJ) and shaken for 30 min at 350 rpm (0.2xg) at room temperature. DA-Bead plate was then washed 3 times with the LT-MX washing station. 5 μ L of detection antibody diluent was added in each used well. The DA-bead was subsequently placed for 5-10 sec on an analog microplate genie shaker as described above, and transferred to the Curiox container and incubated on the orbital shaker for 30 minutes at 350 rpm at room temperature. The DA-Bead plate was then washed 3 times using the LT-MX station. 10 μ L of streptavidin-phycoerythrin diluent was then added in each well and the DA-bead plate was placed for 5-10 sec on the Genie Shaker as described above, transferred to the Curiox container and incubated for 30 min on the orbital shaker at 350 rpm at room temperature. The DA-Bead plate was washed 3 times in the LT-MX station.

EAE Study Milliplex Kit Workflow with DA-Bead

The DA-Bead method followed a conventional Milliplex workflow using an 80% reduction in sample and reagents volume with a few modifications. The DA-Bead plate well surface was initially blocked for 30 min at room temperature with 10 μ L PBS (phosphate Buffered Saline) 1% BSA (Bovine Serum Albumin) and was subsequently washed 1x in the LT-MX (Curiox Biosystems) with a PBS 0.1% BSA, 0.05% Tween-20 wash buffer. The DA-Bead protocol was performed with standard/quality control wells and sample wells with either 5 μ L of beads addition, 5 μ L serum matrix or 5 μ L universal assay buffer addition. 5 μ L Cytokine standard, quality controls or plasma samples were added last in the well. The reagents were then mixed 5x by pipetting. The DA-Bead plate was then placed for 5-10 sec on an analogue microplate Genie Shaker (Scientific Industries Inc, Bohemia, NY) with an intensity scale of 4. To limit evaporation an anti-evaporation lid, which contains a sponge material, is saturated with 12 ml PBS and placed above DA-bead plate during incubation. Additionally, the DA-Bead plate was placed in a Curiox sealed squared contained containing 100 mL PBS soaked Kimwipes during incubation. The container was placed on a 3mm span orbital shaker at 350 rpm speed (0.2xg) and shook overnight at 4°C. The DA-Bead plate was then washed 3X in the LT-MX station with wash buffer. 5 μ L of the detection antibody was added in each used well. The DA-bead plate was placed for 5-10 sec on an analog microplate Genie Shaker as described above, and in the Curiox container on an orbital shaker for 60 min at room temperature. Subsequently 5 μ L streptavidin-phycoerythrin was added to each well. The DA-Bead plate was placed for 5-10 sec on an analog microplate Genie Shaker as described above and placed in Curiox container on orbital shaker for 30 m at room temperature. The DA-Bead plate was then washed 3X in LT-MX station with wash buffer.

Reading of DA-Bead Plate by Luminex Instruments

Preparation of the DA-Bead plate for Bio-Plex 200 or Bio-Plex Magpix system acquisition was performed as follows: After the last wash, 10 μ L of Bio-Plex sheath fluid was added to each well. The DA-Bead plate was placed for 5-10 s on the analogue microplate Genie Shaker. A 96-

well direct reading block (Curiox) was then stamped with 10 mL direct reading fluid (Curiox) and was transferred to the DA-bead plate as an insert. Only a residual layer of liquid is retained on the bottom surface of the direct reading block of ~1 mL. The direct reading fluid liquid acts as a seal between DA-Bead plate surface and bottom surface of the reading block. Next, 55 μ L of Bio-Plex sheath fluid was added to each well and mixed 2 times by pipetting. DA-Bead plate/block assembly was then shaken for 5 min on a 3 mm span orbital shaker at a speed of 350 rpm (0.2xg). The DA-Bead/block assembly was then placed into Bio-Plex 200 or Magpix system and parameters were adjusted to 50 μ L per injection (Bio-Plex Magpix was used in default recommended injection configuration), 50 bead minimal count requirements and 60 s timeout. Gate settings were maintained according to manufacturer's recommendation (Bio-Rad, Hercules, CA).

Data Analysis

Analysis of As24 Study Data

For the As24 study data analysis using the Bio-Plex kit, cytokine standard dilution was based on manufacturer's recommendation with a 4 fold dilution over 8 points. Standards were performed in duplicate. The precision of standards were assessed with intra-assay %CV (coefficient of variation). The intra-assay %CV was generated from the mean of the %CV of four different concentrations of one experiment. Curve fitting for Bio-Plex dataset was derived with the Bio-Plex Manager software. Lower or upper limit of quantitation (LLOQ/ULOQ) for the Bio-Plex dataset was derived with the Bioplex Manager software and was defined as the reliable quantitative range where values could be estimated with 70-130% recovery and a precision below 20 %CV. Sample values were excluded if the value detected was outside of reliable range defined by LLOQ/ULOQ or lower and higher limit of quantitation.

Analysis of EAE Study Data

The Milliplex workflow multiplex cytokine standard dilution for MTH17-MAG-47K was based on manufacturer's recommendation with a 4-fold dilution over 6 points standard curve. The precision of standards were assessed with intra-assay %CV (coefficient of variation). The intra-assay %CV was generated from the mean of the %CV of four different concentrations of one experiment. Curve fitting was performed with Graphpad Prism for the Milliplex based dataset with the most suitable 4 or 5 parameter logistic fitting with weighting ($1/y^2$) to minimize heteroscedasticity. For the Milliplex data set, the lower and upper limit of quantitation was defined as a reliable quantitative range where values could be estimated with 70-130% recovery and a precision below 25 %CV. Quality control QC1, a standard of known concentration acted in low concentration range while QC2 acted in high concentration range. A concentration observed within the expected range was considered as 100% recovery. When measurements were higher than the upper range of the expected, the percentage recovery was considered <100%. When measurements were lower than the lower range of the expected, the percentage recovery was considered less than 100%. Sample values which were outside of reliable quantitative range were excluded of the data analysis.

2.3 RESULTS

Analysis of Assay Standards

Standard Deviation of Bead Counts

Two commercial Luminex kit panels were evaluated in this study: a Bio-Plex (8-plex) kit used for mouse splenocyte supernatant analysis and a Milliplex (25-plex) kit used for mouse plasma samples analysis. In order to evaluate the performance of Curiox DA-Bead technology, we compared side by side the conventional Luminex protocol with the Curiox Luminex miniaturization DA-Bead protocol. Luminex assays generally require a minimal of 50 bead counts for each analyte in each well to reach qualification of data. Therefore, the conventional method uses an excess of bead amounts (~2000 beads/analyte/well) at the start of the assay as it needs to maintain an ideal volume/bead surface ratio, account for beads loss events during washing steps, and bead aggregation. The Curiox miniaturization DA-bead protocol uses 1/5th of beads (~400 beads/analyte/well) as compared to conventional protocol but still satisfies the minimal 50 bead counts/analyte requirements for all analytes tested (**Fig. 2A** and **Supplementary Fig. 1**). Interestingly, variability in standard deviation of bead counts was generally higher in conventional plates than in DA-Bead plates in both Bio-Plex and Milliplex kit panels.

Accuracy

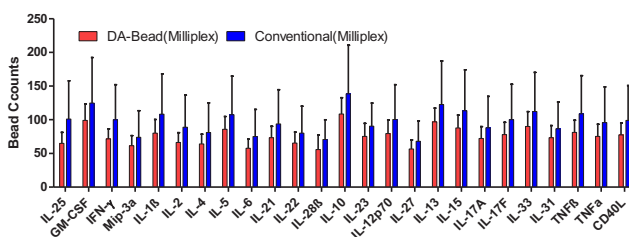
The performance equivalence of cytokine standards between both methods were analysed as follows: Observed calculated concentrations of cytokine standards for all analytes were generated using standard curves and correlated in paired dataset between both methods with $R^2=0.98$ for Bio-Plex kit workflow and $R^2=0.99$ for Milliplex kit workflow (**Fig. 2B**). Standard curves from the Bio-Plex or Milliplex analysis showed comparability between data from the DA-Bead method and data from conventional plate method (**Supplementary Fig. 3** and **4**). Symmetry of the standard curves between both methods was maintained. Accuracy of cytokine standards from the overall dataset was within a 70-130% acceptance criteria but started to deviate from this range at high concentrations (>10,000 pg/ml) for both DA-Bead and conventional plate based method (**Fig. 2C** and **Supplementary Fig. 3** and **4**). Internal quality control samples provided for the Milliplex assay were also evaluated for accuracy in assay with both methods (**Supplementary Table 2**). Acceptable recovery in 90-110% range was observed for all analytes tested with high quantity and low quantity quality controls on both methods, which strongly suggested good equivalence in performance with the DA-Bead workflow as compared to traditional workflow.

Sensitivity

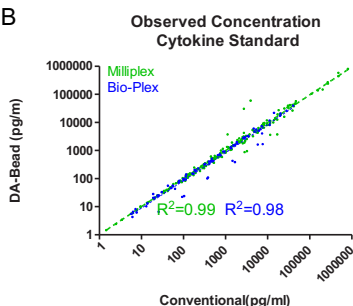
Reliable sensitivity of the assay defined by a low limit of quantitation was achieved using the DA-Bead method for all analytes in the Milliplex kit except for IL-6 and IL-10, which both showed decreased sensitivity or IL-13 which showed improved sensitivity (**Table 1**). Bio-Plex kit's reliable sensitivity defined by LLOQ was improved using the DA-Bead method as

compared to the conventional plate for IL-2, IL-4, IL-5, IFN- γ and TNF- α , while the conventional method showed improved LLOQ for IL-12, GM-CSF and IL-10 (**Table 2**). The upper limits of quantitation were similar for both platforms except IL-12p70, TNF- α in Milliplex panel (**Table 1**). ULOQ with Bio-Plex panel was closely similar for both platforms with IL-4, IL-5, IL-10, IL-12, GM-CSF and TNF- α but showed superior performance with IL-2 in DA-Bead method or IFN- γ in conventional method (**Table 2**).

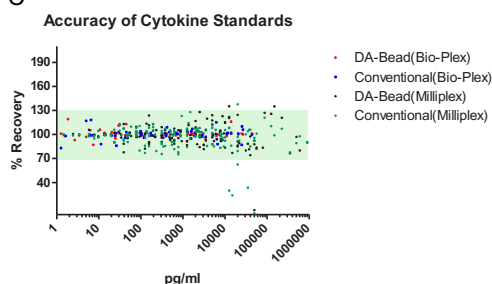
A



B



C



■ **Figure 2.** Fundamental Luminex cytokine assay performance characteristics: (A) average bead counts of complete Milliplex dataset. Each bar and error bar represent the mean and standard deviation of bead counts based on measurements of all 42 wells using the DA-Bead method (red) or the conventional method (blue). (B) Correlation of cytokine standards. Calculated observed concentration derived from the cytokine standards curves for the conventional method and the DA-Bead method were paired and correlated for Milliplex based cytokine panel (green) or Bio-Plex based cytokine panel (blue). The R^2 value was calculated by using Spearman correlation analysis. (C) Accuracy analysis of cytokine standards. Calculated recovery for all cytokine concentration points from Milliplex and Bio-Plex panel was calculated. The delineated dotted lines indicate the acceptable recovery of 70–130%. Results are shown as DA-Bead Bio-Plex panel (red), conventional Bio-Plex panel (blue), DA-Bead Milliplex panel (black), conventional Milliplex panel (green).

■ **Table 1.** Summary of key parameters of cytokine standard in Milliplex assay with serum matrix.

Analytes	Limit of Quantitation#					
	Low(pg/ml)		High(pg/ml)		Intra-Assay %CV*	
	DA-Bead	Conventional	DA-Bead	Conventional	DA-Bead	Conventional
IL-25	585.9	585.9	600000	600000	11.7	13.3
GM-CSF	34.2	34.2	8750	8750	10.1	18.6
IFN- γ	7.8	7.8	8000	8000	9.0	11.2
Mip-3alpha	48.8	48.8	3125	3125	16.5	15.3
IL-1 β	14.7	14.7	15000	15000	7.9	15.1
IL-2	5.9	5.9	6000	6000	3.5	20.3
IL-4	1.5	1.5	1500	1500	9.3	18.9
IL-5	19.5	19.5	5000	5000	18.3	15.9
IL-6	31.3	7.8	8000	8000	13.4	19.1
IL-21	19.5	19.5	20000	5000	11.3	16.3
IL-22	2.4	2.4	2500	2500	9.5	17.8
IL-28 β	127.0	127.0	8125	8125	6.6	12.6
IL-10	78.1	19.5	20000	20000	8.4	12.3
IL-23	341.8	341.8	350000	350000	9.3	17.2
IL-12p70	19.5	19.5	20000	5000	7.4	17.4
IL-27	878.9	878.9	900000	900000	12.6	13.5
IL-13	39.1	156.3	40000	40000	8.9	12.2
IL-15	34.2	34.2	35000	35000	7.5	17.1
IL-17A	39.1	39.1	40000	40000	9.1	19.1
IL-17F	9.8	9.8	10000	10000	10.3	12.8
IL-33	78.1	78.1	80000	20000	7.6	16.0
IL-31	48.8	48.8	50000	50000	7.2	9.6
TNF β	488.3	488.3	500000	500000	12.3	14.4
TNF α	3.4	3.4	3500	875	8.2	22.9
CD40L	48.8	48.8	50000	50000	8.2	17.5

#High and low limit of quantitation are defined with restriction based on highest or lowest standard point with a concentration backfit of 70-130% and <25% CV.

* Intra-Assay %CV based on average of CV of 2nd, 3rd, 4th and 5th standard dilution duplicate.

Precision

Precision of the assay in Milliplex workflow which used a serum matrix component was <25% intra-assay %CV for conventional workflow but <20% intra-assay %CV for the DA-Bead method for all analytes, suggesting better consistency between replicates in DA-Bead

(**Tables 1** and **2**). Precision of the assay in the Bio-Plex workflow, which used a cell media as a matrix, was < 15% intra-assay %CV for both conventional and DA-Bead workflow (**Table 2**).

■ **Table 2.** Summary of key parameters of cytokine standard in Bio-Plex assay with cell media reconstitution.

Analytes	LLOQ		ULOQ		Intra-Assay %CV*	
	DA-Bead	Conventional	DA-Bead	Conventional	DA-Bead	Conventional
IL-2	3.3	13.5	45792	14222	5.1	2.6
IL-4	6.1	24	25342	21648	6.1	2.5
IL-5	2.2	7.3	7519	7809	13.1	1.7
IL-10	1.2	1	20620	20874	5.3	2.9
IL-12	6.4	1.5	26764	28389	8.3	10.1
GM-CSF	51	9.9	11620	11839	12.7	5.1
IFN- γ	1.5	6.1	6370	28102	5.9	2.6
TNF α	2.4	40.9	44362	43867	5.4	6.7

#LLOQ/ULOQ are defined as the reliable range of the curve with a concentration backfit of 70-130% and <20% CV.

* Intra-Assay %CV based on average of CV of 2nd, 3rd, 4th and 5th standard dilution duplicate.

Overall, it was concluded from analysis with standard cytokine or quality controls that the DA-Bead miniaturized Luminex cytokine assay method showed a comparable consistency/precision, accuracy, sensitivity and dynamic range as a conventional protocol.

Comparison of Sample Results Using the Conventional Versus DA-Bead Method

To further compare the conventional method to the DA-Bead method, a set of 24 re-stimulated mouse splenocytes supernatant samples and 56 mouse plasma samples were subjected to parallel analysis with Bio-Plex or Milliplex based panels, respectively. Using the Spearman test, correlations were found with supernatant sample values for all analytes between both methods with a $R^2=0.92$ (**Fig. 3A**). Correlations were also found with plasma sample values for all analytes with a $R^2=0.93$ (**Fig. 3B**).

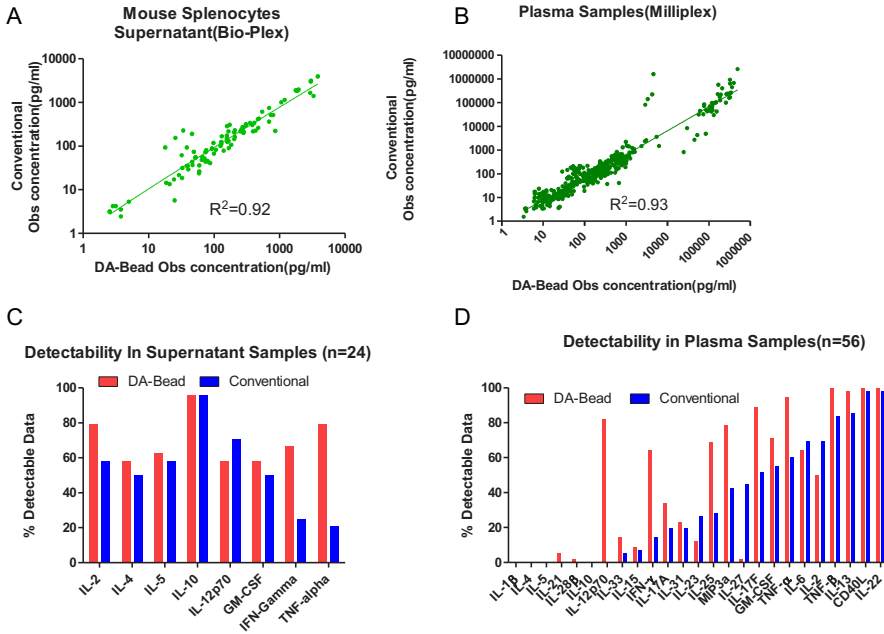


(Fig. 3D). Although some cytokines such as IL-27, IL-2 and IL-23 were less able to be detected using the DA-Bead method, and displayed 80% detectable data for IL-12p70 while these data were undetectable with the conventional method.

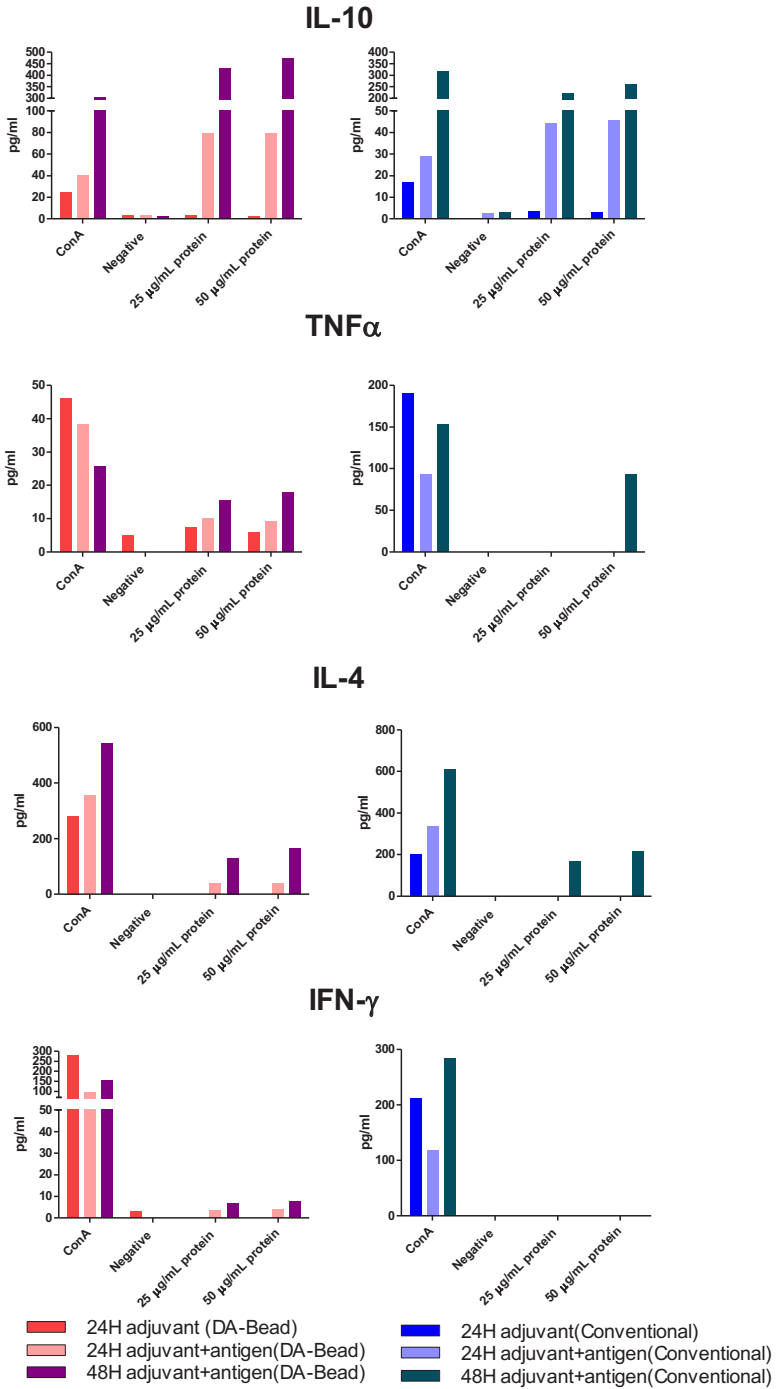
As24 Study with Bio-Plex Kit

To understand further the impact of this difference in ability to detect analytes with the DA-Bead method, re-stimulated mouse splenocyte supernatant samples were analysed using both the DA-Bead method and conventional method. These splenocytes were stimulated for different lengths of time, specifically 24 and 48 h and supernatants were taken at and tested at both time points. Luminex results showed a similar profile of IL-10 increased secretion with both the DA-Bead method and the conventional method suggesting equivalence in analyte detection (Fig. 4A and Supplementary Fig. 6). Interestingly, DA-Bead Luminex analysis could detect cytokines at 24 h and with lower amount of As24 protein, 25 µg/mL, such as TNF-α, IL-4 and IFN-γ. However, the conventional method could only detect TNF-α, IL-4 after 48 h of stimulation and with a higher concentration of As24 protein at 50 µg/mL. These results support the general observation made on improved analyte detectability with the DA-Bead method (Fig. 3C).

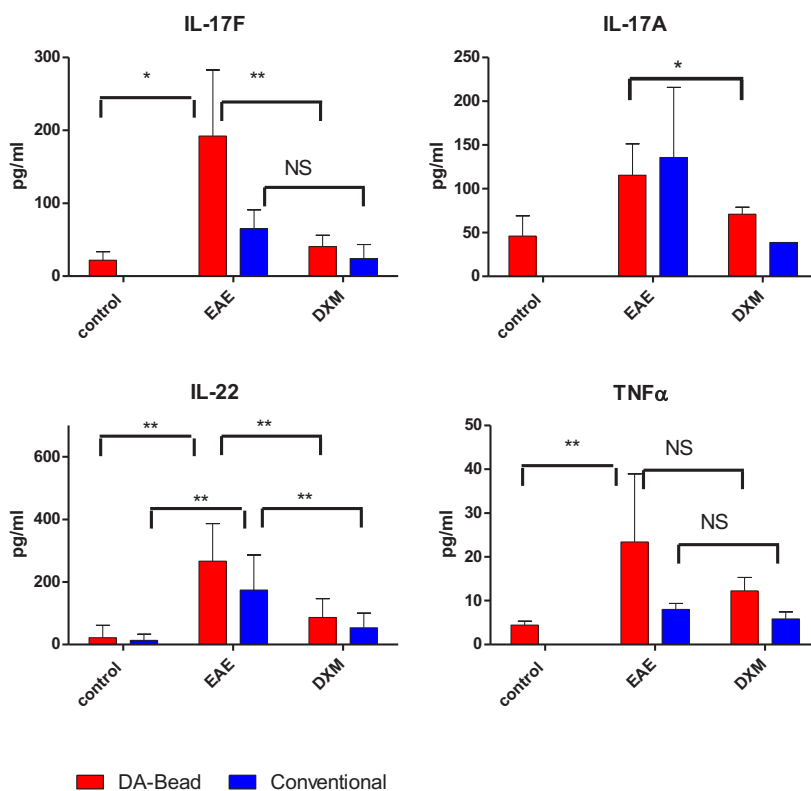
EAE Study with Milliplex Kit

We analyzed the plasma samples from the EAE study using both the DA-Bead and conventional methods, similarly to the analysis of the As24 study as above. Plasma sample sets used in Milliplex analysis was recovered from naive C57BL/6 mice and mice immunized with myelin oligodendrocyte glycoprotein (MOG₃₅₋₅₅) to induce EAE. Profiling of cytokine expression with both the DA-Bead and conventional methods highlighted remarkable differences. IL-17F showed a significant difference with DA-Bead method between control and EAE group or between the EAE and DXM groups ($p=0.03$ and $p=0.0078$ respectively) in Wilcoxon matched pairs signed rank test (Fig. 4B and Supplementary Fig. 7). The conventional method lacked a detectable baseline in the control group and showed no statistical significance between the EAE and DXM groups with IL-17F. Furthermore, IL-17A showed significant difference with DA-Bead method between EAE and DXM group ($p=0.014$) when the conventional method showed no difference. IL-22 was highly elevated upon EAE induction and efficiently suppressed by DXM with both methods. Statistical significance was equivalent with the DA-Bead method ($p=0.0039$) as compared to the conventional method ($p=0.0039$). TNF-α levels in the control group were undetectable by the conventional method and no statistical significance between the EAE and DXM groups. The DA-Bead method showed statistical significant difference with TNF-α between the control and EAE groups ($p=0.0078$) but was not significant between the EAE and DXM groups. Overall the analysis presented here, strongly suggests that the DA-Bead method is effective in improving confidence in detectable cytokine level changes in mouse plasma samples recovered from an EAE based experimental mouse model.

A



B



■ **Figure 4.** Effect of DA-Bead method on functional sample analysis: (A) supernatant sample analysis from Bio-Plex panel depicting observed concentration data generated from the DA-Bead method (left panels) or the conventional method (right panels) with IL-10, TNF α , IL-4 and IFN- γ analytes. (B) Plasma sample analysis derived from an autoimmune encephalomyelitis (EAE) mouse study. Data was generated with Milliplex panel and depict observed concentration data generated from the DA-Bead platform (red) or conventional platform (blue) for IL-17A, IL-17F, IL-22 and TNF α analyte. Mean and standard deviation is presented based on 8 mouse measurements within each group. *P<0.05, **P<0.01, ***P<0.001, NS: not significant. Statistical degree of significance was derived from Wilcoxon matched paired signed rank test.

2.4 DISCUSSION

Although miniaturization and automation of Luminex cytokine assays have previously been reported with a microfluidic based chip method, it has a steep learning curve for implementation (Sasso et al., 2012) and currently remains a workflow challenge when multiple samples need to be analysed. Conversion of Luminex cytokine assays to using smaller volumes can be achieved using 384 well plates but remains only possible for labs equipped with advanced automated systems and more sophisticated and expensive Luminex readers, like the Flexmap3D (Luminex Corporation, Austin, Texas). The DA-Bead method using the wall-less plate maintains a 96-well format uses small volumes, and is compatible with any Luminex reader from oldest models such as Luminex 100, Luminex 200 up to high end Flexmap3D model or Magpix. DA-Bead method can be performed with a traditional 1-10 μ L multichannel or single channel pipet and does not require advanced automation. By reducing commercial Luminex cytokine kit reagents by 80% and maintaining a similar 96-well plate format, the DA-Bead method remains straightforward and easy to implement for the everyday Luminex user (**Supplementary Table 1**). This significant reduction in kit reagents means that one Luminex cytokine kit could be used up to 5 times, and that therefore the costs per assay are significantly reduced.

In this study we compared the DA-Bead method with the conventional method using two different commercial Luminex cytokine kits: a Bio-Plex 8-plex kit and a 25-plex Milliplex kit. We have observed a reduction in the variability in bead counts when using the DA-Bead method as compared to the conventional method. These findings support previous observations of increased stochastic bead count variance when the amount of beads was increased such as in common microtiter plate assays (Hanley, 2008).

Cytokine standards displayed few differences in the lower or upper limit of quantitation between the conventional method and the DA-Bead method in both Bio-Plex and Milliplex kits, and were similar for >70% of the analytes. Most of the differences observed in both kits could be explained by that the lowest or highest standard point was affected by either very low fluorescence reading or fluorescence signal saturation, respectively, accuracy beyond acceptable 70-130% recovery range or inconsistencies above tolerated intra-assay %CV. Generally consistency using the DA-Bead method had a %CV<20%. Both samples from supernatant or plasma displayed good equivalence on both methods with paired detected sample analysis with $R^2>0.9$. Overall the DA-Bead method performed very similar to the conventional method.

The relatively superior performance of the DA-Bead miniaturized method over the conventional method can most likely be attributed to the fact that the DA-Bead method uses smaller volumes than the conventional method and incorporates a unique washing method uniquely designed to prevent bead loss. Beads are also potentially minimally aggregated in

the well during the wash due to the reduced amount of beads/well used in the method which make beads to spread across the surface of a well.

The DA-Bead method has shown improved sensitivity for detecting secreted cytokines in the supernatant of splenocytes re-activated with a recombinant protein, As24. Both methods were able to detect IL-4, and TNF- α but the DA-Bead method could detect cytokines after 24 h of incubation with 25 $\mu\text{g}/\text{mL}$ of stimulant antigen, while the conventional method required a 48 h incubation and 50 $\mu\text{g}/\text{mL}$ of stimulant antigen to reach detectable levels. Remarkably, IFN- γ was only detected using the DA-Bead method. IFN- γ along with IL-4 and IL-10 have been previously associated to be elevated after immunization with As24 and therefore is a valid functional marker picked up in our Luminex analysis with DA-Bead method (Islam et al., 2005; Chen et al., 2012).

Similarly, the DA-Bead method also displayed improved sensitivity in detecting disease and treatment induced modulation in plasma cytokine levels in a mouse model of EAE measured at an early time point before manifestation of clinical disease. In our study, dexamethasone (DXM) was found to suppress IL-17F, IL-17A and IL-22 levels significantly in an EAE model as detected by the DA-Bead method but only IL-22 levels reached statistical significance when assayed with the conventional Luminex method. This result aligns with a very recent study performed with ELISA highlights the specificity and importance of IL-17 and IL-22 cytokine secretion by T-cells in active brain lesions of multiple sclerosis human patients (Wing et al., 2016). The inhibition by DXM of IL-17 and IL-22 cytokines as identified by our results with the DA-Bead method could suggest a tandem inhibition mechanism by DXM since both IL-22 and IL-17F appear as very specific to EAE/multiple sclerosis. Our findings also agree with ELISA results in a recent study in which DXM could suppress IL-17F in an EAE mouse model upon a packing of myelin oligodendrocyte glycoprotein (MOG) with DXM into acetalated dextran particles (Peine et al., 2014).

Given the similarity in the workflow between the methods and benefits of increased sensitivity, low sample requirement, and reduced experimental costs with the DA-bead method, future studies with more complex biological samples will help towards establishing this method as a viable alternative to the currently practiced conventional method. Additionally, these results are independent of sample type, detection reagents, or commercial vendor. A promising avenue for new biomarker discovery with a synergy between Luminex technology and the DA-Bead method is now open to be fully explored.

Acknowledgements

Funding to support the As24 and EAE studies was provided by the Michelson Medical Research Foundation and Merck Research Laboratories, respectively.

Conflicts of Interest

L. Versteeg, B. Zhan, Z. Liu, and C.M. Beaumier are involved in the development of vaccines against neglected tropical diseases including ascariasis. All other authors declare no conflict of interest.

Supplementary Material

Supplementary data from this manuscript can be found online at <http://dx.doi.org/10.1016/j.jim.2016.11.003>.

2.5 REFERENCES

- Breen, E.J., Polaskova, V. and Khan, A., 2015, Bead-based multiplex immuno-assays for cytokines, chemokines, growth factors and other analytes: median fluorescence intensities versus their derived absolute concentration values for statistical analysis. *Cytokine* 71, 188-98.
- Chen, N., Yuan, Z.G., Xu, M.J., Zhou, D.H., Zhang, X.X., Zhang, Y.Z., Wang, X.W., Yan, C., Lin, R.Q. and Zhu, X.Q., 2012, *Ascaris suum* enolase is a potential vaccine candidate against ascariasis. *Vaccine* 30, 3478-82.
- Constantinescu, C.S., Farooqi, N., O'Brien, K. and Gran, B., 2011, Experimental autoimmune encephalomyelitis (EAE) as a model for multiple sclerosis (MS). *Br J Pharmacol* 164, 1079-106.
- Giljohann, D.A. and Mirkin, C.A., 2009, Drivers of bdiagnostic development. *Nature* 462, 461-4.
- Hanley, B.P., 2008, Variance in multiplex suspension array assays: a distribution generation machine for multiplex counts. *Theor Biol Med Model* 5, 3.
- Houser, B., 2012, Bio-Rad's Bio-Plex(R) suspension array system, xMAP technology overview. *Arch Physiol Biochem* 118, 192-6.
- Ingle, G.S. and Scales, S.J., 2014, DropArray, a wall-less 96-well plate for uptake and immunofluorescence microscopy, confirms CD22 recycles. *Traffic* 15, 255-72.
- Islam, M.K., Miyoshi, T. and Tsuji, N., 2005, Vaccination with recombinant *Ascaris suum* 24-kilodalton antigen induces a Th1/Th2-mixed type immune response and confers high levels of protection against challenged *Ascaris suum* lung-stage infection in BALB/c mice. *Int J Parasitol* 35, 1023-30.
- Kozak, K.R., Wang, J., Lye, M., Chuh, J., Takkar, R., Kim, N., Lee, H., Jeon, N.L., Lin, K., Zhang, C., Wong, W.L. and DeForge, L.E., 2013, Micro-volume wall-less immunoassays using patterned planar plates. *Lab Chip* 13, 1342-50.
- Le Guezennec, X., Phong, M., Nor, L. and Kim, N., 2014, Miniaturization of mitotic index cell-based assay using "wall-less" plate technology. *Assay Drug Dev Technol* 12, 129-35.
- Le Guezennec, X., Quah, J., Tong, L. and Kim, N., 2015, Human tear analysis with miniaturized multiplex cytokine assay on "wall-less" 96-well plate. *Mol Vis* 21, 1151-61.
- Lin, A., Salvador, A. and Carter, J.M., 2015, Multiplexed Microsphere Suspension Array-Based Immunoassays. *Methods Mol Biol* 1318, 107-18.
- Lomba, K.S., Beiler, T.F., Sete, M.R., Pires, F.R. and Figueredo, C.M., 2015, Use of minimally invasive gingival biopsies in the study of inflammatory mediators expression and their correlation with gingival fluid in patients with chronic periodontitis. *Indian J Dent Res* 26, 126-30.
- Peine, K.J., Guerau-de-Arellano, M., Lee, P., Kanthamneni, N., Severin, M., Probst, G.D., Peng, H., Yang, Y., Vangundy, Z., Papenfuss, T.L., Lovett-Racke, A.E., Bachelder, E.M. and Ainslie, K.M., 2014, Treatment of experimental autoimmune encephalomyelitis by codelivery of disease associated Peptide and dexamethasone in acetalated dextran microparticles. *Mol Pharm* 11, 828-35.
- Quinones, G.A., Moore, T.I., Nicholes, K., Lee, H., Kim, S., Sun, L., Jeon, N.L. and Stephan, J.P., 2013, Application of a new wall-less plate technology to complex multistep cell-based investigations using suspension cells. *Blood* 121, e25-33.
- Sasso, L.A., Johnston, I.H., Zheng, M., Gupte, R.K., Undar, A. and Zahn, J.D., 2012, Automated microfluidic processing platform for multiplexed magnetic bead immunoassays. *Microfluid Nanofluidics* 13, 603-612.

- Staples, E., Ingram, R.J., Atherton, J.C. and Robinson, K., 2013, Optimising the quantification of cytokines present at low concentrations in small human mucosal tissue samples using Luminex assays. *J Immunol Methods* 394, 1-9.
- Stenzen, J.A. and Poschenrieder, A.J., 2015, Bioanalytical chemistry of cytokines--a review. *Anal Chim Acta* 853, 95-115.
- Tsuji, N., Suzuki, K., Kasuga-Aoki, H., Isobe, T., Arakawa, T. and Matsumoto, Y., 2003, Mice intranasally immunized with a recombinant 16-kilodalton antigen from roundworm *Ascaris* parasites are protected against larval migration of *Ascaris suum*. *Infect Immun* 71, 5314-23.
- Wei, Y., Gadaria-Rathod, N., Epstein, S. and Asbell, P., 2013, Tear cytokine profile as a noninvasive biomarker of inflammation for ocular surface diseases: standard operating procedures. *Invest Ophthalmol Vis Sci* 54, 8327-36.
- Wing, A.C., Hygino, J., Ferreira, T.B., Kasahara, T.M., Barros, P.O., Sacramento, P.M., Andrade, R.M., Camargo, S., Rueda, F., Alves-Leon, S.V., Vasconcelos, C.C., Alvarenga, R. and Bento, C.A., 2016, Interleukin-17- and interleukin-22-secreting myelin-specific CD4(+) T cells resistant to corticoids are related with active brain lesions in multiple sclerosis patients. *Immunology* 147, 212-20.



CHAPTER 3

Location and Expression Kinetics of Tc24 in Different Life Stages of *Trypanosoma Cruzi*

Leroy Versteeg,^{1,2,3} Rakesh Adhikari,^{1,2} Cristina Poveda,^{1,2} Maria Jose Villar-Mondragon,^{1,2}
Kathryn M Jones,^{1,2} Peter J Hotez,^{1,2,4} Maria Elena Bottazzi,^{1,2,4} Edwin Tijhaar,³ Jeroen Pollet^{1,2}

¹ Department of Pediatrics, National School of Tropical Medicine, Baylor College of Medicine,
One Baylor Plaza, Houston, Texas, United States of America,

² Texas Children's Hospital Center for Vaccine Development, Baylor College of Medicine, Houston,
Texas, United States of America,

³ Cell Biology and Immunology Group, Wageningen University, Wageningen, The Netherlands,

⁴ Department of Biology, Baylor University, Waco, Texas, United States of America

Manuscript published in PLOS Neglected Tropical Diseases 15, no. 9 (September 3, 2021).

■ <https://doi.org/10.1371/journal.pntd.0009689>

ABSTRACT

Tc24-C4, a modified recombinant flagellar calcium-binding protein of *Trypanosoma cruzi*, is under development as a therapeutic subunit vaccine candidate to prevent or delay progression of chronic Chagasic cardiomyopathy. When combined with Toll-like receptor agonists, Tc24-C4 immunization reduces parasitemia, parasites in cardiac tissue, and cardiac fibrosis and inflammation in animal models. To support further research on the vaccine candidate and its mechanism of action, murine monoclonal antibodies (mAbs) against Tc24-C4 were generated. Here, we report new findings made with mAb Tc24-C4/884 that detects Tc24WT and Tc24-C4, as well as native Tc24 in *T. cruzi* on ELISA, western blots, and different imaging techniques. Surprisingly, detection of Tc24 by Tc24-C/884 in fixed *T. cruzi* trypomastigotes required permeabilization of the parasite, revealing that Tc24 is not exposed on the surface of *T. cruzi*, making a direct role of antibodies in the induced protection after Tc24-C4 immunization less likely. We further observed that after immunostaining *T. cruzi* infected cells with mAb Tc24-C4/884, the expression of Tc24 decreases significantly when *T. cruzi* trypomastigotes enter host cells and transform into amastigotes. However, Tc24 is then upregulated in association with parasite flagellar growth linked to re-transformation into the trypomastigote form, prior to host cellular escape. These observations are discussed in the context of potential mechanisms of vaccine immunity.

3.1 INTRODUCTION

Chagas disease is a neglected tropical disease caused by the protozoan *Trypanosoma cruzi*. Approximately 6–8 million people are infected, with the highest prevalence in Latin America. [1] From individuals who become chronically infected with the disease, 30–40% develop cardiomyopathy, arrhythmias, and megaviscera. [2] There are only two anti-trypanosomal drugs, nifurtimox and benznidazole, which are licensed to treat Chagas disease. Because both drugs have severe adverse side effects and exhibit low efficacy in the chronic phase of infection, there is an urgent need for alternative, complementary or more effective treatments. [3,4] Prophylactic and therapeutic vaccines are considered potential immune strategies to control *T. cruzi* infection and/or progression of disease.[5]

A promising vaccine candidate antigen is the 24-kDa flagellar calcium-binding protein (FCaBP) of *Trypanosoma cruzi*. FCaBP is an immunogenic protein that is located in the flagellum of *T. cruzi*. Low levels of polymorphism of the gene encoding FCaBP suggest that this can be an effective vaccine candidate against multiple *T. cruzi* strains. [6] FCaBP comprises four EF-hand calcium-binding motifs, of which the third and fourth are able to bind calcium. [7] While the exact function is yet to be elucidated, it is hypothesized that FCaBP acts as a calcium sensor and is involved in regulating Ca²⁺ dependent cell signaling pathways in the parasite. [8] In the Chagas vaccine field FCaBP, in this field commonly known as Tc24, [9] was shown to have immunoprotective properties in a BALB/c acute lethal mouse model. [10] The antigen was further explored as a DNA vaccine in dogs, [11] and as a recombinant protein nanoparticle vaccine in mice. [12] A suitable platform was developed for the large scale production of recombinant Tc24 [13] and Tc24 was selected as one of the key antigens under consideration for a human therapeutic Chagas disease vaccine [14] supported by multiple preclinical studies with a recombinant Tc24 vaccine. [12,15,16]

As previously published, to prevent aggregation of recombinant Tc24 during the production process, four cysteine codons were replaced by serine codons. The resulting antigen, designated Tc24-C4, showed less aggregation while secondary structure and immunogenicity was not altered, and the production process was found to be suitable for technology transfer in preparation for its production under current Good Manufacturing Practices (cGMP). [17,18] It was further shown in a mouse model that vaccination with Tc24-C4 improved the efficacy of benznidazole treatment and reduced myocarditis and fibrosis during acute *T. cruzi* infection. [19,20]

T. cruzi has a complex life cycle that involves two different stages of the parasite during infection in the vertebrate host. [21] Trypomastigotes are the parasitic stage with developed flagella that can be found in the bloodstream and in the extracellular spaces of the host. Once trypomastigotes enter a host cell, they discard their long flagella, and transform to the amastigote stage and a truncated flagellum remains. [22,23] They then divide several times by binary fission. Following division, the amastigotes transform back to trypomastigotes,

exhibiting continuous flagellar movement. Eventually, the host cell wall ruptures and trypomastigotes are released in the extracellular space and bloodstream. [24]

Revealing the location and the presence of Tc24 in the different stages of the *T. cruzi* parasites may help explain the protection mechanism of Tc24 as a vaccine antigen. It was previously hypothesized that Tc24 is located in the flagellar pocket of the parasite, [13,25,26] which would suggest that antibodies could bind to the trypomastigotes, possibly preventing cell invasion. However, in the broader field of trypanosomatids research, it has been shown that flagellar calcium-binding proteins are typically localized intracellularly on the flagellar membrane, [27,28] specifically anchoring to the inner leaflet of the flagellar membrane. [7,29–31] In this case, a humoral response would unlikely be effective to prevent a trypomastigote from infecting host cells. Here, we developed and described anew monoclonal antibody (mAb) with specificity to Tc24-C4, which was used to localize native Tc24 in *T. cruzi* by different microscopic techniques. Fluorescence confocal microscopy and imaging flow cytometry revealed that Tc24 is expressed intracellularly, and is stage-specific amplified in association with a transformation from the amastigote to trypomastigote form and released by cellular rupture. The implications for *T. cruzi* vaccine mechanism are further discussed.

3.2 MATERIALS AND METHODS

Ethics statement

Animal studies were approved by the Institutional Animal Care and Use Committee of Baylor College of Medicine and were performed in strict compliance with The Guide for Care and Use of Laboratory Animals (8th Edition). [32]

T. cruzi strain

T. cruzi MHOM/MX/0000/H1 (H1) strain was used for all experiments. This strain was originally identified in the Yucatan area of Mexico, and is classified as Discrete Typing Unit (DTU) Tc1.[33,34]

Production of Tc24-WT and Tc24-C4

Tc24-WT and Tc24-C4 were produced according to previously published methods. [17] Briefly, DNA coding for Tc24-WT and Tc24-C4 was codon-optimized, chemically synthesized and cloned into the *E. coli* expression vector pET41a and transformed into *E. coli* BL21 (DE3). For the Tc24-C4 construct, all four cysteines in the Tc24-WT sequence were replaced by serine residues. For recombinant protein expression, 10 L of BSM media in a fermentor was inoculated with the transformed *E. coli*. After the media reached the desired cell density, IPTG was added to induce the Tc24-WT expression. After the fermentation, the biomass was collected and

homogenized using an EmulsiFlex C3 (Avestin, Canada) (for Tc24-WT) or EmulsiFlex C55 (Avestin, Canada) (for Tc24-C4). The extracted proteins were further purified using Q Sepharose XL columns and size-exclusion chromatography (SEC) methods.

Preparation of *T. cruzi* lysate

Lysate from *T. cruzi* trypomastigotes and amastigotes was made using a previously published method. [35] The lysate was prepared without any detergents to keep the protein structures stable. To prepare trypomastigotes, VERO cells were infected with *T. cruzi* trypomastigotes at a multiplicity of infection (MOI) of 5 and incubated at 37°C with 5% CO₂. After 5 days, the trypomastigotes were harvested from the culture supernatant. To prepare amastigotes, infected cells were infected for 6 hrs before extracellular (trypomastigote) parasites were removed. Cells were further incubated for an additional 48 hrs, followed by removal from the flask using Accutase (Innovative Cell Technologies, Cat# AT104). Cells were centrifuged for 5 min at 300 x g and resuspended in PBS. To release the intracellular amastigotes, the cells were transferred to a gentleMACS M Tube (Miltenyi Biotech, Cat# 130-093-236) and dissociated using a gentleMACS Octo Dissociator (Miltenyi Biotech) following protocol "Protein_01_01". [36] Afterwards 1.5 mL fractions of the dissociated cell material were loaded onto pre-equilibrated PD10 columns to separate the intracellular amastigotes from cell debris according to previous published methods. [37] Additional PBS was added to the top of the column, while 1mL fractions of eluted material were collected. Following visual assessment under a light microscope, the intracellular amastigote-containing fractions were pooled and pelleted by centrifugation at 3,000 x g for 5min. Two washes of the intracellular amastigotes were performed using centrifugation and resuspension in PBS to remove VERO cell debris.

To create the lysate, purified parasites were disrupted by three freeze/thaw cycles in PBS containing protease inhibitor cocktail (cOmplete ultra-tablets, Roche). Parasite lysate was then sonicated three times for 15 s each and subsequently centrifuged for 30 min at 15,000 x g. The protein concentration of the soluble fraction was determined by using a BCA protein assay kit (ThermoFisher, Cat# 23225). The final *T. cruzi* lysate samples were stored at -80° C until use.

Development of Tc24-C4 specific B-cell hybridoma's

Female BALB/c mice of 6–8 weeks old were immunized three times intraperitoneally (i.p.), two weeks between immunizations, with 100 µg Tc24-C4 +Freund's complete adjuvant as first immunization and 50 µg Tc24-C4 +Freund's incomplete adjuvant for booster immunizations. One week after the third immunization, the mice were bled via retro-orbital sinus puncture and titers were determined by indirect ELISA and western blot. The mouse with the highest serum reactivity in ELISA and western blot was selected to perform the fusion. The mouse received a final i.p. boost with 100 µg of Tc24-C4 and five days after the final boost, mice were humanely euthanized and spleens were harvested. Splenocytes were obtained by grinding the spleen through a steel mesh screen to generate a single-cell suspension. A

fusion between splenocytes from the chosen Tc24-C4 immunized mouse and the mouse SP2/0 myeloma cell line was performed using standard PEG fusion methodology. Newly formed hybridomas from the fusion were plated in ClonaCell Medium D (StemCell Technologies, Inc.), a semi-solid methylcellulose-based selection media, and allowed to grow for twelve days prior to identifying, picking, and transferring individual hybridoma clones to wells of 96-well tissue culture plates using the ClonaCell Easy Pick robot (StemCell Technologies). The hybridomas were grown for three days and supernatants of hybridomas were screened by indirect ELISA for reactivity to Tc24-C4. Those hybridomas showing a strong ELISA reaction were transferred to 24-well tissue culture plates and the supernatants were screened again by ELISA and Western blot for reactivity to Tc24-C4. Hybridoma clone #884 was selected and adapted to IMDM culture medium +15% fetal bovine serum (FBS) and cryopreserved in liquid nitrogen.

Production and purification of Tc24-C4 specific monoclonal antibodies

The B cell hybridoma clone #884 was thawed and seeded at 100,000 cells/mL in 10 cm diameter suspension culture dishes in a volume of 20 mL. Hybridomas were grown for 8–10 days in 15% FBS with ultra-low IgG (ThermoFisher, Cat# 16250078) in IMDM culture media with addition of 2–3 mL new culture media every 3–5 days. Once the viability of the clones became lower than 50%, the culture supernatant containing the secreted antibodies was harvested. The cells were spun down at 300 x g for 5min, and the supernatant was stored at 4° C. A Pellicon XL50 with Ultracel 30 kDa Membrane, Cscreen, 50 cm², and LabScale TFF system was used for concentration of the supernatant and buffer exchange to 20 mM of NaH₂PO₄ +20mM of Na₂HPO₄ solution. The antibodies were then individually purified using HiTrap Protein G HP Columns (GE, Cat#. GE17-0404-01). Approximately 8 mg of mAb Tc24-C4/884 was obtained from 400 mL of culture supernatant.

Enzyme-Linked ImmunoSorbent Assays (ELISAs)

Plates were coated with 100 µL 0.3125 µg/mL recombinant Tc24-C4 or Tc24-WT (produced in *E. coli*) in 1X KPL coating solution (Sera Care, Cat# 5150–0014) and incubated overnight at 4°. For coating of the *T. cruzi* lysate a concentration of 10 µg/mL was used. The next day plates were tapped dry and blocked overnight with 200 µL/well 0.1% BSA in 1x PBS +0.05% Tween-20 (PBST). The next day coating solution was decanted, plates were sealed and stored at -20° until further use. mAb Tc24-C4/884 was added at a starting concentration of 20 µg/ mL and diluted two-fold across. After two hrs, plates were washed 4x with PBST using a plate washer. Goat anti-mouse IgG (H+L) antibodies conjugated with HRP (LSBio, Cat# LS-C55886) were diluted 4000 times in 0.1% BSA in PBST, and subsequently 100 µL was added per well. Plates were incubated for 1 hour. After 1 hour of incubation, the plates were washed 5x with PBST using the plate washer. Next, 100 µL SureBlue TMB substrate (SeraCare, Cat# 5120–0077) was added per well. Plates were developed in the dark at room temperature, and the reaction was stopped after exactly 4 min using 100 µL 1M HCl. The optical density at 450 nm (OD450) was measured using a spectrophotometer (Epoch 2, BioTek).

To determine the isotype of mAb Tc24-C4/884, plates were coated overnight at 4° C with 0.1 µg/mL with the mAbs. The next day plates were tapped dry and blocked overnight with 200 µL/well 0.1% BSA in PBST at 4° C. The following day goat anti-mouse IgG1, IgG2a and IgG2b antibodies conjugated to HRP (LSBio Cat #LS-C346714-1, Cat# LS-C346721-1 and Cat# LS-C346730-1 respectively) were diluted 4,000 times in 0.1% BSA in PBST and 100 µL each antibody was added to another well. After 1-hour incubation, the plates were washed 5x with PBST using the plate washer. SureBlue TMB substrate was removed from 4° C refrigerator and 100 µL was added per well. Plates were developed in the dark, and the reaction was stopped at exactly 4 min using 100 µL 1M HCl. The absorbance at 450 nm was measured using a spectrophotometer (Epoch 2, Biotek).

Western blots and Coomassie Brilliant Blue staining

Reduced and non-reduced Tc24-C4 (0.25 µg), Tc24-WT (0.25 µg) and *T. cruzi* trypomastigote lysate (2 µg) were loaded on 4–12% Bis-Tris gels together with a SeeBlue Plus2 marker (Thermo Fisher Scientific). After running for approximately 2 hrs at 100 V, the gel was transferred to western blots using an iBlot 2 Dry Blotting System (Thermo Fisher Scientific). Western blot was soaked in methanol for one minute and subsequently blocked for 2 hrs with 5% non-fat dry milk in PBST. The western blot was then incubated overnight with 1 µg/mL of mAb Tc24-C4/884 in 1% non-fat dry milk in PBST. After incubation, the Western blot was washed 4 times with PBST followed by 1-hour incubation with 1:5000 diluted goat anti-mouse IgG alkaline phosphatase (KPL, Cat# 0751-1806) in PBST. After incubation, it was washed 4 times with PBST and 1 time with PBS. Finally, immunodetection was performed using BCIP/NBT substrate (VWR, Cat# 50-81-00).

To compare the expression of Tc24 in trypomastigotes to the expression in amastigotes, we loaded Tc24-C4 (0.5 µg), *T. cruzi* trypomastigote lysate (1.5 µg) and *T. cruzi* amastigote lysate (1.5 µg) on two 4–12% Bis-Tris gels as described above. One gel was used for western blotting to detect Tc24 in the lysate samples, the other gel was stained with Coomassie Brilliant Blue to show that equal an amount of trypomastigote and amastigote lysate material was loaded on the gels.

Linear epitope prediction assays

Linear epitope prediction for mAb Tc24-C4/884 was performed using PEPperMAP Linear Epitope Mapping (PEPperPRINT). [38] Briefly, peptides of 15 amino acids length were synthesized, covering the theoretical amino acid sequence of Tc24-C4, including GSGSGG linkers added to the C- and N-terminus. Each peptide had an overlap of 14 amino acids between neighboring peptides. This resulted into 211 unique peptide sequences, which were printed on a microarray plate in duplicate. Control peptide sequences HA (YPYDVPDYAG) and c-Myc (EQKLISEEDL) were also included. The microarray was incubated with 1 or 10 µg/mL Tc24-C4/884 followed by staining with goat anti-mouse IgG (H+L) DyLight 680 and mouse mAb

anti-HA (12CA5) DyLight 800. Plate readout was performed using an LI-COR Odyssey Imaging System at 680 nm (red) and 800 nm (green).

Competitive ELISA

The specificity of Tc24-C4/884 to the epitope TAEAKQR(R) was confirmed using a competitive ELISA. Four different peptides were purchased (GenScript Biotech) which included 1) TAEAKQRR: the expected epitope, 2) PREKTAEAKQRRIEL: the expected epitope with the flanking peptide sequences used in the linear epitope prediction assay (PEPperPRINT), 3) RIRQAIPREKTAEAK: peptide sequence containing the partial expected epitope sequence TAEAK, and 4) PAALFKELDKNGTGS: a randomly selected peptide sequence from Tc24 closer to the C-terminus of the protein. Peptides were serially diluted and pre-incubated with Tc24-C4/884, allowing the peptides to bind to the mAb. The tested molar ratios between peptide: Tc24-C4/884 started at 125:1 and continued in a two-fold dilution fashion until ratio 0.002:1 was reached. After one hour, mAb-peptide samples were transferred to aTc24-C4 coated ELISA plate and samples were incubated for two hrs. Following 4 washes with PBST, bound mAb was detected by goat anti-mouse IgG (H+L) antibodies conjugated with HRP (LSBio, Cat# LS-C55886). After one hour incubation, followed by 5 washes with PBST, SureBlue TMB substrate (SeraCare, Cat# 5120-0077) was used for signal development. After 1M HCl was used to stop the color reaction, the optical density at 450 nm (O.D.450) was measured using a spectrophotometer (Epoch 2, BioTek).

Tc24-C4 protein primary sequence alignment

To check for the conservation of the epitope of mAb Tc24-C4/884 between different *Trypanosoma* species, primary protein sequences of Tc24 were compared to each other. The protein sequence of the flagellar calcium-binding protein (protein entry P07749, UniProt.org) was used to perform a BLAST search to find similar protein sequences. The BLAST result file was screened for the epitope TAEAKQR(R). The protein sequences that contained the epitope were aligned using the Align tool on UniProt.com. FCaBP primary sequences of *T. brucei* and *T. Congolense* were added as a reference in **Supplementary Fig. 4**.

Fluorescence confocal microscopy

T. cruzi trypomastigotes were thawed and resuspended in fixation buffer (BD Biosciences) to fixate parasites, or in fixation/permeabilization buffer (BD Biosciences, Cat# 554714) to fixate and permeabilize parasites. Poly-L-Lysine-coated glass slides were placed in 6-well plates and resuspended trypomastigotes were added to the wells. The plate was then centrifuged for 20 min at 1500 x g at 4° C to coat the trypomastigotes to the glass slides. Then the fix or fix/perm buffer was removed and trypomastigotes were washed 3 times with 2% FBS in PBS (staining buffer) for fixed parasites or 1x perm/wash buffer for fixed/permeabilized parasites. Trypomastigotes were then incubated with either 10 µg/mL mAb Tc24-C4/884,

1:1000 diluted Tc24-C4 polyclonal mouse antisera, or 1:1000 diluted naïve mouse antisera. After 1 hour at 4° C trypomastigotes were washed 3 times followed by an incubation 4° C with 10 µg/mL anti mouse IgG Alexa Fluor 488 antibody. After 1 hour, parasites were washed 4 times with assay buffer and subsequently incubated for 10 min with 1 µM DAPI to stain the nuclei. Finally, after 2 washes with assay buffer glass slides were mounted on microscopy slides and dried overnight before microscopy analysis.

For additional fluorescence confocal microscopy analysis of *T. cruzi* infected cells, VERO cells (ATCC, Cat# CCL-81) and mouse primary cardiac fibroblasts (Cellbiologics, Cat# C576049) were used. VERO cells are commonly used for *in vitro* *T. cruzi* infection studies, [39] and mouse primary cardiac fibroblasts were used since they are a natural cell target for *T. cruzi in vivo*. [40] VERO cells and mouse primary cardiac fibroblasts were grown on a Poly-L-Lysine coated glass slides and infected with *T. cruzi* trypomastigotes at a MOI of 3. After 4 days, cells were fixed and permeabilized with BD fix/perm solution (BD Biosciences) followed by staining steps. For the VERO cells staining of native Tc24 was performed using mAb Tc24-C4/884 followed by goat anti-mouse IgG (H+L) Alexa Fluor 488 as a secondary antibody. DAPI was used to stain the nuclei, and CyTRAK Orange (eBioscience) to stain the DNA and cytoplasm. For the infected mouse primary cardiac fibroblasts, staining of the parasites was performed using an amastigote-specific surface protein (SSP4)-specific mouse IgG1 antibody and a secondary anti-mouse IgG Alexa Fluor 488 antibody. Staining of native Tc24 was performed using a biotinylated mAb Tc24-C4/884 using streptavidin-Alexa Fluor 555 as a secondary antibody. Filamentous actin was stained used phalloidin-iFluor 647, and the nucleus of the cardiac fibroblasts and parasites were stained using DAPI. The sample was analyzed using a Leica SP8 system and an HC PL APO 63x/1.40 oil objective was used. Post-processing of the image was performed using Fiji (ImageJ) and LAS X(Leica).

Imaging flow cytometry

VERO cells were grown in 6-well culture plates and incubated with *T. cruzi* trypomastigotes at a MOI of 3. After 6 hrs the trypomastigotes were washed off, and cells were further incubated at 37° C. At 6 hrs, 12 hrs, 24 hrs, 48 hrs and 96 hrs post infection, cells were removed from the 6-well plate using Accutase (Innovative Cell Technologies, Cat# AT104) and stained for Tc24 and SSP4. Briefly, cells were fixed and permeabilized with BD fix/perm solution (BD Biosciences, Cat# 554714) followed by staining using an amastigote-specific surface protein (SSP4)-specific mouse IgG1 antibody (BEI Resources, Cat# NR-50892) and a secondary anti-mouse IgG Alexa Fluor 488 antibody. Staining of native Tc24 was performed using a biotinylated mAb Tc24-C4/884, using streptavidin-Alexa Fluor 647 as a secondary antibody. Nuclei of the VERO cells were stained using DAPI. Cells were then analyzed using an Amnis ImagestreamX Mark II (Luminex, Austin) and images were analyzed and processed using IDEAS software. To compare the expression of Tc24 and SSP4 between the different time points, threshold masks Threshold(M11, Ch11 Tc24, 60) and Threshold(M02, Ch02 SSP4, 80) were created and used to create features Mean Pixel Threshold (M11, Ch11 Tc24, 60) _Ch11 Tc24

and Mean Pixel Threshold (M02, Ch02 SSP4, 80)_Ch02 SSP4. The Mean Fluorescent Intensity (MFI) of the complete populations was calculated and plotted in a histogram.

3.3 RESULTS

Characterization of Tc24-C4/884 monoclonal antibody

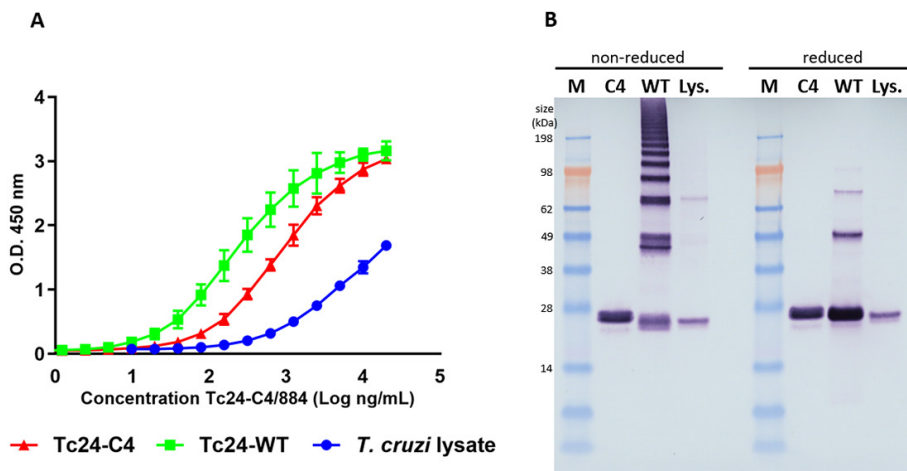
mAb Tc24-C4/884 binds to recombinant Tc24-C4 and Tc24-WT, and native Tc24 in *T. cruzi* lysate.

To evaluate whether the monoclonal antibody Tc24-C4/884 generated against recombinant Tc24-C4 protein and produced in *E. coli* could recognize recombinant Tc24-C4, Tc24-WT as well as native Tc24, different concentrations of the monoclonal antibody were used in an ELISA assay with plates coated with either Tc24-C4, Tc24-WT or a *T. cruzi* lysate (as a source of native Tc24).

The results in **Fig. 1A** show that mAb Tc24-C4/884 detects Tc24-C4, Tc24-WT and native Tc24 in *T. cruzi* lysate. The results show the highest OD450 signal for Tc24-WT and Tc24-C4, and a lower OD450 signal for *T. cruzi* lysate. The signal for Tc24-WT is higher than for Tc24-C4, which might be caused by disulfide bond aggregation of Tc24-WT, leading to more coated molecules in the plate. The relatively low OD450 signal in ELISA on the *T. cruzi* lysate compared to the signals obtained with a coat of Tc24-C4 or Tc24-WT, can be explained by the low concentration of native Tc24 in *T. cruzi* lysate and the excess of other *T. cruzi* proteins in the lysate that compete with Tc24 for binding to the ELISA plate. Therefore, the amount of native Tc24 that actually bound to the ELISA plates is likely to be much lower than for the purified recombinant proteins Tc24-C4 and Tc24-WT. Furthermore, antibody isotyping of mAb Tc24-C4/884 revealed that this antibody is part of the IgG1 class (see **Supplementary Fig. 1**).

After examining the binding of mAb Tc24-C4/884 against different versions of Tc24 on ELISA, it was further evaluated whether the mAb could detect different forms of Tc24 on a western blot. In **Fig. 1B** it was shown that Tc24-C4/884 detects SDS-denatured reduced and non-reduced Tc24-C4, Tc24-WT and native Tc24 from *T. cruzi* lysate. Since there was no significant difference observed in band intensity between denatured reduced and non-reduced versions of Tc24, this suggests that Tc24-C4/884 is specific against a linear epitope.

The difference in S-S bridge formation between Tc24-WT and Tc24-C4 can be observed in these western blots. Tc24-WT has four free cysteines, which allow the protein to form multimers under non-reducing conditions, as seen for Tc24-WT (**Fig. 1B**). As previously published, when the four free cysteines are removed in Tc24-C4, the multimerization of the protein is strongly reduced. [17]

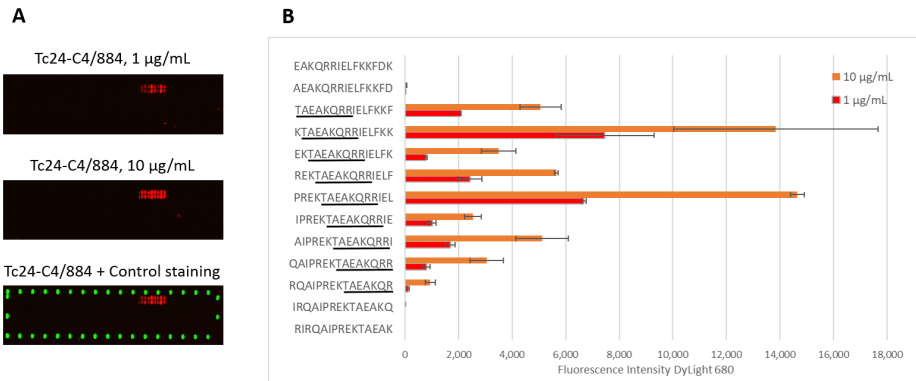


■ **Figure 1. mAb Tc24-C4/884 recognizes Tc24-C4, Tc24-WT and native Tc24 in *T. cruzi* lysate in ELISA and Western blot.** A) The binding of mAb Tc24-C4/884 to Tc24-C4 (red), Tc24-WT (green) and native Tc24 in *T. cruzi* trypomastigote lysate (blue) by ELISA. All ELISAs were performed in triplicate. B) Detection of reduced and nonreduced Tc24-C4, Tc24-WT and native Tc24 by Tc24-C4/884 by western blot. M: SeeBlue Plus3 marker. C4: Tc24-C4. WT: Tc24-WT, Lys.: *T. cruzi* trypomastigote lysate.

Monoclonal antibody Tc24-C4/884 binds to linear epitope sequence TAEAKQR(R)

To investigate to which linear epitope mAb Tc24-C4/884 binds, linear epitope mapping was performed. Peptides of 15 amino acids lengths, with 14 amino acid sequence overlap between successive peptides, were printed on a microarray and binding of mAb Tc24-C4/884 at two different concentrations was tested. A positive signal was observed in a set of adjacent peptides at both concentrations, with stronger signals at the higher concentration of 10 $\mu\text{g}/\text{mL}$ (**Fig. 2**). **Fig. 2B** shows the measured fluorescence intensity started to increase strongly at peptide sequence TAEKQRRIELFKKF and reduced again at sequence RQAIPREKTAEAKQR. These results show that the consensus sequence of the linear epitope recognized by Tc24-C4/884 is TAEAKQR(R). The last arginine (R) is not elemental, but the signal is significantly weaker without the last arginine added. The variation in binding of Tc24-C4/884 with the different peptides that all contain the consensus epitope can be due to structural (e.g. linear or helical) differences between the whole 15-mer peptides. Additionally, a competitive ELISA confirmed that the specificity of Tc24-C4/884 is the epitope TAEAKQR(R), since pre-incubation of Tc24-C4/884 with peptides containing the TAEAKQR(R) sequence reduced the binding of the mAb to Tc24-coated ELISA plates, while peptides without the epitope sequence or with just that partial sequence did not (**Supplementary Fig. 2**). The consensus sequence recognized by mAb Tc24-C4/884 maps in an alpha helix on the first EF-hand of Tc24 (**Supplementary Fig. 3**).

To predict whether the epitope TAEAKQR(R) is conserved within different *Trypanosoma* species and if Tc24-C4/884 will probably detect those proteins, amino acid sequences from different *Trypanosoma* spp. were downloaded from the UniProt protein sequence database and aligned. This alignment shows that epitope TAEAKQR(R) is conserved within *T. cruzi* Cl Brener, *T. cruzi* Dm28c, *T. cruzi* marinkellei and *T. rangeli* (Supplementary Fig. 4).

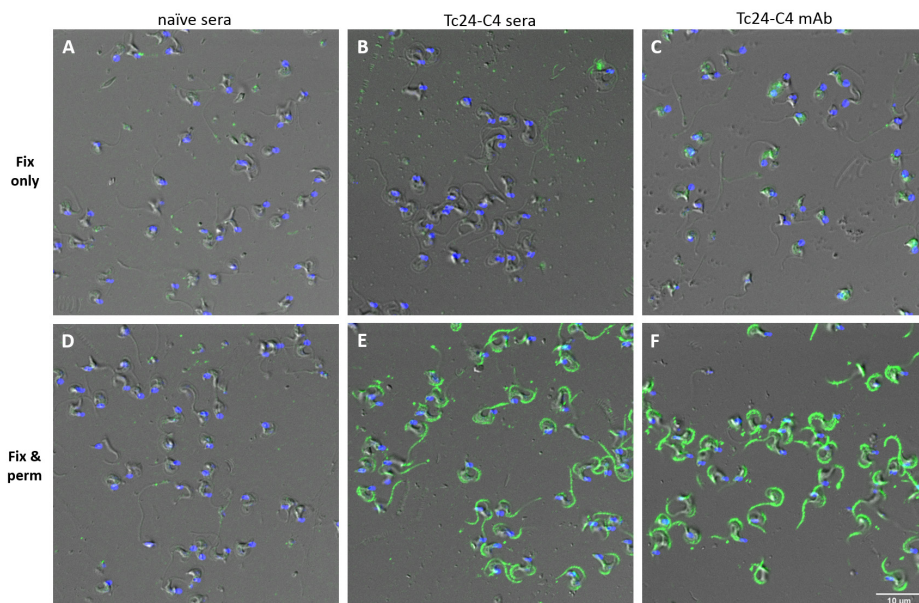


■ **Figure 2. Linear epitope mapping of monoclonal antibody Tc24-C4/884.** A) Scan of the microarray showing an increased intensity of DyLight 680 (red) in a stretch of adjacent peptide sequences when 1 and 10 µg/mL Tc24-C4/884 was used. DyLight 800 was used as a positive control (green). B) Measured median Fluorescent Intensity of DyLight 680 plotted with their corresponding peptide sequences. The consensus sequence is underlined in black.

Studying the location and presence of Tc24 in *T. cruzi* parasites using the characterized antibody

Tc24 is not exposed on the surface of *T. cruzi* trypomastigotes

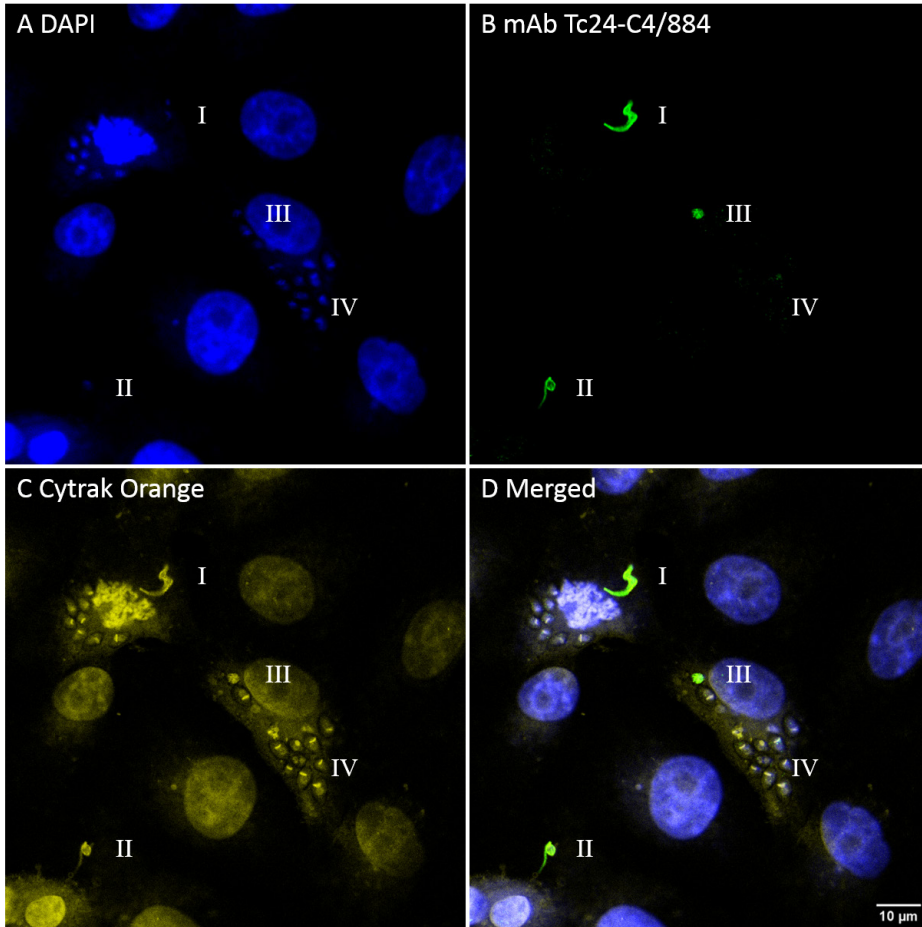
To understand more about the location of Tc24 in *T. cruzi*, including the exposure of Tc24 on the surface, it was examined whether Tc24-C4/884 and Tc24-C4 antisera from Tc24-C4 –vaccinated mice could detect Tc24 in fixed only or in fixed and permeabilized *T. cruzi* trypomastigotes. **Fig. 3** shows that mAb Tc24-C4/884 binds strongly to *T. cruzi* trypomastigotes, which have been fixed and permeabilized, but not to trypomastigotes that were fixed but not permeabilized (fixed-only). Also, when trypomastigotes were incubated with pooled polyclonal anti-Tc24-C4 mice sera, IgG antibodies were only able to bind when trypomastigotes were fixed and permeabilized as well, confirming the observations seen with the mAb Tc24-C4/884. Pooled sera from naïve mice did not show IgG binding to fixed-only or fixed and permeabilized trypomastigotes. These results show that Tc24 is not exposed on the surface of the trypomastigotes but is present intracellularly.



■ **Figure 3. Antibodies recognizing Tc24 binds strongly to fixed and permeabilized *T. cruzi* trypomastigotes but not to fixed only trypomastigotes.** Staining of fixed-only (fix only) or fixed and permeabilized (fix & perm) *T. cruzi* trypomastigotes with mAb Tc24-C4/884, Tc24-C4 polyclonal antisera or naïve sera followed by staining with goat anti-mouse IgG (H+L) Alexa Fluor 488 (green). After staining DAPI (blue) was used to stain the nucleus and kinetoplast. Pixel size of images: 60 nm x60 nm.

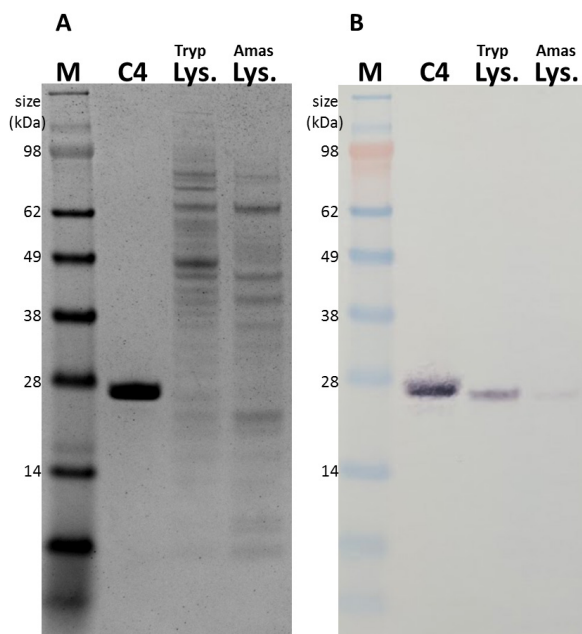
Tc24 is not equally expressed in different stages of *T. cruzi*

After it was found that mAb Tc24-C4/884 can detect native Tc24 in fixed and permeabilized trypomastigotes, it was tested if Tc24 could be detected during all stages of the infection of host cells. Green Monkey Kidney cells (VERO) were infected with *T. cruzi* trypomastigotes. After 72 hrs cells were fixed and permeabilized, and Tc24 was detected using Tc24-C4/884. **Fig. 4B** shows the staining of mAb Tc24-C4/884 to Tc24 in the *T. cruzi* parasites at different stages of the parasite's life cycle, indicated by "I", "II", "III" and "IV". The morphological features of "I" indicates that this is either an extracellular or a recently internalized trypomastigote. The parasite stage labeled with "II" has a round shape with reduced flagella, indicating it has been internalized for a longer period of time and is transforming to the amastigote stage. The single parasite labeled with "III" has lost its flagella and has the morphology of an amastigote but still lacks the disk-shaped kinetoplast which is distinct for replicating amastigotes. [41] The nuclear stain (DAPI) in **Fig. 4A** and the DNA and cytoplasmic stain (CyTRAK Orange) in **Fig. 4C** clearly shows the presence of replicating amastigotes in the cytoplasm of the infected cell (labeled "IV"), and is confirmed by the presence of disk-shaped kinetoplasts. However, these amastigotes do not show staining with mAb Tc24-C4/884 (**Fig. 4B**). This strongly suggests that Tc24 expression is strongly reduced in amastigotes after multiple divisions inside a host cell.



■ **Figure 4. Fluorescence confocal microscopy images of VERO cells infected with *T. cruzi* showing the different Tc24 expression in parasitic stages.** Different transitions between trypomastigote and amastigote can be observed in I, II, III and IV. I: trypomastigote, II: trypomastigote with reduced flagella, III: complete transition to amastigote, IV: amastigotes with multiple divisions. A) In blue, DAPI nuclear stain. B) In green, mAb Tc24-C4/884 stained by goat anti-mouse IgG (H+L) Alexa Fluor 488. C) In yellow, CyTRAK Orange DNA and cytoplasmic stain. D) Merged image of A-C. Pixel size of images: 102 nm x102 nm.

To confirm the observation that Tc24 is not equally expressed in trypomastigotes and amastigotes, Tc24 in *T. cruzi* lysate from trypomastigotes and amastigotes was analyzed using western blotting (**Fig. 5B**). Detection of Tc24 by mAb Tc24-C4/884 revealed a much stronger Tc24 band in the trypomastigote than in the amastigote lysate, further proving that Tc24 expression is reduced in amastigotes compared to trypomastigotes. A second SDS-PAGE gel loaded with the same samples was stained with Coomassie Brilliant Blue to show that a similar amount of lysate was loaded on the gels (**Fig. 5A**).



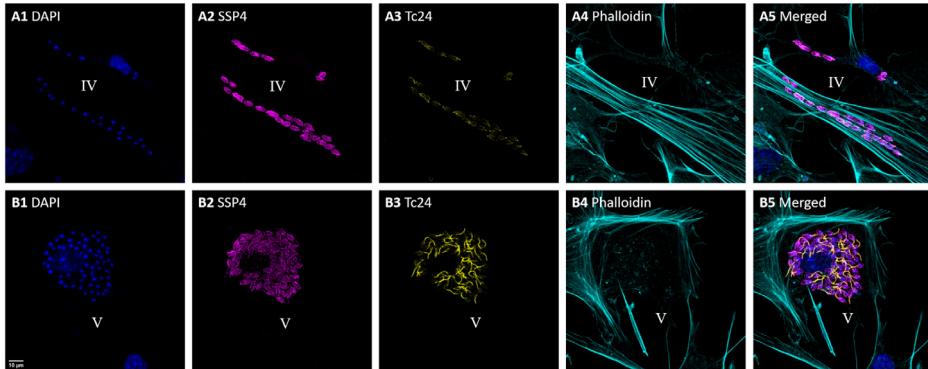
■ **Figure 5.** Expression of Tc24 is reduced in *T. cruzi* amastigotes compared to *T. cruzi* trypomastigotes. A) Coomassie Brilliant blue stained SDS-PAGE gel, and B) Detection of Tc24 in reduced Tc24-C4, *T. cruzi* trypomastigote lysate and *T. cruzi* amastigote lysate by Tc24-C4/884 using western blot M: SeeBlue Plus3 marker. C4: Tc24-C4. Tryp Lys.: *T. cruzi* trypomastigote lysate. Amas Lys.: *T. cruzi* amastigote lysate.

Expression of Tc24 is reduced in amastigotes but restores during transformation to trypomastigote stage.

To further explore the expression of Tc24 during infection of *T. cruzi* in host cells, mouse primary cardiac fibroblasts were infected with *T. cruzi* and after 72 hrs the presence of Tc24 and an amastigote surface protein (SSP4) were examined. SSP4 is specific to the amastigote stage, and is not expressed in trypomastigotes. [42] In **Fig. 6** two different stages of infected cardiac fibroblasts are shown. **Fig. 6A1–A5** are all from two infected cardiac fibroblasts and represent stage “IV” (like in **Fig. 4**), and **Fig. 6B1–B5** show one infected cardiac fibroblast which represents stage “V”. Stage “V” represents *T. cruzi* amastigotes that are transforming back to trypomastigotes. Besides DAPI, Tc24 and SSP4, filamentous actin detection by Phalloidin was used to visualize the boundaries of each cell (**Fig. 6A4–B4**). Merged images of all channels were given in **Fig. 6A5–B5**.

Fig. 6A1 shows *T. cruzi* amastigotes spread in the cytoplasm of the cell, while in the event of **Fig. 6B1** they are more concentrated around the nucleus. The cardiac fibroblast in **Fig. 6B1** is infected with more *T. cruzi* amastigotes than the cardiac fibroblasts in **Fig. 6A1**, suggesting the fibroblast has been infected for a longer period of time. Interestingly, while the

T. cruzi amastigotes stained very strongly for SSP4 (**Fig. 6A2**), they stained dim and diffuse for Tc24 (**Fig. 6A3**). On the contrary, in infected cardiac fibroblasts with many *T. cruzi* amastigotes, indicating continued replication of the parasite, much more expression of Tc24 was observed (**Fig. 6B3**). Here *T. cruzi* amastigotes showed overall more staining for Tc24, and staining was even more increased around a structure that appears to be the growth of new flagella. This suggests that these amastigotes are transforming back to trypomastigotes.

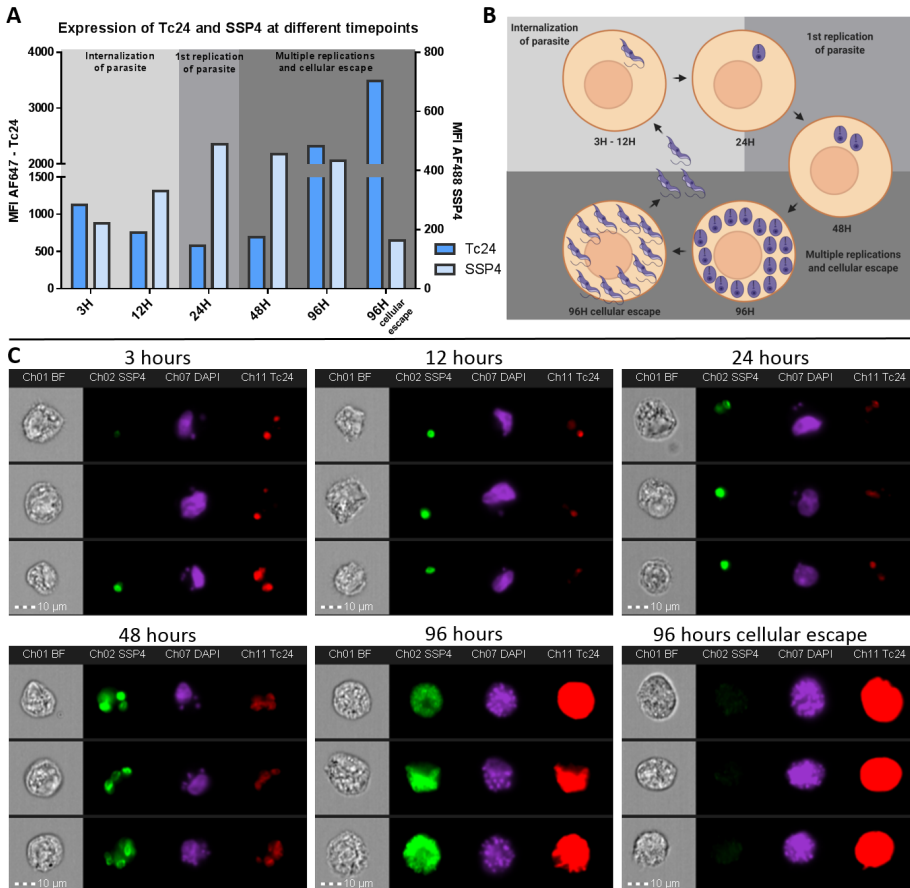


■ **Figure 6. Fluorescence confocal microscopy images of mouse primary cardiac fibroblasts infected with *T. cruzi* show the return of Tc24 expression.** Two images were acquired that represent different stages of infection. In A1-A5 two infected cardiac fibroblasts can be seen with only approximately 20 and 6 amastigotes inside, representing stage IV: amastigotes with several (2–4) divisions. In B1-B5 an infected cardiac fibroblast can be seen hosting 60 amastigotes inside, which represents stage V: transformation from amastigote back to trypomastigote. 1) In blue, DAPI nuclear stain. 2) In magenta, detection of the amastigote specific protein SSP-4 using a specific IgG1 antibody followed by staining with anti-IgG1 Alexa Fluor 488. 3) In yellow, detection of Tc24 using biotinylated Tc24-C4/884 followed by staining with streptavidin–Alexa Fluor 555. 4) In cyan, filamentous actin stained with Phalloidin iFluor 647. 5) Merged image of 1–4. Pixel size of images: 120 nm x120 nm.

The number of *T. cruzi* amastigotes in an infected cell increases quickly, since amastigotes divide by binary fission approximately every 18–25 hrs. [43] Therefore, it can be expected that the cardiac fibroblasts in **Fig. 6A** was infected recently and only 2–4 amastigote divisions have happened. The stage of the amastigotes in **Fig. 6A** is therefore very similar to the amastigotes at stage “IV” in **Fig. 4**. In **Fig. 6B**, the cardiac fibroblasts contained many amastigotes, so there the cell has been infected for a longer period of time and considerably more divisions took place. When an infected cell contains many amastigotes, indicative of continued divisions, the amastigotes start transforming back to trypomastigotes, which involves the growth of flagella (**Fig. 6B3** and **6B5**). **Fig. 6B** shows the moment when the transformation from amastigote of trypomastigote stage happens. This can be considered stage “V”, which comes after stage “IV” shown in **Fig. 4**.

Expression of Tc24 is reduced after cellular invasion but increases prior to cellular escape

To further confirm and quantify the expression of Tc24 and SSP4 by *T. cruzi* trypomastigotes and amastigotes, VERO cells were examined using imaging flow cytometry at different time points after infection. The cells were infected with *T. cruzi* trypomastigotes and subsequently fixed and stained for Tc24 and SSP4 at 3 hrs, 6 hrs, 12 hrs, 24 hrs, 48 hrs and 96 hrs after the start of the infection. In the first 24 hrs after infection, the expression of Tc24 is reduced while the expression of SSP4 is increased (**Fig. 7A**). Expression of Tc24 is reduced at 12 hrs and 24 hrs compared to 3hrs, the period in which the trypomastigote is transforming to an amastigote (**Fig. 7B**). In the same period, SSP4 expression is increased when the trypomastigote transforms to an amastigote (**Fig. 7A** and **7C**). At 48 hrs, the amastigotes remain expressing similar levels of Tc24 and SSP4 as at 24 hrs. However, at 96 hrs there is a large increase in Tc24 expression, which is thought to be caused by the transformation of amastigotes back to trypomastigotes. Due to the combination of the high expression of Tc24 and the large amount of trypomastigotes in a host cell at this time point, individual parasites can no longer be distinguished and the whole host cell shows up red (**Fig. 7C**, 96 hrs). Expression of SSP4 remained similar as at 48 hrs. Interestingly, by inspecting the individual images of the 96 hrs time point, a small subpopulation was identified which showed very high expression of Tc24 and no expression of SSP4. A manual gate was drawn (**Supplementary Fig. 5**) to identify this subpopulation (**Fig. 7A** and **7C**, 96 hrs cellular escape). The fully reduced expression of SSP4 suggests that these parasites are completely transformed from amastigotes to trypomastigotes and will escape the host cell shortly. Since the host cell will rupture when the trypomastigotes escape, this population of cells will not accumulate over time. Overall, this dataset showed that Tc24 expression in *T. cruzi* after cellular invasion decreases but expression increased again when the parasite transforms back to the trypomastigote stage.



■ **Figure 7** Imaging Flow Cytometry reveals a change in expression of Tc24 and SSP4 during different infection timepoints of *T. cruzi*. VERO cells were infected with *T. cruzi* and 3 hrs, 6 hrs, 12 hrs, 24 hrs, 48 hrs and 96 hrs after start infection fixed and permeabilized. VERO cells were then stained for Tc24 and SSP4. Nuclei were stained using DAPI. A) The MFI of Tc24 and SSP4 from the total population of *T. cruzi*-infected VERO cells was plotted in a histogram. The left y-axis depicts the MFI for Tc24 and the right y-axis depicts the MFI for SSP4. B) A schematic representation of the transformation of *T. cruzi* trypomastigotes to amastigotes and back to trypomastigotes in the VERO host cell is shown. Prepared using Biorender. com C) Image gallery of three events of each infection time point representing the complete population. Presented are brightfield, Tc24 (red), SSP4 (green) and DAPI (magenta).

3.4 DISCUSSION

We provide new information on the cell biology and localization of a flagellar calcium-binding protein called Tc24, and we discuss the underlying mechanisms linked to protective immunity for this antigen or its derivatives. The Tc24-C4/884 antibody recognizes a linear epitope in Tc24 and showed a strong affinity to recombinant Tc24-C4, Tc24-WT and native

Tc24 in *T. cruzi* lysate. This epitope is located on the first EF-hand of the Tc24 protein. Since only the third and the fourth EF-hand bind calcium, [7] it is anticipated that binding of Tc24-C4/884 does not interfere with calcium-binding by Tc24. Tc24 shows low diversity in protein sequence within *T. cruzi* stains. [6] By comparing the flagellar calcium-binding protein amino acid sequences of different *Trypanosoma spp*, it was found that the epitope recognized by Tc24-C4/884 is conserved between *T. cruzi* Cl Brener, *T. cruzi* Dm28c, *T. cruzi* marinkellei and *T. rangeli*. The conservation of the Tc24-C4/884 epitope in these *Trypanosoma* species suggests that the antibody can be used to detect Tc24 in these species, but the antibody cannot be used for a *T. cruzi*-specific serological test due to cross-reactivity with Tc24 from *T. rangeli*.

Images made by fluorescence confocal microscopy revealed that mAb Tc24-C4/884 as well as polyclonal Tc24-C4 antisera were only able to bind to Tc24 when *T. cruzi* trypomastigotes were fixed and permeabilized, but not when trypomastigotes were fixed only. This indicates that Tc24 is not exposed on the outside of trypomastigotes. This finding was somewhat surprising since it has previously been suggested that Tc24 is located on the outside of the *T. cruzi* parasites and antibodies against Tc24 can be generated that show complement-mediated trypanolytic activity. [10,44] The data supporting these suggestions in these manuscripts was however limiting; it was not tested whether antibodies against Tc24 could bind Tc24 without permeabilizing the parasite, and complement-mediated trypanolytic activity by Tc24 antisera was not shown to be significantly different from controls. [10] Additionally, our microscopic analysis clearly shows that Tc24 is located along the whole flagellar membrane of trypomastigotes and is not concentrated in just the flagellar pocket, as earlier described. [13,18,26] Consequently, if Tc24 is not exposed on the surface of the parasite, antibody-mediated immune responses against Tc24 cannot opsonize the parasites and will not induce antibody-mediated phagocytosis nor anti-Tc24 mediated complement lysis of *T. cruzi*.

In-line with the current *T. cruzi* literature, [29] our images acquired by fluorescence confocal microscopy confirmed that Tc24 is expressed differentially during the trypomastigote and amastigote stages. Tc24 expression was high in the flagellum of trypomastigotes and reduced in replicating amastigotes, and this observation was confirmed by the much stronger detection of Tc24 in trypomastigote than amastigote lysate by western blotting. To add further, we used imaging flow cytometry analysis to quantify the decrease of Tc24 expression after *T. cruzi* infects a host cell and the increase at later time points in infection and cellular escape. While expression of Tc24 was found to decrease right after cellular invasion, SSP4 (surface marker of the amastigote stage) expression increased. Of note, in **Fig. 4B** it looks like there is no expression of Tc24 in the replicating amastigotes (stage IV), while there is a dim Tc24 signal visible at 24 hrs and 48 hrs in **Fig. 7**. This difference can be explained by the difference in imaging techniques. While confocal microscopy used for Fig. 4 only collected emitted light from a thin slice of the sample, in imaging flow cytometry emitted light was collected from the complete depth of the sample. Therefore, more emitted light was acquired in the imaging flow cytometry experiment of **Fig. 7** and a dim signal of Tc24 could be observed at 24 hrs and 48 hrs post infection, while this was for these time points not visible by confocal microscopy (**Fig. 4**).

T. cruzi flagellar-derived proteins like Tc24 are of special interest as vaccine candidates, since flagellar proteins are among the first proteins presented on the MHC of infected cells to CD8+ T cells. [22] Upon host cell entry, the *T. cruzi* flagellum reduces by approximately 90%, [45] gets “discarded” and flagellar-derived proteins become available to MHC class I processing and subsequent presentation to CD8+ T cells. Furthermore, the strain-invariant nature and abundance in flagellar-stage parasites of flagellar proteins make them very interesting vaccine targets. Immunization with paraflagellar rod proteins for example, have already shown to be protective against *T. cruzi* infection in mice through a T cell-dependent manner, while antiparaflagellar rod antibodies do not bind to live parasites. [46–48] Similarly, a cytotoxic T cell (CTL) response might be the key mechanism of Tc24 as a vaccine candidate, allowing for very effective elimination of *T. cruzi*-infected host cells and clear infection. [49,50]

The location and expression of Tc24 in *T. cruzi* trypomastigotes and amastigotes has direct consequences for Tc24 vaccine-induced protection. Due to the absence of Tc24 on the surface of the parasite, antibody-mediated immune response against Tc24 will not be able to opsonize the parasites and therefore also not to induce antibody mediated lysis or phagocytosis of the parasites. Our study does not entirely rule out the possibility of effector humoral immunity to Tc24. Because *T. cruzi* secretes Tc24 as soluble proteins and in extracellular vesicles (EVs), [51,52] it has been suggested that Tc24 might be involved in immune-evasion strategies or interference with host signaling pathways. [52,53] By inducing Tc24-specific antibodies in the host, the function of soluble Tc24 and Tc24 in EVs might be disabled and the protective immune response improved. Additionally, soluble Tc24 and Tc24 in EVs could be targeted by inducing catalytic antibodies that degrade Tc24 through IgM-mediated hydrolysis. [16,25] While it is yet to be elucidated what the effect of secreted Tc24 is on the host immune response, it is clear that Tc24 is an important target for cell-mediated immunity. Indeed, since *T. cruzi* is an intracellular pathogen most of its lifecycle, it is thought that a cytotoxic T cell response might be very effective in eliminating *T. cruzi*-infected host cell and clear the infection. [49,50] This is supported by the observation that antibody mediated depletion of CD8+ T cells in a *T. cruzi* infection model, resulted in increased susceptibility towards infection. [54] Villanueva-Lizama *et al.* showed that PBMC-derived effector memory T cells from chagasic patients produced IFN- γ and proliferated strongly after invitro re-stimulation with Tc24. [55] Immunization with Tc24 vaccine candidates showed robust cell-mediated immune responses that had protective effects in mouse models. [12,15,19] These studies suggest that a cell-mediated immune response is crucial to eliminate *T. cruzi* and clear the infection. Therefore, we hypothesized that the observed vaccine-induced protection by Tc24 immunization is mostly driven by cell-mediated immunity and Tc24 specific antibodies are unlikely to be directly involved in killing of *T. cruzi* parasites.

In summary, the results obtained using the monoclonal antibody Tc24-C4/884 yielded new insights into the location of the Tc24 protein and the expression of Tc24 in different stages of *Trypanosoma cruzi*. We found that Tc24 is not exposed on the surface of *T. cruzi* parasites. It is regulated in association with parasite-life cycle stages and transformation

between amastigote and trypomastigote stages. Opportunities for Tc24-C4 vaccine-induced immunity include antibodies to soluble or EV bound Tc24 that might interfere with a possible immune-evasive function of Tc24, as well as a Th1-mediated response and CTLs clearing *T. cruzi*-infected cells.

Author Contributions

Conceptualization: LV, KMJ, PJH, MEB, ET and JP. Data curation: LV, RA, CP, MJV and JP. Formal analysis: LV, ET and JP. Funding acquisition: PJH and MEB. Investigation: LV, MEB, ET and JP. Methodology: LV, KMJ, PJH, ET and JP. Supervision: KMJ, PJH, MEB, ET and JP. Validation: LV, ET and JP. Visualization: LV. Writing –original draft: LV. Writing –review & editing: LV, RA, CP, MJV, KMJ, PJH, MEB, ET and JP.

(Leroy Versteeg, Rakesh Adhikari, Cristina Poveda, Maria Jose Villar-Mondragon, Kathryn M. Jones, Peter J. Hotez, Maria Elena Bottazzi, Edwin Tijhaar, Jeroen Pollet)

Acknowledgments

We would kindly thank Dr. Kristyn Hoffmann for providing technical assistance with working with the mouse primary cardiac fibroblasts. We would like to thank Dr. Alexandre Carisey from the Texas Children's Hospital William T. Shearer Center for Human Immunobiology for his expert assistance in the confocal microscopy experiments. We would kindly thank Dr. Amal El-Mabhouth for providing technical assistance with analyzing the imaging flow cytometry dataset. We especially like to mention Kurt Christensen and Karen Moberg for their support in the development of the mAbs.

Supplementary Material

Supplementary data from this manuscript can be found online at <https://doi.org/10.1371/journal.pntd.0009689>

3.5 REFERENCES

1. Rassi A, Rassi A, Marin-Neto JA. Chagas disease. *Lancet Lond Engl*. 2010; 375: 1388–1402. [https://doi.org/10.1016/S0140-6736\(10\)60061-X](https://doi.org/10.1016/S0140-6736(10)60061-X)
2. Perez-Molina JA, Molina I. Chagas disease. *Lancet Lond Engl*. 2018; 391: 82–94. [https://doi.org/10.1016/S0140-6736\(17\)31612-4](https://doi.org/10.1016/S0140-6736(17)31612-4)
3. Coura JR, Castro SL de. A Critical Review on Chagas Disease Chemotherapy. *Mem Inst Oswaldo Cruz*. 2002; 97: 3–24. <https://doi.org/10.1590/s0074-02762002000100001> PMID: 11992141
4. Morillo CA, Marin-Neto JA, Avezum A, Sosa-Estani S, Rassi A, Rosas F, et al. Randomized Trial of Benznidazole for Chronic Chagas' Cardiomyopathy. *N Engl J Med*. 2015; 373: 1295–1306. <https://doi.org/10.1056/NEJMoa1507574> PMID: 26323937
5. Bivona AE, Alberti AS, Cerny N, Trinitario SN, Malchiodi EL. Chagas disease vaccine design: the search for an efficient *Trypanosoma cruzi* immune-mediated control. *Biochim Biophys Acta Mol Basis Dis*. 2020; 1866: 165658. <https://doi.org/10.1016/j.bbadis.2019.165658> PMID: 31904415
6. Arnal A, Villanueva-Lizama L, Teh-Poot C, Herrera C, Dumonteil E. Extent of polymorphism and selection pressure on the *Trypanosoma cruzi* vaccine candidate antigen Tc24. *Evol Appl*. n/a. <https://doi.org/10.1111/eva.13068> PMID: 33294015
7. Buchanan KT, Ames JB, Asfaw SH, Wingard JN, Olson CL, Campana PT, et al. A Flagellum-specific Calcium Sensor. *JBiol Chem*. 2005; 280: 40104–40111. <https://doi.org/10.1074/jbc.M505777200> PMID: 16148003
8. Landfear SM, Ignatushchenko M. The flagellum and flagellar pocket of trypanosomatids. *Mol Biochem Parasitol*. 2001; 115: 1–17. [https://doi.org/10.1016/s0166-6851\(01\)00262-6](https://doi.org/10.1016/s0166-6851(01)00262-6) PMID: 11377735
9. Krautz GM, Peterson JD, Godsel LM, Krettli AU, Engman DM. Human antibody responses to *Trypanosoma cruzi* 70-kD heat-shock proteins. *Am J Trop Med Hyg*. 1998; 58: 137–143. <https://doi.org/10.4269/ajtmh.1998.58.137> PMID: 9502594
10. Taibi A, Plumas-Marty B, Guevara-Espinoza A, Schöneck R, Pessoa H, Loyens M, et al. *Trypanosoma cruzi*: immunity-induced in mice and rats by trypomastigote excretory-secretory antigens and identification of a peptide sequence containing a T cell epitope with protective activity. *J Immunol*. 1993; 151: 2676–2689. PMID: 7689612
11. Quijano-Hernandez IA, Bolio-González ME, Rodríguez-Buenfil JC, Ramírez-Sierra MJ, Dumonteil E. Therapeutic DNA vaccine against *Trypanosoma cruzi* infection in dogs. *Ann NY Acad Sci*. 2008; 1149: 343–346. <https://doi.org/10.1196/annals.1428.098> PMID: 19120245
12. Barry MA, Wang Q, Jones KM, Heffernan MJ, Buhaya MH, Beaumier CM, et al. A therapeutic nanoparticle vaccine against *Trypanosoma cruzi* in a BALB/c mouse model of Chagas disease. *Hum Vaccines Immunother*. 2016; 12: 976–987. <https://doi.org/10.1080/21645515.2015.1119346> PMID: 26890466
13. Martínez-Campos V, Martínez-Vega P, Ramírez-Sierra MJ, Rosado-Vallado M, Seid CA, Hudspeth EM, et al. Expression, purification, immunogenicity, and protective efficacy of a recombinant Tc24 antigen as a vaccine against *Trypanosoma cruzi* infection in mice. *Vaccine*. 2015; 33: 4505–4512. <https://doi.org/10.1016/j.vaccine.2015.07.017> PMID: 26192358
14. Dumonteil E, Bottazzi ME, Zhan B, Heffernan MJ, Jones K, Valenzuela JG, et al. Accelerating the development of a therapeutic vaccine for human Chagas disease: rationale and prospects. *Expert Rev Vaccines*. 2012; 11: 1043–1055. <https://doi.org/10.1586/erv.12.85> PMID: 23151163

15. Barry MA, Versteeg L, Wang Q, Pollet J, Zhan B, Gusovsky F, et al. A therapeutic vaccine prototype induces protective immunity and reduces cardiac fibrosis in a mouse model of chronic *Trypanosoma cruzi* infection. *PLoS Negl Trop Dis*. 2019; 13: e0007413. <https://doi.org/10.1371/journal.pntd.0007413> PMID: 31145733
16. Gunter SM, Versteeg L, Jones KM, Keegan BP, Strych U, Bottazzi ME, et al. Covalent vaccination with *Trypanosoma cruzi* Tc24 induces catalytic antibody production. *Parasite Immunol*. 2018; 40: e12585. <https://doi.org/10.1111/pim.12585> PMID: 30132929
17. Seid CA, Jones KM, Pollet J, Keegan B, Hudspeth E, Hammond M, et al. Cysteine mutagenesis improves the production without abrogating antigenicity of a recombinant protein vaccine candidate for human chagas disease. *Hum Vaccines Immunother*. 2017; 13: 621–633. <https://doi.org/10.1080/21645515.2016.1242540> PMID: 27737611
18. Biter AB, Weltje S, Hudspeth EM, Seid CA, McAtee CP, Chen W-H, et al. Characterization and Stability of *Trypanosoma cruzi* 24-C4 (Tc24-C4), a Candidate Antigen for a Therapeutic Vaccine Against Chagas Disease. *J Pharm Sci*. 2018; 107: 1468–1473. <https://doi.org/10.1016/j.xphs.2017.12.014> PMID: 29274820
19. Jones K, Versteeg L, Damania A, Keegan B, Kendricks A, Pollet J, et al. Vaccine-linked chemotherapy improves benznidazole efficacy for acute Chagas disease. *Infect Immun*. 2018; IAI.00876-17. <https://doi.org/10.1128/IAI.00876-17> PMID: 29311242
20. Cruz-Chan JV, Villanueva-Lizama LE, Versteeg L, Damania A, Villar MJ, Gonzalez-Lopez C, et al. Vaccine-linked chemotherapy induces IL-17 production and reduces cardiac pathology during acute *Trypanosoma cruzi* infection. *Sci Rep*. 2021; 11: 3222. <https://doi.org/10.1038/s41598-021-82930-w> PMID: 33547365
21. Onyekwelu KC. Life Cycle of *Trypanosoma cruzi* in the Invertebrate and the Vertebrate Hosts. *Biol Em Trypanosoma Cruziem*. 2019 [cited 9Jun 2020]. <https://doi.org/10.5772/intechopen.84639>
22. Kurup SP, Tarleton RL. The *Trypanosoma cruzi* Flagellum Is Discarded via Asymmetric Cell Division following Invasion and Provides Early Targets for Protective CD8+ T Cells. *Cell Host Microbe*. 2014; 16: 439–449. <https://doi.org/10.1016/j.chom.2014.09.003> PMID: 25299330
23. Arias-del-Angel JA, Santana-Solano J, Santilla nM, Manning-Cela RG. Motility patterns of *Trypanosoma cruzi* trypomastigotes correlate with the efficiency of parasite invasion invitro. *Sci Rep*. 2020; 10: 15894. <https://doi.org/10.1038/s41598-020-72604-4> PMID: 32985548
24. Teixeira DE, Benchimol M, Crepaldi PH, Souza W de. Interactive Multimedia to Teach the Life Cycle of *Trypanosoma cruzi*, the Causative Agent of Chagas Disease. *PLoS Negl Trop Dis*. 2012; 6:e1749. <https://doi.org/10.1371/journal.pntd.0001749> PMID: 22970330
25. Gunter SM, Jones KM, Zhan B, Essigmann HT, Murray KO, Garcia MN, et al. Identification and Characterization of the *Trypanosoma cruzi* B-cell Superantigen Tc24. *Am J Trop Med Hyg*. 2016; 94: 114–121. <https://doi.org/10.4269/ajtmh.15-0438> PMID: 26598565
26. Filardy AA, Guimarães-Pinto K, Nunes MP, Zukeram K, Fliess L, Pereira L, et al. Human Kinetoplastid Protozoan Infections: Where Are We Going Next? *Front Immunol*. 2018;9. <https://doi.org/10.3389/fimmu.2018.00009> PMID: 29403493
27. Eyford BA, Kaufman L, Salama -Alber O, Loveless B, Pope ME, Burke RD, et al. Characterization of Calflagin, a Flagellar Calcium-Binding Protein from *Trypanosoma congolense*. *PLoS Negl Trop Dis*. 2016; 10: e0004510. <https://doi.org/10.1371/journal.pntd.0004510> PMID: 27055052
28. Xu X, Olson CL, Engman DM, Ames JB. NMR structure of the calflagin Tb24 flagellar calcium binding protein of *Trypanosoma brucei*. *Protein Sci Publ Protein Soc*. 2012; 21: 1942–1947. <https://doi.org/10.1002/pro.2167> PMID: 23011904

29. Godsel LM, Engman DM. Flagellar protein localization mediated by acalcium-myristoyl/palmitoyl switch mechanism. *EMBO J*. 1999; 18: 2057–2065. <https://doi.org/10.1093/emboj/18.8.2057> PMID: 10205160
30. Wingard JN, Ladner J, Vanarotti M, Fisher AJ, Robinson H, Buchanan KT, et al. Structural Insights into Membrane Targeting by the Flagellar Calcium-binding Protein (FCaBP), a Myristoylated and Palmitoylated Calcium Sensor in *Trypanosoma cruzi*. *J Biol Chem*. 2008; 283: 23388–23396. <https://doi.org/10.1074/jbc.M803178200> PMID: 18559337
31. Engman DM, Krause KH, Blumin JH, Kim KS, Kirchoff LV, Donelson JE. A novel flagellar Ca²⁺-binding protein in trypanosomes. *J Biol Chem*. 1989; 264: 18627–18631. PMID: 2681200
32. National Research Council (US) Committee for the Update of the Guide for the Care and Use of Laboratory Animals. *Guide for the Care and Use of Laboratory Animals*. 8th ed. Washington(DC): National Academies Press (US); 2011. Available: <http://www.ncbi.nlm.nih.gov/books/NBK54050/> <https://doi.org/10.1258/la.2010.010031> PMID: 21123303
33. Martinez I, Nogueira B, Martinez-Hernandez F, Espinoza B. Microsatellite and Mini-Exon Analysis of Mexican Human DTU I *Trypanosoma cruzi* Strains and Their Susceptibility to Nifurtimox and Benznidazole. *Vector Borne Zoonotic Dis*. 2013; 13: 181–187. <https://doi.org/10.1089/vbz.2012.1072> PMID: 23421890
34. Ruiz-Sanchez R, Leon MP de, Matta V, Reyes PA, Lopez R, Jay D, et al. *Trypanosoma cruzi* isolates from Mexican and Guatemalan acute and chronic chagasic cardiopathy patients belong to *Trypanosoma cruzi* I. *Mem Inst Oswaldo Cruz*. 2005; 100: 281–283. <https://doi.org/10.1590/s007402762005000300012> PMID: 16113869
35. Villanueva-Lizama LE, Cruz-Chan JV, Versteeg L, Teh-Poot CF, Hoffman K, Kendrick A, et al. TLR4 agonist protects against *Trypanosoma cruzi* acute lethal infection by decreasing cardiac parasite burdens. *Parasite Immunol*. 2020; 42: e12769. <https://doi.org/10.1111/pim.12769> PMID: 32592180
36. Marques AF, Nakayasu E, Almeida IC. Purification of extracellular and intracellular amastigotes of *Trypanosoma cruzi* from mammalian host-infected cells. 8Nov 2011 [cited 16 May 2021]. <https://doi.org/10.1038/protex.2011.265>
37. Dumoulin PC, Burleigh BA. Methods for the Investigation of *Trypanosoma cruzi* Amastigote Proliferation in Mammalian Host Cells. In: Michels PAM, Ginger ML, Zilberstein D, editors. *Trypanosomatids: Methods and Protocols*. New York, NY: Springer US; 2020. pp. 535–554. https://doi.org/10.1007/9781-0716-0294-2_32 PMID: 32221941
38. Linear Epitope Mapping. In: PEPperPRINT [Internet]. 15 Jul 2019 [cited 6 Jun 2020]. Available: <https://www.pepperprint.com/applications/linear-epitope-mapping/>
39. Duran-Rehbein GA, Vargas-Zambrano JC, Cue llar A, Puerta CJ, Gonzalez JM. Mammalian cellular culture models of *Trypanosoma cruzi* infection: a review of the published literature. *Parasite*. 2014; 21. <https://doi.org/10.1051/parasite/2014022> PMID: 24836940
40. Hoffman Kristyn A., Reynolds Corey, Bottazzi Maria Elena, Hotez Peter, Jones Kathryn. Improved Biomarker and Imaging Analysis for Characterizing Progressive Cardiac Fibrosis in a Mouse Model of Chronic Chagasic Cardiomyopathy. *J Am Heart Assoc*. 2019; 8:e01336 5. <https://doi.org/10.1161/JAHA.119.013365> PMID: 31718442
41. Cavalcanti DP, Shimada MK, Probst CM, Souto-Padron TCBS, de Souza W, Goldenberg S, et al. Expression and subcellular localization of kinetoplast-associated proteins in the different developmental stages of *Trypanosoma cruzi*. *BMC Microbiol*. 2009; 9:120. <https://doi.org/10.1186/1471-2180-9-120> PMID: 19497120

42. Moran-Utrera Y, Lopez-Monteon A, Rosales-Encina JL, Mendez-Bolaina E, Ramos-Ligonio A. *Trypanosoma cruzi* SSP4 Amastigote Protein Induces Expression of Immunoregulatory and Immunosuppressive Molecules in Peripheral Blood Mononuclear Cells. *J Trop Med.* 2012;2012. <https://doi.org/10.1155/2012/829139> PMID: 23209478
43. MacLean LM, Thomas J, Lewis MD, Cotillo I, Gray DW, De Rycker M. Development of *Trypanosoma cruzi* in vitro assays to identify compounds suitable for progression in Chagas' disease drug discovery. *PLoS Negl Trop Dis.* 2018;12. <https://doi.org/10.1371/journal.pntd.0006612> PMID: 30001347
44. Krautz GM, Kissinger JC, Krettli AU. The Targets of the Lytic Antibody Response against *Trypanosoma cruzi*. *Parasitol Today.* 2000; 16: 31–34. [https://doi.org/10.1016/s0169-4758\(99\)01581-1](https://doi.org/10.1016/s0169-4758(99)01581-1) PMID: 10637586
45. Michailowsky V, Luhrs K, Rocha MOC, Fouts D, Gazzinelli RT, Manning JE. Humoral and Cellular Immune Responses to *Trypanosoma cruzi*-Derived Paraflagellar Rod Proteins in Patients with Chagas' Disease. *Infect Immun.* 2003; 71: 3165–3171. <https://doi.org/10.1128/IAI.71.6.3165-3171.2003> PMID: 12761095
46. Wrightsman RA, Miller MJ, Saborio JL, Manning JE. Pure paraflagellar rod protein protects mice against *Trypanosoma cruzi* infection. *Infect Immun.* 1995; 63: 122–125. <https://doi.org/10.1128/iai.63.1.122125.1995> PMID: 7806347
47. Miller MJ, Wrightsman RA, Stryker GA, Manning JE. Protection of mice against *Trypanosoma cruzi* by immunization with paraflagellar rod proteins requires T cell, but not B cell, function. *J Immunol Baltim Md* 1950. 1997; 158: 5330–5337.
48. Miller MJ, Wrightsman RA, Manning JE. *Trypanosoma cruzi*: protective immunity in mice immunized with paraflagellar rod proteins is associated with a T-helper type 1 response. *Exp Parasitol.* 1996; 84: 156–167. <https://doi.org/10.1006/expr.1996.0101> PMID: 8932765
49. Cardoso MS, Reis-Cunha JL, Bartholomeu DC. Evasion of the Immune Response by *Trypanosoma cruzi* during Acute Infection. *Front Immunol.* 2016;6. <https://doi.org/10.3389/fimmu.2016.00006> PMID: 26834747
50. Tarleton RL. CD8+ T Cells in *Trypanosoma cruzi* Infection. *Semin Immunopathol.* 2015; 37: 233–238. <https://doi.org/10.1007/s00281-015-0481-9> PMID: 25921214
51. Bautista-Lopez NL, Ndao M, Camargo FV, Nara T, Annoura T, Hardie DB, et al. Characterization and Diagnostic Application of *Trypanosoma cruzi* Trypomastigote Excreted-Secreted Antigens Shed in Extracellular Vesicles Released from Infected Mammalian Cells. *J Clin Microbiol.* 2017; 55: 744–758. <https://doi.org/10.1128/JCM.01649-16> PMID: 27974541
52. Bayer-Santos E, Aguilar-Bonavides C, Rodrigues SP, Cordero EM, Marques AF, Varela-Ramirez A, et al. Proteomic analysis of *Trypanosoma cruzi* secretome: characterization of two populations of extracellular vesicles and soluble proteins. *J Proteom eRes.* 2013; 12: 883–897. <https://doi.org/10.1021/pr300947g> PMID: 23214914
53. Marcilla A, Martin-Jaular L, Trelis M, Menezes-Neto Ade, Osuna A, Bernal D, et al. Extracellular vesicles in parasitic diseases. *J Extracell Vesicles.* 2014; 3:25040. <https://doi.org/10.3402/jev.v3.25040> PMID: 25536932
54. Tarleton RL. Depletion of CD8+ T cells increases susceptibility and reverses vaccine-induced immunity in mice infected with *Trypanosoma cruzi*. *J Immunol.* 1990; 144: 717–724. PMID: 2104903
55. Villanueva-Lizama LE, Cruz-Chan JV, Aguilar-Cetina Adel C, Herrera-Sanchez LF, Rodriguez-Perez JM, Rosado-Vallado ME, et al. *Trypanosoma cruzi* vaccine candidate antigens Tc24 and TSA-1 recall memory immune response associated with HLA-A and -B supertypes in Chagasic chronic patients from Mexico. *PLoS Negl Trop Dis.* 2018; 12: e0006240. <https://doi.org/10.1371/journal.pntd.0006240> PMID: 29377898



CHAPTER 4

Enlisting the mRNA Vaccine Platform to Combat Parasitic Infections

Leroy Versteeg^{1,2,3}, Mashal M. Almutairi^{4,5,6}, Peter J. Hotez^{2,7,8,9} and Jeroen Pollet^{1,2}

¹ Departments of Pediatrics, National School of Tropical Medicine, Baylor College of Medicine, One Baylor Plaza, BCM113, Houston, TX 77030, USA

² Texas Children's Hospital Center for Vaccine Development, Baylor College of Medicine, 1102 Bates Street, Houston, TX 77030, USA; hotez@bcm.edu

³ Cell Biology and Immunology Group, Wageningen University & Research, De Elst 1, 6708 WD Wageningen, The Netherlands

⁴ Prince Naif Health Research Center, King Saud University, Riyadh 11451, Saudi Arabia; mmalmutairi@KSU.EDU.SA

⁵ Department of Pharmacology and Toxicology, College of Pharmacy, King Saud University, Riyadh 11451, Saudi Arabia

⁶ Vaccines and Biologics Research Unit, College of Pharmacy, King Saud University, Riyadh 11451, Saudi Arabia

⁷ Departments of Pediatrics and Molecular Virology & Microbiology, National School of Tropical Medicine, Baylor College of Medicine, One Baylor Plaza, BCM113, Houston, TX 77030, USA

⁸ Hagler Institute for Advanced Study at Texas A&M University, College Station, TX 77843, USA

⁹ Department of Biology, Baylor University, Waco, TX 76798, USA

Manuscript published in *Vaccines* 7, no. 4 (December 2019): 122.

■ <https://doi.org/10.3390/vaccines7040122>

ABSTRACT

Despite medical progress, more than a billion people still suffer daily from parasitic infections. Vaccination is recognized as one of the most sustainable options to control parasitic diseases. However, the development of protective and therapeutic vaccines against tropical parasites has proven to be exceptionally challenging for both scientific and economic reasons. For certain parasitic diseases, traditional vaccine platforms are not well-suited, due to the complexity of the parasite life cycles and the parasite's ability to evade the human immune system. An effective anti-parasite vaccine platform needs to have the ability to develop and test novel candidate antigens fast and at high-throughput; it further needs to allow for multivalent combinations and must evoke a strong and well-defined immune response. Anti-parasitic vaccines need to be safe and economically attractive, especially in the world's low- and middle-income countries. This review evaluates the potential of in vitro transcribed mRNA vaccines as a new class of preventive and therapeutic vaccine technologies for parasitic infections.

Keywords: messenger RNA; multivalent vaccines; CD8+ T cells; neglected tropical diseases

4.1 INTRODUCTION

A Pressing Need for Vaccines Against Parasitic Diseases

Over the last few decades, vaccines have eliminated and reduced numerous infectious diseases. In 1980, smallpox became the first infectious disease to be eradicated thanks to an effective vaccine [1]. Polio cases have been declining since the WHO Global Polio Eradication initiative started in 1988, and cases are at a record low number. As a result, polio is now almost eradicated [2]. Other diseases, like measles, diphtheria, tetanus, rubella, and mumps, have seen a significant reduction in incidence and mortality since the introduction of vaccines [3].

In contrast to the public health gains from vaccinating children against virus and bacterial agents of disease, so far, human parasitic infectious diseases remain a major burden and have largely resisted successful vaccine development efforts. Soil-transmitted helminths and schistosomes are thought to affect as much as a quarter of the world's population [4]. Protozoa that infect humans can cause severe disease (malaria and kinetoplastid infections, including Chagas disease, leishmaniasis, sleeping sickness) [5]. Shown in **Table 1** are some of the most important human parasitic diseases and their disease burden in terms of global prevalence, disability-adjusted life years (DALYs), and deaths, as recently estimated by the Global Burden of Disease Study (2017), an initiative of the Institute of Health Metrics and Evaluation (IHME) and the Gates Foundation. Altogether, it is estimated that nearly two billion people worldwide are infected with at least one (neglected) tropical parasitic disease, while many of these same individuals are “poly-parasitized” with multiple parasitic diseases [6]. Their health impact is substantial. Malaria is a leading cause of death in resource-poor nations, especially in sub-Saharan Africa, while other parasitic diseases exert their adverse health effects by causing profound disability as measured in DALYs [7]. Still another effect is that the disabling features of these parasitic infections often translate to reduced economic productivity so that they actually thwart economic achievements and gains [8]. Finally, it can be noted that while neglected parasitic infections dominate in resource-poor countries, there is increasing evidence for their high prevalence rates among poor and indigenous populations living in wealthier countries, including the United States, Europe, and Australia, a phenomenon sometimes referred to as “blue marble health” [9].

While for all parasitic infections listed in **Table 1** specific treatment options like antihelminthic, antitrypanosomal, and other antiparasitic drugs are available, there are often issues preventing their successful application in endemic regions, such as severe side-effects, low-efficacy, drug-resistance, and reinfection. Nonetheless, the mainstay of parasitic disease control globally has relied on large-scale mass treatment programs and allied measures. A package of essential anti-parasitic medicines now reaches more than one billion people annually for the treatment of soil-transmitted helminth infections, schistosomiasis, lymphatic filariasis, and onchocerciasis. In the case of lymphatic filariasis and onchocerciasis, this approach may lead to the elimination of these diseases as a public health program in the

coming decade, with additional or collateral benefits for additional neglected infections, including scabies [11]. However, for hookworm infection and schistosomiasis, there is an expectation that additional control tools, such as vaccines, will be required in order to effect elimination efforts [12,13]. Similarly, for malaria, tremendous gains have been achieved through the administration of antimalarial drugs and insecticide-treated bed nets, but a vaccine will still be required to go the last mile for this ancient scourge. We urgently need a new generation of vaccines for high-prevalence parasitic infections, such as malaria, leishmaniasis, Chagas disease, hookworm infection, and schistosomiasis [14]. However, there are only a handful of licensed vaccines against parasites available and, with the exception of the malaria vaccine, Mosquirix (RTS, S), which was approved by the European Medicine Agency (EMA) in 2015 and is just now being introduced in three African nations [15], all are for veterinary applications [16]. If parasitic infections cause such a large worldwide burden and vaccines can offer a solution, then why are there no vaccines available?

■ **Table 1.** Prevalence, disability-adjusted life years (DALYs), and mortality of the most impactful parasitic diseases in 2017 [10].

Disease/Parasite	Prevalence	DALY's	Deaths
Ascariasis <i>Ascaris lumbricoides</i>	447,008,998	860,833	3206
Trichuriasis <i>Trichuris trichiura</i>	289,617,741	212,664	N/A
Hookworm disease <i>Ancylostoma duodenale</i> and <i>Necator americanus</i>	229,217,130	845,010	N/A
Schistosomiasis <i>Schistosoma spp.</i>	142,788,542	1,431,447	8837
Malaria <i>Plasmodium spp.</i>	136,085,123	45,014,578	619,827
Chagas disease <i>Trypanosoma cruzi</i>	6,196,959	232,143	7853
Leishmaniasis <i>Leishmania sp.</i>	4,130,197	774,211	7527
Sleeping Sickness <i>Trypanosoma brucei</i>	4896	78,990	1364

Why Does Commercial Vaccine Development Steer Clear of Parasitic Infectious Diseases?

The relatively low interest in the commercial development of vaccines for parasitic diseases can be explained by the following factors:

Lack of Knowledge of the Biological Complexity of Parasites

Eukaryotic parasites have large and complex genomes that can challenge the successes of the reverse vaccinology programs now benefiting the development of vaccines to prevent “small genome” bacterial and viral infections. Moreover, many parasites have complex life cycles. Several have developed sophisticated strategies to evade and modulate the host immune system, and sometimes they even exist as different stages within one host [17]. There is often poor knowledge on how the parasite evades the immune system, what the function

of specific parasite proteins is, and what antigens should go into an effective vaccine, yielding a protective immune response.

Parasitic Infections Mainly Impact Poor People in Regions of Low Economic Power

These infections often occur in tropical countries with weak economies. Mostly, the poorest of the poor are affected because they typically live in inadequate conditions with poor hygienic conditions and an increased risk of exposure to insect and other disease vectors [18]. In addition, access to healthcare in these regions is often limited, making the development of anti-parasitic vaccines even more important. When parasitic infections do occur in wealthier countries, they disproportionately affect impoverished or indigenous populations who are often not prioritized by government leaders. The term “antipoverty vaccines” has been invoked to describe neglected parasitic disease vaccines because of their simultaneous impact on both public health and economic development [18]. However, from an investment perspective, the fact that these technologies would primarily benefit the poor has had a chilling effect on the traditional investment community targeting new pharmaceuticals.

Most Parasites Cause Chronic Disease and Disabilities but Do Not Kill the Host

Co-evolution between parasites and their hosts have made them capable of establishing chronic infections that can last for decades [19]. Only malaria is a significant killer. As a result, parasitic infections are either not recognized or underestimated for the severe burden they cause.

Limitations of the Traditional Vaccine Platforms

Because of the complexity of parasitic infections, conventional vaccine platforms, such as live attenuated, killed whole parasite or subunit vaccines, including recombinant protein strategies, may not always be effective. Vaccine development for parasitic infections is often hindered by limitations of production and/or inadequate immune responses [20]. There is also the expense associated with traditional vaccine platforms, which might not be linked to a traditional return on investment [14].

From the bench to the clinic, a multitude of attempts have been made to develop efficacious human vaccines for parasitic diseases. Although many anti-parasitic vaccine candidates showed promising results in preclinical models, they either lacked protective capacity in the field or experienced other issues. For example, while a prophylactic live-attenuated vaccine against leishmaniasis showed great protection, it was discontinued due to safety problems because one vaccinated individual presented primary lesions after vaccination [21,22]. A leading recombinant malaria vaccine candidate, MSP-1⁴², tested in children in Kenya, induced high antibody titers but failed to protect against infection [23,24], while Mosquirix is only partially protective [15]. It was found that malaria parasites altered dendritic cell functionality and weakened their ability to support memory B cell survival.

Enlisting mRNA Vaccine Technology to Control Parasitic Diseases

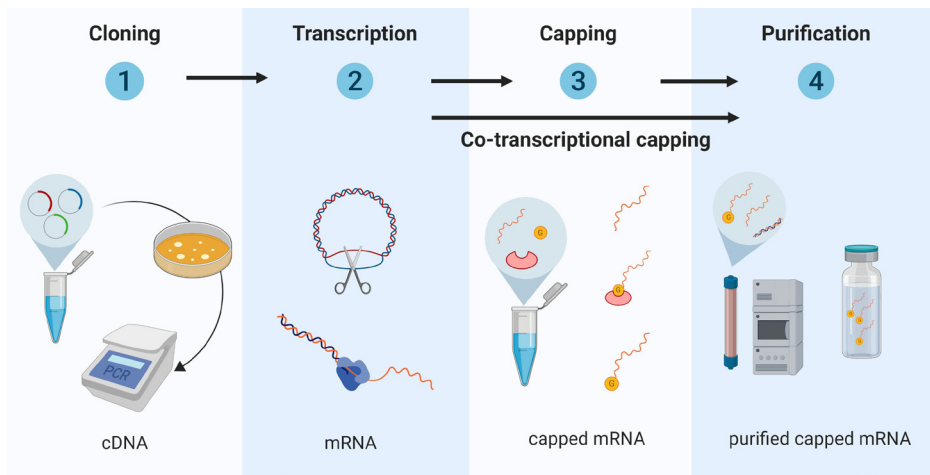
To find a vaccine-based solution for parasitic infections, novel vaccine platform technologies need to be considered. In this review, we discuss the application of in vitro transcribed (IVT) mRNA vaccines for the development of novel vaccines against parasitic infections. We will give a comprehensive introduction of the mRNA vaccine platform with relevance to making mRNA vaccines against parasitic infections. We will discuss the potent immune response of exogenous RNA and highlight the platform's advantages and limitations for each of the critical vaccine development topics (production, formulation, immunology, stability, and safety). Moreover, we will go over some recently published studies on mRNA vaccines for parasitic diseases and briefly introduce our development plan for an mRNA vaccine to protect against Chagas disease. An accompanying manuscript in this special issue (Poveda et al.) [25] reviews the necessary product characterizations for the initial evaluation of mRNA vaccine antigen candidates, and for more detailed information on the mRNA technology beyond the application for parasitic diseases, we refer the reader to a few excellent recent reviews on the topic [26–31].

4.2 MESSENGER RNA VACCINE TECHNOLOGY

Design and Development of In Vitro Transcribed mRNA

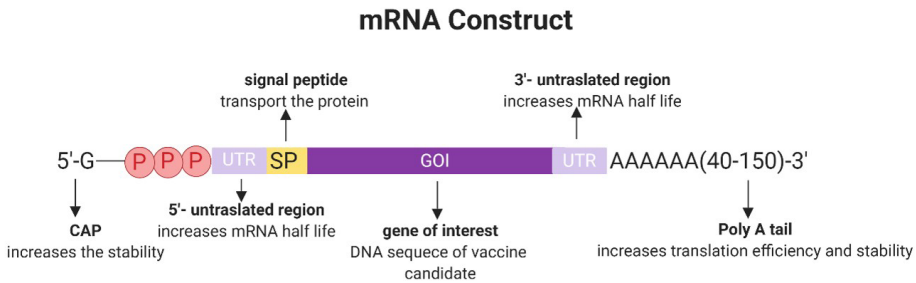
Messenger RNA vaccines apply IVT mRNA as a blueprint to produce vaccine antigens in vivo, in a patient. The translated pathogen-specific antigens will induce a specific immune response, depending on the type of the cell that was transfected, and the immunogenicity of both the mRNA product and the encoded antigen.

In vitro mRNA synthesis usually starts with the cloning of the target antigen into a DNA plasmid and its subsequent linearization, although PCR products and synthetic oligonucleotides can also serve as templates for a cell-free in vitro transcription reaction with recombinant RNA polymerase and nucleoside triphosphates [30]. After transcription, the DNA template is removed using RNase-free DNases, and in order to increase mRNA stability and translation efficiency, the transcriptional product is enzymatically capped. Finally, the mRNA product is purified to remove any remaining DNA template, double-stranded RNA, and other contaminations by HPLC [32,33] (**Figure 1**). The quality of the mRNA transcript is a critical factor, requiring testing for stability, integrity, identity, purity, and homogeneity, as is testing for the desired innate immune response prior to animal testing [25].



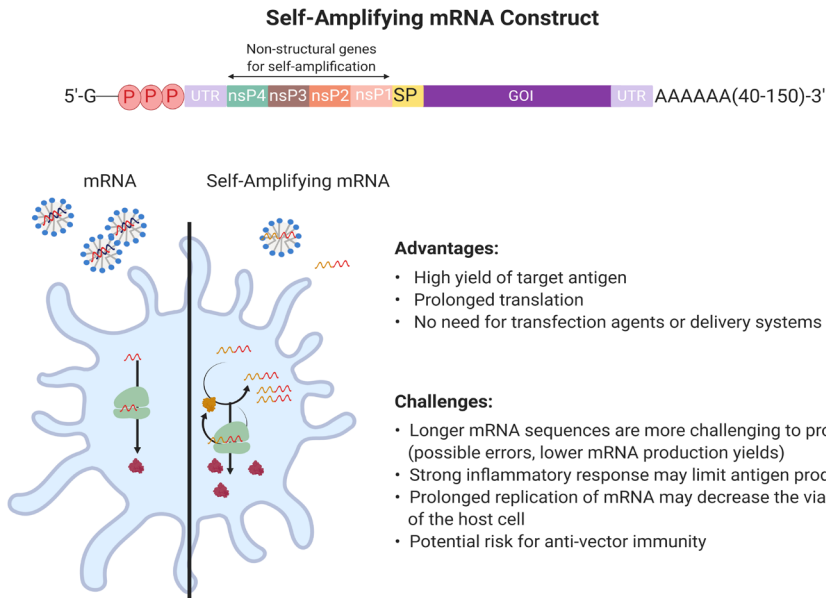
■ **Figure 1.** Messenger RNA production steps: (1) DNA construct is cloned in *Escherichia coli* (*E. coli*) bacteria, then purified and amplified; (2) linearized DNA constructs are transcribed; (3) transcripts are either capped during transcription or capped post-transcription; and (4) purified by chromatography.

Typically, IVT mRNA is comprised of a protein-encoding open reading frame (ORF) flanked by two untranslated regions (UTRs), to support translation (**Figure 2**). A signal peptide (SP) may be added to the ORF to facilitate the secretion of the encoded vaccine antigen candidate. The transcript should further contain a 3' poly(A) tail to improve intracellular stability and translational efficiency. It has been shown that while an increase in poly(A) tail length generally enhances the efficiency of polysome formation, leading to improved protein expression [31], there appears to be an optimal length of 120 and 150 nucleotides [34]. At the 5' end, the RNA is capped with 7-methyl-guanosine triphosphate (m7G) to protect against RNases [35,36]. Because of the presence of two free 3'-OH on both guanine moieties of the cap structure, approximately one-third of the mRNAs have a cap incorporated in the reverse orientation. These reverse cap structures bind poorly to eIF4E, the cap-binding protein, and therefore decrease translational efficiency [35]. In order to solve the problem, anti-reverse cap analogs (ARCAs) have been developed. ARCAs have only one 3'-OH group, which inhibits the incorporation in the reverse orientation seen with cap analogs. Further improvement of the capping efficiency was made by CleanCap[®], a co-transcriptional capping method. CleanCap[®] yields a naturally occurring Cap1 structure, which results in an increased mRNA transcription efficiency compared with ARCA cap analogs [37].



■ **Figure 2.** A typical mRNA construct with supporting untranslated regions, poly(A) tail, and an optional signal peptide sequence attached to the coding sequence.

Multiple groups have developed self-replicating or replicon mRNA vaccine products in order to make mRNA transfection more efficient [38,39]. The construction of a self-amplifying mRNA includes non-structural parts of the genome of positive-strand viruses, e.g., Sindbis virus, Semliki Forest virus, or Venezuelan equine encephalitis virus [40], which encode for their own RNA replication system [41,42] (**Figure 3**). The viral structural protein sequences are replaced with the sequence of the antigen of interest. This mRNA platform has the capability of self-replication through the synthesis of an RNA-dependent RNA polymerase complex, leading to multiple copies of the antigen-encoding mRNA and higher levels of the heterologous target antigen. In a specific study on mRNA vaccines against influenza, self-amplifying mRNA vaccines produced high antibody titers *in vivo* after injecting only 50 ng mRNA, an amount that is 40 times lower than that used for conventional transfections [43]. While delivery and transfection systems can be used to improve the stability and the cellular uptake of self-amplifying RNA, an advantage of self-amplifying mRNA vaccines is that they do not strictly require an additional delivery system. Due to the design of the alphavirus vectors and its larger size (9–11 kilobases), naked self-amplifying RNA is picked up by mostly antigen-presenting cells [38]. It should be noted that the production and purification of longer mRNAs is more challenging and that amplification of mRNA in the host cell can result in a strong inflammatory response, limiting antigen production [44]. In addition, a memory immune response against the replication proteins may limit repeated use, similar to other vaccine platforms applying viral vectors [26].



■ **Figure 3.** Top: self-amplifying mRNA construct: the sequences of four non-structural proteins (nsPs) from an alpha virus are inserted between the first untranslated region (UTR) and the gene of interest (GOI); bottom left: Schematic of a cell transfected with either a regular mRNA vaccine or a self-amplifying mRNA, illustrating the higher yield of translated protein by the self-amplifying construct; bottom right) Advantages and disadvantages of self-amplifying mRNA.

Messenger RNA Delivery

Naked mRNA can be taken up by many cell types, and has been used successfully for *in vivo* transfection after intranodal and intradermal administration [26,28,45]. However, with the exception of self-amplifying mRNA (see the previous section), transfection with naked exogenous mRNA is generally not very effective when administered through classic vaccination routes. From the sequences that are taken up by the cells, only a fraction will get into the cytoplasm and most of the internalized mRNA will get entrapped and degraded in lysosomes. *In vivo* cell transfection can be significantly improved by specific mRNA delivery vehicles and transfection systems [26]. These transfection agents help the exogenous mRNA escape from the endosome into the cytoplasm before being degraded in a lysosome. In addition, the physicochemical properties of the mRNA-transfection complex can influence cellular delivery and organ distribution. Other recent reviews on the mRNA vaccine platform have given a comprehensive and complete overview of current mRNA delivery and transfection systems [43,46]. The most used systems are *in vivo* electroporation, protamine, cationic nanoemulsion, modified dendrimer nanoparticles, cationic liposomes, cationic polysaccharide particles, cationic polymers, and different versions of cationic lipid nanoparticles (LNPs) [26,47], many of which are now commercially available.

The site of injection is equally important. Multiple injection routes have been explored in the literature [26,30], and in clinical trials, mRNA vaccines have been delivered intradermally, intravenously, and intramuscularly (Clinical trial ID NCT02241135, NCT03014089, NCT03076385, NCT03325075, NCT03345043, NCT03382405, NCT03392389, NCT03713086).

Immune Profile of mRNA Vaccines

Recent research has dramatically improved our understanding of immune activation and immune response induced by mRNA and mRNA vaccines [32,48–52]. The innate immune response has been studied extensively because exogenous mRNA triggers the same host cell receptors as triggered by an RNA virus infection [48,53]. It has been demonstrated that mRNA vaccines can elicit strong CD8+ T cells responses, which are essential in targeting intracellular pathogens [51]. Type I interferons, released through innate immune activation, have been shown to be important activation markers in this context. In addition, a potent CD4+ T cell response has proven to be essential in supporting CD8+ T cell activation and the activation of B cells to differentiate into antibody-secreting plasma cells and memory B cells.

Induction of the Innate Immune Response by mRNA Vaccines

Two major groups of RNA sensors have been identified that are involved in activation of the innate immune system upon mRNA recognition, Toll-like receptors (TLRs) and retinoic acid-inducible gene-I (RIG-I) receptors. TLRs recognize viral agents before the infection is even established, while the RIG family is triggered when viral agents are present in the cytoplasm and viral infection has been established [54]. TLR3, TLR7, and TLR8 are all located in the endosomal compartment of antigen-presenting cells (APCs), including dendritic cells, macrophages, and monocytes. TLR3 detects double-stranded RNA and is the only TLR that acts through the NF- κ B pathway, while all the other TLRs act through the MyD88-dependent signaling cascade [55]. TLR7 and TLR8 both detect single-stranded RNA. All pathways lead to the production of type I interferons (IFN α / β) [48]. RIG-I-like receptor family (RLR), located in the cytoplasm, detects single- and double-stranded RNA. LGP2 (Laboratory of Genetics and Physiology 2) is an RLR that has shown to be important in antiviral signaling [56]. MDA5 (melanoma differentiation-associated protein 5) detects double-stranded RNA over 2000 base pairs in size. Upon activation, both RIG-I and MDA5 recruit IPS-1 (alternatively called MAVS), which ultimately activates NF- κ B and IRF3 and the production of type I interferons. In addition, it was recently discovered that the NOD (nucleotide-binding oligomerization domain)-like receptor (NLR) NOD2 is activated by uncapped GU-rich single-strand RNA sequences [57]. Just like RIG-I and MDA5, NOD2 recruits IPS-1 to activate IRF3, which leads to the production of IFN- β .

Type I interferons are important in every aspect of the response against mRNA vaccines because they modulate processes like antigen expression, the function of APCs, and the differentiation of T cells [51]. It has further been shown that the production of type I interferons can be both beneficial and detrimental for mRNA vaccines depending on the timing of the

“signal” [58]. It is thought that TCR signaling needs to happen before IFN signaling, to elicit the desired T cell response (STAT4 will be activated in the T cell), including CD8 T cell differentiation and proliferation to cytotoxic T cells [59–61]. When IFN signaling happens before the TCR is activated, STAT1 is activated and anti-proliferation and pro-apoptosis events are initiated [62,63]. Type I interferons are recognized by T cells through the IFN α / β -receptor (IFNAR) on the cell surface. Thus, while mRNA can be very potent, it can also shut down protein production through a host-cell defense mechanism to keep viruses from producing viral proteins.

It is therefore suggested that the interferon Type I response should be controlled, in order to improve translation of the mRNA vaccine candidate and consequently increase vaccine potency [32,44]. The innate immune response against exogenous mRNA can be minimized by avoiding the activation of TLR receptors, by using highly purified transcripts (complete removal of production byproducts, such as dsRNA and DNA template) and modified nucleosides (replacing uridine for pseudouridine) [25,62]. Another strategy is to suppress the receptors by co-expressing mRNA encoding immune evasion proteins, such as vaccinia virus proteins E3, K3, and B18 [64–66]. These proteins can locally and temporarily suppress PKR and IFN pathway activation and enhance expression of mRNA-encoded genes of interest. This option is especially interesting for self-amplifying mRNA because in vivo replicated mRNA cannot be purified or made with modified nucleosides.

Cellular and Humoral Immune Responses to mRNA Vaccines

Potent T cell responses through mRNA vaccination are achieved by targeting professional APCs, i.e., dendritic cells (DCs). Depending on the route of mRNA processing by the APCs, peptides derived from the mRNA can be presented on the major histocompatibility complex (MHC) class I or II of the APCs (**Figure 4**). In order to establish successful T cell activation and differentiation from naive T cells to effector cells, T cells must receive three different signals. Signal 1 involves the activation of the T cell receptor (TCR) by recognition of a peptide that is presented on the MHC of APCs. Signal 2 involves the binding of co-stimulatory molecules, such as CD80 and CD86, by CD28 on the T cells. Signal 3 consists of secreted cytokines that are then sensed by the T cell. A combination of all these signals will result in T cell activation and differentiation.

The humoral response is orchestrated by circulating antibodies secreted by B cells. It has been demonstrated that antigen-specific antibodies can be induced by mRNA vaccines [67–71]. B cells can be activated by circulating antigens binding to the B cell receptor (BCR). For mRNA vaccines, the availability of extracellular protein for B cell recognition can be enhanced by adding a secretion signal peptide to the RNA sequence or the addition of an MHC class II targeting sequence of a lysosomal or endosomal protein, such as LAMP (lysosomal-associated membrane protein) [72,73], which will allow the transfected cells to secrete the protein. Circulating proteins are taken up by B cells and peptides are displayed on the B cell's MHC class II. T follicular helper (T_{fh}) cells, CD4⁺ T cells that have previously been activated by DCs displaying the MHC-II/peptide combination, will bind to the peptide-

MHC class II of the B cells presenting the same peptide and subsequently release activation signals, including co-stimulatory molecules and cytokines (**Figure 4**). Antigen-experienced Tfh cells trigger the formation and maintenance of germinal centers (GCs) within secondary lymphoid organs, where B cell proliferation, class switching, and differentiation into memory B cells and antibody-secreting plasma cells take place [70]. It was shown in the literature that vaccination of mice with mRNA generates robust antigen-specific Tfh cell responses and an increased number of GC B cells, which results in long-lived high-affinity antibodies [71]. It was also proven that mRNA vaccine candidates can induce potent antibody responses against immunosubdominant targets [74], which are often important conserved regions on parasites and are ideal for vaccine development.

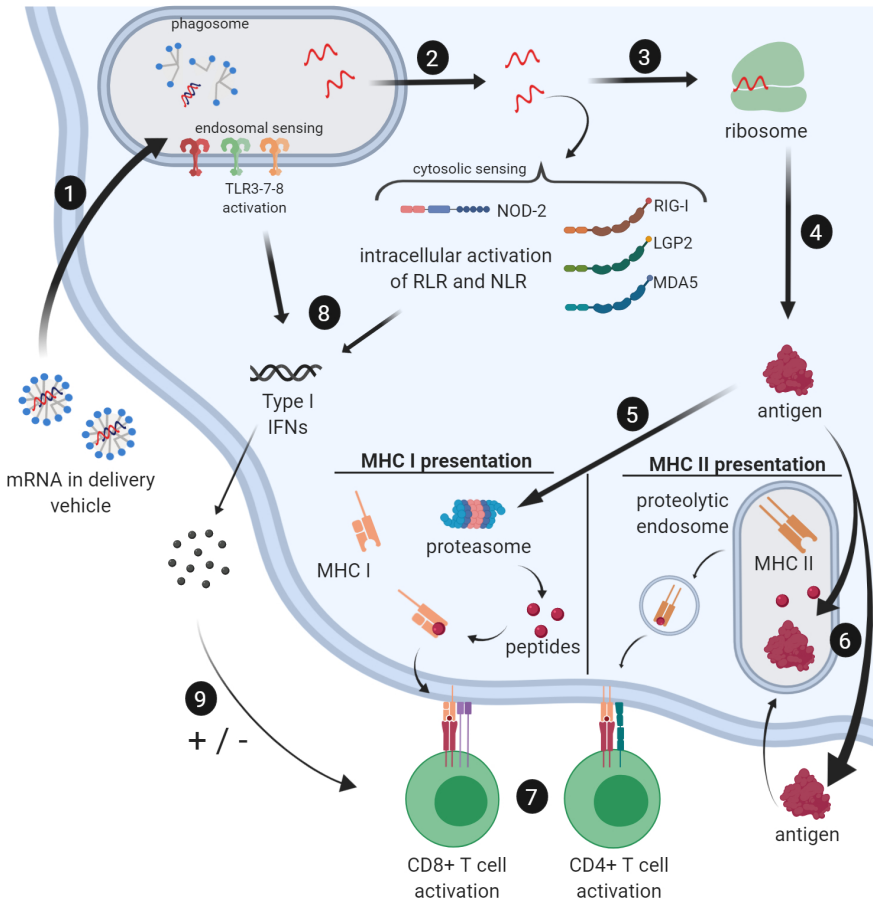
Advantages and Limitations of the mRNA Platform for Vaccine Development Against Parasitic Infections

While several vaccines against parasitic infections in humans have been developed at the pre-clinical stage, and some are even in early clinical trials, so far, only the malaria vaccine has made it to licensure. An effective vaccine should boost the immune response in a fashion that exceeds the “natural” innate and adaptive immune response. Most licensed vaccines also induce a memory immune response that provides long-term protection against infection. We will discuss the advantages and disadvantages of the mRNA vaccine development platform in this context.

Production and Development

The production and purification process of IVT mRNA can be standardized, therefore avoiding the need for costly product-specific production and purification steps. While it faces the same regulatory requirements and needs for quality control as a recombinant protein [25], the mRNA purification process is less complicated [26]. Due to the standardization of the production and purification process, the development time for new vaccine candidates can be dramatically reduced, which allows for the rapid testing of more vaccine candidates by high-throughput screening [28,31]. The relatively simple, low-cost production process is a crucial benefit because regardless of the scientific and medical prospects, parasitic vaccines need to become accessible for people living in low-income countries [75].

On a lab-scale, new widely available kits allow for high-yield transcription reactions for the synthesis of capped RNA. The current costs of producing capped RNA are, however, still high at the larger scale, but, for example, more effective capping enzymes could lower cost [76]. Several companies and research institutes have built facilities for the GMP-grade large-scale synthesis (up to kilograms amounts) of capped, polyadenylated RNA. FDA-compliant enzymes and reagents to synthesize capped RNA have become available [29,77].



■ **Figure 4.** Messenger RNA-encoded vaccine antigen processing in antigen presenting cells (APCs). (1) mRNA encapsulated in the delivery vehicle is taken up by the host cell. After the delivery vehicle is digested, mRNA is recognized by Toll-like receptors (TLRs) and/or escapes from the phagosome (2). Different cytosolic pathogen recognition receptors can then recognize the mRNA. (3) mRNA is translated by the host's ribosome and antigen is formed. (4) After the antigen is formed, it can be processed through different pathways. (5) The antigen is broken down to peptides by the host proteasome; peptides are accepted by major histocompatibility complex class I (MHC I). The MHC class I-peptide complex then travels to the cell membrane where it is presented to the immune system. (6) The antigen is secreted and ingested by an endosome or alternatively enters the endosome without secretion, achieved by adding signaling molecules and sequences. The antigen is then degraded by endosomal proteases and peptides are bound by major histocompatibility class II (MHC II). The MHC class II-peptide complex then travels to the cell membrane where it is presented to the immune system. (7) CD8+ and CD4+ T cell activation can be achieved through the presentation of the peptide on MHC class I and MHC class II, respectively. Co-stimulatory molecules and cytokines need to be present for successful activation. (8) TLR3-7-8 and NOD2, RIG-I, LGP2, and MDA5 can be activated by mRNA, subsequently triggering the production of type I interferons. (9) Secreted type I interferons can have a positive or negative effect on T cell activation. The activation level of the type I innate immune response triggered by mRNA can be controlled by the application of modified nucleosides, improved RNA purification, and low-immunogenic delivery systems.

Multivalent mRNA Vaccines

The mRNA platform allows for the simultaneous expression of multiple proteins, eliciting immunity to different epitopes from different targets [78–80]. Several antigens can either be combined into one mRNA sequence or a mixture of shorter RNA sequences, each translating into a different protein antigen that can be transfected together. The development of multivalent vaccines consisting of several antigens can even include a pan-parasitic approach, creating a vaccine, for example, targeting the multiple helminths that typically infect children in endemic areas. Additionally, not all individuals respond to the same parasitic antigens. Multivalent vaccines have a greater number of protective epitopes and thus should be efficacious in a greater proportion of the population. However, in multivalent vaccines, the optimal association or combination of antigens must be assessed to obtain synergistic effects. Additionally, mRNA vaccine mixtures may even encode immune evasive proteins [65,81] or co-stimulatory proteins that may further enhance the activation and differentiation of T cells [82].

Strong Cellular Immune Responses

The immune profile triggered by mRNA vaccines has been discussed in detail above. When taken up by APCs, the mRNA vaccine induces a very strong T-cell response. However, with the use of signal markers, the immune response can be steered towards an increased humoral response. Because of the relatively simple option of multivalency, the platform also allows the combination of two mRNA antigens to be processed through different pathways; i.e., the mRNA sequences taken up by APCs without signal peptide will induce more T-cell responses, while other sequences that include a signal peptide will induce an antibody-mediated response.

Stability

Previously, RNA was associated with low stability because of the omnipresence of RNases. However, the stability of IVT mRNA at -80°C can be guaranteed for many months to years when the mRNA is properly capped and purified under sterile conditions [29,83,84]. In fact, a lyophilized mRNA vaccine for rabies has proven to be extremely thermostable [83]; its potency did not drop significantly over several months when the vaccine was stored at oscillating temperatures between 4 and 56°C . This will be relevant as there is often a lack of a functional cold chain in many of the regions endemic for tropical parasites.

Once administered *in vivo* or *in vitro*, the stability of mRNA is limited. In mice, measurable levels of protein translation were found up to 10 days ($5\ \mu\text{g}$ dose), depending on the route of the delivery [71,85,86]. When using higher doses or with the application of self-amplifying RNA, RNA can be translated at high levels for several weeks [43,87]. The stability *in vivo* can be improved when the mRNA is encapsulated or linked to a protective delivery system [28,88–90]. However, it should be noted that from the vaccine safety perspective, the low half-life of the mRNA is typically regarded as an advantage.

Safety Profile

The flipside of having a very potent product, such as mRNA, is the possibility of uncontrolled inflammatory reactions and possible toxicity. However, because of the transient character of mRNA and the relatively low doses (<100 µg) typically administered for vaccination, the risk is minimal. In addition, the inflammatory nature of mRNA can be further controlled by working with highly purified transcripts as well as modified nucleosides [32,34,67]. A report on the first in-human phase 1 clinical trial (NCT02241135) for an mRNA rabies vaccine (CV7201, CureVac, Tübingen Germany) concluded that the administration of the mRNA vaccine encoding a rabies virus glycoprotein was generally safe and reasonably tolerable [52]. Some limited local and systemic adverse reactions were noted; however, this is generally the case with most potent vaccine products. It will be interesting to see if the inflammatory nature of mRNA can be further controlled using an improved construct in an upcoming clinical study (NCT03713086). Unfortunately, a prostate cancer immunotherapy mRNA vaccine candidate (CV9104, CureVac, Tübingen, Germany), based on the same RActive® technology, has failed to meet the primary endpoint of improving overall survival in a phase IIb clinical trial (NCT01817738).

When compared to traditional vaccines, it is evident that using a gene construct coding for the antigen avoids the risks associated with whole-cell pathogens. In comparison to DNA vaccines, it is often noted that RNA cannot integrate into the host DNA (unless by a retrovirus), and from a regulatory perspective, mRNA vaccines are not considered a gene therapy product [91]. Furthermore, the manufacturing of IVT mRNA does not involve any animal-derived products. A side-by-side list of all the advantages and the disadvantages of traditional and novel oligonucleotide-based vaccine platforms is shown in **Table 2**.

Despite different pre-clinical and even clinical studies existing that have shown the utility of mRNA vaccines against cancer, viral, and bacterial diseases, only a few studies have addressed parasitic diseases. Here, we discuss the few examples of mRNA vaccines against different parasitic infections.

■ **Table 2.** Advantages and disadvantages of different vaccine platforms for parasitic diseases.

Vaccine Platform	Advantages	Disadvantages
Killed/Attenuated Parasites	Very potent Multivalent by nature Simple formulation, no adjuvants required	Manufacturing challenge Requires stringent quality control Risk for infection
Subunit/Recombinant Protein	Non-infectious Strong humoral response	Need for additional immunostimulants (adjuvant) Need to develop new production process and stability assays for each new antigen Multivalent formulations can be challenging
Viral Vector	Strong innate immune response Strong cellular and humoral responses	Potential risk for infection Inflammation could cause risk for adverse reactions Pre-existing immunity against the vector Mixed results immunogenicity in humans
DNA	Non-infectious Rapid development and production using standardized production pipeline Options for multivalency Strong T cell responses	Poor immunogenicity in humans Potential risk at genetic integration
RNA	Non-infectious Degradable and no risk for genetic integration Rapid development and production using standardized production pipeline Production free of any animal-derived products Options for multivalency Very potent innate immune response Strong T cell responses	RNases can cause stability issues Inflammation could cause risk for adverse reactions Although becoming rapidly more affordable the current production costs are high

4.3 MESSENGER RNA VACCINES AGAINST PARASITIC INFECTIONS

Toxoplasma Gondii Infection

Chahal et al. have shown the possibility to achieve protective immunity against lethal doses of different infectious diseases using a dendrimer-RNA nanoparticle vaccine platform [79]. Modified dendrimer nanoparticles (MDNPs) were developed containing mRNA replicons encoding for antigens from either H1N1 influenza, Ebola virus, or the protozoan *Toxoplasma gondii*. In the case of *T. gondii*, self-amplifying mRNA constructs based on the Venezuelan

equine encephalitis virus (VEEV) replicase proteins encoded for six different conserved *T. gondii* antigens, which are expressed by the protozoan throughout its lifecycle. Thirty-two days after a single vaccination, the mice were challenged with a lethal dose of *T. gondii* type II strain Prugniaud, and all vaccinated mice survived the lethal challenge, while the mice in the control group all died within 12 days.

Luo et al. demonstrated the potential of a self-amplifying mRNA vaccine candidate against *T. gondii* infection [92]. A lipid nanoparticle (LNP) was developed containing a self-replicating RNA vector RREP based on non-structural proteins of Semliki Forest virus (SFV) and an RNA sequence encoding for *T. gondii* nucleoside triphosphate hydrolase-II (NTPase-II). While vaccinating mice with the naked self-amplifying mRNA construct RREP-NTPase-II already induced strong specific immunoglobulin (IgG) titers and IFN- γ production, the immune responses were even more pronounced when the mRNA construct was delivered by the LNP. Mice that received the RREP-NTPase-II LNP vaccine candidate showed an increased survival time and survival rate versus control groups after being challenged with 10^3 tachyzoites of the RH strain. In addition, in a chronic animal model, in which mice were challenged with 20 tissue cysts of the PRU strain, mice who received RREP-NTPase-II and RREP-NTPase-II LNP showed a 46.4% and 62.1% reduction, respectively, in brain cysts when compared to the phosphate buffered saline (PBS) control group. The results indicated that vaccination with RREP-NTPase-II mRNA vaccine candidates can enhance resistance against acute and chronic challenges of *T. gondii*.

Malaria

Garcia et al. proved that protective immunity against malaria infection can be achieved by neutralizing the *Plasmodium* macrophage migration inhibitory factor (PMIF) utilizing the self-amplifying mRNA vaccine [93]. PMIF is an orthologue of the mammalian macrophage migration inhibitory factor (MIF) and secretion of PMIF by *Plasmodium* attenuates the host's immune response. To improve host immunity, mice were vaccinated twice with a self-amplifying mRNA replicon encoding PMIF. It was observed that after vaccinations, PMIF specific CD4+ cells were increased, the anti-PMIF IgG titer increased 4-fold, and these antibodies blocked the pro-inflammatory action of PMIF without altering the functionality of host MIF. More importantly, a challenge with *Plasmodium* showed that vaccination with the PMIF mRNA enhanced the control of parasites and prevented re-infection.

Leishmania Donovanii Infection

Recently, it was shown that protection against *Leishmania donovani* infection was accomplished by vaccinating mice with a heterologous mRNA—a subunit vaccine strategy. Duthie et al. developed a naked mRNA replicon encoding for the *LEISH-F2* gene [40]. When this F2-RNA was given as a prime vaccination and mice were boosted with the recombinant LEISH-F2 protein in glucopyranosyl lipid A in a stable oil-in-water emulsion (SLA-SE), a significant reduction in the parasite burden in the liver was observed. Other vaccination strategies, including homologous vaccination with either F2-RNA or LEISH-F2 SLA-SE, did not

reduce parasite burdens compared to the control. In addition, the successful heterologous vaccine strategy was shown to induce very strong IFN- γ secretions and antigen-specific Th1 responses by splenocytes, while vaccination with F2-RNA alone showed low antigen-specific Th1 responses and very low IgG responses and vaccination with LEISH-F2 SLA-SE alone showed slightly larger Th1 responses and strong IgG responses. These differences demonstrate the importance of how the antigen is produced and presented to the immune system.

4.4 CONCLUDING REMARKS AND PROSPECTS OF NEW MRNA VACCINES FOR PARASITIC DISEASES

The IVT mRNA platform is currently one of the fastest growing vaccine technologies [26,94,95]. Similar to other oligonucleotide-based vaccine technologies, mRNA can be made using a standardized production process, allowing for multiple vaccine candidates to be screened within a reasonable time frame. The present-day costs of production are still high, however, the prospect of the low cost of standardized production may soon be realized through improved transcription and mRNA capping techniques and increased competition between GMP RNA production facilities. Different mRNA vaccine candidates can potentially be combined in multivalent vaccines. mRNA triggers a type-I innate immune response, leading to a strong CD8+ T cell response even without additional adjuvants. The immune reaction can also be steered towards antibody production by incorporating effective signal peptides. These features, mostly lacking in traditional vaccine platforms, make this platform very attractive for the development of vaccines against parasitic diseases. From a regulatory standpoint, mRNA products are less complex and safer than whole cell, DNA, or recombinant protein vaccines. Several mRNA vaccine candidates (for infectious diseases and cancers) have now found a pathway into the clinic and it will be interesting to study the immune reaction in humans. Hopefully, the additional potency of RNA versus DNA will push mRNA vaccines to surpass the clinical track record of DNA vaccines.

We foresee hundreds of new mRNA vaccine research results published in the next few years and expect several will be focused on parasitic diseases. We are currently developing an mRNA vaccine as part of our vaccine program against Chagas disease [96–98], a neglected tropical disease caused by the protozoan *Trypanosoma cruzi* resulting in cardiomyopathy and death. Although *T. cruzi* has been studied for decades now, no vaccine has been able to induce a 100% immune protection [87]. However, there is a consensus on what the properties of a protective vaccine would be. Ideally, an anti-*T. cruzi* vaccine should induce specific CD8+ T cells targeting conserved epitopes from both immunodominant and subdominant, or cryptic, *T. cruzi* antigens [99]. When applied as a therapeutic vaccine, a more balanced immune response is needed, in order to avoid triggering excessive host inflammation or autoimmunity [97]. Although there is a certain learning curve and the technology is in constant development, in our experience, the mRNA platform promises to be an effective vaccine tool to rapidly produce and screen different targets and induce potent CD8+ T cells responses against multiple

antigens/epitopes of *T. cruzi* in a relatively easy manner. By these criteria, we conclude that the mRNA vaccine platform might become ideally suited for the development of neglected parasitic disease vaccines, on the condition that the costs of production continue to drop.

Author Contributions

Leroy Versteeg: original draft preparation, figure preparation, revision and editing; Mashal M. Almutairi: original draft preparation, figure preparation, revision and editing; Peter J. Hotez: secure funding, writing, revision and editing; Jeroen Pollet: original draft preparation, figure preparation, revision and editing.

Funding

The authors acknowledge support from the Robert J. and Helen C. Kleberg Foundation and Texas Children's Hospital, supporting the development of a vaccine against Chagas Disease. We are also grateful to King Saud University for supporting a joint training program with Baylor College of Medicine.

Acknowledgments

The authors like to thank Maria Elena Bottazzi and Ulrich Strych for proofreading and editing.

Conflicts of Interest

The authors are involved in and receive funding for the development of vaccines against neglected and emerging tropical diseases.

4.5 REFERENCES

1. Fenner, F. Global Eradication of Smallpox. *Rev Infect Dis* **1982**, *4*, 916–930.
2. Norrby, E.; Uhnoo, I.; Brytting, M.; Zakikhany, K.; Lepp, T.; Olin, P. [Polio close to eradication]. *Lakartidningen* **2017**, *114*, 1–5.
3. Achievements in Public Health, 1900–1999 Impact of Vaccines Universally Recommended for Children -- United States, 1990–1998 Available online: <https://www.cdc.gov/mmwr/preview/mmwrhtml/00056803.htm#00003753.htm> (accessed on May 28, 2019).
4. Jourdan, P.M.; Lambertson, P.H.L.; Fenwick, A.; Addiss, D.G. Soil-transmitted helminth infections. *The Lancet* **2018**, *391*, 252–265.
5. Filardy, A.A.; Guimarães-Pinto, K.; Nunes, M.P.; Zukeram, K.; Fliess, L.; Pereira, L.; Oliveira Nascimento, D.; Conde, L.; Morrot, A. Human Kinetoplastid Protozoan Infections: Where Are We Going Next? *Front. Immunol.* **2018**, *9*.
6. Vos, T.; Abajobir, A.A.; Abate, K.H.; Abbafati, C.; Abbas, K.M.; Abd-Allah, F.; Abdulkader, R.S.; Abdulle, A.M.; Abebo, T.A.; Abera, S.F.; et al. Global, regional, and national incidence, prevalence, and years lived with disability for 328 diseases and injuries for 195 countries, 1990–2016: a systematic analysis for the Global Burden of Disease Study 2016. *The Lancet* **2017**, *390*, 1211–1259.
7. Kyu, H.H.; Abate, D.; Abate, K.H.; Abay, S.M.; Abbafati, C.; Abbasi, N.; Abbastabar, H.; Abd-Allah, F.; Abdela, J.; Abdelalim, A.; et al. Global, regional, and national disability-adjusted life-years (DALYs) for 359 diseases and injuries and healthy life expectancy (HALE) for 195 countries and territories, 1990–2017: a systematic analysis for the Global Burden of Disease Study 2017. *The Lancet* **2018**, *392*, 1859–1922.
8. Hotez, P.J.; Fenwick, A.; Savioli, L.; Molyneux, D.H. Rescuing the bottom billion through control of neglected tropical diseases. *Lancet* **2009**, *373*, 1570–1575.
9. Hotez, P.J.; Damania, A.; Naghavi, M. Blue Marble Health and the Global Burden of Disease Study 2013. *PLOS Neglected Tropical Diseases* **2016**, *10*, e0004744.
10. Global Health Data Exchange, I. GBD Results Tool | GHDx Available online: <http://ghdx.healthdata.org/gbd-results-tool?params=gbd-api-2017-permalink/4c9d166de41065b7a285b59edcf47405> (accessed on May 3, 2019).
11. Hotez, P.J.; Fenwick, A.; Molyneux, D.H. Collateral Benefits of Preventive Chemotherapy — Expanding the War on Neglected Tropical Diseases. *New England Journal of Medicine* **2019**, *380*, 2389–2391.
12. Stylianou, A.; Hadjichrysanthou, C.; Truscott, J.E.; Anderson, R.M. Developing a mathematical model for the evaluation of the potential impact of a partially efficacious vaccine on the transmission dynamics of *Schistosoma mansoni* in human communities. *Parasit Vectors* **2017**, *10*, 294.
13. Bartsch, S.M.; Hotez, P.J.; Hertenstein, D.L.; Diemert, D.J.; Zapf, K.M.; Bottazzi, M.E.; Bethony, J.M.; Brown, S.T.; Lee, B.Y. Modeling the Economic and Epidemiologic Impact of Hookworm Vaccine and Mass Drug Administration (MDA) in Brazil, a High Transmission Setting. *Vaccine* **2016**, *34*, 2197–2206.
14. Bottazzi, M.E.; Hotez, P.J. “Running the Gauntlet”: Formidable challenges in advancing neglected tropical diseases vaccines from development through licensure, and a “Call to Action.” *Human Vaccines & Immunotherapeutics* **2019**, *0*, 1–8.
15. Anonymous Mosquirix H-W-2300 Available online: <https://www.ema.europa.eu/en/mosquirix-h-w-2300> (accessed on Aug 18, 2019).
16. Morrison, W.I.; Tomley, F. Development of vaccines for parasitic diseases of animals: Challenges and opportunities. *Parasite Immunology* **2016**, *38*, 707–708.

17. Abath, F.G.C.; Montenegro, S.M.L.; Gomes, Y.M. Vaccines against human parasitic diseases: an overview. *Acta Tropica* **1998**, *71*, 237–254.
18. Hotez, P.J. The global fight to develop antipoverty vaccines in the anti-vaccine era. *Hum Vaccin Immunother* **2018**, *14*, 2128–2131.
19. Perry, G.H. Parasites and human evolution. *Evol. Anthropol.* **2014**, *23*, 218–228.
20. Rogier, C. [Challenge of developing anti-parasite vaccines in the tropics]. *Med Trop (Mars)* **2007**, *67*, 328–334.
21. Nadim, A.; Javadian, E.; Tahvildar-Bidruni, G.; Ghorbani, M. Effectiveness of leishmanization in the control of cutaneous leishmaniasis. *Bull Soc Pathol Exot Filiales* **1983**, *76*, 377–383.
22. Sacks, D.L. Vaccines against tropical parasitic diseases: a persisting answer to a persisting problem. *Nature Immunology* **2014**, *15*, 403–405.
23. Ogutu, B.R.; Apollo, O.J.; McKinney, D.; Okoth, W.; Siangla, J.; Dubovsky, F.; Tucker, K.; Waitumbi, J.N.; Diggs, C.; Wittes, J.; et al. Blood Stage Malaria Vaccine Eliciting High Antigen-Specific Antibody Concentrations Confers No Protection to Young Children in Western Kenya. *PLoS One* **2009**, *4*.
24. Wykes, M.N. Why haven't we made an efficacious vaccine for malaria? *EMBO Rep* **2013**, *14*, 661.
25. Cristina Poveda; Biter, A.B.; Bottazzi, Maria Elena; Strych, Ulrich Establishing preferred product characterization for the evaluation of RNA vaccine antigens. *Vaccines* **2019**, *In press*.
26. Pardi, N.; Hogan, M.J.; Porter, F.W.; Weissman, D. mRNA vaccines — a new era in vaccinology. *Nature Reviews Drug Discovery* **2018**, *17*, 261–279.
27. Pollard, C.; De Koker, S.; Saelens, X.; Vanham, G.; Grooten, J. Challenges and advances towards the rational design of mRNA vaccines. *Trends in Molecular Medicine* **2013**, *19*, 705–713.
28. Zhang, C.; Maruggi, G.; Shan, H.; Li, J. Advances in mRNA Vaccines for Infectious Diseases. *Front. Immunol.* **2019**, *10*.
29. Liu, M.A. A Comparison of Plasmid DNA and mRNA as Vaccine Technologies. *Vaccines* **2019**, *7*, 37.
30. Sahin, U.; Karikó, K.; Türeci, Ö. mRNA-based therapeutics — developing a new class of drugs. *Nature Reviews Drug Discovery* **2014**, *13*, 759–780.
31. Maruggi, G.; Zhang, C.; Li, J.; Ulmer, J.B.; Yu, D. mRNA as a Transformative Technology for Vaccine Development to Control Infectious Diseases. *Molecular Therapy* **2019**, *27*, 757–772.
32. Karikó, K.; Muramatsu, H.; Ludwig, J.; Weissman, D. Generating the optimal mRNA for therapy: HPLC purification eliminates immune activation and improves translation of nucleoside-modified, protein-encoding mRNA. *Nucleic Acids Res.* **2011**, *39*, e142.
33. Baiersdörfer, M.; Boros, G.; Muramatsu, H.; Mahiny, A.; Vlatkovic, I.; Sahin, U.; Karikó, K. A Facile Method for the Removal of dsRNA Contaminant from In Vitro-Transcribed mRNA. *Molecular Therapy - Nucleic Acids* **2019**, *15*, 26–35.
34. Holtkamp, S.; Kreiter, S.; Selmi, A.; Simon, P.; Koslowski, M.; Huber, C.; Türeci, O.; Sahin, U. Modification of antigen-encoding RNA increases stability, translational efficacy, and T-cell stimulatory capacity of dendritic cells. *Blood* **2006**, *108*, 4009–4017.
35. Pasquinelli, A.E.; Dahlberg, J.E.; Lund, E. Reverse 5' caps in RNAs made in vitro by phage RNA polymerases. *RNA* **1995**, *1*, 957–967.
36. Stepinski, J.; Waddell, C.; Stolarski, R.; Darzynkiewicz, E.; Rhoads, R.E. Synthesis and properties of mRNAs containing the novel “anti-reverse” cap analogs 7-methyl(3'-O-methyl)GpppG and 7-methyl(3'-deoxy)GpppG. *RNA* **2001**, *7*, 1486–1495.

37. Vaidyanathan, S.; Azizian, K.T.; Haque, A.K.M.A.; Henderson, J.M.; Hendel, A.; Shore, S.; Antony, J.S.; Hogrefe, R.I.; Kormann, M.S.D.; Porteus, M.H.; et al. Uridine Depletion and Chemical Modification Increase Cas9 mRNA Activity and Reduce Immunogenicity without HPLC Purification. *Mol Ther Nucleic Acids* **2018**, *12*, 530–542.
38. Lundstrom, K. Self-Replicating RNA Viruses for RNA Therapeutics. *Molecules* **2018**, *23*, 3310.
39. Brito, L.A.; Kommareddy, S.; Maione, D.; Uematsu, Y.; Giovani, C.; Berlanda Scorza, F.; Otten, G.R.; Yu, D.; Mandl, C.W.; Mason, P.W.; et al. Self-amplifying mRNA vaccines. *Adv. Genet.* **2015**, *89*, 179–233.
40. Duthie, M.S.; Van Hoesven, N.; MacMillen, Z.; Picone, A.; Mohamath, R.; Erasmus, J.; Hsu, F.-C.; Stinchcomb, D.T.; Reed, S.G. Heterologous Immunization With Defined RNA and Subunit Vaccines Enhances T Cell Responses That Protect Against *Leishmania donovani*. *Front Immunol* **2018**, *9*, 2420.
41. Johanning, F.W.; Conry, R.M.; LoBuglio, A.F.; Wright, M.; Sumerel, L.A.; Pike, M.J.; Curiel, D.T. A Sindbis virus mRNA polynucleotide vector achieves prolonged and high level heterologous gene expression in vivo. *Nucleic Acids Res* **1995**, *23*, 1495–1501.
42. Zhou, X.; Berglund, P.; Rhodes, G.; Parker, S.E.; Jondal, M.; Liljeström, P. Self-replicating Semliki Forest virus RNA as recombinant vaccine. *Vaccine* **1994**, *12*, 1510–1514.
43. Vogel, A.B.; Lambert, L.; Kinnear, E.; Busse, D.; Erbar, S.; Reuter, K.C.; Wicke, L.; Perkovic, M.; Beissert, T.; Haas, H.; et al. Self-Amplifying RNA Vaccines Give Equivalent Protection against Influenza to mRNA Vaccines but at Much Lower Doses. *Mol. Ther.* **2018**, *26*, 446–455.
44. Pepini, T.; Pulichino, A.-M.; Carsillo, T.; Carlson, A.L.; Sari-Sarraf, F.; Ramsauer, K.; Debasitis, J.C.; Maruggi, G.; Otten, G.R.; Geall, A.J.; et al. Induction of an IFN-Mediated Antiviral Response by a Self-Amplifying RNA Vaccine: Implications for Vaccine Design. *The Journal of Immunology* **2017**, *198*, 4012–4024.
45. Tan, L.; Sun, X. Recent advances in mRNA vaccine delivery. *Nano Res.* **2018**, *11*, 5338–5354.
46. Guan, S.; Rosenecker, J. Nanotechnologies in delivery of mRNA therapeutics using nonviral vector-based delivery systems. *Gene Therapy* **2017**, *24*, 133–143.
47. Shin, H.; Park, S.-J.; Yim, Y.; Kim, J.; Choi, C.; Won, C.; Min, D.-H. Recent Advances in RNA Therapeutics and RNA Delivery Systems Based on Nanoparticles. *Advanced Therapeutics* **2018**, *1*, 1800065.
48. Chen, N.; Xia, P.; Li, S.; Zhang, T.; Wang, T.T.; Zhu, J. RNA sensors of the innate immune system and their detection of pathogens. *IUBMB Life* **2017**, *69*, 297–304.
49. Pollard, C.; Rejman, J.; De Haes, W.; Verrier, B.; Van Gulck, E.; Naessens, T.; De Smedt, S.; Bogaert, P.; Grooten, J.; Vanham, G.; et al. Type I IFN Counteracts the Induction of Antigen-Specific Immune Responses by Lipid-Based Delivery of mRNA Vaccines. *Molecular Therapy* **2013**, *21*, 251–259.
50. Meyer, M.; Huang, E.; Yuzhakov, O.; Ramanathan, P.; Ciaramella, G.; Bukreyev, A. Modified mRNA-Based Vaccines Elicit Robust Immune Responses and Protect Guinea Pigs From Ebola Virus Disease. *The Journal of Infectious Diseases* **2018**, *217*, 451–455.
51. De Beuckelaer, A.; Grooten, J.; De Koker, S. Type I Interferons Modulate CD8+ T Cell Immunity to mRNA Vaccines. *Trends in Molecular Medicine* **2017**, *23*, 216–226.
52. Alberer, M.; Gnad-Vogt, U.; Hong, H.S.; Mehr, K.T.; Backert, L.; Finak, G.; Gottardo, R.; Bica, M.A.; Garofano, A.; Koch, S.D.; et al. Safety and immunogenicity of a mRNA rabies vaccine in healthy adults: an open-label, non-randomised, prospective, first-in-human phase 1 clinical trial. *The Lancet* **2017**, *390*, 1511–1520.
53. Liu, M.A. Immunologic basis of vaccine vectors. *Immunity* **2010**, *33*, 504–515.
54. Lee, B.L.; Barton, G.M. Trafficking of endosomal Toll-like receptors. *Trends in Cell Biology* **2014**, *24*, 360–369.

55. Takeuchi, O.; Akira, S. Pattern recognition receptors and inflammation. *Cell* **2010**, *140*, 805–820.
56. Rodriguez, K.R.; Bruns, A.M.; Horvath, C.M. MDA5 and LGP2: Accomplices and Antagonists of Antiviral Signal Transduction. *Journal of Virology* **2014**, *88*, 8194–8200.
57. Sabbah, A.; Chang, T.H.; Harnack, R.; Frohlich, V.; Tominaga, K.; Dube, P.H.; Xiang, Y.; Bose, S. Activation of innate immune antiviral responses by Nod2. *Nature Immunology* **2009**, *10*, 1073–1080.
58. Tough, D.F. Modulation of T-cell function by type I interferon. *Immunology & Cell Biology* **2012**, *90*, 492–497.
59. Agarwal, P.; Raghavan, A.; Nandiwada, S.L.; Curtsinger, J.M.; Bohjanen, P.R.; Mueller, D.L.; Mescher, M.F. Gene Regulation and Chromatin Remodeling by IL-12 and Type I IFN in Programming for CD8 T Cell Effector Function and Memory. *The Journal of Immunology* **2009**, *183*, 1695–1704.
60. De Beuckelaer, A.; Pollard, C.; Van Lint, S.; Roose, K.; Van Hoecke, L.; Naessens, T.; Udhayakumar, V.K.; Smet, M.; Sanders, N.; Lienenklaus, S.; et al. Type I Interferons Interfere with the Capacity of mRNA Lipoplex Vaccines to Elicit Cytolytic T Cell Responses. *Molecular Therapy* **2016**, *24*, 2012–2020.
61. Wiesel, M.; Crouse, J.; Bedenikovic, G.; Sutherland, A.; Joller, N.; Oxenius, A. Type-I IFN drives the differentiation of short-lived effector CD8+ T cells in vivo. *European Journal of Immunology* **2012**, *42*, 320–329.
62. Tanabe, Y.; Nishibori, T.; Su, L.; Arduini, R.M.; Baker, D.P.; David, M. Cutting Edge: Role of STAT1, STAT3, and STAT5 in IFN- $\alpha\beta$ Responses in T Lymphocytes. *The Journal of Immunology* **2005**, *174*, 609–613.
63. Terawaki, S.; Chikuma, S.; Shibayama, S.; Hayashi, T.; Yoshida, T.; Okazaki, T.; Honjo, T. IFN- α Directly Promotes Programmed Cell Death-1 Transcription and Limits the Duration of T Cell-Mediated Immunity. *The Journal of Immunology* **2011**, *186*, 2772–2779.
64. Beissert, T.; Koste, L.; Perkovic, M.; Walzer, K.C.; Erbar, S.; Selmi, A.; Diken, M.; Kreiter, S.; Türeci, Ö.; Sahin, U. Improvement of In Vivo Expression of Genes Delivered by Self-Amplifying RNA Using Vaccinia Virus Immune Evasion Proteins. *Human Gene Therapy* **2017**, *28*, 1138–1146.
65. Sarén, T.; Ramachandran, M.; Martikainen, M.; Yu, D. Insertion of the Type-I IFN Decoy Receptor B18R in a miRNA-Tagged Semliki Forest Virus Improves Oncolytic Capacity but Results in Neurotoxicity. *Molecular Therapy - Oncolytics* **2017**, *7*, 67–75.
66. Yoshioka, N.; Dowdy, S.F. Enhanced generation of iPSCs from older adult human cells by a synthetic five-factor self-replicative RNA. *PLOS ONE* **2017**, *12*, e0182018.
67. Pardi, N.; Hogan, M.J.; Pelc, R.S.; Muramatsu, H.; Andersen, H.; DeMaso, C.R.; Dowd, K.A.; Sutherland, L.L.; Scarce, R.M.; Parks, R.; et al. Zika virus protection by a single low-dose nucleoside-modified mRNA vaccination. *Nature* **2017**, *543*, 248–251.
68. Hekele, A.; Bertholet, S.; Archer, J.; Gibson, D.G.; Palladino, G.; Brito, L.A.; Otten, G.R.; Brazzoli, M.; Buccato, S.; Bonci, A.; et al. Rapidly produced SAM(®) vaccine against H7N9 influenza is immunogenic in mice. *Emerg Microbes Infect* **2013**, *2*, e52.
69. Charles A Janeway, J.; Travers, P.; Walport, M.; Shlomchik, M.J. B-cell activation by armed helper T cells. *Immunobiology: The Immune System in Health and Disease. 5th edition* **2001**.
70. Lindgren, G.; Ols, S.; Liang, F.; Thompson, E.A.; Lin, A.; Hellgren, F.; Bahl, K.; John, S.; Yuzhakov, O.; Hassett, K.J.; et al. Induction of Robust B Cell Responses after Influenza mRNA Vaccination Is Accompanied by Circulating Hemagglutinin-Specific ICOS+ PD-1+ CXCR3+ T Follicular Helper Cells. *Front. Immunol.* **2017**, *8*.
71. Pardi, N.; Hogan, M.J.; Naradikian, M.S.; Parkhouse, K.; Cain, D.W.; Jones, L.; Moody, M.A.; Verkerke, H.P.; Myles, A.; Willis, E.; et al. Nucleoside-modified mRNA vaccines induce potent T follicular helper and germinal center B cell responses. *Journal of Experimental Medicine* **2018**, *215*, 1571–1588.

72. Bonehill, A.; Heirman, C.; Tuyvaerts, S.; Michiels, A.; Breckpot, K.; Brasseur, F.; Zhang, Y.; Van Der Bruggen, P.; Thielemans, K. Messenger RNA-electroporated dendritic cells presenting MAGE-A3 simultaneously in HLA class I and class II molecules. *J. Immunol.* **2004**, *172*, 6649–6657.
73. Simon, G.G.; Hu, Y.; Khan, A.M.; Zhou, J.; Salmon, J.; Chikhlikar, P.R.; Jung, K.-O.; Marques, E.T.A.; August, J.T. Dendritic Cell Mediated Delivery of Plasmid DNA Encoding LAMP/HIV-1 Gag Fusion Immunogen Enhances T Cell Epitope Responses in HLA DR4 Transgenic Mice. *PLOS ONE* **2010**, *5*, e8574.
74. Pardi, N.; Parkhouse, K.; Kirkpatrick, E.; McMahon, M.; Zost, S.J.; Mui, B.L.; Tam, Y.K.; Karikó, K.; Barbosa, C.J.; Madden, T.D.; et al. Nucleoside-modified mRNA immunization elicits influenza virus hemagglutinin stalk-specific antibodies. *Nat Commun* **2018**, *9*, 1–12.
75. Submitted by WHO European Region; Member States through the WHO/UNICEF; Joint Reporting Form for 2013 *Review of vaccine price data*; 2013; p. 60;.
76. Muttach, F.; Muthmann, N.; Rentmeister, A. Synthetic mRNA capping. *Beilstein J Org Chem* **2017**, *13*, 2819–2832.
77. Fuchs, A.-L.; Neu, A.; Sprangers, R. A general method for rapid and cost-efficient large-scale production of 5' capped RNA. *RNA* **2016**, *22*, 1454–1466.
78. Magini, D.; Giovani, C.; Mangiavacchi, S.; Maccari, S.; Cecchi, R.; Ulmer, J.B.; Gregorio, E.D.; Geall, A.J.; Brazzoli, M.; Bertholet, S. Self-Amplifying mRNA Vaccines Expressing Multiple Conserved Influenza Antigens Confer Protection against Homologous and Heterosubtypic Viral Challenge. *PLOS ONE* **2016**, *11*, e0161193.
79. Chahal, J.S.; Khan, O.F.; Cooper, C.L.; McPartlan, J.S.; Tsosie, J.K.; Tilley, L.D.; Sidik, S.M.; Lourido, S.; Langer, R.; Bavari, S.; et al. Dendrimer-RNA nanoparticles generate protective immunity against lethal Ebola, H1N1 influenza, and *Toxoplasma gondii* challenges with a single dose. *PNAS* **2016**, *113*, E4133–E4142.
80. John, S.; Yuzhakov, O.; Woods, A.; Deterling, J.; Hassett, K.; Shaw, C.A.; Ciaramella, G. Multi-antigenic human cytomegalovirus mRNA vaccines that elicit potent humoral and cell-mediated immunity. *Vaccine* **2018**, *36*, 1689–1699.
81. Michel, T.; Golombek, S.; Steinle, H.; Hann, L.; Velic, A.; Macek, B.; Krajewski, S.; Schlensak, C.; Wendel, H.P.; Avci-Adali, M. Efficient reduction of synthetic mRNA induced immune activation by simultaneous delivery of B18R encoding mRNA. *Journal of Biological Engineering* **2019**, *13*, 40.
82. Van Lint, S.; Goyvaerts, C.; Maenhout, S.; Goethals, L.; Disy, A.; Benteyn, D.; Pen, J.; Bonehill, A.; Heirman, C.; Breckpot, K.; et al. Preclinical evaluation of TriMix and antigen mRNA-based antitumor therapy. *Cancer Res.* **2012**, *72*, 1661–1671.
83. Stitz, L.; Vogel, A.; Schnee, M.; Voss, D.; Rauch, S.; Mutzke, T.; Ketterer, T.; Kramps, T.; Petsch, B. A thermostable messenger RNA based vaccine against rabies. *PLOS Neglected Tropical Diseases* **2017**, *11*, e0006108.
84. Jones, K.L.; Drane, D.; Gowans, E.J. Long-term storage of DNA-free RNA for use in vaccine studies. *BioTechniques* **2007**, *43*, 675–681.
85. Kirschman, J.L.; Bhosle, S.; Vanover, D.; Blanchard, E.L.; Loomis, K.H.; Zurla, C.; Murray, K.; Lam, B.C.; Santangelo, P.J. Characterizing exogenous mRNA delivery, trafficking, cytoplasmic release and RNA–protein correlations at the level of single cells. *Nucleic Acids Res* **2017**, *45*, e113.
86. Pardi, N.; Tuyishime, S.; Muramatsu, H.; Kariko, K.; Mui, B.L.; Tam, Y.K.; Madden, T.D.; Hope, M.J.; Weissman, D. Expression kinetics of nucleoside-modified mRNA delivered in lipid nanoparticles to mice by various routes. *Journal of Controlled Release* **2015**, *217*, 345–351.

87. Thran, M.; Mukherjee, J.; Pönisch, M.; Fiedler, K.; Thess, A.; Mui, B.L.; Hope, M.J.; Tam, Y.K.; Horscroft, N.; Heidenreich, R.; et al. mRNA mediates passive vaccination against infectious agents, toxins, and tumors. *EMBO Mol Med* **2017**, *9*, 1434–1447.
88. Lundstrom, K. Latest development on RNA-based drugs and vaccines. *Future Sci OA* **2018**, *4*.
89. Sun, Y.; Zhao, Y.; Zhao, X.; Lee, R.J.; Teng, L.; Zhou, C. Enhancing the Therapeutic Delivery of Oligonucleotides by Chemical Modification and Nanoparticle Encapsulation. *Molecules* **2017**, *22*.
90. Islam, M.A.; Reesor, E.K.; Xu, Y.; Zope, H.R.; Zetter, B.R.; Shi, J. Biomaterials for mRNA delivery. *Biomater Sci* **2015**, *3*, 1519–1533.
91. Hinz, T.; Kallen, K.; Britten, C.M.; Flamion, B.; Granzer, U.; Hoos, A.; Huber, C.; Khleif, S.; Kreiter, S.; Rammensee, H.-G.; et al. The European Regulatory Environment of RNA-Based Vaccines. *Methods Mol. Biol.* **2017**, *1499*, 203–222.
92. Luo, F.; Zheng, L.; Hu, Y.; Liu, S.; Wang, Y.; Xiong, Z.; Hu, X.; Tan, F. Induction of Protective Immunity against *Toxoplasma gondii* in Mice by Nucleoside Triphosphate Hydrolase-II (NTPase-II) Self-amplifying RNA Vaccine Encapsulated in Lipid Nanoparticle (LNP). *Front. Microbiol.* **2017**, *8*.
93. Baeza Garcia, A.; Siu, E.; Sun, T.; Exler, V.; Brito, L.; Hekele, A.; Otten, G.; Augustijn, K.; Janse, C.J.; Ulmer, J.B.; et al. Neutralization of the Plasmodium- encoded MIF ortholog confers protective immunity against malaria infection. *Nature Communications* **2018**, *9*, 2714.
94. mRNA Vaccines and Therapeutics Market Forecast 2019-2029. *Visiongain*, London, UK, **2019**
95. Iavarone, C.; O'hagan, D.T.; Yu, D.; Delahaye, N.F.; Ulmer, J.B. Mechanism of action of mRNA-based vaccines. *Expert Review of Vaccines* **2017**, *16*, 871–881.
96. Beaumier, C.M.; Gillespie, P.M.; Strych, U.; Hayward, T.; Hotez, P.J.; Bottazzi, M.E. Status of vaccine research and development of vaccines for Chagas disease. *Vaccine* **2016**, *34*, 2996–3000.
97. Jones, K.; Versteeg, L.; Damania, A.; Keegan, B.; Kendricks, A.; Pollet, J.; Cruz-Chan, J.V.; Gusovsky, F.; Hotez, P.J.; Bottazzi, M.E. Vaccine-linked chemotherapy improves benznidazole efficacy for acute Chagas disease. *Infect. Immun.* **2018**, IAI.00876-17.
98. Barry, M.A.; Versteeg, L.; Wang, Q.; Pollet, J.; Zhan, B.; Gusovsky, F.; Bottazzi, M.E.; Hotez, P.J.; Jones, K.M. A therapeutic vaccine prototype induces protective immunity and reduces cardiac fibrosis in a mouse model of chronic *Trypanosoma cruzi* infection. *PLoS Neglected Tropical Diseases* **2019**, *13*, e0007413.
99. Dos Santos Virgilio, F.; Pontes, C.; Dominguez, M.R.; Ersching, J.; Rodrigues, M.M.; Vasconcelos, J.R. CD8(+) T cell-mediated immunity during *Trypanosoma cruzi* infection: a path for vaccine development? *Mediators Inflamm.* **2014**, *2014*, 243786.



CHAPTER 5

Immunopeptidomic MHC-I Profiling and Immunogenicity Testing Identifies Tcj2 as a New Chagas Disease mRNA Vaccine Candidate

Leroy Versteeg^{1,2}, Rakesh Adhikari¹, Gonteria Robinson¹, Jungsoon Lee¹, Junfei Wei¹, Brian Keegan¹, William K. Russell³, Cristina Poveda¹, Maria Jose Villar¹, Kathryn Jones^{1,4}, Maria Elena Bottazzi^{1,4,5}, Peter Hotez^{1,4,5}, Edwin Tijhaar^{2 *}, Jeroen Pollet^{1 *}

¹ Texas Children's Hospital Center for Vaccine Development, Department of Pediatrics, Division of Tropical Medicine, Baylor College of Medicine, Houston, Texas, USA

² Cell Biology and Immunology Group, Wageningen University & Research, Wageningen, The Netherlands

³ University of Texas Medical Branch, Mass Spectrometry Facility, UTMB Health, Galveston, USA

⁴ Department of Molecular Virology and Microbiology, Baylor College of Medicine, Houston, TX, USA

⁵ Department of Biology, Baylor University, Waco, TX, USA

* Contributed equally to this work

ABSTRACT

Trypanosoma cruzi is a protozoan parasite that causes Chagas disease. Globally 6 to 7 million people are infected by this parasite of which 20-30% will progress to develop Chronic Chagasic Cardiomyopathy (CCC). Despite its high disease burden, no clinically approved vaccine exists for the prevention or treatment of CCC. Developing vaccines that can stimulate *T. cruzi*-specific CD8+ cytotoxic T cells and eliminate infected cells requires targeting parasitic antigens presented on major histocompatibility complex-I (MHC-I) molecules. We utilized mass spectrometry-based immunopeptidomics to investigate which parasitic peptides are displayed on MHC-I of *T. cruzi* infected cells. Through duplicate experiments, we identified an array of unique peptides that could be traced back to 17 distinct *T. cruzi* proteins. Notably, six peptides were derived from Tcj2, a trypanosome chaperone protein and member of the DnaJ (heat shock protein 40) family, showcasing its potential as a viable candidate vaccine antigen with cytotoxic T cell inducing capacity. Upon testing Tcj2 as an mRNA vaccine candidate in mice, we observed a strong memory cytotoxic CD8+ T cell response along with a Th1-skewed humoral antibody response. *In vitro* co-cultures of *T. cruzi* infected cells with splenocytes of Tcj2-immunized mice restricted the replication of *T. cruzi*, demonstrating the protective potential of Tcj2 as a vaccine target. Moreover, antisera from Tcj2-vaccinated mice displayed no cross-reactivity with DnaJ in lysates from mouse and human indicating a decreased likelihood of triggering autoimmune reactions. Our findings highlight how immunopeptidomics can identify new vaccine targets for Chagas disease, with Tcj2 emerging as a promising new mRNA vaccine candidate.

Keywords: *Trypanosoma cruzi*, immunopeptidomics, mass spectrometry, peptides, MHC class I, heat shock protein 40, DnaJ, cytotoxic CD8+ T cells, protozoa, neglected tropical disease

5.1 INTRODUCTION

Chagas disease is a neglected tropical disease caused by the protozoan parasite *Trypanosoma cruzi*. Approximately 6-7 million people worldwide are affected by the disease, resulting in 10,000-50,000 deaths per year, and an estimated 65-100 million are at risk of contracting the infection (1,2). After the acute stage of the infection, generally with flu-like symptoms, patients can develop chronic disease in 30-40% of cases, and 20-30% of all chronic cases involving Chagasic cardiomyopathy (CCC), characterized by arrhythmias, heart aneurysms or failure, stroke, megacolon or megaesophagus (3,4). Chagas disease is endemic in 21 Latin American countries, where it has been confined to rural and poor areas where transmission by the *Triatoma* (kissing bug) vector is the main route of infection (4). However, due to transmission of the disease through blood transfusion, organ transplantation or by congenital transmission, Chagas disease is a growing concern for non-endemic countries in North America, Europe, Australia, and Asia that import cases through migration and globalization (3,5). Furthermore, it is estimated that the global economic burden of Chagas disease is almost \$7 billion, exceeding that of global diseases like rotavirus and cervical cancer (6). While the anti-trypanosomal drugs benznidazole and nifurtimox are approved for use, they have poor efficacy in the chronic phase and significant side effects (7). Much effort has been made to find new solutions to cure Chagas disease, such as vaccines and other immunotherapies, as well as better drugs (8,9).

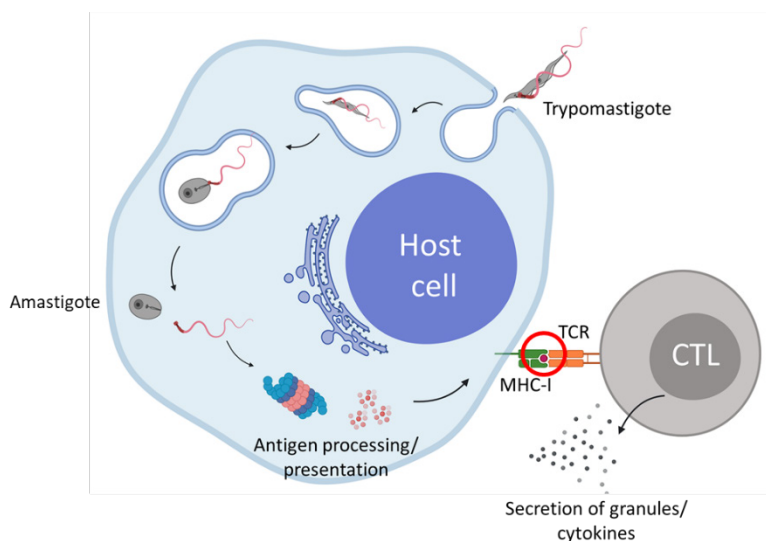
During *T. cruzi* infection, extracellular trypomastigotes penetrate host cells, subsequently infiltrate the phagolysosome and eventually enter the host cell cytoplasm (**Figure 1**). Here, they proliferate and evade the humoral immune response. During this intracellular stage, parasite-derived proteins that are discarded or secreted are processed by the proteasome and presented on MHC-I. This MHC-I presentation at the cell surface is crucial as it enables antigen specific cytotoxic CD8+ T cells (CTLs) to recognize, and subsequently kill, the *T. cruzi* infected cells. These antigen specific CTLs play an essential role in cell-mediated immunity and the control of *T. cruzi* infections (10,11). Importantly, it is thought that most trypomastigote and amastigote proteins are not directly available for MHC-I presentation, because they are still contained within the parasite, therefore not accessible for processing by the proteasome localized in the cytoplasm. Knowing which *T. cruzi* peptides are displayed on MHC-I of infected cells gives crucial insights for selecting appropriate candidate vaccine antigens that can induce cytotoxic T cell able to kill *T. cruzi* infected cells.

Immunopeptidomics is the science that studies the peptides that are presented on major histocompatibility complex (MHC) proteins on the surface of cells (red circle, Figure 1). Within the last decade, major advances in the field of liquid chromatography – mass spectrometry (LC-MS/MS) have led to a significant increase in sensitivity and accuracy of data acquisition and prediction, which now allow the identification of MHC presented peptides at a superior sensitivity (12,13). The repertoire of MHC-presented peptides, or so-called immunopeptidome, contains information of the health state of cells and is continuously

surveilled by T cells (14,15). Importantly, when a pathogen infects cells, pathogen-derived peptides will be presented by MHC-I (16). The identification of pathogen-derived peptides presented on MHC by immunopeptidomics has already been done numerous times for various viruses (17–20), protozoans (12,21–23) and bacteria (24–27). The results of these studies give insights into which pathogen derived peptides are presented on the surface of infected cells, thereby identifying the proteins that are accessible to the MHC-I presentation pathway. These proteins will be prime targets for inducing antigen specific CTLs that can kill infected target cells. Importantly, identification of peptides presented by *T. cruzi* infected cells has to this date not been performed. Thus, in combination with genomics and machine learning algorithms, immunopeptidomics offers new and innovative reverse vaccinology opportunities to address Chagas disease.

In recent years, mRNA vaccines have undergone significant development and are recognized as potent inducers of cell-mediated immunity, including MHC-I restricted CTLs(28,29). The advantages of this vaccine platform for anti-parasitic vaccines have been previously described and include the option of multivalency, rapid development and production, stability and strong induction of CTLs (30–32). Promising results of mRNA vaccines for parasitic diseases have already been reported for malaria, toxoplasmosis and leishmaniasis (33–35). The use of mRNA vaccines for Chagas disease has been proposed, and recently we published our work characterizing an mRNA vaccine construct encoding the flagellar calcium-binding protein Tc24 from *T. cruzi* (30,36–38).

Here, we report on the identification of a novel mRNA vaccine target for Chagas disease using immunopeptidomics. Through the analysis of the immunopeptidome of *T. cruzi* infected cells, using mass-spectrometry-based immunopeptidomics, we identified 24 unique *T. cruzi* peptides, derived from 17 different *T. cruzi* proteins. Of these proteins, Tcj2 – a known *T. cruzi* chaperone protein and part of the DnaJ (heat shock protein 40) family - was identified as a primary candidate vaccine antigen, since multiple unique Tcj2-derived peptides were identified in repeat experiments. Therefore, a Tcj2 mRNA vaccine was developed, and its immunogenicity tested *in vitro* and *in vivo* using a mouse model. The results revealed that when Tcj2 mRNA was formulated in lipid nanoparticles (LNPs), it provoked a robust immune response, displaying characteristics considered critical for a successful Chagas disease vaccine. Overall, our findings underscore the potential of immunopeptidomics in the identification of vaccine candidate antigens for parasitic diseases and highlights Tcj2-encoding mRNA formulated in LNPs as a promising vaccine candidate for Chagas disease.



- **Figure 1.** Immunopeptidomics identifies which peptides derived from *T. cruzi* antigens can be detected by CD8+ cytotoxic T cells (CTLs). After a *T. cruzi* trypomastigote invades a host cell, it enters the cytosol and transforms into the amastigote stage. During this process, several parasitic proteins become available for antigen processing by the proteasome followed by peptide presentation on MHC-I. This presentation can activate CTLs which secrete granules and cytokines to clear the infected cells. Immunopeptidomics will help us understand which proteins become available for the antigen processing and presentation machinery. Red encircled is the key event where immunopeptidomics is used to learn information on which peptides are presented. Created with Biorender.com

5

5.2 RESULTS

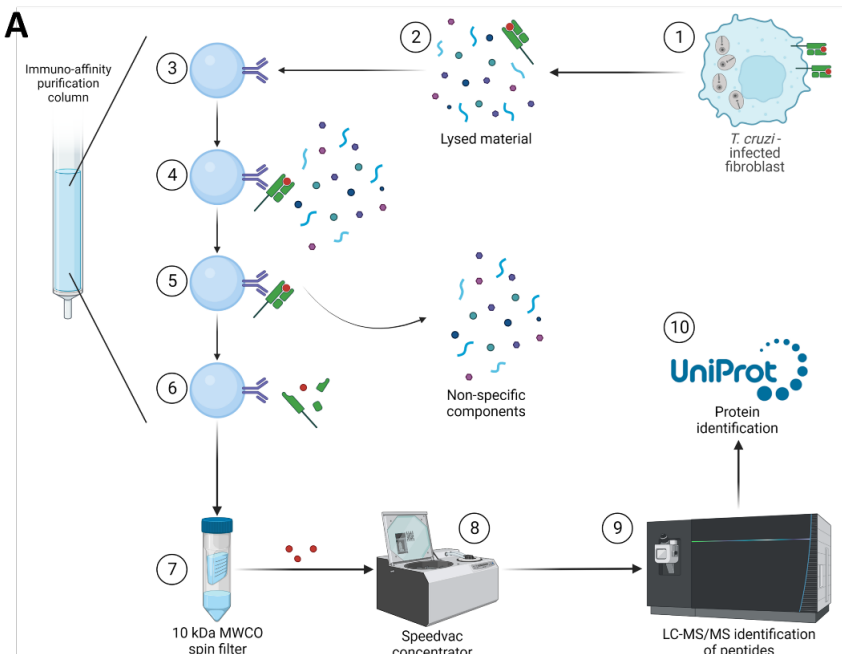
Analysis of peptides presented on MHC-I of *T. cruzi* – infected cells

To analyze which proteins from *T. cruzi* are subject to antigen processing followed by presentation on MHC-I, the immunopeptidome of *T. cruzi* - infected cells was analyzed as shown in **Figure 2A**. Murine MC57G fibroblasts were infected with *T. cruzi* Tulahuen trypomastigotes for 48 hours, followed by lysing the infected fibroblasts and isolation of the MHC-I – peptide complexes using an immunoaffinity column that consisted of the anti-mouse MHC-I mAb (clone M1/42), covalently coupled to cross-linked agarose resin. Flow cytometry analysis showed increased binding of the M1/42 mAb to mouse MHC-I (H-2) expressing MC75G cells after 48-hour infection with *T. cruzi* compared to uninfected controls, suggesting a significant upregulation of MHC-I expression due to infection (**Figure 2B**).

Two immunopeptidomics experiments (technical replicates) were performed using lysate from *T. cruzi* - infected fibroblasts. Following the analysis of the peptides by LC-MS/MS, peptides were identified using available protein FASTA databases from *T. cruzi* and mouse. To

further increase the specificity of the results, only peptide lengths between 8 and 15 amino acids (aa) were selected since these lengths have shown to bind most likely to MHC-I (H2-K^b and H2-D^b) (39). In the first experiment (#1) a total of 6 *T. cruzi* peptides were identified, as well as 1191 murine peptides (**Figure 2C**). When the experiment was repeated (experiment #2), 20 and 1475 peptides were identified from *T. cruzi* and mouse, respectively. When the immunopeptidome of non-infected fibroblasts was analyzed, 619 peptides from mouse and no peptides from *T. cruzi* were identified, indicating that mouse peptides are not mis-identified as *T. cruzi* peptides.

The length distribution of the identified peptides is displayed (**Figure 2D**). For *T. cruzi* peptides, the observed length was equally distributed between 8-14 aa with an average of 11.3. Interestingly, for murine self-peptides approximately 40% (experiment #1 39.5%, experiment #2 39.9%) of the peptides 8-15 aa in length were 8 or 9 aa long. In contrast, murine self-peptide length from non-infected fibroblasts showed a much higher number of peptides around 8 and 9 aa (68.7%). This suggests an increase in the length of peptides presented on MHC-I during *T. cruzi* infection, a phenomenon that has been described previously for *T. gondii* infection (22).



■ **Figure 2** continues on the next page

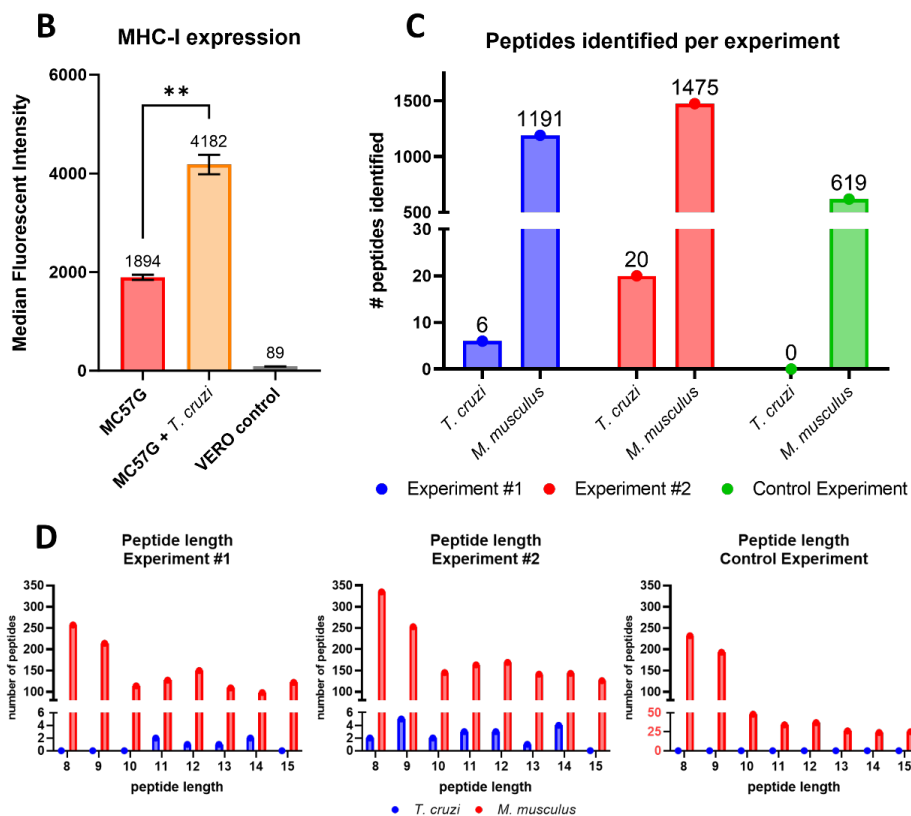


Figure 2. Isolation and identification of the peptides presented on MHC-I of *T. cruzi* infected MC57G fibroblast cells. A) Schematic overview of the immunopeptidomics workflow. 1: MC57G murine fibroblasts were co-cultured for 48 hours with *T. cruzi* Tulahuen trypomastigotes. 2: Infected fibroblasts were harvested and lysed using a non-denaturing lysis buffer. 3: Immuno-affinity purification column was prepared by covalently linking MHC-I – specific mAbs (M1/42) to AminoLink Plus resin. 4: Lysed fibroblast material was loaded on the column, allowing the peptide-loaded MHC-I complexes to bind. 5: Four different wash buffers were used to remove the non-specific components. 6: Acetic acid was used to elute the peptide - MHC-I complexes from the column and dissociate the peptide from the MHC-I. 7: A spin filter column separated the peptide fraction from the MHC-I molecules. 8: Peptides were concentrated using a speedvac concentrator. 9: concentrated peptides were analyzed using LC-MS/MS for their sequence. 10: using the *T. cruzi* proteome from UniProt *T. cruzi* proteins were identified. Mouse self-proteins were identified using the C57BL/6J proteome. Figure prepared with Biorender.com. B) *T. cruzi* infected and non-infected MC57G fibroblasts, as well as green monkey kidney (VERO) cells were stained with anti-mouse MHC-I Alexa Fluor 488. Cells were analyzed by flow cytometry and data was reported as median fluorescent intensity (MFI). Mean and standard deviation are shown and were calculated from six technical replicates. Statistical significance: **: $p < 0.01$. C) Number of MHC-I binding peptides identified from *T. cruzi* or mouse for each experiment. D) Distribution of the peptide length for each experiment.

Peptides from Tcj2 (*T. cruzi* DnaJ 2) protein are presented on MHC-I from *T. cruzi* - infected cells

24 unique *T. cruzi* peptides, originating from 17 unique proteins were identified from the two immunopeptidomics experiments with *T. cruzi* infected cells (**Table 1**, more details in **Supplementary Table 1**). Notably, six different peptides were linked to *T. cruzi* DnaJ 2 (Tcj2) (**Table 1**, Protein Group 2), with their peptide sequences located throughout the Tcj2 protein (**Supplementary Figure 2**). The Tcj2 derived peptides AFYTGKTIKLA and VKETKFYDSLGL were identified in both immunopeptidomics experiments. Tcj2 was the only *T. cruzi* protein that was identified by both experiments, increasing the confidence of being a protein that is well processed and presented on MHC-I of *T. cruzi* infected cells.

The DNAJ heat shock protein family, also known as heat shock protein 40 (HSP40), represents a highly conserved group of proteins throughout evolutionary history. Five different DnaJ proteins have been described for *T. cruzi*, and the DnaJ-derived peptides found in our immunopeptidomics experiments, are derived from one of these DnaJ proteins, described as *T. cruzi* DnaJ 2 (Tcj2) (40,41). In comparison, more than 40 DnaJ proteins have been described in humans (42). They are molecular chaperones of heat shock protein 70 (HSP70) and are involved in protein (re) folding (40). It has been described that DnaJ proteins are located in all cellular compartments of *T. cruzi*, and it has been suggested that DnaJs are potentially secreted proteins (43). Furthermore, comparative proteome analysis of trypomastigote and amastigote stages of *T. cruzi* suggested that Tcj2 are similarly expressed in both stages of the parasite (44). Notably, our immunopeptidomics data revealed the presence of a DnaJ chaperone protein (**Table 1**, Protein Group 15). Unlike Tcj2, this chaperone protein, while related, is not classified as a DnaJ protein and exhibits a low sequence identity of 32.6% with Tcj2. In the context of vaccine development two critical aspects of a vaccine target come into play: its degree of conservation across diverse parasitic strains and its dissimilarity from host self-proteins, ensuring it does not provoke autoimmunity. For *T. cruzi* over 6000 *T. cruzi* strains, classified into six Discrete Typing Units (DTUs) have been described (45). Therefore, Tcj2 protein sequence alignments were conducted to address these questions. When comparing the Tcj2 sequence between the different genetic groups of *T. cruzi*, it was observed that Tcj2 is very conserved (**Supplementary Figure 1**). Between 9 different *T. cruzi* strains from the three available DTUs, only twice a difference is a single residue was observed. Next, the amino acid sequence of Tcj2 was blasted using BLASTp and compared to human and mouse DnaJ proteins with the highest sequence identity to Tcj2 (**Supplementary Figure 2**). It can be observed that there is a considerable degree of identity (43.0% identity and 60.0% similarity) between human DnaJA4 and *T. cruzi* Tcj2 protein. However, enough differences in amino acids in the sequence are present which make overlapping T cell epitopes of 8-15 amino acids unlikely. DnaJ-homolog protein sequence between human and mouse showed a high degree of similarity (93.2% identity) which consequently, resulted in comparable similarities between mouse and *T. cruzi* (42.5% identity and 60.7% similarity) as observed for human and *T. cruzi*. Overall, this suggests a reduced risk of auto-immune reaction induction to host DnaJ through complete amino

acid sequence identity when using *T. cruzi* Tcj2 (DnaJ) as a vaccine target (46). Additionally, sequence alignments between Tcj2 (DnaJ) and DnaJ-homologs from other trypanosomes were performed. Sequence identity showed a considerable degree of overlap for *T. brucei brucei* (72.41% identity) (**Supplementary Figure 3**), as well as for *T. congolense* (71.79% identity) and *T. vivax* (72.10% identity) (alignments not shown). *T. rangeli* showed a lower degree of overlap with *T. cruzi* with 45.69% identity. For *T. brucei brucei*, *T. congolense* and *T. vivax*, multiple stretches of identical amino acid sequences are present which could serve as overlapping epitopes for antibodies and CTLs. For example, the peptide sequence GEGDQIPGVR from *T. cruzi* Tcj2 found by immunopeptidomics is also present in the DnaJ-homolog of *T. brucei brucei* and *T. vivax*. Overall, these observations suggest that a *T. cruzi* Tcj2 (DnaJ) vaccine candidate antigen has the potential to cross-protect against other trypanosomes infections.

In vitro immunogenicity testing of Tcj2-expressing mRNA vaccine

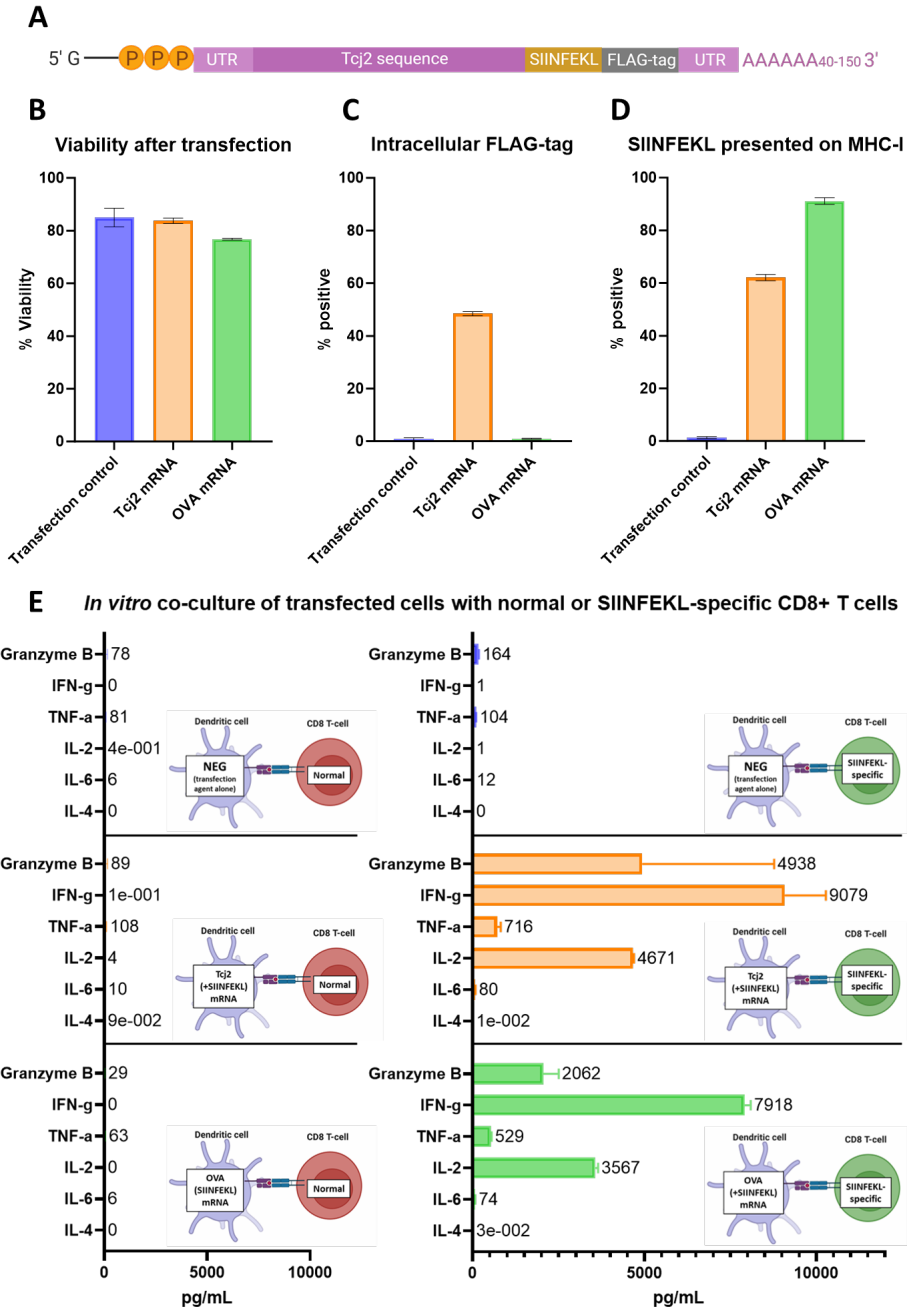
An mRNA vaccine construct was designed based on the Tcj2 protein sequence from *T. cruzi* (**Fig. 3A**). On the 3' - end of the Tcj2 sequence, the amino acid sequence SIINFEKL was added, followed by a FLAG-tag. SIINFEKL (OVA 257-264) is a sequence naturally occurring in the chicken ovalbumin protein that has a high affinity to H-2K^b (MHC-I expressed by C57BL/6J mice). An antibody is available that allows detection of MHC-I antigen presentation of this model epitope, as well as MHC-I/SIINFEKL tetramers for the quantification of SIINFEKL-specific CD8⁺ T cells (47). A FLAG-tag was added to evaluate the translation of the complete mRNA construct, which can be measured intracellularly by flow cytometry using a FLAG-tag specific antibody.

■ **Table 1.** List of all *T. cruzi* peptides presented on MHC-I and their source proteins. The 24 unique peptides traced back to 17 *T. cruzi* proteins. The identified heat shock protein DnaJ (protein group 2) is one of 5 DnaJ (heat shock protein 40) proteins described for *T. cruzi* that is identified in literature as TcJ2.

Protein Group	Peptide	Length	-10lgP	Unique	Identified in experiment #	Protein Accession	Protein Description
1	ASYDALETANKMGLL	15	41,91	Y	1	Q4E2Y1	60S ribosomal protein L23a putative
	LNIKHLDDRDVS	12	34,91	Y	2		
	VKETKFYDSLGL	11	33,21	Y	1+2		
2	AFYTGKTIKLA	11	32,99	Y	1+2	Q4D832	Heat shock protein DnaJ, putative
	LEAFYTGKTIKLA	13	31,76	Y	1		
	SNEISDLR	8	22,18	Y	2		
	GEGDQIPGVR	10	15,31	Y	2		
3	AEFAKMEEQNKKFF	15	32,11	Y	1	Q4D3A5, Q4D3A7, Q4D7V4	Kinetoplastid membrane protein KMP-11
4	MTYKPIVHGRPGVG	14	31,24	Y	2	Q4DGGZ5	40S ribosomal protein S15, putative
	KERTFHKFTYRGL	14	18,43	Y	2		
5	LYALYRQKKEKPRN	14	30,62	Y	2	Q4DTQ1	40S ribosomal protein S23, putative
6	LFSGMKVLR	11	30,3	Y	2	Q4DY30, Q4DY32	RNA-binding protein, putative
	LFSGMKVLR	9	21,87	Y	2		
7	DVFVNGKKPVVD	12	26,87	Y	2	Q4DAW5	Cytochrome C oxidase subunit VI, putative
8	IVPVPFIKV	9	26,35	Y	2	Q4D289	Neurobeachin/beige-like protein, putative
9	SAAGATLLVENF	12	24,47	Y	1	Q4DRE3, Q4CW14	Uncharacterized protein
10	LVRHMASKDRSARL	14	23,6	Y	2	Q4DCN9	Glyceraldehyde-3-phosphate dehydrogenase
11	DQGSADIVN	9	23,54	Y	2	Q4D976, Q4E5Z1	ATP-dependent DEAD/H RNA helicase, putative
12	AEFAESKV	8	23,25	Y	2	Q4DNZ9	Nfu_N domain-containing protein
13	PAVVAPPPQ	9	22,63	Y	2	Q4CNA5, Q4DPR2	OTU domain-containing protein

■ **Table 1.** List of all *T. cruzi* peptides presented on MHC-I and their source proteins. The 24 unique peptides traced back to 17 *T. cruzi* proteins. The identified heat shock protein DnaJ (protein group 2) is one of 5 DnaJ (heat shock protein 40) proteins described for *T. cruzi* that is identified in literature as Tcj2. (continued)

Protein Group	Peptide	Length	-10lgP	Unique	Identified in experiment #	Protein Accession	Protein Description
14	VAAKRSATSAKLG	13	21,63	Y	2	Q4CY60, Q4D3G1	Uncharacterized protein
15	SSSEKDYKILG	12	20,75	Y	2	Q4D7B1, Q4DVP6	Chaperone DnaJ protein, putative
16	GVLATGASLA	10	20,67	Y	2	Q4DH33, Q4DY72	Uncharacterized protein
17	ASVWAGNIS	9	20,62	Y	2	Q4DBX3	Uncharacterized protein



■ **Figure 3.** *In vitro* evaluation of Tcj2 mRNA showed the translation and antigen presentation of the mRNA construct, as well as the activation of SIINFEKL-specific CD8+ T cells. DC2.4 cells were transfected with mRNA with Lipofectamine MessengerMAX, or without mRNA (transfection control). After a 24-hour incubation, cells were subjected to analysis. A) Schematic representation of Tcj2 mRNA construct. B) Cell viability measured after transfection. C) Detection of the translated FLAG-tag sequence

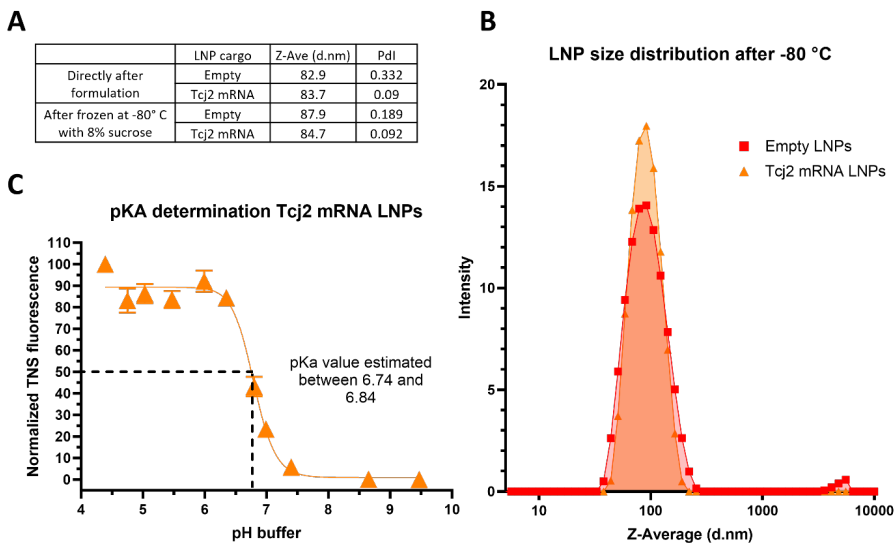
by intracellular flow cytometry staining using a FLAG-specific antibody. D) Presentation of SIINFEKL on surface MHC-I (H-2K^b) measured by flow cytometry using an antibody specific for the combination of SIINFEKL presented by H-2K^b. E) Cytokines secreted by C57BL/6J “normal” or SIINFEKL specific OT-1 CD8+ T cells after co-culture with transfected cells. DC2.4 cells were transfected for 24 hours and then counted and seeded. Splenocytes were added in a ratio of 1:10 (DC2.4 : splenocytes) and the co-culture was incubated for 24 hours before the supernatant was collected and analyzed for cytokines by Luminex. Figure prepared with Biorender.com. From all experiments, mean and standard deviations are shown from triplicate experiments.

After a 24-hour transfection with Tcj2 mRNA and Lipofectamine MessengerMAX, the viability of the mouse dendritic cell line DC2.4 cells was analyzed. Results (**Figure 3B**) showed that Tcj2 mRNA has no impact on the viability of the cells compared with transfection agent only (84% versus 85%, respectively). Transfection with Ovalbumin mRNA, which was used as a positive control for the MHC-I presentation of SIINFEKL peptide, decreased the viability slightly to 77%. More than 40% of the Tcj2 mRNA transfected cells were positive for intracellular FLAG-tag staining of this epitope located at the C-terminal end of the protein. This shows that the Tcj2 mRNA was completely translated (**Figure 3C**). As expected, no FLAG-tag was detected in cells transfected with Ovalbumin mRNA or in transfection control cells. Additionally, almost 60% of the cells transfected with the Tcj2 mRNA were positive for SIINFEKL presentation on MHC-I, as revealed by the H-2K^b SIINFEKL specific antibody (**Figure 3D**), followed by 80% for the positive Ovalbumin mRNA control. These results show that the Tcj2 mRNA is translated and that peptides derived from the produced protein are presented on MHC-I. Furthermore, when Tcj2 mRNA transfected DC2.4 cells were co-cultured with splenocytes from transgenic C57BL/6J OT-1 mice, which contain high numbers of CD8+ T cells specific for the SIINFEKL epitope presented on H-2K^b, an increase in Granzyme B, IFN- γ , TNF- α and IL2- was measured (**Figure 3E**). Production of IL2- suggests the activation of T cells and Granzyme B, IFN- γ and TNF- α hallmarks the activation of CD8+ cytotoxic T cells. Moreover, the results looked similar in the co-culture where DC2.4 cells were transfected with Ovalbumin mRNA, demonstrating that the SIINFEKL peptide presented on MHC-I is responsible for activating the OT1- CD8+ T cells. No increase in Granzyme B, IFN- γ , TNF- α and IL2- was measured when splenocytes from non-transgenic (= “normal”) C57BL/6J mice were used. Overall, the data suggests that the Tcj2 mRNA construct was translated *in vitro*, antigen presented on MHC-I, and induced CD8+ T cell activation of naïve antigen specific T cells.

Preparation of Tcj2 mRNA LNPs

Following *in vitro* validation of the translatability of the Tcj2-encoding mRNA construct and its subsequent presentation on MHC-I and activation of antigen-specific CD8+ T cells, Tcj2-encoding mRNA was formulated in lipid nanoparticles (LNPs) for further *in vivo* assessment of this mRNA vaccine. To serve as a negative control, LNPs without mRNA (empty LNPs) were also prepared. Based on the Ribogreen assay, the loading efficiency of the encapsulated mRNA was 85%. Dynamic Light Scattering (DLS) analysis indicated that both Tcj2 mRNA LNPs and empty LNPs exhibited sizes within the range of 80-90 nm, which is considered suitable for mRNA LNP immunogenicity studies (**Figure 4A**) (48). Freezing at -80° C followed by thawing did not

significantly affect the LNP diameter (Z-ave), with measurements of 83.7 d.nm versus 84.7 d.nm for Tcj2 mRNA LNPs and 82.9 d.nm versus 87.9 d.nm for empty LNPs before and after freezing, respectively. Furthermore, polydispersity index (Pdl) of Tcj2 mRNA LNPs was measured to be low before and after freeze/thaw, indicating a small variation in particle size (**Figure 4A and 4C**). For the empty LNPs a Pdl of 0.331 was measured, surpassing the acceptance criterion of 0.25, although it decreased to 0.189 after freeze/thaw. The higher Pdl values observed in the empty LNPs can be attributed to the absence of mRNA in the formulation, which is crucial for proper LNP formation. To further characterize the Tcj2 mRNA LNPs and determine whether they are suitable for intramuscular (IM) delivery, the surface charge of the LNPs was examined by measuring the pKa (acid dissociation constant). The pKa of LNPs has been previously shown to be a determining factor for immunogenicity, influencing factors such as endosomal escape delivery and cellular uptake (49). As shown in **Figure 4B**, the pKa of the LNP's surface falls within a range of 6.740 and 6.841, what is within the optimal pKa range of 6.6-6.9 for IM delivery (49). In summary, results indicated that the mRNA encapsulation, the diameter, the polydispersity index, and the surface charge of the LNPs all fall within the desired range for LNP mRNA vaccines.



■ **Figure 4. Freeze/thawed Tcj2 mRNA LNPs showed desired diameter, polydispersity index and pKa range for immunogenicity studies.** A) Tcj2 mRNA LNPs and empty LNPs were analyzed by Dynamic Light Scattering (DLS), directly after formulation and after storage at -80° C. Diameter in nm (Z-Ave (d.nm)) and polydispersity index (Pdl) of LNPs were reported. B) Distribution of the size of the Tcj2 mRNA LNPs and empty LNPs. C) pKa of the surface of Tcj2 mRNA LNPs was analysed through a TNS fluorescence assay.

Tcj2 mRNA LNPs elicit robust antigen-specific T cells and humoral immune responses

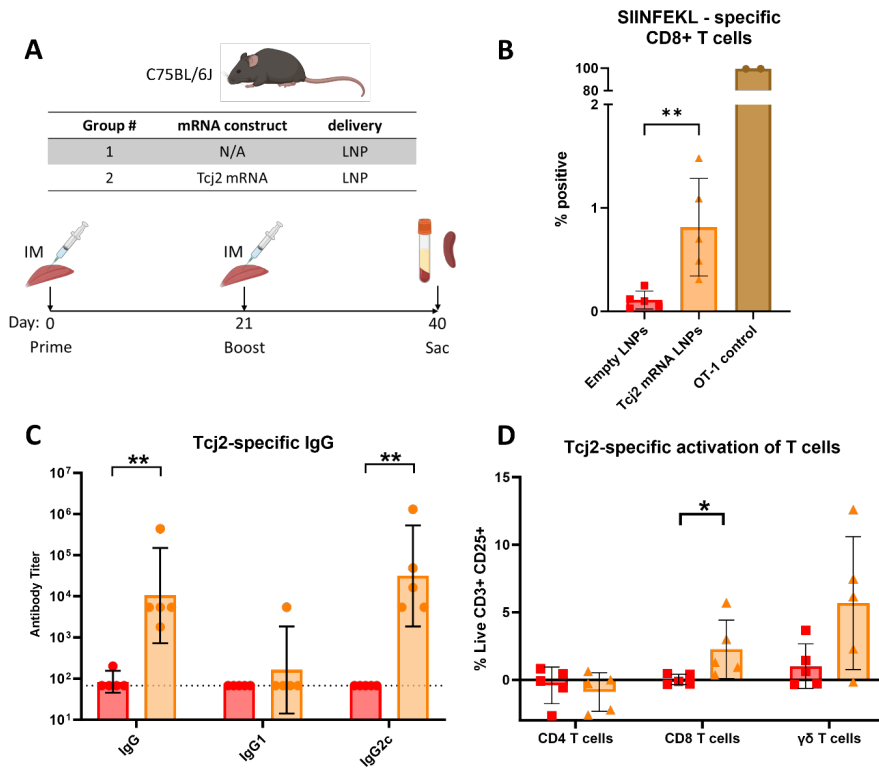
To evaluate the immunogenicity of the Tcj2 mRNA vaccine candidate, five mice were immunized with Tcj2 mRNA LNPs on day 0 followed by a boost at day 21 (**Figure 5A**). As a control, five mice were immunized with empty LNPs. At day 40, mice were euthanized, and sera and spleens were collected for immune evaluation.

To evaluate whether the Tcj2 mRNA had elicited the generation of antigen-specific T cells, the percentage of SIINFEKL specific CD8⁺ T cells in splenocytes of immunized mice (**Figure 5B**) was determined by SIINFEKL tetramer staining. Immunizations with Tcj2 mRNA LNPs resulted in a significant increase in SIINFEKL-specific CD8⁺ T cells compared to empty LNPs (mean 0.81% for Tcj2 mRNA LNPs versus 0.11% for empty LNPs). The location of the mRNA sequence encoding for SIINFEKL at the 3' end of the mRNA construct indicates successful delivery of Tcj2 mRNA to antigen-presenting cells (APCs), subsequent translation into protein, and processing for presentation on MHC-I to CD8⁺ T cells, leading to the generation of SIINFEKL-specific CD8⁺ T cells and potentially Tcj2-specific CD8⁺ T cells. Furthermore, splenocytes from the transgenic OT-1 mice, used as a positive control for SIINFEKL tetramer staining, exhibited nearly all CD8⁺ T cells being SIINFEKL specific (mean 99.59%).

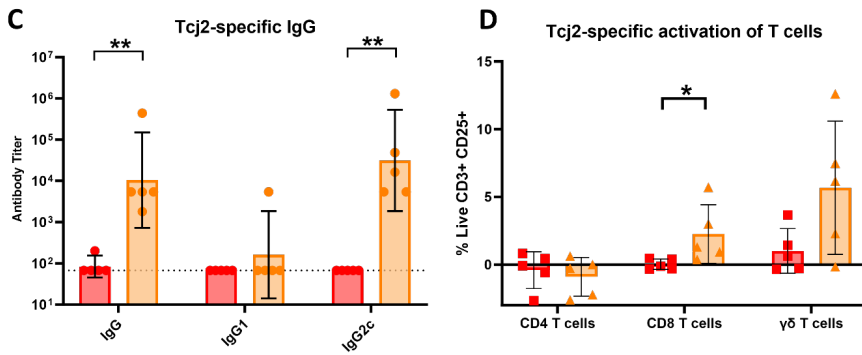
To assess Tcj2 antigen-specific responses, recombinant Tcj2 (rTcj2) was prepared in *E. coli* (**Supplementary Figure 4**). The protein was then utilized in ELISAs to determine the generation of Tcj2-specific antibodies and in *in vitro* restimulation assays to evaluate antigen-specific T cell responses. Immunizations with Tcj2 mRNA LNPs induced a significant increase in Tcj2-specific IgG and IgG2c titers, while specific IgG1 titers were not increased compared to the empty LNP control (**Figure 5C**). The strong increase in IgG2c but not IgG1 suggest a skewed humoral immune response towards Th1 (50). Testing *T. cruzi* trypomastigote lysate on western blot with sera from Tcj2 mRNA LNP immunized mice confirmed that the induced Tcj2 antibodies recognize native Tcj2 from *T. cruzi* (**Supplementary Figure 5**). Importantly, native DnaJ in lysates from uninfected mouse and human cell lines was not recognized, indicating that the Tcj2-specific antibodies do not cross-react with human and mouse DnaJ. Presence of human DNAJA4, which of all human DnaJ's shares the highest protein sequence identity with Tcj2, was confirmed in the HEK293T lysate by western blot (**Supplementary Figure 6**). Furthermore, Tcj2 antisera did also not show cross-reactivity with the much more homologous DnaJ in *T. brucei* lysate (**Supplementary Figure 5**).

To assess the cellular immune response against Tcj2, splenocytes were *in vitro* restimulated for 48 hours with rTcj2 protein, followed by analysis by flow cytometry. The expression of CD25, a late activation marker expressed on T cells, was significantly upregulated by CD8⁺ T cells after restimulation, as well as an observable trend ($p = 0.095$) in increase for $\gamma\delta$ T cells (**Figure 5D**). CD4⁺ T cells displayed minimal changes in CD25 expression, implying a lesser role in the immune response against Tcj2 when compared to CD8⁺ T cells and $\gamma\delta$

T cells. This was further observed when the production of intracellular cytokines IFN- γ , TNF- α , IL-17A, and cytolytic compounds granzyme B and perforin were analyzed. Significant increases in production of granzyme B, IFN- γ , perforin and TNF- α were observed in CD8+ T cells (**Figure 5E**). For $\gamma\delta$ T cells, a significant increase in the production of Granzyme B was observed (**Figure 5F**). No significant changes in cytokine production were observed by CD4+ T cells after restimulation (**Supplementary Figure 7**) but an observable trend in increase in granzyme B and IFN- γ was observed. These findings suggest that CD8+ T cells and $\gamma\delta$ T cells were stronger activated by Tcj2 mRNA LNP compared to CD4+ T cells.



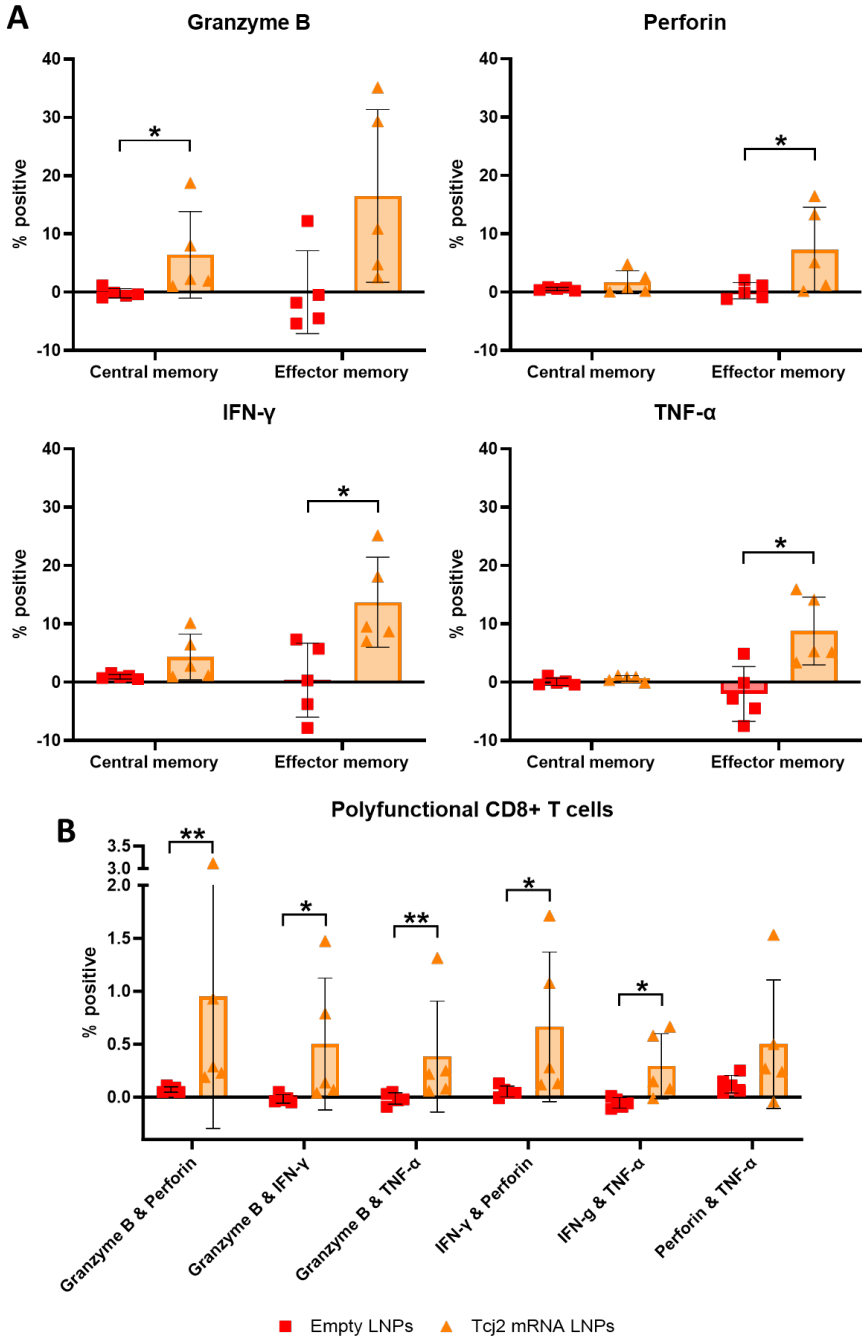
■ Figure 5 continues on the next page



■ **Figure 5. Tcj2 mRNA LNPs elicited humoral and cellular immune responses in a mouse immunogenicity study.** A) Schematic description of mouse model, study groups and immunization schedule. Figure prepared with Biorender.com. B) SIINFEKL-specific CD8⁺ T cells measured by SIINFEKL tetramer staining. C) Tcj2-specific IgG, IgG1 and IgG2c was measured using an indirect ELISA coated with rTcj2 protein. The baseline antibody titer was set at 67 and is highlighted by the dotted line. D) Antigen-specific activation of T cells was measured after *in vitro* restimulation with rTcj2 protein by analyzing CD25 late activation marker expression. E) Cytokines and cytolytic compounds produced by CD8⁺ T cells after *in vitro* restimulation with rTcj2 protein. F) Cytokines produced by γδ T cells after *in vitro* restimulation with rTcj2 protein. For data presented in figures D, E and F: values from non-stimulated cells were subtracted from rTcj2 protein stimulated cells to obtain antigen-specific cytokine production. Statistical significance: *: $p < 0.05$, **: $p < 0.01$, ***: $p < 0.001$. For panel B, D, E and F the mean and standard deviation are shown, while for C the geometric mean with 95% confidence intervals is shown.

Immunizations with Tcj2 mRNA LNPs induced significant memory CD8⁺ T cells response with cytotoxic features

To improve our understanding of the antigen-specific CD8⁺ T cell response induced by immunization with Tcj2 mRNA LNPs, central and memory CD8⁺ T cells were examined for their production of cytolytic enzymes and cytokines after *in vitro* restimulation with rTcj2. Central memory CD8⁺ T cells producing granzyme B were significantly increased, and a trend ($p = 0.056$) in an increased percentage of effector memory CD8⁺ T cells was observed (**Figure 6A**). Effector memory CD8⁺ T cells producing perforin, IFN- γ and TNF- α were also significantly increased, and central memory CD8⁺ T cells also exhibited an observable increase in IFN- γ . Additionally, polyfunctionality of CD8⁺ T cells was investigated, as measured by the ability to produce more than one cytolytic enzyme or cytokine (**Figure 6B**). The results showed that polyfunctional CD8⁺ T cells producing granzyme B & perforin, granzyme B & IFN- γ , granzyme B & TNF- α , IFN- γ & perforin and IFN- γ & TNF- α were significantly increased compared to the empty LNP control. To summarize, immunizations with Tcj2 mRNA LNPs led to a robust increase in central and effector memory CD8⁺ T cells that produce cytolytic enzymes and cytokines upon restimulation, as well as an increase in CD8⁺ T cells that demonstrate polyfunctionality.

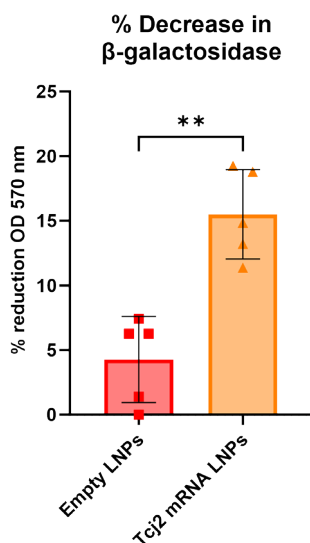


■ **Figure 6. Tc2 mRNA LNP immunizations induced antigen-specific cytokine production in central memory and effector memory CD8+ T cells, as well as increase in cytokine producing polyfunctional CD8+ T cells.** A) antigen-specific central memory (CD62^{high} and CD44^{high}) and effector memory (CD62^{low} and CD44^{high}) CD8+ T cells were analyzed for production of granzyme B, perforin, IFN- γ or

TNF- α . B) Antigen-specific CD8⁺ T cells were analyzed for the production of two cytolytic enzymes or cytokines. For data presented in figures A and B: values from non-stimulated cells were subtracted from rTcj2 protein stimulated cells to obtain antigen-specific cytokine production. Statistical significance: *: $p < 0.05$, **: $p < 0.01$. For all panels in this figure the mean and standard deviation are shown.

Splenocytes from Tcj2 mRNA LNPs immunized mice decreased *T. cruzi* parasite load *in vitro*

To evaluate whether the observed cytotoxic properties from the CD8⁺ T cells would show functional protectiveness against *T. cruzi* infection, splenocytes from Tcj2 mRNA LNP – immunized mice were co-cultured with *T. cruzi* – infected MC75G mouse fibroblasts. A transgenic *T. cruzi* (Tulahuen, clone C4 +*lacZ*) parasite strain was used that expresses β -galactosidase, which allows for the utilization of a colorimetric reaction with chlorophenol red- β -D-galactopyranoside (51). The enzymatic activity is directly proportional to the number of parasites, and can therefore be used to measure parasite load *in vitro*. The results of the co-culture between *T. cruzi* – infected fibroblasts and splenocytes showed a significant reduction of 15.5% in β -galactosidase activity compared to splenocytes from empty LNP-immunized mice (4.3%), where 100% reduction was achieved after *in vitro* treatment with 100 μ M benznidazole (Figure 7). This observation suggests that parasite load was reduced by Tcj2 mRNA LNP-immunized splenocytes.



■ **Figure 7. Splenocytes from Tcj2 mRNA LNP – immunized mice decrease *T. cruzi* infection *in vitro*.** *T. cruzi* – infected MC57G mouse fibroblasts were co-cultured with splenocytes from immunized mice for 72 hours. *T. cruzi* parasites expressed the LacZ gene which encodes for the enzyme β -galactosidase, used to convert a substrate which directly correlated to the parasite load in each well. *T. cruzi* – infected fibroblasts treated with a high dose of benznidazole were run in parallel and used to calculate the %-reduction of parasite load. Statistical significance: **: $p < 0.01$. Mean and standard deviation are shown.

5.3 DISCUSSION

Mass-Spectrometry based immunopeptidomics has emerged as a powerful tool to identify new vaccine targets for cancers and infectious pathogens. For Chagas disease, a parasitic infection characterized by intracellular replication of *T. cruzi*, it is most relevant to analyze the peptides presented on MHC-I, since these peptides can be recognized by CD8+ T cells and are a target for CTLs to eliminate infected cells (11,52). Most proteins from *T. cruzi* are unsuitable for vaccine development in stimulating a defensive cellular immune response, as they are unlikely to efficiently engage the MHC-I antigen presentation pathway upon infection. Utilizing immunopeptidomics data, we can pinpoint the proteins that are capable of MHC-I presentation and subsequent recognition by CTLs.

Analysis of the immunopeptidome of *T. cruzi* infected fibroblasts revealed 24 unique *T. cruzi* peptides presented on MHC-I, along with over one thousand murine self-peptides. H2-K^b and H2-D^b MHC-I haplotypes were immunoaffinity isolated from *T. cruzi* infected and uninfected murine MC57G fibroblast cells, using the anti-H2 M1/42 mAb (53). Upon *T. cruzi* infection of fibroblasts, an increase in M1/42 binding to the cells was observed, demonstrating an upregulation of MHC-I presentation. Contradicting reports suggesting MHC-I downregulation by *T. cruzi* as a strategy to evade T cell immune detection, while upregulation has also been observed (54–56). The upregulation of MHC-I molecules observed in our study may also explain the higher abundance of mouse self-peptides in the infected fibroblast samples compared to the uninfected sample.

The identified 24 unique MHC-I presented *T. cruzi* peptides were originating from 17 distinct proteins, reflecting the availability of these proteins for processing and presentation on MHC-I of murine fibroblasts. Notably, Tcj2 protein was identified as the source of six different peptides, and Tcj2 was the only protein identified in both immunopeptidomics experiments, making Tcj2 our most promising vaccine candidate antigen for inducing MHC-I restricted cytotoxic T cells. Of the other 17 proteins, several are known to be involved in intracellular endogenous processes, such as ribosomal proteins, oxidases, dehydrogenases, helicases, and heat shock proteins, indicating their intracellular localization and functions. However, KMP-11, one of the 17 identified proteins, is a membrane protein that has been shown to be at least partially exposed on the surface of *T. cruzi* trypomastigotes, since KMP-11 antisera can affect parasite invasion and flagellar motility (57). Three proteins remain uncharacterized even after blasting their protein sequence, leaving their subcellular localization and functions to be determined. Remarkably, no trans-sialidases derived peptides were found, while it has been observed that these proteins are highly expressed in trypomastigotes, located on the outside of the plasma membrane, sometimes GPI-anchored, and are immunodominant for CD8+ T cells during natural infection (58,59). Given that trans-sialidase – specific CD8+ T cells did not recognize *T. cruzi* – infected cells within the first 48 hours after infection in previous research, the timing of our immunopeptidomics MHC-I profiling of *T. cruzi* at 48 post infection, – may

have been too closely aligned with this timeframe, potentially contributing to the absence or limited availability of trans-sialidase peptides (60).

We further focused on the potential of Tcj2 as a promising vaccine candidate. We assessed the antigen's conservation across various Trypanosomes and explored potential cross-reactivity with heat shock proteins in mice and humans. Sequence alignments revealed minimal overlapping peptide sequences shared by Tcj2 and mouse or human DnaJ, suggesting a reduced likelihood of inducing autoimmune reactions to self-DnaJ by Tcj2 mRNA vaccination in mice and humans. Furthermore, during the full duration of the *in vivo* immunogenicity study, the Tcj2 mRNA LNPs injected mice appeared clinically normal, supporting the safety profile of the Tcj2 mRNA vaccine. Additionally, Tcj2-specific antibodies generated through immunizations did not cross-react with native DnaJ expressed in mouse MC57G or human HEK293 cell lines, nor with native DnaJ from *Trypanosoma brucei* (61–63). Protein sequence alignments showed the existence of multiple stretches of identical amino acid sequences between DnaJ from *T. cruzi*, *T. brucei brucei*, *T. congolense* and *T. vivax*, suggesting there are potential overlapping epitopes for CTL for cross-protection between these different trypanosomes. Considering the conserved nature of Tcj2 across different *T. cruzi* DTUs, protection against all *T. cruzi* strains could be possible, but this will be dependent on the expression profile of Tcj2 between different *T. cruzi* DTUs.

Heat shock proteins are critical for maintaining the structural integrity of cellular protein machinery and function in protein folding, as well as in the degradation of misfolded proteins. In protozoans, such as *T. cruzi*, heat shock proteins like Tcj2 play vital roles in the parasite's ability to adapt to hostile and constantly changing environments. *T. cruzi* undergoes transitions between hosts and transmission vectors throughout its lifecycle, as well as switches between intracellular and extracellular stages. These environmental changes encompass variations in pH levels, temperature, oxidative stress, and immune responses (64). Therefore, it comes to no surprise that Tcj2 is described in literature to be expressed in different compartments of the *T. cruzi* trypomastigotes and amastigotes (40,44).

Vaccines targeting DnaJ proteins like Tcj2 have previously demonstrated effectiveness against various microbial pathogens. In the context of a vaccine candidate against typhoid, Saghi et al. administered recombinant DnaJ from *Salmonella enterica serovar Typhi* to mice and observed that this immunization approach induced robust humoral and cellular immune responses, resulting in 70% protection against a lethal challenge with *Salmonella typhimurium*, highlighting the potential of DnaJ as a vaccine target (65). Similarly, in the case of *Ureaplasma urealyticum* infection, DnaJ - immunizations have been shown to elicit a strong humoral and a Th1-mediated cellular immune response, along with a significant decrease in bacterial load and inflammation in the reproductive tract of mice (66). Moreover, Khan et al. demonstrated that vaccination with recombinant DnaJ protein from *Streptococcus pneumoniae* provided protection to 70% of mice against a lethal intranasal challenge with *S. pneumoniae* (67). These

findings collectively underscore the potential effectiveness of DnaJ proteins as a vaccine target against diverse pathogens.

We used our mRNA platform to evaluate the potential of Tcj2 as a vaccine against Chagas disease. *In vitro* assessments confirmed successful translation, MHC-I antigen presentation, and activation of antigen specific CD8+ T cells. When injected in C57BL/6J mice, Tcj2 mRNA induced robust humoral and cellular immune responses, including significant increases in cytotoxic T lymphocytes (CTLs) and associated cytotoxic enzymes and cytokines. Additionally, an *in vitro* killing assay demonstrated that splenocytes from Tcj2 mRNA immunized mice reduced *T. cruzi* infection, indicating the vaccine-induced effector functions. mRNA vaccines have demonstrated remarkable success in eliciting CD8+ T cell responses by efficiently presenting peptides on MHC-I to CD8+ T cells. Given the critical role of these T cells in identifying and killing parasite-infected cells, the mRNA vaccine platform presents a promising avenue for the creation of a Chagas disease vaccine (30). The Tcj2 mRNA construct was designed with a SIINFEKL-tag to assess MHC-I antigen presentation and CD8+T cell activation *in vitro*, along with a FLAG-tag to measure intracellular expression. These tags are very useful for development and evaluation of the mRNA vaccine constructs, but the case of clinical evaluations, these will be removed from the mRNA construct. Notably, high IgG2c antibody titers specific to the rTcj2 protein were detected, and these antibodies were also capable of binding native *T. cruzi* Tcj2 on western blot. Importantly, immune clearance of *T. cruzi* trypomastigotes has been largely attributed to the IgG2 isotype (68). However, it remains unknown whether Tcj2 is exposed on the surface of trypomastigotes and if antibodies could opsonize parasites. Furthermore, Tcj2 has been found to be secreted by trypomastigotes from different strains (Colombiana - TcI, Y strain - TcII, and CL Brener - TcVI) as part of the trypomastigote-derived secretome (69). These secreted proteins could potentially be captured by Tcj2-specific antibodies, and processed by the MHC-I pathway when parasites are intracellular.

Evaluation of the cellular responses following Tcj2 mRNA LNP immunizations revealed the strongest induction of CD8+ T cells, followed by $\gamma\delta$ T cells, while CD4+ T cells exhibited the lowest response. Antigen-specific central and effector memory CD8+ T cells produced cytotoxic enzymes granzyme B and perforin, as well as cytokines IFN- γ and TNF- α . The expansion of central memory CD8+ T cells is important for long-term immunological protection (70), while effector CD8+ T cells play a critical role in controlling ongoing *T. cruzi* infection (71). Moreover, there was also an increase in antigen-specific polyfunctional CD8+ T cells capable of secreting multiple cytokines, indicating a robust T cell response with potential immunological control against infectious diseases (72). Particularly for *T. cruzi* infection, polyfunctional T cell responses have been linked to effective anti-parasitic cell mediated immunity (73,74).

In the case of $\gamma\delta$ T cells, there was a significant increase in granzyme B-secreting cells upon *in vitro* restimulation with rTcj2. Although $\gamma\delta$ T cells have been studied less extensively than CD4+ and CD8+ T cells due to their unique properties, they have been implicated in

parasitic control during the acute phase of *T. cruzi* infection (75). $\gamma\delta$ T cells can act as modulators of Th1 responses and exert infection through cytotoxic action against infected cells (76). Similar observations have been made in other protozoan infections, such as *Plasmodium falciparum*, where they demonstrated the ability to recognize parasite-infected cells and eliminate them through the release of granzyme B (77). This suggests the potential of the increased granzyme B-producing $\gamma\delta$ T cells to exhibit similar effector functions in the context of *T. cruzi* infection.

We observed a minimal increase in antigen-specific CD4+ T cells upon *in vitro* restimulation, suggesting a low level of CD4+ T cell activation in response to the vaccine. This indicates that antigen processing and presentation via MHC-II might be occurring to a lesser extent, although the presence of Tcj2-specific IgG antibodies suggest the help and presence of Tcj2-specific CD4+ T helper cells. The Tcj2 mRNA vaccine is primarily expected to undergo cytosolic antigen processing and presentation on MHC-I, leading to the activation of CD8+ T cells (78). However, the observable trend in increase of CD4+ T cells producing granzyme B and IFN- γ after restimulation with rTcj2, as well as the presence of Tcj2-specific IgG2c antibodies in the sera, suggests also processing and presentation of Tcj2 through the MHC-II pathway. The observed low level induction of antigen-specific CD4+ T cells could be attributed to factors such as the mRNA delivery, the vaccination route, and the immunization schedule, as similar findings have been reported by Peng et al., showing a 10-fold lower activation of CD4+ T cells compared to CD8+ T cells upon antigen-specific restimulation (79).

This study has some limitations. i) MHC-I immunopeptidome screening: The reported experiments were limited to the screening of peptides presented by mouse fibroblasts (a matching model for our *in vivo* experiments). Human cell lines can be considered for complementary studies as well as different cell types, such as skeletal and cardiac muscle cells. The authors acknowledge the possibility that additional replicate studies, potentially at different times of infection, could unveil more peptides and identify additional vaccine antigen candidates. ii) No spectral match validation using synthetic peptides was conducted to validate the peptides identified from Tcj2. iii) Cross-reactive epitopes: structural similarities between peptides from Tcj2 and DnaJ proteins from mouse/human have not been evaluated, hence the risk of cross-reactivity cannot be excluded without further investigation. iv) The Tcj2 mRNA vaccine immunogenicity study: The group sizes were limited, and only one single formulation and a single dose was tested. Further investigations are essential for demonstrating the effectiveness of the Tcj2 mRNA vaccine candidate, including *in vivo* challenge studies and detailed cytokine analysis.

Although constrained by the mentioned limitations, our data showcases a pioneering application of immunopeptidomics in identifying novel vaccine targets for Chagas disease. Moreover, it underscores the mRNA platform's potential for rapid evaluation of new candidate antigens that stimulate antigen-specific CD8+ T cell responses. Further expanding on this work will increase the understanding of MHC-I presentation of *T. cruzi* antigens and identify the

dominant and subdominant protein peptides recognized by CTLs, which may result in more effective vaccines. Based on the *in vitro* and *in vivo* data presented in this study, we consider Tcj2 a potentially strong vaccine antigen for Chagas disease and are currently planning challenge experiments using *T. cruzi* of different DTUs.

5.4 MATERIALS & METHODS

Ethics statement

Animal experiments were performed in full compliance with the Public Health Service Policy and the National Institutes of Health Guide for the Care and Use of Laboratory Animals, 8th edition, under a protocol approved by Baylor College of Medicine's Institutional Animal Care and Use Committee, assurance number D16-00475 (80).

Animals used for studies

Female C57BL/6J and C57BL/6J OT-1 mice were obtained at 5-6 weeks of age from The Jackson Laboratory and allowed to acclimate for one week prior to any manipulation. Mice were housed in groups of 4 in small microisolator caging, with ad libitum food and water and a 12hr light/dark cycle.

Immunopectidomics

Preparation of *T. cruzi* trypomastigotes

To obtain parasites for the immunopectidomics experiments, 500 cm² TripleFlask treated cell culture flasks (ThermoFisher Scientific, Cat# 132913) were seeded with 5×10^6 VERO cells (ATCC, Cat# CCL-81) in cMEM media (MEM + 2% FBS + 1x pen/strep) and incubated overnight at 37° C, 5% CO₂. The following day, *T. cruzi* Tulahuen trypomastigotes (ATCC, Cat# 30266) were added to the flasks at a multiplicity of infection (MOI) of 5 and the flasks were returned to the incubator. After three days, the culture media was refreshed with fresh cMEM to provide optimal conditions for continued cell and parasite growth.

Infection of mouse fibroblasts with *T. cruzi* trypomastigotes

MC57G mouse fibroblasts (ATCC, Cat# CRL-2295) were cultured in cMEM media. To obtain enough peptides for LC-MS/MS analysis, a large quantity of infected cells was prepared to isolate the MHC-I complex from (13). First, fibroblasts were seeded in five 500 cm² TripleFlask treated cell culture flasks (ThermoFisher Scientific, Cat# 132913) in 100 mL cMEM media and incubated at 37° C, 5% CO₂. When the confluency reached >80%, fibroblasts were harvested from the flask using Accutase and counted using a Cellca MX automated cell counter (Nexcelom). Then, 30 culture flasks of 175 cm² were prepared with 8×10^6 cells per flask in 30 mL cMEM media. After a 48-hour incubation at 37° C, fibroblasts in one flask were

removed from the flask and counted. Based on the cell count, the number of parasites required to infect with a multiplicity of infection (MOI) of 7 was calculated.

To measure the MHC-I expression on *T. cruzi* infected MC57G fibroblasts, MC57G cells were seeded in 12-well plates in cMEM media and incubated overnight at 37 °C, 5% CO₂. The next day, *T. cruzi* trypomastigotes were added to the cells at an MOI of 7, and cells were further incubated for 48 hours. At the end of the incubation, extracellular parasites were washed off using 1x PBS, and cells were collected using Accutase. Detection of surface MHC-I was performed using an anti-mouse MHC-I Alexa Fluor 488 antibody (LS Bio, Cat# LS-C811400-50). Data was acquired using an Attune NxT flow cytometer (ThermoFisher Scientific). Data was analyzed using FlowJo and median fluorescent intensity (MFI) was reported (Supplementary Figure 8).

Preparation of lysate of *T. cruzi*-infected cells

At the end of the 48-hour incubation of fibroblasts with *T. cruzi* trypomastigotes, cells were washed twice with PBS of 4 °C followed by detachment from the flask using a cell scraper. Scraped cells were collected in 1x PBS in 50-mL tubes and centrifuged for 10 min at 2000 x g at 4° C. Supernatant was discarded and pellets were either snap frozen in liquid nitrogen and stored at -80° C, or directly lysed.

Lysing the cells was performed by adding twice the volume of lysing buffer (0.5% Igepal CA-630 (Sigma-Aldrich, Cat# I8896), 150 mM NaCl, 50 mM Tris HCl pH 8, cComplete mini protease inhibitor cocktail (Roche, Cat# 11836153001), and mass spectrometry-grade H₂O) to the cell pellet. After resuspending the pellet, the cells were incubated and rotated for 1 hour at 4° C. The lysed cells were then centrifuged for 10 min at 2000 x g to pellet their nuclei. The supernatant was transferred to a new tube and centrifuged for an additional 1 hour at 19,000 x g at 4° C. The supernatant was then filtered through a 0.45 µm and 0.2 µm filter to remove any possible particles that might clog the immunoaffinity purification column. Importantly, filters were prerinced with in succession H₂O, methanol and again H₂O to remove plastic particles from the filter.

Preparation of M1/42 monoclonal antibody

M1/42 (M1/42.3.9.8) is a TIB-126 hybridoma-produced clone of an IgG2c rat monoclonal antibody that specifically binds to H-2 (MHC-I) haplotypes a, b, d, j, k, s, and u in mice (81). TIB-126 hybridomas were purchased from ATCC and cultured in 30 mL complete IMDM media (Iscove's DMEM + 10% FBS (with IgG depleted (ThermoFisher Scientific, Cat # 16250078) + 1x pen/strep) in 175 cm² non-treated tissue culture flasks (Falcon, Cat# 355001) at 37 °C, 5% CO₂. Every 2-3 days, the viability of the cells was assessed and 3 mL of complete IMDM media was added. When the viability dropped below 50%, cell culture supernatant containing M1/42 was harvested by pelleting cells for 5 min at 400 x g. The supernatant was then filtered through a 0.45 µm filter and diluted with IgG binding buffer (Pierce, Cat# 21011) to a final pH of 5-5.5. The low pH is optimal for IgG binding to Protein G, and will improve the yield of the purification

(82). Using a peristaltic pump, the diluted supernatant was loaded onto a HiTrap protein G HP prepacked column (Cytiva, Cat# 45-000-053) that was pre-equilibrated with IgG binding buffer. Subsequently, the column was rinsed with IgG binding buffer followed by the elution of the bound M1/42 using pH 2.8 IgG elution buffer (Pierce, Cat# 21004). Tris-HCl pH 9 was added to the eluted M1/42 to establish a neutral pH, followed by dialysis using a 3,500 MWCO dialysis cassette (ThermoFisher Scientific, Cat# 66110) with 1x PBS pH 7.4 with multiple changes of dialysis buffer to remove traces of Tris. Finally, M1/42 monoclonal antibody (mAb) was analyzed by Coomassie SDS-PAGE to check for purity.

To test the functionality of the M1/42 antibodies, MC57G fibroblasts were first infected with *T. cruzi* Tulahuen trypomastigotes. After 48 hours, cells were rinsed with PBS and detached from flask using Accutase. Cells were incubated for 30 min at 4° C with M1/42 mAb purified from the TIB-126 hybridoma cell line, followed by ten washes with staining buffer (2% FBS in PBS) using the Laminar Wash HT2000 (Curiox Biosystems). Bound M1/42 to MC57G cells was then detected by a 30 min incubation with goat anti-mouse IgG PE (ThermoFisher Scientific, Cat# P-852) at 4 °C. After incubation, cells were washed 15 times, followed by analysis on a Guava Muse flow cytometer (Cytex).

Immuno-affinity purification

To prepare the immunoaffinity purification column, the previously purified M1/42 mAb was covalently linked to AminoLink Plus Coupling Resin (ThermoFisher Scientific, Cat#20501). Following the manufacturers recommendations, 5 mL of settled resin was incubated with 11.5 mg of M1/42 mAb in pH 7.2 1x PBS in a 15-mL tube. Cyanoborohydrate solution was added to a final concentration of 50 mM and resin was rotated overnight at 4° C. The next day resin was washed with coupling buffer followed by a wash with pH 7.5 quenching buffer (1M Tris HCl, pH 7.5). Next, resin was gently rocked for 30 min in 50 mM Cyanoborohydrate in quenching buffer. Then the resin was transferred to two 1.5 cm glass chromatography columns (Bio-Rad, Cat#7374150). After allowing it to settle, resin was washed with 1 M NaCl followed by a final wash with pH 7.2 coupling buffer with 0.05% sodium azide. Columns were then wrapped in aluminum foil to avoid light exposure and stored until use at 4° C.

Isolation and purification of MHC-I – peptide complexes was performed using an adapted method from Purcell and colleagues (83). Mass spectrometry grade H₂O (Optima, Cat# W64) was used to prepare all buffers which were freshly prepared. Briefly, the immunoaffinity purification column, consisting of M1/42 mAb covalently coupled to the AminoLink resin, was equilibrated with wash buffer 1 (0.005% Igepal CA-630, 150 mM NaCl, 50 mM Tris HCl pH 8, 5 mM EDTA, 100 μM PMSF, 1 μg/mL pepstatin A). Then cell lysate was passed over the column for four consecutive times, allowing all the MHC-I-peptide complexes to bind to the column. Next, a series of washes was performed; wash buffer 1 to remove unbound proteins, wash buffer 2 (150 mM NaCl, 50 mM Tris HCl pH 8) to remove detergent, wash buffer 3 (450 mM NaCl, 50 mM Tris HCl) to remove non-specific material, and last wash buffer 4 (50 mM Tris HCl) to remove salt. Finally, 10% acetic acid was used to elute the MHC-I-peptide complexes. The low

pH of the elution buffer will unfold the MHC-I complex, resulting in elution of the peptides from the MHC-I binding cleft. Next, the peptides were separated from the unfolded MHC-I complex using a 10 kDa Amicon Ultra centrifugal filter (MilliPore Sigma, Cat# UFC801024) that was prerinsed with successively milliQ water, methanol, milliQ water, and finally 10% acetic acid. The flow-through was concentrated to 100-250 μ L using a speed vac and then stored at -80° C for LC-MS/MS analysis.

Mass spectrometry

Peptides were cleaned up using a HyperSep C18 cartridge (Thermo 60108-376). Cartridges were rinsed with 500 μ L of 80% Acetonitrile 0.1% formic acid, then with 500 μ L 50% acetonitrile 0.1 % formic acid, and equilibrated with 1 mL of LCMS grade water in 0.1% formic acid. Immunopeptides were loaded onto the cartridge and the cartridge washed with 500 μ L of the 0.1% formic acid solution. Peptides were eluted with 300 μ L of 50% acetonitrile, 0.1% formic acid and then dried in a speed vac and resuspended in 30 μ L of 2% acetonitrile, 0.1% formic acid, 97.9% water and placed in an autosampler vial.

Samples were analyzed by nanoLC-MS/MS (nanoRSLC, ThermoFisher) using an Aurora series (Ion Opticks) reversed phase HPLC column (25 cm length x 75 μ m inner diameter) directly injected into a ThermoScientific Orbitrap Eclipse using a 160 min method (mobile phase A = 0.1% formic acid (Thermo Fisher), mobile phase B = 99.9% acetonitrile with 0.1% formic acid (Thermo Fisher); hold 3% B for 15 min, 3-22% B in 95 min, 22-38% for 24 min, 38%-90% for 2min, hold at 90% for 2min, 90-5% in 2 min, followed by a second quick gradient and equilibration) at a flow rate of 300 μ L/min. Eluted peptide ions were analyzed using a data-dependent acquisition (DDA) method with resolution settings of 120,000 and 7,500 (at m/z 200) for MS1 and MS2 scans, respectively. DDA-selected peptides were fragmented using high energy collisional dissociation (30%).

PEAKS version X software was used to process all data dependent acquisition mass-spectral data (84). Proteins identifications were obtained by searching a database of *Mus Musculus* C57BL/6J obtained from Uniprot (6th October 2017) and a database of *Trypanosoma cruzi* CL Brener obtained from Uniprot (23rd October 2021, UP000002296). The following data analysis parameters were used: enzyme set to none, digest mode set to unspecific, up to three variable modifications including oxidation of methionine as well as deamidation of asparagine and glutamine, parent mass error tolerance of 15 ppm, fragment mass error tolerance of 0.02 Da, charge states between 1 and 7 were accepted, the peptide -10LgP score was left at the default 15 and the protein -10LgP score was left at the default 20 corresponding to protein false discovery rates of 1.6% and 2.5%. Peptide sequence lengths between 8 and 15 amino acids were selected for further analysis.

Protein sequence alignments

To compare the Tcj2 protein sequence between different strains of *T. cruzi*, amino acid sequences of ortholog syntenic genes of Tcj2 of the following strains were downloaded from TriTrypDB.org (accessed on May 23rd, 2023): Dm28c (C4B63_175g9), Sylvio X10/1 (TCSYLVI0_003497), G (TcG_07973), Brazil A4 (TcBrA4_0100200), Berenice (ECC02_009221), Y C6 (TcYC6_0075780), CL Brener Esmeraldo-like (TcCLB.511627.110), TCC (C3747_88g53), and CL (TcCL_ESM07472). Multiple sequence alignments were done using Clustal Omega, and the results were ordered by The Distinct Types Units (DTUs) genetic classification each strain belongs to (85).

Additionally, homologous DnaJ protein sequences of *Trypanosoma rangeli* (TRSC58_00469), *Trypanosoma brucei brucei* (Tb927.2.5160), *Trypanosoma congolense* (TcIL3000_2_1270) and *Trypanosoma vivax* (TvY486_0007950) were also compared to *T. cruzi* Tcj2 by multiple sequence alignment using Clustal Omega.

Comparison of DnaJ-homolog protein sequences between species *Trypanosoma cruzi*, *Mus musculus* and *Homo sapiens* were also performed. *T. cruzi* Tcj2 (Uniprot: Q4D832) was ran through protein BLAST (<https://blast.ncbi.nlm.nih.gov>) and results were filtered for *M. musculus* or *H. sapiens*. From the significant alignment results list, the sequence with the best score (lowest E value) was selected, resulting in DnaJ homolog subfamily A member 4 isoform 2 (NP_067397.1) for *M. musculus* and DnaJ homolog subfamily A member 4 isoform 2 (NP_001123654.1) for *H. sapiens*. Using Clustal Omega the multiple sequence alignment was performed.

mRNA vaccine construct encoding *T. cruzi* Tcj2

A mRNA vaccine construct encoding for *T. cruzi* Tcj2 (Uniprot: Q4D832) was ordered from the RNAcore of Houston Methodist Research Institute. At the C-terminus of the Tcj2 protein, the amino acid sequence SIINFEKL was added, followed by the sequence for a FLAG-tag. The complete sequence was optimized for improved RNA translation. Uridine was replaced by N1-Methylpseudouridine during the *in vitro* transcription of the mRNA to achieve improved translation and vaccine efficacy (86,87). mRNA was capped using CleanCap (Trilink Technology). An automated electrophoresis gel (Tapestation, Agilent) was ran by the RNAcore, to verify the study integrity of the Tcj2 mRNA (**Supplementary Figure 9**).

In vitro testing of Tcj2 mRNA construct

MHC-I presentation

The DC2.4 murine dendritic cell line (Millipore Sigma, Cat# SCC142) was cultured in DC2.4 media (RPMI 1640 + L-glutamine, 10% FBS, 1x pen/strep, 1x non-essential amino acids, 10 mM HEPES, 55 μ M β -mercaptoethanol) and used for *in vitro* transfections. DC2.4 cells were

seeded at 240,000 per well in 12-well culture plates and incubated overnight at 37° C. The following day, cells were transfected with 1 µg Tcj2 mRNA in 2 µL Lipofectamine MessengerMAX (Invitrogen, cat# LMRNA001) and Opti-MEM (Gibco, Cat# 31985062) per well according to manufacturer's instructions. As controls, cells were transfected with 1 µg of ovalbumin expressing mRNA (5MoU modified, TriLink, Cat# L-7210) in 2 µL Lipofectamine MessengerMAX or with transfection agent only. After 24 hours incubation at 37 °C, transfected cells were harvested by a 15-minute incubation with Accutase (Sigma-Aldrich, Cat# A6964) followed by the use of a cell scraper. Cells were washed using DC2.4 media and centrifugation, and cell viability and concentration was measured using ViaStain AO/PI viability dye (Nexcelom, Cat# CS2-0106) and the Cellaca MX automated cell counter (Nexcelom, PerkinElmer).

Intracellular detection of FLAG-tag

The expression of Tcj2 protein after mRNA transfections was assessed by flow cytometry using intracellular staining of the FLAG-tag incorporated in the Tcj2 mRNA construct. For all the washing steps in this protocol the Laminar Wash HT2000 (Curiox Biosystems) was used for improved cell viability and recovery. Briefly, 100,000 transfected cells were added per well in a laminar wash 96-well plate (Curiox, Cat# 96-DC-CL-05) and the plate was incubated for 20 min at 4° C. After the cells were settled, ten washes with staining buffer (2% FBS in PBS) were performed and cells were resuspended in Cytotfix/Cytoperm (BD, Cat# 51-2090KZ). After a 20 min incubation at 4 °C, cells were washed 10x in 1x Perm/Wash buffer (BD, Cat# 51-2091KZ). Then, cells were resuspended in 25 µL 1x Perm/Wash buffer and 1 µL of mouse Fc Block (BD, Cat# 553142) was added and cells were incubated for 5 min at 4° C. Subsequently, anti-FLAG M2-Cy3 antibody (Sigma-Aldrich, Cat# A9594) was diluted 1:100 in 1x Fix/Perm buffer and 45 µL was added to the cells. Following a 30 min incubation at 4° C, cells were washed 15x in staining buffer. Cells were then transferred from the laminar wash plate to 1.5 mL Eppendorf tubes and analyzed for intracellular FLAG-staining using a Guava Muse flow cytometer (Cytex).

Presentation of SIINFEKL peptide on MHC-I

To assess MHC-I presentation of peptides derived from the translated Tcj2 mRNA, DC2.4 cells were stained with fluorophore conjugated antibody that recognizes SIINFEKL peptide bound to H2-K^b. To each well of a laminar wash 96-well plate (Curiox, Cat# 96-DC-CL-05) 100,000 transfected cells were added and the plate was incubated for 20 min at 4 °C. After the cells were settled, ten washes with staining buffer (2% FBS in PBS) were performed using the Laminar Wash HT2000. Cells were then resuspended and 1 µL of mouse Fc Block was added and cells were incubated for 5 min at 4 °C, followed by the addition of 0.625 µL PE anti-mouse H-2K^b bound to SIINFEKL Antibody (Biolegend, Cat# 141604). After a 30 min incubation at 4 °C, cells were washed 15x in staining buffer. Cells were then transferred from laminar wash plate to 1.7 mL Eppendorf tubes and analyzed for intracellular FLAG using a Guava Muse flow cytometer (Cytex).

Activation of SIINFEKL-specific T cells

In vitro co-culture experiments were conducted to examine the activation of naïve CD8⁺ T cells by mRNA transfected cells by measuring the cytokine secretions in the supernatant 24 hours after the start of the co-culture. DC2.4 cells were cultured and transfected with Tcj2 mRNA, Ovalbumin mRNA (positive control), or only the transfection agent Lipofectamine MessengerMAX (negative control) as earlier described. The following day cells were harvested using Accutase and counted using the Cellaca MX automated cell counter. Transfected DC2.4 cells were then seeded in 96-well culture plates at 75,000 cells per well in DC2.4 media and incubated at 37 °C, 5% CO₂. In the meantime, splenocytes from naïve C57BL/6J mice or naïve C57BL/6J OT-1 mice were thawed from -150 °C in DC2.4 media and counted. Five hours after the transfected DC2.4 cells were seeded, 750,000 C57BL/6J or C57BL/6J OT-1 splenocytes were added to designated wells and incubation was continued overnight. After 24 hours, the 96-well culture plate was centrifuged for 5 min at 300 x g to pellet cells, and supernatant was harvested and frozen at -80 °C. To analyze the cytokines that were secreted during the co-culture, a Luminex cytokine assay was performed on the culture supernatants. A MILLIPLIX MAP Mouse CD8⁺ T Cell Magnetic Bead Panel kit (Millipore Sigma, Cat# MCD8MAG-48K) containing the analytes Granzyme B, IFN- γ , TNF- α , IL-2, IL-6 and IL-4 was used in combination DropArray technology according to a previous published method (88).

mRNA vaccine formulation in Lipid Nanoparticles (LNPs)

Tcj2 mRNA LNPs were prepared using the Genvoy ILM kit (Precision Nanosystems, Cat# NWW0042) according to the manufacturer's recommendation. The kit contains PNI ionizable lipid, DSPC, Cholesterol and PNI stabilizer at a mol% of 50, 10, 37.5 and 2.5, respectively. The Tcj2 mRNA LNPs were prepared at N:P ratio (nitrogen to phosphate) of 4:1 and formulated using a NanoAsmblr Ignite (Precision Nanosystems) instrument. LNPs without mRNA were prepared as controls (hence called empty LNPs). After formulation, LNPs were concentrated using 10 kDa spin filter columns and 0.2 μ m sterile filtered. Using a RiboGreen RNA Assay Kit (Invitrogen, Cat# R11490) and 1x TE buffer with and without TritonX100 detergent, the RNA concentration in the LNPs was calculated. The LNPs were then diluted in 1x PBS with a final concentration of 8% sucrose to increase their stability during freezing (79). These vaccine formulations were stored at -80 °C until use.

To characterize the LNPs, average LNP size and polydispersity index was determined by dynamic light scattering (DLS) using a DynaPro Plate Reader II instrument (Wyatt). Samples were diluted in PBS prior to testing.

To measure the pKa (charge) of the surface of the LNPs, a 2-(p-toluidino)-6-naphthalene sulfonic acid (TNS) fluorescent assay was conducted according to methods published by Patel *et al* (49). Data was analyzed using Prism 9 and a four-parameter dose-response curve was fitted to the data points to obtain the pKa (IC₅₀ of the data).

Production of recombinant Tcj2 protein

To produce recombinant Tcj2 protein, a pET41 a(+) expression vector was designed containing the *T. cruzi* Tcj2 sequence (Uniprot: Q4D832) followed by a His6-tag at the C-terminus. The sequence was codon optimized for protein expression in *E. coli* (Genscript). For protein expression, *E. coli* BL21 cells containing Tcj2-pET41a vector were cultured in LB media at 37° C in the presence of kanamycin to an O.D. of 0.6. Subsequently, protein expression was induced with 0.5 mM IPTG at 22° C for 4 hours. Next, *E. coli* cells were harvested by centrifugation followed by cell lysis of the pellet using Bugbuster protein extraction reagent (Millipore, Cat# 70584). The recombinant Tcj2 protein was initially purified by Immobilized Metal Affinity Chromatography (IMAC) using the HisTrap FF column (Cytiva, Cat# 17525501). The sample was applied to this column after first adding 2M urea. The column was washed with IMAC buffer (30 mM Tris-HCl pH 7.5, 500 mM NaCl) with 2 M urea and bound protein was refolded using a linear gradient of 2-0 M urea in IMAC buffer. After further washing the column with IMAC buffer with 20 mM imidazole, bound protein was eluted using a linear gradient of 0-500 mM imidazole in IMAC buffer. Then, the protein was further purified using a Butyl Sepharose column (Cytiva, Cat# 28411001). Therefore, ammonium sulfate salt was added to a final 1 M concentration to the IMAC purified protein. The column was washed with HIC buffer (20 mM Tris-HCl pH 8) with 1 M ammonium sulfate and bound protein was eluted in a linear gradient of 1 – 0 M ammonium sulfate in HIC buffer. Finally, removal of endotoxin was done by incubating the purified rTcj2 protein with Triton X-114, followed by Triton elimination using SM2 beads as earlier described (89). After buffer exchange with 1x PBS by dialysis, final rTcj2 protein was stored at -80° C, and aliquots of rTcj2 were ran by SDS-PAGE followed by Coomassie staining or western blotting detecting HIS-tag using AP-conjugated anti-His tag antibody (ThermoFisher Scientific, Cat# R932-25).

In vivo mouse immunogenicity study

Ten female C57BL/6J mice (The Jackson Laboratory) were used for the *in vivo* immunogenicity study. At 6-8 weeks of age, five mice were immunized with 10 µg Tcj2 mRNA formulated in LNPs. Five other mice received empty LNPs as a negative control. Immunizations were administered intramuscular in the hind muscle with a volume of 50 µL. Twenty-one days after the first immunization, mice received booster immunization in an identical way as described for the primary immunization and were euthanized at day 40. Throughout the study all animals appeared clinically normal.

Processing sera and spleens

At day 40, mice were anesthetized by an intraperitoneal injection with ketamine/xylazine. Blood was collected through a cardiac puncture, followed by the harvest of the spleen. Sera was prepared by allowing the blood to clot in Z-Gel sera collection tubes (Sarstedt, Cat# 101093-958), followed by centrifugation for 5 min at 10,000 x g. The sera were transferred to new tubes and stored at - 80° C until further use. For processing the spleens to single cell

suspensions, all steps were performed at 4 °C or on ice. First, spleens were rinsed in 1x PBS, transferred to gentleMACS C tubes (Miltenyi Biotec, Cat# 130-093-237) and then dissociated to a single cell suspension using the gentleMACS Dissociator (Miltenyi Biotec). After pelleting the splenocytes by centrifugation for 5 min at 300 x g, 1 mL ACK lysing buffer was added to lyse the red blood cells. After 1 min incubation on ice, 20 mL 1x PBS was added to stop the lysing reaction and splenocytes were centrifuged another time. Subsequently, supernatant was discarded and splenocytes were resuspended in complete RPMI (cRPMI) consisting of RPMI 1640 with L-Glutamine, 10% heat-inactivated fetal Bovine serum (FBS) and 1x pen/strep. Splenocytes were passed through a 40 µm strainer, and viability and concentration were assessed using a Cellca MX automated cell counter (Nexcelom, PerkinElmer) and ViaStain AO/PI viability dye (Nexcelom, Cat# CS2-0106). Splenocyte suspensions were stored at 4° C until further use.

SIINFEKL-specific CD8+ T cell analysis

Splenocytes were washed once in 1x PBS and transferred to a laminar wash plate. After a 30 min incubation at 4° C to settle the cells, the laminar wash plate was washed 10x using the Laminar Wash HT2000 (Curiox Biosystems). Splenocytes were resuspended in 1:1000 diluted LIVE/DEAD Fixable Near-IR Dead Cell Stain (Invitrogen, Cat# L34975) and incubated at 4° C. After 30 min, the laminar wash plate was washed for 10x with staining buffer (2% FBS in 1x PBS) followed by the addition of mouse Fc block (BD, Cat# 553141). After a 5 min incubation, splenocytes were stained with Pacific Blue anti-mouse CD3ε (Biolegend, Cat# 100334), PerCP-Cy5.5 Anti-Mouse CD8a (BD, Cat# 551162) and PE labeled SIINFEKL-loaded mouse H-2K^b tetramer (MHC Tetramer Production Facility, Baylor College of Medicine). After a 30 min incubation at 4° C, cells were washed 10x with staining buffer followed by addition of BD Cytotfix buffer (BD, Cat# 554655) to fix the cells. After 30 min at 4° C, cells were washed 15x with staining buffer. Cells were analyzed using an Attune NxT flow cytometer (ThermoFisher Scientific) and data was analyzed using VenturiOne software V6 (Applied Cytometry). Gating strategy can be observed in **Supplementary Figure 10**.

Enzyme-Linked Immunosorbent Assay (ELISA) detecting anti-Tcj2 antibodies

Indirect ELISAs were performed to assess Tcj2-specific antibody titers of total IgG, IgG1 and IgG2c. The 96-well ELISA plates were coated overnight at 4° C with 0.25 µg/mL rTcj2 diluted in KPL coating solution (SeraCare, Cat# 5150-0014). The following day the coating solution was discarded, and wells were blocked for two hours at room temperature with dilution buffer (0.1% Bovine Serum Albumin (BSA) in 1x PBS + 0.05% Tween-20 (PBST)). Mouse serum was serially diluted two-fold in dilution buffer, starting at 1:200. As a negative control, a pool of naïve sera was diluted at 1:200. After blocking, dilution buffer in wells was discarded, wells were washed once using a BioTek 405TS plate washer and PBST, and 100 µL of diluted sera or negative control pooled sera was added to designated wells in duplicate. After a two-hour incubation at room temperature, the plate was washed four times, followed by the addition of 100 µL/well goat anti-mouse IgG HRP (Lifespan Bioscience), goat anti-mouse IgG1 HRP (Lifespan Bioscience), or goat anti-mouse IgG2c HRP (Lifespan Bioscience). After one hour of

incubation at room temperature, the plates were washed five times with PBST followed by a 15 min incubation with 100 μ L/well TMB substrate (KPL). The color reaction was stopped by the addition of 100 μ L/well 1M HCl, and the absorbance at 450 nm was measured using a spectrophotometer (Epoch 2, BioTek). To analyze the results, the OD₄₅₀ values from duplicate wells were first averaged. Then the antibody titer cutoff value was calculated using the formula: average of naïve sera control + 3 x standard deviation of the naïve sera control. Represented are end-point antibody titers, defined as highest serum dilution that still resulted in an OD₄₅₀ value above the cutoff value. When a sample did not show any signal at all and the antibody titer could not be calculated, an arbitrary baseline antibody titer value of 67 was assigned.

Native Tcj2 western blots

Western blots were performed to analyze Tcj2 in *T. cruzi* lysate, as well as testing for cross-reactivity of homologous-DnaJ protein in lysates from MC57G mouse fibroblasts and HEK293T human kidney cells. *T. cruzi* Tulahuen lysate was prepared according to previous published methods (90). For lysates from MC57G and HEK293T cells, cells cultured in flasks were washed three times with 1x PBS to remove culture media and cells were detached from the flask using a cell scraper. Cells were collected by centrifugation and resuspended in 500 μ L RIPA buffer (ThermoFisher Scientific, Cat# 89900) and incubated on ice for 15 min. Then, lysed cells were centrifuged for 15 min at 12,000 x g and the supernatant was collected and filtered through a 0.2 μ m filter. Protein concentration was quantified using a BCA protein quantification kit (ThermoFisher Scientific, Cat# 23225) according to manufacturer's recommendations.

Cell lysate were loaded on a 4-12% Bis-Tris SDS-PAGE gel, using rTcj2 protein as a positive control and Bovine Serum Albumin (BSA) as a negative control. The SDS-PAGE gel was run for 75 min at 140 V, followed by blotting of the proteins to nitrocellulose. The blot was incubated overnight at 4° C with pooled Tcj2 antisera diluted 1:5000 in 1% non-fat dry milk in PBST. Goat anti-mouse IgG alkaline phosphatase (KPL, Cat# 5220-0357) diluted 1:5000 in PBST was used as a secondary detection antibody. For confirmation of human DNAJA4 in HEK293T cell lysate, an anti-human DNAJA4 Polyclonal Antibody (ThermoFisher Scientific, Cat# PA5-65311) was used at a 1:500 dilution and in combination with ECL substrate (Cytiva, Cat# RPN2236).

Analysis of antigen-specific T cells by flow cytometry

To assess the induction of Tcj2 specific T cells by the mRNA vaccine, 1 x 10⁶ live splenocytes were seeded per well in a 96-well culture plate and restimulated with 10 μ g/mL rTcj2 protein in cRPMI media *in vitro*. Unstimulated (negative) and PMA/I (positive) stimulated controls were included for each splenocyte sample. Splenocytes were incubated for 48 hours at 37° C, 5% CO₂, with the last 5 hours in presence of Brefeldin A (BD Biosciences, Cat# 555029) to retain cytokines intracellularly. After this incubation, cells were transferred to a laminar wash 96-well plate (Curiox, Cat# 96-DC-CL-05) and the plate was incubated for 20 min at 4° C. For all the washing steps in this protocol the Laminar Wash HT2000 (Curiox Biosystems) was used for improved cell viability and recovery. After the cells were settled, ten washes with

1x PBS were performed and cells were resuspended in viability dye (Table 2). After a 30 min incubation at 4° C, ten washes with staining buffer (2% FBS in PBS) were performed. Then the Fc receptors CD16/CD32 on the cell surface were blocked with 2 µL mouse Fc Block (BD, Cat# 553142) per well for 5 min, followed by the addition of the surface marker antibody cocktail (containing CD3, CD4, CD8, CD19, CD25, CD44, CD62L, CD127 and TCRγδ, Table 2). After a 30 min incubation at 4° C, ten washes with staining buffer (2% FBS in PBS) were performed and cells were resuspended in Cytofix/Cytoperm (BD, Cat# 51-2090KZ). After a 20 min incubation at 4° C, cells were washed 10x in 1x Perm/Wash buffer (BD, Cat# 51-2091KZ), followed by the addition of the intracellular marker antibody cocktail (containing IL-17A, Granzyme B, IL-10, IFN-γ, TNF-α and perforin, Table 2). Following a 30 min incubation at 4° C, cells were washed 15x in staining buffer. Cells were then transferred from laminar wash plate to 96-well culture plates and analyzed using an Aurora spectral flow cytometer (Cytek). To unmix the raw data, single stained cell and bead controls were used. Further analysis of flow cytometry data was done using FlowJo software. Gating of cell populations was done using Fluorescence minus one (FMO) samples and untreated controls (**Supplementary Figure 11**). The %-values of populations from unstimulated cells were subtracted from %-values from rTcj2-stimulated cells to obtain the antigen-specific results.

■ **Table 2.** Flow cytometry fluorophore-conjugated antibodies and viability dye used for the experiment.

Target	Fluorochrome	Clone mAb	Manufacturer	Catalogue #
CD3	APC/Fire 810	17A2	Biologend	100268
CD4	BV605	RM4-5	BD Biosciences	563151
CD8a	BUV615	53-6.7	BD Biosciences	613004
CD19	BV480	1D3	BD Biosciences	566167
CD25	BB790	PC61	BD Biosciences	624296
CD44	BV570	IM7	BD Biosciences	624298
CD62L	APC-Cy7	MEL-14	BD Biosciences	560514
TCRγδ	PE-Cy5	eBioGL3	Life technologies	15-5711-82
IL-17A	BV786	TC11-18H10	BD Biosciences	564171
Granzyme B	BV421	GB11	BD Biosciences	563389
IFN-γ	PE	XMG1.2	Biologend	505808
TNF-α	BV510	MP6-XT22	Biologend	506339
Perforin	FITC	S16009A	Biologend	154310
Viability	ViaDye™ Red Fixable Viability Dye	N/A	Cytek	R7-60008

***In vitro* T. cruzi – infected fibroblast killing assay**

To measure the cytotoxic effector functions of CD8+ T cells from immunized mice, a co-culture between *T. cruzi* infected MC57G fibroblasts and splenocytes was conducted. First, 15,000 MC57G murine fibroblasts were seeded in 96-well flat-bottom culture plates and incubated overnight at 37 °C, 5% CO₂. The next day, 150,000 β-galactosidase-expressing *T.*

cruzi trypomastigotes (Tulahuen, *LacZ*) (BEI Resources, Cat# NR-18959) were added to the fibroblasts and culture plates were further incubated at 37 °C, 5% CO₂. After 24 hours, media in wells was removed with a multichannel pipet and wells were washed twice with 1x PBS to remove extracellular *T. cruzi* trypomastigotes. Subsequently, 1 x 10⁶ live splenocytes were added to designated wells in complete co-culture media (RPMI 1640 + L-glutamine, 10% FBS, 1x pen/strep, 1x non-essential amino acids, 10 mM HEPES, 55 μM β-mercaptoethanol). In addition, naïve C57BL/6J were added to designated wells as negative controls, as well as 100 μM benznidazole (Sigma, Cat# 419656-1G) as positive control for *T. cruzi* killing. In addition to *T. cruzi* – infected fibroblasts, a similar co-culture was prepared with non-infected fibroblasts. Finally, the co-culture was then incubated for 72 hours. Afterwards, supernatant was harvested for cytokine analysis, and cells were incubated with 1% Igepal-630 in PBS supplemented with 100 μM Chlorophenol Red-β-D- galactopyranoside. After a 4-hour incubation at 37 °C to lyse the cells and convert the substrate, the substrate conversion by β-galactosidase was analyzed by measuring the absorbance at 570 nm using a spectrophotometer (Epoch 2, BioTek). For analysis of the results, OD₅₇₀ values of co-cultures without *T. cruzi* – infected fibroblasts were first subtracted from OD₅₇₀ values from co-cultures with *T. cruzi* – infected fibroblasts to remove background. Then, the OD₅₇₀ values were normalized between maximum killing of intracellular *T. cruzi* parasites (co-culture with 100 μM benznidazole) and no killing of intracellular *T. cruzi* parasites (co-culture with naïve C57BL/6J splenocytes).

Data analysis

All data was plotted with Prism 9 (GraphPad) and analyzed for statistical significance using a non-parametric Mann-Whitney U test. Stars representing statistical significance indicate the following: *: p < 0.05, **: p < 0.01, ***: p < 0.001.

Author contributions

LV, ET and JP designed the study. LV, RA, RG, JL, JW, BK, WR, MJV and CP conducted the experiments. LV and WR analyzed the data. KJ, MEB and PH contributed to the overall scientific strategy and secured funding. LV drafted the manuscript. All authors reviewed and edited the manuscript.

(Leroy Versteeg, Rakesh Adhikari, Gonteria Robinson, Jungsoon Lee, Junfei Wei, Brian Keegan, William Russell, Maria Jose Villar, Cristina Poveda, Kathryn Jones, Maria Elena Bottazzi, Peter Hotez, Edwin Tijhaar, Jeroen Pollet)

Acknowledgements

This research was supported by funding from the Southern Star Medical Research Institute and intramural funds from Texas Children's Hospital Center for Vaccine Development at Baylor College of Medicine. This project was also supported by the Cytometry and Cell Sorting Core at Baylor College of Medicine with funding from the NIH (NIAID P30AI036211, NCI

P30CA125123, and NCRR S10RR024574) and the assistance of Joel M. Sederstrom. The LC-MS/MS analysis was conducted at The University of Texas Medical Branch's Mass Spectrometry Facility and supported by the Cancer Prevention Research Institute of Texas (CPRIT) grant no. RP190682.

The authors would like to extend their sincere appreciation to Dr. Ziyin Li from the Department of Microbiology and Molecular Genetics at UT Health for generously providing the *T. brucei brucei* lysate. Additionally, we would like to express our heartfelt gratitude to all the scientists from the Houston Methodist RNA Core for their invaluable contributions and support in the development and generation of our mRNA.

Competing Interests

Leroy Versteeg, Rakesh Adhikari, Jungsoon Lee, Junfei Wei, Brian Keegan, Maria Jose Villar, Cristina Poveda, Kathryn Jones, Maria Elena Bottazzi, Peter Hotez, and Jeroen Pollet collaborated in the development of Tc24-C4, a vaccine candidate antigen against Chagas Disease that is currently undergoing clinical evaluation. Jeroen Pollet, Maria Elena Bottazzi and Peter Hotez are listed among the inventors on a Chagas disease vaccine patent, submitted by Baylor College of Medicine.

5.5 SUPPLEMENTARY MATERIAL

■ **Supplementary Table 1. List of all the T. cruzi peptides presented on MHC-I.** Properties of each peptide calculated by mass spectrometry are listed. Affinity (in nM) to H2-Kb and H2-Db was calculated using NetMHCpan 4.1 prediction tool.

Protein Group	Experiment #	Peptide	Length	Unique	-10lgP	Mass	ppm	m/z	z	RT	Affinity H2-Kb	Affinity H2-Db	Protein Accession	Description
1	1	ASYDALETANKWGLL	15	Y	41,91	1595,7865	0,5	798,9009	2	86,2	N/A	N/A	Q4E2Y1	60S ribosomal protein L23a putative
2	2	LNKHLDRDRVS	12	Y	34,91	1423,7419	-0,2	475,5878	3	61,22	28214,62	37802,07	Q4D832	Heat shock protein DnaJ, putative
2	1+2	VKETKFDYSLG	11	Y	33,21	1285,6554	0,6	643,8353	2	68,52	17920,22	41675,59	Q4D832	Heat shock protein DnaJ, putative
2	1+2	AFYTGKTIKLA	11	Y	32,99	1211,6914	1,7	606,854	2	87,6	10898,21	37391,63	Q4D832	Heat shock protein DnaJ, putative
2	1	LEAFYTGKTIKLA	13	Y	31,76	1453,818	0,3	485,6134	3	60,25	26681,71	41101,48	Q4D832	Heat shock protein DnaJ putative
2	2	SNEISDLR	8	Y	22,18	932,4563	2	467,2364	2	57,34	32680,68	45089,55	Q4D832	Heat shock protein DnaJ, putative
2	2	GEDQIPGVR	10	Y	15,31	1026,5094	3,5	514,2638	2	65,38	39886,62	45476,61	Q4D832	Heat shock protein DnaJ, putative
3	1	AEFAKKMEEQNKKFF	15	Y	32,11	1873,9396	-0,6	469,4919	4	33,51	N/A	N/A	Q4D3A5, Q4D3A7, Q4D7Y4	Kinetoplastid membrane protein KMP-11
4	2	MTYKPIVHGRPGVG	14	Y	31,24	1510,8079	0,7	504,6102	3	59,06	21686,33	40673,71	Q4DGZ5	40S ribosomal protein S15, putative

Supplementary Table 1. List of all the *T. cruzi* peptides presented on MHC-I. Properties of each peptide calculated by mass spectrometry are listed. Affinity (in nM) to H2-Kb and H2-Db was calculated using NetMHCpan 4.1 prediction tool. (continued)

Protein Group	Experiment #	Peptide	Length	Unique	-10lgP	Mass	ppm	m/z	z	RT	Affinity H2-Kb	Affinity H2-Db	Protein Accession	Description
4	2	KERTFHKFTYRGL	14	Y	18,43	1810,9478	1,2	453,7448	4	54,37	14170,03	41897,56	Q4DGZ5	40S ribosomal protein S15, putative
5	2	LYALYRQKKEKPRN	14	Y	30,62	1806,0264	-0,6	452,5136	4	25,12	37397,3	46108,82	Q4DTQ1	40S ribosomal protein S23, putative
6	2	LFSGMKVLRLR	11	Y	30,3	1318,7908	0,9	330,7053	4	98,62	22021,14	41170,93	Q4DY30, Q4DY32	RNA-binding protein, putative
6	2	LFSGMKVLRL	9	Y	21,87	1049,6056	2,7	350,8767	3	82,71	30434,57	44946,86	Q4DY30, Q4DY32	RNA-binding protein, putative
7	2	DVFVNGKKPVYD	12	Y	26,87	1379,7085	2	690,8629	2	72,43	33411,13	38423,52	Q4DAW5	Cytochrome C oxidase subunit VI, putative
8	2	IVPVPIKVV	9	Y	26,35	1010,6528	1	506,3342	2	36,21	438,25	20813,45	Q4D289	Neurobeachin/beige-like protein, putative
9	1	SAAGATTLVENF	12	Y	24,47	1179,5771	-8,2	590,791	2	51,24	17738,68	19701,81	Q4DRE3, Q4CWL4	Uncharacterized protein
10	2	LVRHMASKDRSARL	14	Y	23,6	1638,91	2,1	410,7357	4	22,39	15446,03	39742,8	Q4DCN9	Glyceraldehyde-3-phosphate dehydrogenase
11	2	DQGSADIVN	9	Y	23,54	917,409	0,7	459,7121	2	58,7	43413,05	46070,42	Q4D976, Q4E5Z1	ATP-dependent DEAD/H RNA helicase, putative
12	2	AFFAESKVV	8	Y	23,25	879,4338	0,4	880,4414	1	51,8	21140,96	39381,89	Q4DNZ9	Nfu_N domain-containing protein

Supplementary Table 1. List of all the *T. cruzi* peptides presented on MHC-I. Properties of each peptide calculated by mass spectrometry are listed. Affinity (in nM) to H2-Kb and H2-Db was calculated using NetMHCpan 4.1 prediction tool. (continued)

Protein Group	Experiment #	Peptide	Length	Unique	-10lgP	Mass	ppm	m/z	z	RT	Affinity H2-Kb	Affinity H2-Db	Protein Accession	Description
13	2	PAVVAPPQ	9	Y	22,63	874,4912	3,1	438,2542	2	67,7	38719,81	43005,38	Q4CNA5, Q4DPR2	OTU domain-containing protein
14	2	VAAKRSATSAKLG	13	Y	21,63	1258,7357	-0,7	420,5855	3	17,87	22122,15	39616,09	Q4CY60, Q4D3G1	Uncharacterized protein
15	2	SSSEKDYKILG	12	Y	20,75	1388,6824	1,8	695,3497	2	83,76	16737,58	35976,43	Q4D7B1, Q4DVP6	Chaperone DnaJ protein, putative
16	2	GVLATGASLA	10	Y	20,67	858,4811	12,6	430,2532	2	57,11	28196,63	35335,65	Q4DH33, Q4DY72	Uncharacterized protein
17	2	ASVVAGNIS	9	Y	20,62	816,4341	-9,8	409,2203	2	46,6	23336,5	26423,14	Q4DBX3	Uncharacterized protein

<i>T. cruzi</i> strain	DTU		
Dm28c	TcI	MVKETKFDYSLGVSPDASVDEIKRAYRRLLAKYHPDKNKDPGSQEKFKVEVSVAECLSDP	60
Sylvio X10/1	TcI	MVKETKFDYSLGVSPDASVDEIKRAYRRLLAKYHPDKNKDPGSQEKFKVEVSVAECLSDP	60
G	TcI	MVKETKFDYSLGVSPDASVDEIKRAYRRLLAKYHPDKNKDPGSQEKFKVEVSVAECLSDP	60
Brazil A4	TcI	MVKETKFDYSLGVSPDASVDEIKRAYRRLLAKYHPDKNKDPGSQEKFKVEVSVAECLSDP	60
Berenice	TcII	MVKETKFDYSLGVSPDASVDEIKRAYRRLLAKYHPDKNKDPGSQEKFKVEVSVAECLSDP	60
Y C6	TcII	MVKETKFDYSLGVSPDASVDEIKRAYRRLLAKYHPDKNKDPGSQEKFKVEVSVAECLSDP	60
CL Brener Esmeraldo-like	TcVI	MVKETKFDYSLGVSPDASVDEIKRAYRRLLAKYHPDKNKDPGSQEKFKVEVSVAECLSDP	60
TCC	TcVI	MVKETKFDYSLGVSPDASVDEIKRAYRRLLAKYHPDKNKDPGSQEKFKVEVSVAECLSDP	60
CL	TcVI	MVKETKFDYSLGVSPDASVDEIKRAYRRLLAKYHPDKNKDPGSQEKFKVEVSVAECLSDP	60

Dm28c	TcI	EKRSRYDQFGEKGVEMESGGIDPTDIFASF FGGSRARGEKPKDIVHEL PVSLEAFYTGK	120
Sylvio X10/1	TcI	EKRSRYDQFGEKGVEMESGGIDPTDIFASF FGGSRARGEKPKDIVHEL PVSLEAFYTGK	120
G	TcI	EKRSRYDQFGEKGVEMESGGIDPTDIFASF FGGSRARGEKPKDIVHEL PVSLEAFYTGK	120
Brazil A4	TcI	EKRSRYDQFGEKGVEMESGGIDPTDIFASF FGGSRARGEKPKDIVHEL PVSLEAFYTGK	120
Berenice	TcII	EKRSRYDQFGEKGVEMESGGIDPTDIFASF FGGSRARGEKPKDIVHEL PVSLEAFYTGK	120
Y C6	TcII	EKRSRYDQFGEKGVEMESGGIDPTDIFASF FGGSRARGEKPKDIVHEL PVSLEAFYTGK	120
CL Brener Esmeraldo-like	TcVI	EKRSRYDQFGEKGVEMESGGIDPTDIFASF FGGSRARGEKPKDIVHEL PVSLEAFYTGK	120
TCC	TcVI	EKRSRYDQFGEKGVEMESGGIDPTDIFASF FGGSRARGEKPKDIVHEL PVSLEAFYTGK	120
CL	TcVI	EKRSRYDQFGEKGVEMESGGIDPTDIFASF FGGSRARGEKPKDIVHEL PVSLEAFYTGK	120

Dm28c	TcI	TIKLAI TRDLCPACNGSGSKVPNASVTCCKECDGRGVLITRSIGPGFIQQM VACPCKR	180
Sylvio X10/1	TcI	TIKLAI TRDLCPACNGSGSKVPNASVTCCKECDGRGVLITRSIGPGFIQQM VACPCKR	180
G	TcI	TIKLAI TRDLCPACNGSGSKVPNASVTCCKECDGRGVLITRSIGPGFIQQM VACPCKR	180
Brazil A4	TcI	TIKLAI TRDLCPACNGSGSKVPNASVTCCKECDGRGVLITRSIGPGFIQQM VACPCKR	180
Berenice	TcII	TIKLAI TRDLCPACNGSGSKVPNASVTCCKECDGRGVLITRSIGPGFIQQM VACPCKR	180
Y C6	TcII	TIKLAI TRDLCPACNGSGSKVPNASVTCCKECDGRGVLITRSIGPGFIQQM VACPCKR	180
CL Brener Esmeraldo-like	TcVI	TIKLAI TRDLCPACNGSGSKVPNASVTCCKECDGRGVLITRSIGPGFIQQM VACPCKR	180
TCC	TcVI	TIKLAI TRDLCPACNGSGSKVPNASVTCCKECDGRGVLITRSIGPGFIQQM VACPCKR	180
CL	TcVI	TIKLAI TRDLCPACNGSGSKVPNASVTCCKECDGRGVLITRSIGPGFIQQM VACPCKR	180

Dm28c	TcI	GKGTDMREEDKCDSCRQQI IKDKKIFEIFVEKGMHRGDNATFRGEGDQIPGVR LSGDII	240
Sylvio X10/1	TcI	GKGTDMREEDKCDSCRQQI IKDKKIFEIFVEKGMHRGDNATFRGEGDQIPGVR LSGDII	240
G	TcI	GKGTDMREEDKCDSCRQQI IKDKKIFEIFVEKGMHRGDNATFRGEGDQIPGVR LSGDII	240
Brazil A4	TcI	GKGTDMREEDKCDSCRQQI IKDKKIFEIFVEKGMHRGDNATFRGEGDQIPGVR LSGDII	240
Berenice	TcII	GKGTDMREEDKCDSCRQQI IKDKKIFEIFVEKGMHRGDNATFRGEGDQIPGVR LSGDII	240
Y C6	TcII	GKGTDMREEDKCDSCRQQI IKDKKIFEIFVEKGMHRGDNATFRGEGDQIPGVR LSGDII	240
CL Brener Esmeraldo-like	TcVI	GKGTDMREEDKCDSCRQQI IKDKKIFEIFVEKGMHRGDNATFRGEGDQIPGVR LSGDII	240
TCC	TcVI	GKGTDMREEDKCDSCRQQI IKDKKIFEIFVEKGMHRGDNATFRGEGDQIPGVR LSGDII	240
CL	TcVI	GKGTDMREEDKCDSCRQQI IKDKKIFEIFVEKGMHRGDNATFRGEGDQIPGVR LSGDII	240

Dm28c	TcI	IIFEQKPHPVFTRKGDHLMERTISLAEALTGFTLNIXHLDRDVSITSTGVWPSK LWC	300
Sylvio X10/1	TcI	IIFEQKPHPVFTRKGDHLMERTISLAEALTGFTLNIXHLDRDVSITSTGVWPSK LWC	300
G	TcI	IIFEQKPHPVFTRKGDHLMERTISLAEALTGFTLNIXHLDRDVSITSTGVWPSK LWC	300
Brazil A4	TcI	IIFEQKPHPVFTRKGDHLMERTISLAEALTGFTLNIXHLDRDVSITSTGVWPSK LWC	300
Berenice	TcII	IIFEQKPHPVFTRKGDHLMERTISLAEALTGFTLNIXHLDRDVSITSTGVWPSK LWC	300
Y C6	TcII	IIFEQKPHPVFTRKGDHLMERTISLAEALTGFTLNIXHLDRDVSITSTGVWPSK LWC	300
CL Brener Esmeraldo-like	TcVI	IIFEQKPHPVFTRKGDHLMERTISLAEALTGFTLNIXHLDRDVSITSTGVWPSK LWC	300
TCC	TcVI	IIFEQKPHPVFTRKGDHLMERTISLAEALTGFTLNIXHLDRDVSITSTGVWPSK LWC	300
CL	TcVI	IIFEQKPHPVFTRKGDHLMERTISLAEALTGFTLNIXHLDRDVSITSTGVWPSK LWC	300

Dm28c	TcI	VSREGMPINNTGGVERGDLVKFHVVPYSAQSLQSNIEIDLKILHYPPQOSP PPSAML C	360
Sylvio X10/1	TcI	VSREGMPINNTGGVERGDLVKFHVVPYSAQSLQSNIEIDLKILHYPPQOSP PPSAML C	360
G	TcI	VSREGMPINNTGGVERGDLVKFHVVPYSAQSLQSNIEIDLKILHYPPQOSP PPSAML C	360
Brazil A4	TcI	VSREGMPINNTGGVERGDLVKFHVVPYSAQSLQSNIEIDLKILHYPPQOSP PPSAML C	360
Berenice	TcII	VSREGMPINNTGGVERGDLVKFHVVPYSAQSLQSNIEIDLKILHYPPQOSP PPSAML C	360
Y C6	TcII	VSREGMPINNTGGVERGDLVKFHVVPYSAQSLQSNIEIDLKILHYPPQOSP PPSAML C	360
CL Brener Esmeraldo-like	TcVI	VSREGMPINNTGGVERGDLVKFHVVPYSAQSLQSNIEIDLKILHYPPQOSP PPSAML C	360
TCC	TcVI	VSREGMPINNTGGVERGDLVKFHVVPYSAQSLQSNIEIDLKILHYPPQOSP PPSAML C	360
CL	TcVI	VSREGMPINNTGGVERGDLVKFHVVPYSAQSLQSNIEIDLKILHYPPQOSP PPSAML C	360

Dm28c	TcI	HLSETNIDLEKAKRRRQTGGDDDDAPQGHGTACTTQQ	399
Sylvio X10/1	TcI	HLSETNIDLEKAKRRRQTGGDDDDAPQGHGTACTTQQ	399
G	TcI	HLSETNIDLEKAKRRRQTGGDDDDAPQGHGTACTTQQ	399
Brazil A4	TcI	HLSETNIDLEKAKRRRQTGGDDDDAPQGHGTACTTQQ	399
Berenice	TcII	HLSETNIDLEKAKRRRQTGGDDDDAPQGHGTACTTQQ	399
Y C6	TcII	HLSETNIDLEKAKRRRQTGGDDDDAPQGHGTACTTQQ	399
CL Brener Esmeraldo-like	TcVI	HLSETNIDLEKAKRRRQTGGDDDDAPQGHGTACTTQQ	399
TCC	TcVI	HLSETNIDLEKAKRRRQTGGDDDDAPQGHGTACTTQQ	399
CL	TcVI	HLSETNIDLEKAKRRRQTGGDDDDAPQGHGTACTTQQ	399

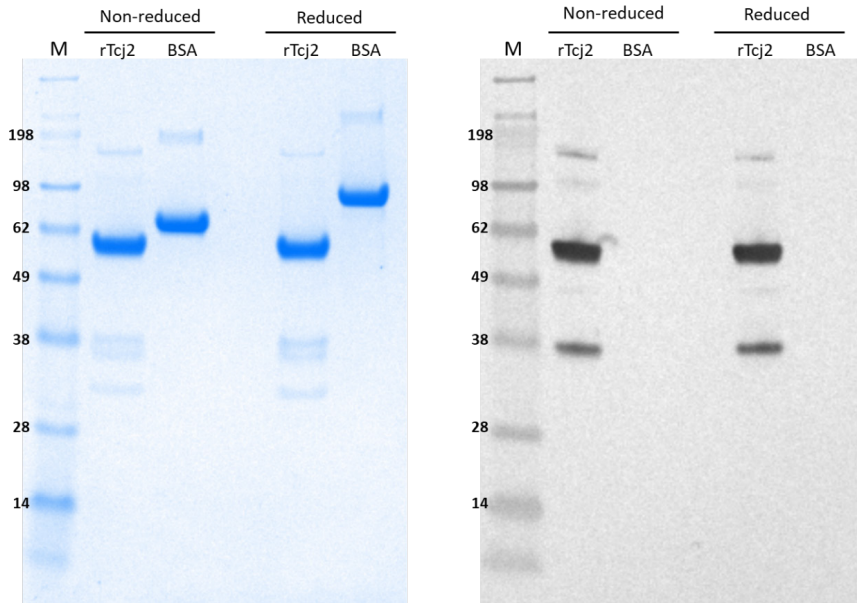
■ **Supplementary Figure 1. Amino acid sequence of Tcj2 protein is very conserved between different Discrete Typing Units (DTUs) of *T. cruzi*.** Multiple sequence alignment of DnaJ (Tcj2) protein sequence of different *T. cruzi* strains, obtained from TriTripDB.org (accessed on May 23rd, 2023). The two mutations in amino acid residues are highlighted in red.

Trypanosoma cruzi	MVKETK FYDSL GVSPDASVDEIKRAYRRLALKYHPDKNKDPGSQEKFKVESVAYECLSDP	60
Mus musculus	MVKETQYYDILGVKPSASPEEIKKAYRKLALKYHPDKNPDEG--EKFKLISQAYEVLSDP	58
Homo sapiens	MVKETQYYDILGVKPSASPEEIKKAYRKLALKYHPDKNPDEG--EKFKLISQAYEVLSDP	58
	*****:* ** *.* ** :***:***:***** * * ** * : * ** **	
Trypanosoma cruzi	EKRSRYDQFGEKGVEMESGG---IDPTDIFASFFGGG-RARGEPKPKDIVHEL PSL EA	115
Mus musculus	KKRDIYDQGGEQAIKEGGSGSPSFSSPMDIFDMFFGGGGRMTRERRGNVHQLSVTL	118
Homo sapiens	KKRDVYDQGGEQAIKEGGSGSPSFSSPMDIFDMFFGGGGRMARERRGNVHQLSVTL	118
	:** . ** ** :. : . * . * ** ** . * * : : ** : * **	
Trypanosoma cruzi	FYTGKTIKLA ITRDRLCPACNGSGSKVPNASVTCKEDGRGVKLITRSIGPGFIQQMQVA	175
Mus musculus	LYNGITKKLALQKNVICEKCEGIGGKGG-SVEKCLCKGRGMQVHIQQIGPMVQQIQTV	177
Homo sapiens	LYNGVTKKLALQKNVICEKCEGVGGKGG-SVEKCLCKGRGMQIHIQQIGPMVQQIQTV	177
	:* . * ** : : : * * . * * . : . * * . ** : : : . ** : * ** .	
Trypanosoma cruzi	CPKCRGKGTDMREEDKCDSCRGGQIKKDKKIFEIFVEKGMHRGNATFR EGDQIPGV RL	235
Mus musculus	CIECKGQGERINPKDRCECSGAKVTREKKIEVHVEKGMKDQKILFHGEDQPEL	236
Homo sapiens	CIECKGQGERINPKDRCECSGAKVIREKKIEVHVEKGMKDQKILFHGEDQPEL	236
	* : * : * . : . : * : . * * : : : ** : . ** : * : : * : * * * * :	
Trypanosoma cruzi	SGDIIIFEQPHPVFTRKGDHLMERTISLAEALTGFT LN IKHLDDRDV SITS --TGW	293
Mus musculus	PGDVIIVLDQKDHVVFQRRGQDLIMKMKIQLSEALCGFKTIKTLDDRVLVSSKSGEVI	296
Homo sapiens	PGDVIIVLDQKDHVVFQRRGHDLMKMKIQLSEALCGFKTIKTLDNRLVITSKAGEVI	296
	** : * : : * * * * * . * . * . * : . * . * * * * . * * * * : * : * * :	
Trypanosoma cruzi	DPSKLCVSRGEMPIPNITGGVERGDLVVKFHWYPSAQS LSNET SLRKILHYPPQQSP	353
Mus musculus	KHGDLKICIRNEGMPYK-APLEKGMIIQFLVVFPEKQWLSQEKLPLQLEALLP--PRQKV	353
Homo sapiens	KHGDLRCVRDEGMPYK-APLEKGIILIIQFLVIFPEKHWSLEKLPQLEALLP--PRQKV	353
	. . . * : * * * * : . : * : * : : * * : * . : * . : : * . * * * .	
Trypanosoma cruzi	PPSAMLCHLSETNIDLEKEAKRRRQTGGDDDDAPQGHGTACTQQ	399
Mus musculus	RITDDMDQVELKEFNPNEQSWRQHREAYEEDDEEP--RAGVQCQTA	397
Homo sapiens	RITDDMDQVELKEFCPNEQNWRQHREAYEEDDEGP--QAGVQCQTA	397
	: : : . . : : : * : : . : * : * * : * . *	

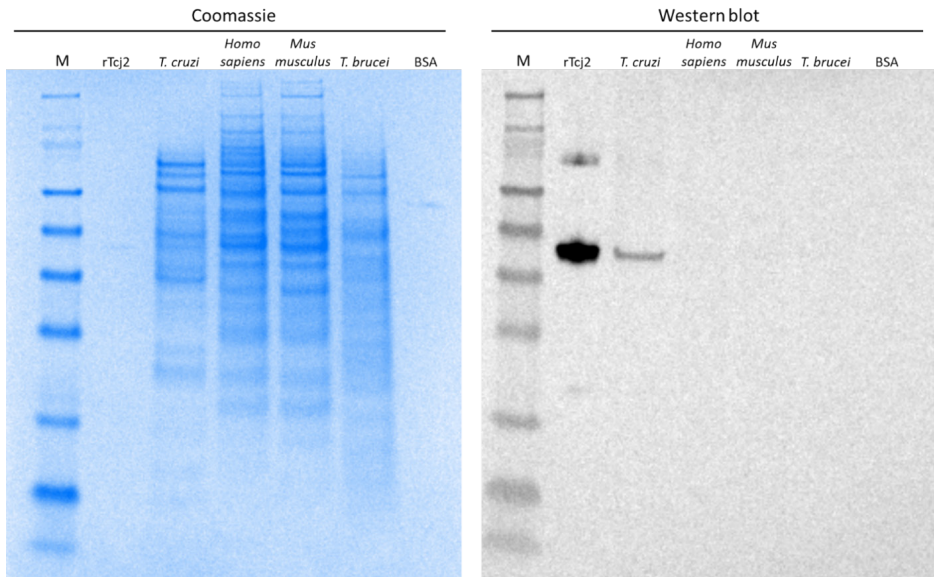
■ **Supplementary Figure 2. Multiple Sequence Alignment (Clustal Omega) between Tcj2 from *Trypanosoma cruzi* and DnaJ homolog from *Mus musculus* and *Homo sapiens*.** The colored sequences represent the six peptides that were found by immunopeptidomics. Sequence identity is 42% between *T. cruzi* and *M. musculus* (dnaJ homolog subfamily A member 4 isoform 2). Sequence identity is 43% between *T. cruzi* and *H. sapiens* (dnaJ homolog subfamily A member 4 isoform 2).

Trypanosoma cruzi	MVKERTKFDYSLGVSPDASVDEIKRAYRRLALKYHPDKNKDPSGQSEKFKVSVAYECLSDP	60
Trypanosoma brucei brucei	MVKETKYDVALGVPNASEDDIKRAYRKLALKYHPDKNKEPGANEKFKVSVAYECLSDV	60
	*****:*:*:* *:* *:* *****:*****:*:*:*****	
Trypanosoma cruzi	EKRSRVYDQFGEKGVEMESGGIDPTDIFASFFGGSRARGEKPKKDIVHELVPVLEAFYTGK	120
Trypanosoma brucei brucei	EKRRRYDQFGEKGVSEGVGIDPSDIFSFFGGRRARGEAKPKDIVHQQPVPLETIFYNGK	120
	*****:*:* *:* *:* *****:*****:*:*:*:*:* *:* *:* *:	
Trypanosoma cruzi	TIKLAIIRDRLCPACNGSGSKVPNASVTCKECDGRGVKLIITRSIGPGFIQQMQVACPCKR	180
Trypanosoma brucei brucei	TIKLAIIRDRLCDSNGSGSKDPKVSRCVCECDGRGVKIITRSIGPGFVQQMQVACPRCG	180
	***** *:* *:* ***** *:* * * *****:*****:*****:*	
Trypanosoma cruzi	GKGTDMREEDKCDSCRGGQIKKDKKIFEIFVEKGMHRGDNATFRGEGDQIPGVRLSGDII	240
Trypanosoma brucei brucei	GKGTDIKEEHKCSQCRGGQIVKDKKVFVVEKGMHQHDSVTFQEGEDQIPGVRLSGDII	240
	*****:*:* *:* *:* ***** *:*:*:* *:*:*:*:* *:* *:* *****	
Trypanosoma cruzi	IIFEQKPHPVFTRKGDHLMERTISLAEALTGFTLNLIKHLDDRDSITSTGVDPVPSKLWC	300
Trypanosoma brucei brucei	IILDEKPHPVFTRKGDHLIHHKISLAEALTGFTMNIKHLDERAISIRSTNVIDPQKLWS	300
	::*:*****:*:*:*:*:*:*****:*****:* *:* *:* *:* *:* *:	
Trypanosoma cruzi	VSREGMPIPNTGGVERGDLVVKFHVYPSAQSLQSNESDLRKLILHYPPQSQSPPPSAML	360
Trypanosoma brucei brucei	VSREGMPIPGTGGTERGDLVIKFDVVYPSAQSLSGDGIPLRRILGYPKQEEPAPATEH	360
	***** *:* *:* *****:*:* *****:.. *:* *:* * * *:* * * *	
Trypanosoma cruzi	HLSETNIDLEKAKRRRQTGGDDDDA-PQGHGTGATCTQQ	399
Trypanosoma brucei brucei	TLAVTYVDLREARRRRTAANDDDDAGQHVHTGATCTQQ	400
	: *:*:*:*:* *:* *:* *:* *:* *:* *:* *:* *:* *:* *:* *:* *:	

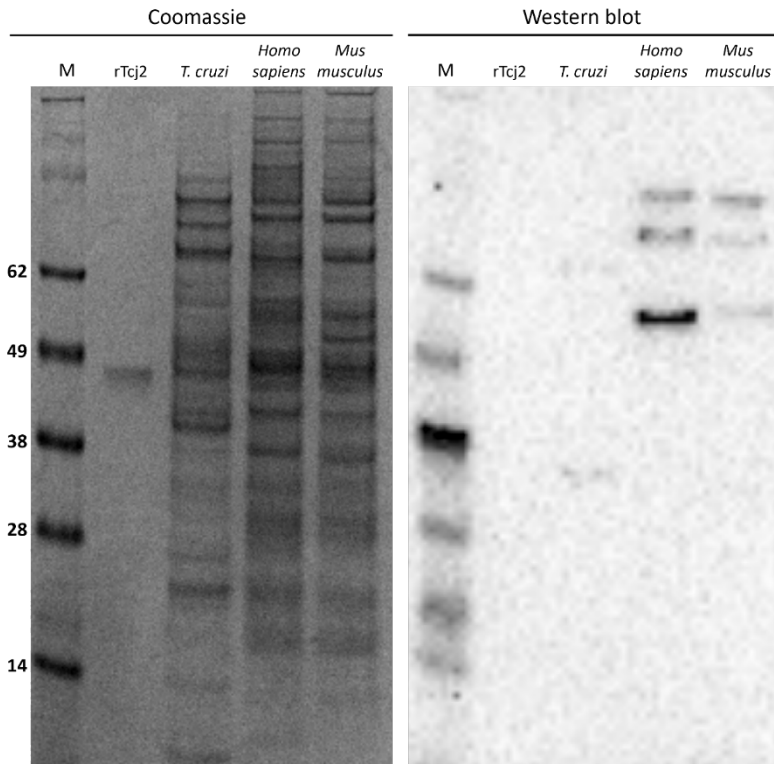
■ **Supplementary Figure 3. Multiple Sequence Alignment (Clustal Omega) between Tcj2 from *Trypanosoma cruzi* and Tbj2 from *Trypanosoma brucei*.** Protein sequence obtained from TriTripDB.org (accessed on July 3rd, 2023).



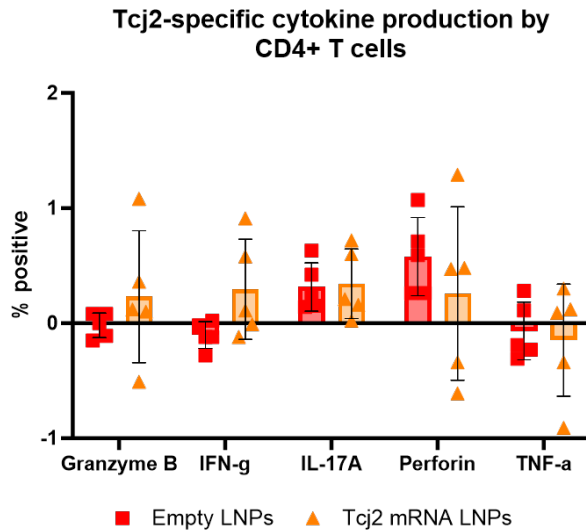
■ **Supplementary Figure 4. Recombinant *T. cruzi* Tcj2 was expressed in *E. coli* and purified.** Coomassie stained SDS-PAGE gel and western blot detecting HIS-tag showed a main band at the expected size of 45 kDa. Three bands smaller than the main band were observed, of which one band contained the HIS-tag. Densitometry analysis estimated the purity of the main band to be 76%.



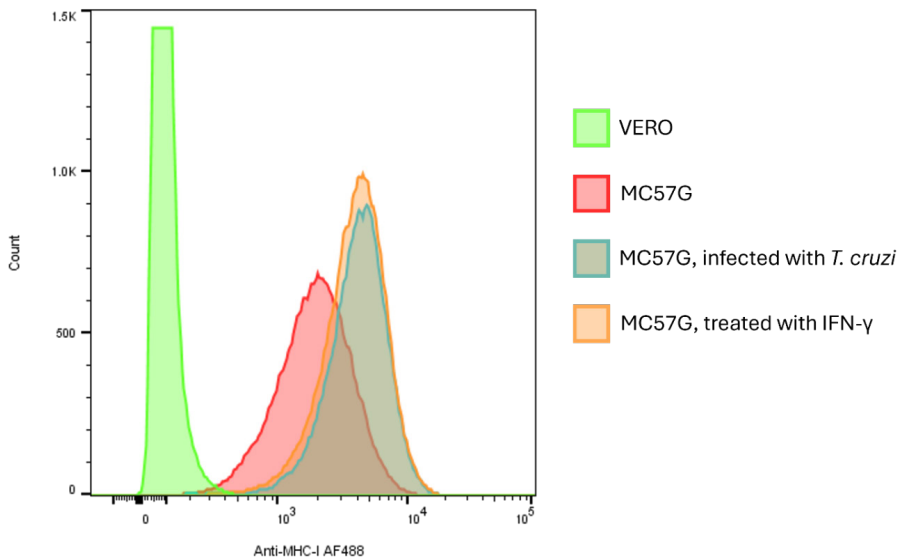
- **Supplementary Figure 5. Tcj2 antisera recognizes native Tcj2 in *T. cruzi* lysate, but not DnaJ-homologs in lysate from *H. sapiens*, *M. musculus* and *T. brucei*.** 20 ng rTcj2 protein, as well as 3 μ g of lysates from *T. cruzi* Tulahuen, *H. sapiens* (HEK293T), *M. musculus* (MC57G) and *T. brucei* *brucei*, were run on reduced SDS-PAGE gels and either stained with Coomassie Blue or subjected to western blotting followed by incubation with Tcj2 antisera from Tcj2 LNP-vaccinated mice. 20 ng Bovine Serum Albumin (BSA) protein was added as negative control.



■ **Supplementary Figure 6. Western blot confirming the presence of human DNAJA4 in HEK292T cell lysate.** 100 ng rTcj2 protein, as well as 3 μ g of lysates from *T. cruzi* Tulahuen, *H. sapiens* (HEK293T) and *M. musculus* (MC57G) were ran on reduced SDS-PAGE gels and either stained with Coomassie Blue or subjected to western blotting followed by incubation with anti-human DNAJA4 polyclonal antibody.

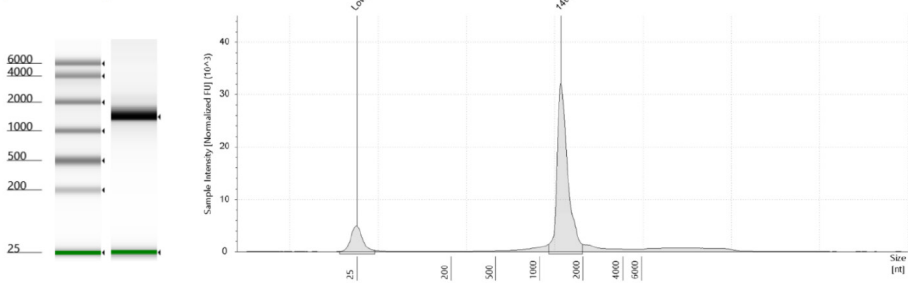


- **Supplementary Figure 7. Cytokines produced by CD4+ T cells after *in vitro* restimulation with rTcj2 protein.** No significant changes in cytokine production were observed by CD4+ T cells after restimulation, but an observable trend in increase in granzyme B and IFN- γ was observed. Data values from non-stimulated cells were subtracted from rTcj2 protein stimulated cells to obtain antigen-specific cytokine production.

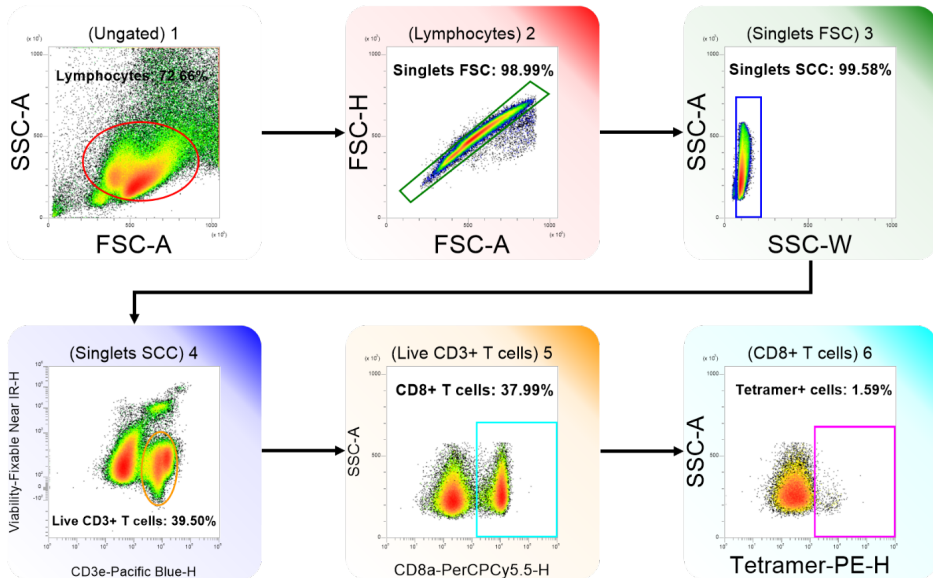


- **Supplementary Figure 8. Histogram plot showing the expression of MHC-I by *T. cruzi* infected and noninfected MC57G mouse fibroblasts.** Cells were infected with *T. cruzi* for 48 hours followed by flow cytometric staining. As a positive control for upregulated MHC-I expression, cells were incubated for 24 hours with recombinant mouse IFN- γ . VERO cells that do not have mouse MHC-I were used as a negative control.

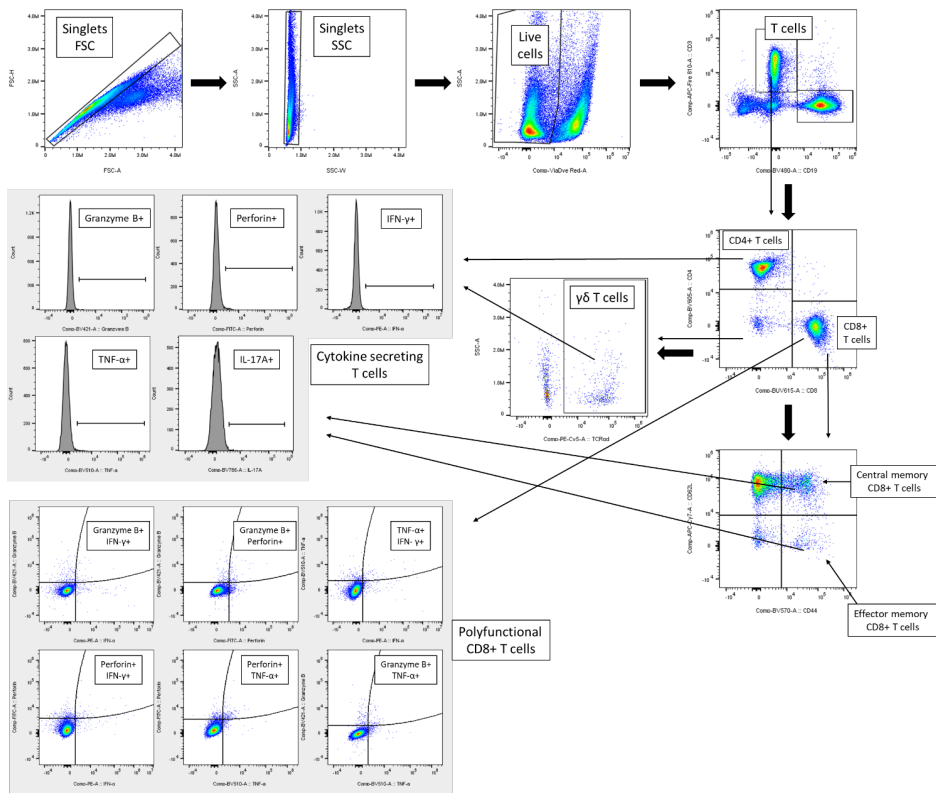
TapeStation Image:



- **Supplementary Figure 9. Electrophoresis gel showing the robust integrity of Tcj2 mRNA.** TapeStation automated electrophoresis was performed to analyze the size and integrity of the Tcj2 mRNA construct. A strong single band was observed, calculated to be 1404 nucleotides, which was the expected size. The second band at 25 nucleotides represents a positive control that is run within the sample.



- **Supplementary Figure 10. Flow cytometry gating strategy to analyze SIINFEKL-specific CD8+ T cells.** After lymphocytes and singlets were selected, live CD3+ T cells were gated, followed by CD8+ T cells, followed by gating on SIINFEKL tetramer PE positive cells.



■ **Supplementary Figure 11. Flow cytometry gating strategy to analyze in vitro rTcj2-restimulated splenocytes.** First live T cells were gated, followed by gating on CD4+, CD8+ or $\gamma\delta$ T cells. CD8+ T cells were further separated by central memory or effector memory CD8+ T cells. For all cell populations intracellular cytokine production was measured. Additionally, CD8+ T cells were also analyzed for polyfunctionality, meaning the intracellular production of two cytokines.

5.6 REFERENCES

1. Lidani KCF, Andrade FA, Bavia L, Damasceno FS, Beltrame MH, Messias-Reason IJ, et al. Chagas Disease: From Discovery to a Worldwide Health Problem. *Front Public Health* [Internet]. 2019 [cited 2023 Apr 5];7. Available from: <https://www.frontiersin.org/articles/10.3389/fpubh.2019.00166>
2. Gómez-Ochoa SA, Rojas LZ, Echeverría LE, Muka T, Franco OH. Global, Regional, and National Trends of Chagas Disease from 1990 to 2019: Comprehensive Analysis of the Global Burden of Disease Study. *Glob Heart*. 2022;17(1):59.
3. Jones KM, Poveda C, Versteeg L, Bottazzi ME, Hotez PJ. Preclinical advances and the immunophysiology of a new therapeutic Chagas disease vaccine. *Expert Rev Vaccines*. 2022 Jun 23;0(0):1–19.
4. Pérez-Molina JA, Molina I. Chagas disease. *The Lancet*. 2018 Jan 6;391(10115):82–94.
5. Neglected Infectious Diseases in the Americas: Success Stories and Innovation to Reach the Neediest - PAHO/WHO | Pan American Health Organization [Internet]. [cited 2023 Apr 5]. Available from: <https://www.paho.org/en/documents/neglected-infectious-diseases-americas-success-stories-and-innovation-reach-neediest-0>
6. Lee BY, Bacon KM, Bottazzi ME, Hotez PJ. Global economic burden of Chagas disease: a computational simulation model. *Lancet Infect Dis*. 2013 Apr 1;13(4):342–8.
7. Pérez-Molina JA, Pérez-Ayala A, Moreno S, Fernández-González MC, Zamora J, López-Velez R. Use of benznidazole to treat chronic Chagas' disease: a systematic review with a meta-analysis. *J Antimicrob Chemother*. 2009 Dec;64(6):1139–47.
8. Padilla AM, Wang W, Akama T, Carter DS, Easom E, Freund Y, et al. Discovery of an orally active benzoxaborole prodrug effective in the treatment of Chagas disease in non-human primates. *Nat Microbiol*. 2022 Oct;7(10):1536–46.
9. Jones K, Versteeg L, Damania A, Keegan B, Kendricks A, Pollet J, et al. Vaccine-linked chemotherapy improves benznidazole efficacy for acute Chagas disease. *Infect Immun*. 2018 Jan 8;IAI.00876-17.
10. Dos Santos Virgilio F, Pontes C, Dominguez MR, Ersching J, Rodrigues MM, Vasconcelos JR. CD8(+) T cell-mediated immunity during *Trypanosoma cruzi* infection: a path for vaccine development? *Mediators Inflamm*. 2014;2014:243786.
11. Tarleton RL. CD8+ T cells in *Trypanosoma cruzi* infection. *Semin Immunopathol*. 2015 May;37(3):233–8.
12. Connelley T, Nicastrì A, Sheldrake T, Vrettou C, Fisch A, Reynisson B, et al. Immunopeptidomic Analysis of BoLA-I and BoLA-DR Presented Peptides from *Theileria parva* Infected Cells. *Vaccines*. 2022 Nov;10(11):1907.
13. Kuznetsov A, Voronina A, Govorun V, Arapidi G. Critical Review of Existing MHC I Immunopeptidome Isolation Methods. *Molecules*. 2020 Jan;25(22):5409.
14. Shapiro IE, Bassani-Sternberg M. The impact of immunopeptidomics: From basic research to clinical implementation. *Semin Immunol*. 2023 Mar 1;66:101727.
15. Huang R, Zhao B, Hu S, Zhang Q, Su X, Zhang W. Adoptive neoantigen-reactive T cell therapy: improvement strategies and current clinical researches. *Biomark Res*. 2023 Apr 17;11(1):41.
16. Leddy OK, White FM, Bryson BD. Leveraging Immunopeptidomics To Study and Combat Infectious Disease. *mSystems*. 6(4):e00310-21.

17. Yaciuk JC, Skaley M, Bardet W, Schafer F, Mojsilovic D, Cate S, et al. Direct Interrogation of Viral Peptides Presented by the Class I HLA of HIV-Infected T Cells. *J Virol*. 2014 Nov 15;88(22):12992–3004.
18. Wölk B, Trautwein C, Büchele B, Kersting N, Blum HE, Rammensee HG, et al. Identification of Naturally Processed Hepatitis C Virus-Derived Major Histocompatibility Complex Class I Ligands. *PLOS ONE*. 2012 Jan 3;7(1):e29286.
19. Johnstone C, Lorente E, Barriga A, Barnea E, Infantes S, Lemonnier FA, et al. The Viral Transcription Group Determines the HLA Class I Cellular Immune Response Against Human Respiratory Syncytial Virus. *Mol Cell Proteomics*. 2015 Apr 1;14(4):893–904.
20. de Wit J, Emmelot ME, Meiring H, van Gaans-van den Brink JAM, van Els CACM, Kaaijk P. Identification of Naturally Processed Mumps Virus Epitopes by Mass Spectrometry: Confirmation of Multiple CD8+ T-Cell Responses in Mumps Patients. *J Infect Dis*. 2020 Jan 14;221(3):474–82.
21. Draheim M, Wlodarczyk MF, Crozat K, Saliou JM, Alayi TD, Tomavo S, et al. Profiling MHC II immunopeptidome of blood-stage malaria reveals that cDC1 control the functionality of parasite-specific CD4 T cells. *EMBO Mol Med*. 2017 Nov;9(11):1605–21.
22. McMurtrey C, Trolle T, Sansom T, Remesh SG, Kaefer T, Bardet W, et al. Toxoplasma gondii peptide ligands open the gate of the HLA class I binding groove. Gilmore MS, editor. *eLife*. 2016 Jan 29;5:e12556.
23. Mou Z, Li J, Boussoffara T, Kishi H, Hamana H, Ezzati P, et al. Identification of broadly conserved cross-species protective Leishmania antigen and its responding CD4+ T cells. *Sci Transl Med*. 2015 Oct 21;7(310):310ra167.
24. Bettencourt P, Müller J, Nicastrì A, Cantillon D, Madhavan M, Charles PD, et al. Identification of antigens presented by MHC for vaccines against tuberculosis. *Npj Vaccines*. 2020 Jan 3;5(1):1–14.
25. Mayer RL, Verbeke R, Asselman C, Aernout I, Gul A, Eggermont D, et al. Immunopeptidomics-based design of mRNA vaccine formulations against *Listeria monocytogenes*. *Nat Commun*. 2022 Oct 14;13(1):6075.
26. Karunakaran KP, Rey-Ladino J, Stoykov N, Berg K, Shen C, Jiang X, et al. Immunoproteomic Discovery of Novel T Cell Antigens from the Obligate Intracellular Pathogen *Chlamydia* 1. *J Immunol*. 2008 Feb 15;180(4):2459–65.
27. Karunakaran KP, Yu H, Jiang X, Chan Q, Goldberg MF, Jenkins MK, et al. Identification of MHC-Bound Peptides from Dendritic Cells Infected with *Salmonella enterica* Strain SL1344: Implications for a Nontyphoidal *Salmonella* Vaccine. *J Proteome Res*. 2017 Jan 6;16(1):298–306.
28. Guerrero G, Picozza M, D’Orso S, Placido R, Pirronello M, Verdiani A, et al. BNT162b2 vaccination induces durable SARS-CoV-2-specific T cells with a stem cell memory phenotype. *Sci Immunol*. 2021 Nov 2;6(66):eabl5344.
29. Chen M, Venturi V, Munier CML. Dissecting the Protective Effect of CD8+ T Cells in Response to SARS-CoV-2 mRNA Vaccination and the Potential Link with Lymph Node CD8+ T Cells. *Biology*. 2023 Jul 22;12(7):1035.
30. Versteeg L, Almutairi MM, Hotez PJ, Pollet J. Enlisting the mRNA Vaccine Platform to Combat Parasitic Infections. *Vaccines*. 2019 Dec;7(4):122.
31. You H, Jones MK, Gordon CA, Arganda AE, Cai P, Al-Wassiti H, et al. The mRNA Vaccine Technology Era and the Future Control of Parasitic Infections. *Clin Microbiol Rev*. 2023 Jan 10;36(1):e00241-21.
32. Barbier AJ, Jiang AY, Zhang P, Wooster R, Anderson DG. The clinical progress of mRNA vaccines and immunotherapies. *Nat Biotechnol*. 2022 Jun;40(6):840–54.

33. Baeza Garcia A, Siu E, Sun T, Exler V, Brito L, Hekele A, et al. Neutralization of the Plasmodium-encoded MIF ortholog confers protective immunity against malaria infection. *Nat Commun.* 2018 Jul 13;9(1):2714.
34. Chahal JS, Khan OF, Cooper CL, McPartlan JS, Tsosie JK, Tilley LD, et al. Dendrimer-RNA nanoparticles generate protective immunity against lethal Ebola, H1N1 influenza, and *Toxoplasma gondii* challenges with a single dose. *Proc Natl Acad Sci.* 2016 Jul 19;113(29):E4133–42.
35. Duthie MS, Van Hoeven N, MacMillen Z, Picone A, Mohamath R, Erasmus J, et al. Heterologous Immunization With Defined RNA and Subunit Vaccines Enhances T Cell Responses That Protect Against *Leishmania donovani*. *Front Immunol.* 2018;9:2420.
36. Maldonado E, Morales-Pison S, Urbina F, Solari A. Vaccine Design against Chagas Disease Focused on the Use of Nucleic Acids. *Vaccines.* 2022 Apr;10(4):587.
37. Michel-Todó L, Reche PA, Bigey P, Pinazo MJ, Gascón J, Alonso-Padilla J. In silico Design of an Epitope-Based Vaccine Ensemble for Chagas Disease. *Front Immunol [Internet].* 2019 [cited 2020 Apr 14];10. Available from: <https://www.frontiersin.org/articles/10.3389/fimmu.2019.02698/full>
38. Poveda C, Leão AC, Mancino C, Taraballi F, Chen YL, Adhikari R, et al. Heterologous mRNA-protein vaccination with Tc24 induces a robust cellular immune response against *Trypanosoma cruzi*, characterized by an increased level of polyfunctional CD8+ T-cells. *Curr Res Immunol.* 2023 Jan 1;4:100066.
39. Stevens J, Wiesmüller KH, Walden P, Joly E. Peptide length preferences for rat and mouse MHC class I molecules using random peptide libraries. *Eur J Immunol.* 1998;28(4):1272–9.
40. Tibbetts RS, Jensen JL, Olson CL, Wang FD, Engman DM. The DnaJ family of protein chaperones in *Trypanosoma cruzi*! Note: Nucleotide sequence data reported in this paper have been submitted to the GenBank data base with the following accession numbers: tcj1, L42541; tcj2, L42549; tcj3, L46818; tcj4, L46819.1. *Mol Biochem Parasitol.* 1998 Mar 15;91(2):319–26.
41. Edkins AL, Ludewig MH, Blatch GL. A *Trypanosoma cruzi* heat shock protein 40 is able to stimulate the adenosine triphosphate hydrolysis activity of heat shock protein 70 and can substitute for a yeast heat shock protein 40. *Int J Biochem Cell Biol.* 2004 Aug 1;36(8):1585–98.
42. Qiu XB, Shao YM, Miao S, Wang L. The diversity of the DnaJ/Hsp40 family, the crucial partners for Hsp70 chaperones. *Cell Mol Life Sci CMLS.* 2006 Nov 1;63(22):2560–70.
43. Watanabe Costa R, Batista MF, Meneghelli I, Vidal RO, Nájera CA, Mendes AC, et al. Comparative Analysis of the Secretome and Interactome of *Trypanosoma cruzi* and *Trypanosoma rangeli* Reveals Species Specific Immune Response Modulating Proteins. *Front Immunol [Internet].* 2020 [cited 2022 Nov 6];11. Available from: <https://www.frontiersin.org/articles/10.3389/fimmu.2020.01774>
44. Paba J, Ricart CAO, Fontes W, Santana JM, Teixeira ARL, Marchese J, et al. Proteomic Analysis of *Trypanosoma cruzi* Developmental Stages Using Isotope-Coded Affinity Tag Reagents. *J Proteome Res.* 2004 Jun 1;3(3):517–24.
45. Brenière SF, Waleckx E, Barnabé C. Over Six Thousand *Trypanosoma cruzi* Strains Classified into Discrete Typing Units (DTUs): Attempt at an Inventory. *PLoS Negl Trop Dis.* 2016 Aug 29;10(8):e0004792.
46. Tagliamonte M, Cavalluzzo B, Mauriello A, Ragone C, Buonaguro FM, Tornesello ML, et al. Molecular mimicry and cancer vaccine development. *Mol Cancer.* 2023 Apr 26;22(1):75.
47. Dersh D, Yewdell JW, Wei J. A SIINFEKL-Based System to Measure MHC Class I Antigen Presentation Efficiency and Kinetics. *Methods Mol Biol Clifton NJ.* 2019;1988:109–22.
48. Hassett KJ, Higgins J, Woods A, Levy B, Xia Y, Hsiao CJ, et al. Impact of lipid nanoparticle size on mRNA vaccine immunogenicity. *J Controlled Release.* 2021 Jul 10;335:237–46.

49. Patel P, Ibrahim NM, Cheng K. The Importance of Apparent pKa in the Development of Nanoparticles Encapsulating siRNA and mRNA. *Trends Pharmacol Sci*. 2021 Jun;42(6):448–60.
50. Nazeri S, Zakeri S, Mehrizi AA, Sardari S, Djadid ND. Measuring of IgG2c isotype instead of IgG2a in immunized C57BL/6 mice with *Plasmodium vivax* TRAP as a subunit vaccine candidate in order to correct interpretation of Th1 versus Th2 immune response. *Exp Parasitol*. 2020 Sep;216:107944.
51. Buckner FS, Verlinde CL, La Flamme AC, Van Voorhis WC. Efficient technique for screening drugs for activity against *Trypanosoma cruzi* using parasites expressing beta-galactosidase. *Antimicrob Agents Chemother*. 1996 Nov;40(11):2592–7.
52. Garg N, Nunes MP, Tarleton RL. Delivery by *Trypanosoma cruzi* of proteins into the MHC class I antigen processing and presentation pathway. *J Immunol*. 1997 Apr 1;158(7):3293–302.
53. Wang L, Li X, Yang S, Chen X, Li J, Wang S, et al. Proteomic identification of MHC class I-associated peptidome derived from non-obese diabetic mouse thymus and pancreas. *J Proteomics*. 2023 Jan 6;270:104746.
54. Overtvelt LV, Andrieu M, Verhasselt V, Connan F, Choppin J, Vercruyse V, et al. *Trypanosoma cruzi* down-regulates lipopolysaccharide-induced MHC class I on human dendritic cells and impairs antigen presentation to specific CD8+ T lymphocytes. *Int Immunol*. 2002 Oct 1;14(10):1135–44.
55. Camargo R, Faria LO, Kloss A, Favali CBF, Kuckelkorn U, Kloetzel PM, et al. *Trypanosoma cruzi* Infection Down-Modulates the Immunoproteasome Biosynthesis and the MHC Class I Cell Surface Expression in HeLa Cells. *PLOS ONE*. 2014 Apr 21;9(4):e95977.
56. Stryker GA, Nickell SP. *Trypanosoma cruzi*: Exposure of Murine Cells to Live Parasites *in Vitro* Leads to Enhanced Surface Class I MHC Expression Which Is Type I Interferon-Dependent. *Exp Parasitol*. 1995 Dec 1;81(4):564–73.
57. Finkelsztein EJ, Diaz-Soto JC, Vargas-Zambrano JC, Suesca E, Guzmán F, López MC, et al. Altering the motility of *Trypanosoma cruzi* with rabbit polyclonal anti-peptide antibodies reduces infection to susceptible mammalian cells. *Exp Parasitol*. 2015 Mar;150:36–43.
58. Martin DL, Weatherly DB, Laucella SA, Cabinian MA, Crim MT, Sullivan S, et al. CD8+ T-Cell responses to *Trypanosoma cruzi* are highly focused on strain-variant trans-sialidase epitopes. *PLoS Pathog*. 2006 Aug;2(8):e77.
59. Rodríguez-Bejarano OH, Avendaño C, Patarroyo MA. Mechanisms Associated with *Trypanosoma cruzi* Host Target Cell Adhesion, Recognition and Internalization. *Life*. 2021 Jun;11(6):534.
60. Kurup SP, Tarleton RL. The *Trypanosoma cruzi* Flagellum Is Discarded via Asymmetric Cell Division following Invasion and Provides Early Targets for Protective CD8+ T Cells. *Cell Host Microbe*. 2014 Oct 8;16(4):439–49.
61. Luo Y, Huang X, Yang J, Huang L, Li R, Wu Q, et al. Proteomics analysis of G protein-coupled receptor kinase 4-inhibited cellular growth of HEK293 cells. *J Proteomics*. 2019 Sep 15;207:103445.
62. Batra J, Tripathi S, Kumar A, Katz JM, Cox NJ, Lal RB, et al. Human Heat shock protein 40 (Hsp40/DnaJB1) promotes influenza A virus replication by assisting nuclear import of viral ribonucleoproteins. *Sci Rep*. 2016 Jan 11;6(1):19063.
63. Ludewig MH, Boshoff A, Horn D, Blatch GL. *Trypanosoma brucei* J protein 2 is a stress inducible and essential Hsp40. *Int J Biochem Cell Biol*. 2015 Mar 1;60:93–8.
64. Shonhai A, G. Maier A, M. Przyborski J, L. Blatch G. Intracellular Protozoan Parasites of Humans: The Role of Molecular Chaperones in Development and Pathogenesis. *Protein Pept Lett*. 2011 Feb 1;18(2):143–57.

65. Sagi SSK, Paliwal P, Bansal A, Mishra C, Khan N, Mustoori SR, et al. Studies on immunogenicity and protective efficacy of DnaJ of *Salmonella Typhi* against lethal infection by *Salmonella Typhimurium* in mice. *Vaccine*. 2006 Nov 30;24(49):7135–41.
66. Guo F, Tang Y, Zhang W, Yuan H, Xiang J, Teng W, et al. DnaJ, A Promising Vaccine Candidate Against *Ureaplasma Urealyticum* Infectio [Internet]. 2021 [cited 2022 Mar 5]. Available from: <https://doi.org/10.21203/rs.3.rs-1132437/v1>
67. Khan MohdN, Bansal A, Shukla D, Paliwal P, Sarada SKS, Mustoori SR, et al. Immunogenicity and protective efficacy of DnaJ (hsp40) of *Streptococcus pneumoniae* against lethal infection in mice. *Vaccine*. 2006 Sep 11;24(37):6225–31.
68. Brodskyn CI, da Silva AMM, Takehara HA, Mota I. Characterization of antibody isotype responsible for immune clearance in mice infected with *Trypanosoma cruzi*. *Immunol Lett*. 1988 Aug 1;18(4):255–8.
69. Hosseini N. Isolation And Characterization Of α -Gal-Containing Extracellular Vesicles (evs) From Three Major Genotypes Of *Trypanosoma Cruzi*: Potential Biomarkers Of Chagas Disease. Open Access Theses Diss [Internet]. 2020 Jan 1; Available from: https://scholarworks.utep.edu/open_etd/2986
70. Bixby LM, Tarleton RL. Stable CD8+ T Cell Memory during Persistent *Trypanosoma cruzi* Infection. *J Immunol Baltim Md 1950*. 2008 Aug 15;181(4):2644–50.
71. Pack AD, Collins MH, Rosenberg CS, Tarleton RL. Highly competent, non-exhausted CD8+ T cells continue to tightly control pathogen load throughout chronic *Trypanosoma cruzi* infection. *PLoS Pathog*. 2018;14(11):e1007410.
72. Imai N, Tawara I, Yamane M, Muraoka D, Shiku H, Ikeda H. CD4+ T cells support polyfunctionality of cytotoxic CD8+ T cells with memory potential in immunological control of tumor. *Cancer Sci*. 2020 Jun;111(6):1958–68.
73. Sanchez Alberti A, Bivona AE, Matos MN, Cerny N, Schulze K, Weißmann S, et al. Mucosal Heterologous Prime/Boost Vaccination Induces Polyfunctional Systemic Immunity, Improving Protection Against *Trypanosoma cruzi*. *Front Immunol* [Internet]. 2020 [cited 2023 Jun 20];11. Available from: <https://www.frontiersin.org/articles/10.3389/fimmu.2020.00128>
74. Chowdhury IH, Lokugamage N, Garg NJ. Experimental Nanovaccine Offers Protection Against Repeat Exposures to *Trypanosoma cruzi* Through Activation of Polyfunctional T Cell Response. *Front Immunol* [Internet]. 2020 [cited 2023 Jun 20];11. Available from: <https://www.frontiersin.org/articles/10.3389/fimmu.2020.595039>
75. Cardillo F, de Pinho RT, Antas PRZ, Mengel J. Immunity and immune modulation in *Trypanosoma cruzi* infection. *Pathog Dis*. 2015 Dec 1;73(9):ftv082.
76. da Mota JB, Echevarria-Lima J, Kyle-Cezar F, Melo M, Bellio M, Scharfstein J, et al. IL-18R signaling is required for $\gamma\delta$ T cell response and confers resistance to *Trypanosoma cruzi* infection. *J Leukoc Biol*. 2020 Oct 1;108(4):1239–51.
77. Hernández-Castañeda MA, Happ K, Cattalani F, Wallimann A, Blanchard M, Fellay I, et al. $\gamma\delta$ T Cells Kill *Plasmodium falciparum* in a Granzyme- and Granulysin-Dependent Mechanism during the Late Blood Stage. *J Immunol Author Choice*. 2020 Apr 1;204(7):1798–809.
78. De Beuckelaer A, Grooten J, De Koker S. Type I Interferons Modulate CD8+ T Cell Immunity to mRNA Vaccines. *Trends Mol Med*. 2017 Mar 1;23(3):216–26.
79. Peng L, Renauer PA, Ökten A, Fang Z, Park JJ, Zhou X, et al. Variant-specific vaccination induces systems immune responses and potent in vivo protection against SARS-CoV-2. *Cell Rep Med*. 2022 May 17;3(5):100634.

80. National Research Council (US) Committee for the Update of the Guide for the Care and Use of Laboratory Animals. Guide for the Care and Use of Laboratory Animals [Internet]. 8th ed. Washington (DC): National Academies Press (US); 2011 [cited 2023 Aug 21]. (The National Academies Collection: Reports funded by National Institutes of Health). Available from: <http://www.ncbi.nlm.nih.gov/books/NBK54050/>
81. Stallcup KC, Springer TA, Mescher MF. Characterization of an anti-H-2 monoclonal antibody and its use in large-scale antigen purification. *J Immunol Baltim Md* 1950. 1981 Sep;127(3):923–30.
82. Watanabe H, Matsumaru H, Ooishi A, Feng Y, Odahara T, Suto K, et al. Optimizing pH Response of Affinity between Protein G and IgG Fc. *J Biol Chem*. 2009 May 1;284(18):12373–83.
83. Purcell AW, Ramarathinam SH, Ternette N. Mass spectrometry–based identification of MHC-bound peptides for immunopeptidomics. *Nat Protoc*. 2019 Jun;14(6):1687–707.
84. Zhang J, Xin L, Shan B, Chen W, Xie M, Yuen D, et al. PEAKS DB: de novo sequencing assisted database search for sensitive and accurate peptide identification. *Mol Cell Proteomics MCP*. 2012 Apr;11(4):M111.010587.
85. Zingales B, Andrade SG, Briones MRS, Campbell DA, Chiari E, Fernandes O, et al. A new consensus for *Trypanosoma cruzi* intraspecific nomenclature: second revision meeting recommends TcI to TcVI. *Mem Inst Oswaldo Cruz*. 2009 Nov;104:1051–4.
86. Anderson BR, Muramatsu H, Nallagatla SR, Bevilacqua PC, Sansing LH, Weissman D, et al. Incorporation of pseudouridine into mRNA enhances translation by diminishing PKR activation. *Nucleic Acids Res*. 2010 Sep;38(17):5884–92.
87. Pardi N, Weissman D. Nucleoside Modified mRNA Vaccines for Infectious Diseases. *Methods Mol Biol Clifton NJ*. 2017;1499:109–21.
88. Versteeg L, Le Guezennec X, Zhan B, Liu Z, Angagaw M, Woodhouse JD, et al. Transferring Luminex cytokine assays to a wall-less plate technology: Validation and comparison study with plasma and cell culture supernatants. *J Immunol Methods*. 2017 Jan 1;440(Supplement C):74–82.
89. Teodorowicz M, Perdijk O, Verhoek I, Govers C, Savelkoul HFJ, Tang Y, et al. Optimized Triton X-114 assisted lipopolysaccharide (LPS) removal method reveals the immunomodulatory effect of food proteins. *PLOS ONE*. 2017 Mar 29;12(3):e0173778.
90. Versteeg L, Adhikari R, Poveda C, Villar-Mondragon MJ, Jones KM, Hotez PJ, et al. Location and expression kinetics of Tc24 in different life stages of *Trypanosoma cruzi*. *PLoS Negl Trop Dis*. 2021 Sep 3;15(9):e0009689.



CHAPTER 6

| General Discussion

The overall goal of my thesis was to advance the development and evaluation of cost-effective vaccines for parasitic diseases that fall under the category of Neglected Tropical Diseases (NTDs), with a particular focus on Chagas disease. As outlined in section 1.7, my objectives were to advance knowledge on current vaccine targets for Chagas disease by using mRNA vaccines as a new vaccine platform. I further aimed to improve existing techniques to assess vaccine-induced immune responses and applied alternative approaches to the identification of new vaccine targets that can be targeted by CD8+ T cells.

6.1 ENHANCING OUR UNDERSTANDING OF THE TC24 VACCINE TARGET

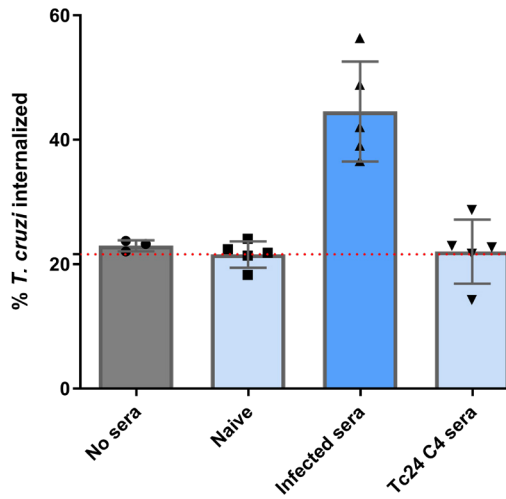
As described in this thesis, Tc24 is a flagellar calcium-binding protein (FCaBP) from *T. cruzi*. The modified and recombinant protein version, Tc24-C4, has shown promising results when formulated with a TLR-4 agonist as a therapeutic vaccine candidate (1–3). However, there was limited understanding regarding the location of Tc24 in the parasite, its expression during different parasitic stages, and the mechanisms of immune-protection elicited by Tc24-immunization. When mAbs against Tc24-C4 were developed, the opportunity to study localization and expression level of Tc24 in trypomastigotes and amastigotes became available. In **Chapter 3**, it is shown that trypomastigote permeabilization was required to detect Tc24, demonstrating that Tc24 was located on the inside of the parasite and not exposed on the surface of *T. cruzi* trypomastigotes. Follow-up experiments showed that Tc24 expression was drastically reduced after trypomastigotes entered host cells and started amastigogenesis, although Tc24 expression was still high in the “early” amastigote stage. Expression of Tc24 remained low within replicating amastigotes. Then, when amastigotes transitioned back to trypomastigotes, coinciding with the growth of the flagellum, expression of Tc24 was significantly increased again. These findings contribute to a better understanding of the location and expression kinetics of Tc24 in *T. cruzi*.

6.1.1 Tc24’s location and the implications for immunity

The finding that Tc24 is not located on the outside of the parasite conflicted with the working hypothesis in the Chagas disease vaccine research field that Tc24 is located in the flagellar pocket of the parasite and can be targeted by Tc24-specific antibodies (4,5). However, when we performed a search in the parasitology literature using the term flagellar calcium-binding protein (FCaBP), which is a different name for the Tc24 protein, we found that the location of these calcium-sensing proteins was also described to be the inner leaflet of the flagellar membrane. For instance, *Trypanosoma brucei* expresses an FCaBP, named Tb24, and it is also targeted to the inner leaflet of the flagellar membrane (6). Also, in the case of *Trypanosoma congolense*, FCaBP is called Calflagin, and it was reported that Calflagin associates strongly with the plasma membrane around the flagella (7). Similarly, for *T. cruzi*, FCaBP has been reported to be associated with the inner leaflet of the flagellar membrane (8).

These studies strongly supported our finding that Tc24 is not exposed on the outside of the parasite. This finding has implications for the immune mechanisms that are responsible for the observed (partial) protection against *T. cruzi* infection induced by the Tc24-C4 vaccine. The absence of Tc24 on the parasite's surface makes it highly unlikely that an antibody-mediated immune response against Tc24 will facilitate classical antibody-mediated complement lysis or opsonization/phagocytosis of *T. cruzi* since Tc24-specific antibodies will not be able to bind to intact parasites.

To confirm the inability of Tc24 antibodies to opsonize *T. cruzi* trypomastigotes, I conducted an *in vitro* experiment measuring phagocytosis of fluorescently labeled trypomastigotes by RAW 264.7 macrophages after parasites were incubated with Tc24-C4 antisera. The results in **Figure 1** show that trypomastigotes pre-incubated with Tc24-C4 antisera did not result in increased macrophage phagocytosis, similar to pre-incubation with naïve mouse sera or no sera. In contrast, sera from *T. cruzi*-infected mice showed a strong increase in phagocytosis by macrophages, indicating the presence of opsonizing antibodies. These observations showed that Tc24-specific antibodies have minimal to no phagocytosis enhancing activity, and were in line with the observation that Tc24-specific antibodies do not bind to intact trypomastigotes. Other recombinant protein vaccines have been evaluated that elicit antibody responses that are effective and can bind to the surface of *T. cruzi*, such as Cruzipain (Cz), a *T. cruzi* cysteine protease that is secreted and present on the surface of amastigotes and in the flagellar pocket of trypomastigotes, and Tc52, a *T. cruzi* protein with significant homology with glutathione S-transferase, which is suggested to be surface exposed on amastigotes and trypomastigotes (9–11). These candidate vaccines induced antibodies that inhibited infection of non-phagocytotic cells *in vitro*, as well as trypomastigote lysis through complement activation in the case of Tc52 (12,13). While I did not study cellular inhibition of infection and parasite lysis through complement activation for Tc24-specific antibodies, I hypothesize that we would not see any effect due to the unavailability of Tc24 on the cell surface.



■ **Figure 1. *T. cruzi* trypomastigotes phagocytosed by murine macrophages.** Trypomastigotes strain H1 parasites were labelled with violet proliferation dye 450 and incubated for 1 hour with 1:10 diluted, heat-inactivated antisera from Tc24-C4 vaccinated, *T. cruzi*-infected, or naïve mice. Subsequently, trypomastigotes were washed and co-cultured with mouse RAW 264.7 macrophages for 3 hours. Afterwards, macrophages were collected from wells by trypsinization, and analyzed for internalized parasites using imaging flow cytometry.

Although Tc24-specific antibodies cannot bind on the surface of the parasite, they might interact with secreted forms of Tc24, exerting protective functions. Mass spectrometry analysis of the secretome of *T. cruzi* revealed the presence of Tc24 in the soluble protein fraction, as well as its presence in extracellular vesicles (EVs) (14,15). While it has been confirmed for some *T. cruzi* proteins that they are exposed on the outside of EVs, such as trans-sialidases, the exact location of Tc24 in the EVs is not known (16). However, since Tc24 is located on the inner leaflet of the flagellar membrane, it would be expected that Tc24, and other proteins present in the cytosol, end up on the inside of the EVs when they bud off *T. cruzi*'s plasma membrane and would therefore still not be accessible for antibodies.

Further research should determine whether Tc24 antibodies could bind to Tc24-containing EVs, potentially neutralizing and preventing their interaction with host cells and counteracting their functions. Although *T. cruzi* is believed to secrete soluble proteins and extracellular vesicles to modulate host cell responses to favor survival and replication (17), specific reasons why Tc24 would be secreted as a soluble protein or as part of EVs remain unknown, but could include interference with host signaling pathways, immune-evasion strategies (14,18), acting as a “smokescreen protein”, diverting attention from more critical parasite targets (19,20), or involvement in polyclonal B cell activation to weaken the specific humoral response (21).

However, the main question is whether Tc24(-C4) specific antibodies contribute to protection. To test if Tc24-specific antibodies contribute to protection, serum transfer studies could be conducted. Herein, serum from immunized mice would be transferred to naïve mice, who would then be challenged with *T. cruzi* to assess whether the antibodies confer protection. If protection is observed, studies can be conducted to elucidate the role of soluble or EV-containing Tc24 during *T. cruzi* infection. Understanding the role of Tc24 outside the parasite could lead to opportunities for Tc24-specific antibodies to disrupt its activities and improve the protection against Chagas disease.

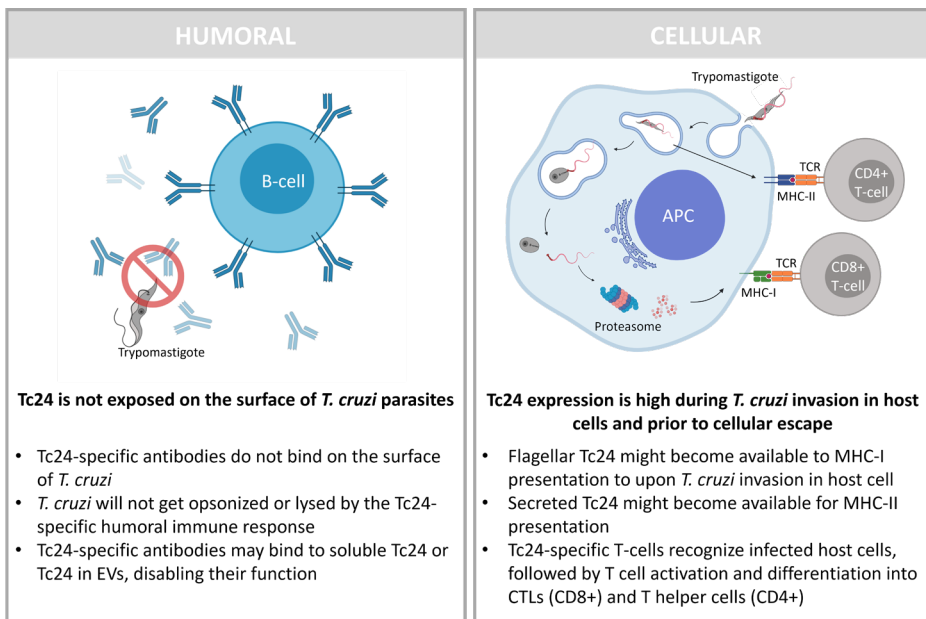
6.1.2 Current hypotheses on Tc24-induced protection

While the role of secreted Tc24 in the host immune response against *T. cruzi* remains to be elucidated, Tc24 is believed to be an important target for cell-mediated immunity (**Figure 2**). The response of CD8+ T cells plays a vital role in the eradication of *T. cruzi*-infected cells, as these cells can identify *T. cruzi*-derived peptides on the MHC-I of infected cells via their T cell receptor (TCR) (19,22). It has been established that *T. cruzi* peptides from specific proteins can be presented on MHC-I during infection, whereby they become available for antigen processing and presentation, as previously observed with amastigote surface proteins (23). Furthermore, Garg *et al.* have demonstrated that *T. cruzi* proteins that are secreted or released (such as glycosylphosphatidylinositol (GPI)- anchored) by the parasite inside host cells are a major source of peptides for MHC-I presentation, while cytoplasmic or transmembrane proteins were not significantly processed and presented on MHC-I (24). Additionally, flagellar proteins are also a source for MHC-I presentation after the trypomastigote discards its flagella during amastigogenesis.

Since Tc24 is located along the flagellar membrane, Tc24 proteins are likely part of the discarded proteins, and I therefore hypothesized that Tc24 is available for antigen processing and presentation on MHC-I after trypomastigote invasion of host cells. Tc24-specific CD8+ T cells, like memory CD8+ T cells elicited from immunization with Tc24, can recognize these infected host cells, followed by proliferation and differentiation into CTLs that are capable of eliminating infected cells. Furthermore, the secretion of Tc24 as soluble protein or via EVs by extracellular *T. cruzi* trypomastigotes may also aid in MHC-II presentation. During the initial stage of host cell invasion, when expression of Tc24 in trypomastigotes is still high, secreted Tc24 in the phagolysosome may become available for MHC-II presentation followed by presentation to CD4+ T cells. Tc24 vaccine-induced CD4+ T cells can become activated, and after proliferation and differentiation into T helper cells they secrete cytokines to skew the immune response. T helper cells can also assist the activation of CD8+ T cells by CD40 ligand and the secretion of IL-2 (25). Additionally, CD4+ T helper cells can enhance the efficiency of macrophages killing phagocytosed parasites by either the expression of CD40 ligand, or the secretion of IFN- γ . (26)

As amastigotes replicate intracellularly, Tc24 expression is low, but increases again when amastigotes revert to trypomastigotes. Notably, non-replicating amastigotes have been reported during chronic *T. cruzi* infection, displaying dormancy, and these parasites might remain a high expression of Tc24 (27). The high expression of Tc24 in dormant parasites and amastigotes reverting to trypomastigotes could offer another opportunity for CD8+ T cells to identify *T. cruzi*-infected cells. Analyzing the killing of *T. cruzi*-infected cells by Tc24-specific CD8+ T cells, through *in vitro* killing assays or microscopy, could test these hypotheses. Overall, the expression kinetics of Tc24 could impact the presentation of Tc24 by infected cells and the subsequent recognition and elimination by CD8+ T cells.

In conclusion, for prophylactic vaccination with Tc24, a robust CD8+ and CD4+ T cells response should be elicited, which can result in the generation of memory CD8+ and CD4+ T cells. These memory T cells can quickly respond to *T. cruzi* exposures by recognizing Tc24 on MHC-I and MHC-II, providing a fast response and robust protection.



■ **Figure 2. Findings and implications on Tc24 – induced protection.** Left) humoral immune response implications. Right) Cellular immune response implications. Written in bold are the findings, and in bulletpoints are the implications.

6.1.3 Mode of action for the therapeutic recombinant Tc24-C4 candidate vaccine

The Tc24-C4 candidate subunit vaccine is currently being prepared for clinical trials, with the goal to be used as a therapeutic vaccine (28). The mechanism of vaccine-induced protection is initiated by APCs, phagocytosing the Tc24-C4 protein followed by MHC-II presentation. This leads to the activation of CD4+ T helper cells, which in turn assist CTLs, macrophages, and B cells as described above. The addition of a TLR4 agonist as an adjuvant skews the immune response towards a T helper 1 (Th1) profile, hallmarked by the production of IFN- γ (29). CD4+ Th1 cells are major producers of IFN- γ , as well as other Th1 cytokines like IL-2 and TNF- α (30). Furthermore, IFN- γ may promote cross-presentation of Tc24-C4 protein on MHC-I by APCs, although this form of antigen presentation is generally less efficient than presentation of exogenous protein on MHC-II to CD4+ T cells. Given that there is already a natural immune response against Tc24 during *T. cruzi* infection, which elicits a population of Tc24-specific CD8+ T cells, the Tc24-C4 candidate subunit vaccine acts as a booster, re-stimulating CD4+ T cells, which in their turn enhance the CD8+ T cells response and macrophage killing of parasites. On the contrary, while Tc24-C4 also induces a strong Tc24-specific antibody response, the protective capacity of these antibodies remains to be elucidated in light of the location of Tc24 in the parasite.

In summary, the findings presented on the location and expression of Tc24 bring new insights on the mechanisms of Tc24 vaccine-induced protection, highlighting the role of cell-mediated immunity. Further research can explore the potential roles of Tc24-specific antibodies.

6.2 ADVANCING STATE OF THE ART TECHNIQUES AND IMPLEMENTING NEW METHODOLOGIES IN VACCINE RESEARCH

Studying the immune response induced by vaccination is key to developing effective vaccines. While existing techniques to analyze the immune response work very well, some still pose limitations due to various factors, such as cost restrains and sample volume. In this thesis, the methodology to conduct cytokine analyses by Luminex was optimized, described in **Chapter 2**, making it more affordable for vaccine development studies. In **Chapter 3**, imaging flow cytometry (IFC) was utilized as an emerging tool that combines flow cytometry with fluorescent microscopy, allowing for the quantification of morphological and spatial features of cells. Additionally, other fields of research were explored for state-of-the-art methodologies that could enhance vaccine research for NTDs. Immunopeptidomics was applied as a novel method to identify novel vaccine targets for Chagas disease in **Chapter 5**. Although mass spectrometry is a relatively expensive tool to use for NTD research, and I aimed to apply affordable methodologies in this thesis, the use of services from available mass spectrometry

cores makes the methodology more cost-effective. Furthermore, I also enhanced the design of our mRNA vaccine constructs with the SIINFEKL and FLAG-tag sequences, which allowed for rapid screening of the translation and antigen presentation of these mRNA constructs *in vitro*.

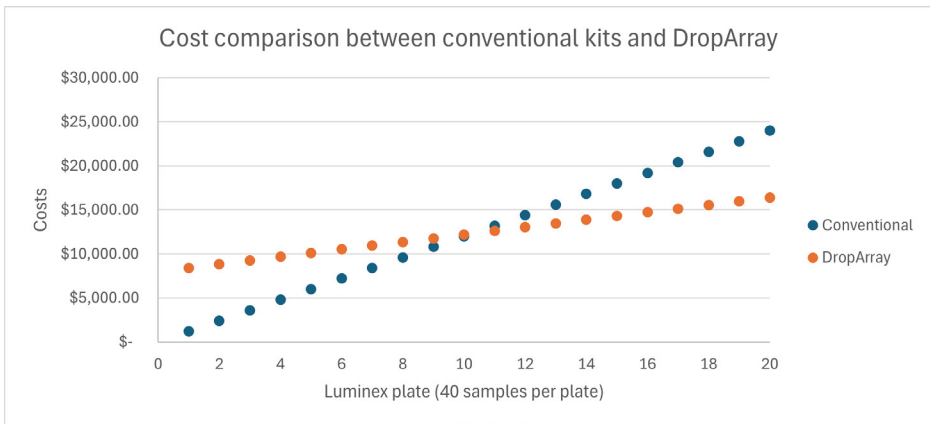
6.2.1 Adapting DropArray technology for cytokine profiling

The analysis of cytokines, chemokines, antibodies, and other analytes is essential for the assessment of candidate vaccines. In the Texas Children's Center for Vaccine Development, we routinely evaluate immune responses against candidate vaccines by conducting cytokine analysis using Luminex technology. In this thesis in **Chapter 5**, we used Luminex to analyze the cytokine profiles in co-culture experiments.

Enzyme-linked immunosorbent assay (ELISA) is an established technique to look at analytes of interest, such as cytokines. However, ELISA is limited to assaying individual analytes and multiple analytes require multiple ELISAs, consuming significantly more sample volume (50-100 μ L samples per well in a 96-well plate) and cost. Therefore, multiplex techniques that allow for the simultaneous measurement of multiple analytes within the same assay are very valuable.

Furthermore, while ELISA uses enzyme amplification or chromogenic substrate conversion, Luminex uses fluorescence to read results, which is a more sensitive technique (31). Luminex is based on xMAP (Multi-Analyte Profiling) technology and uses polystyrene beads (microspheres) uniquely dyed with distinct proportions of red and near-infrared fluorophores to distinguish each analyte (32). A drawback to this technology is that a specific instrument is required to acquire the data. Alternatively, other technologies exist that measure analytes like cytokines levels, such as the cytometric bead array (CBA), which however requires a flow cytometer, an instrument that is significantly more expensive than a Luminex instrument.

From a cost perspective, Luminex is one of the most competitive-priced technologies to perform multiplex cytokine analysis. Yet, after a MapPix Luminex instrument was acquired in our lab, an issue was the costs of the commercial kits to perform the Luminex assays. By implementing DropArray technology, which allows five assays to be run with a single kit, and despite the initial purchase of a DropArray plate washer (\$8,000), costs were reduced significantly (**Figure 3**). This improved methodology reduces the financial burden for cytokine profiling in vaccine research, particularly in the field of NTD research where funding is more limited.



■ **Figure 3.** The costs per Luminex plate are very cheap when using the dropArray technology. The initial costs of the DropArray methodology include the purchase of the DropArray plate washer.

Developing new methodologies, as well as adapting existing technologies, will drive vaccine research when costs can be saved, workflow is made easier, or assays become more sensitive.

6.2.2 Immunopeptidomics as a new approach to *T. cruzi* vaccine target identification

CD8+ T cells are considered crucial for protection against *T. cruzi*, enabling the immune system to recognize infected host cells, following by the release of cytotoxic enzymes including granzymes and perforin, which will induce apoptosis of infected host cells. These cells with intracellular *T. cruzi* parasites will then be ingested and destroyed by phagocytotic cells, ultimately clearing the infection. This is especially important in the chronic phase, where parasite burden is minimal in the blood stream and humoral immunity may be less effective. Notably, while in principle all *T. cruzi* peptides could be presented on MHC-II, assuming they display sufficient affinity to MHC-II, by APCs after taking up the antigen, for MHC-I presentation only *T. cruzi* peptides that gain access to the cytosol of the host cells (and not those that remain within the parasite) can be presented. Exceptions may exist where APCs present exogenous antigens on MHC-I through cross-presentation, but for infected host cells like muscle cells, cross-presentation is not possible (33). Therefore, it is important to understand which *T. cruzi* proteins are presented on MHC-I of infected cells, as this is important for selecting effective vaccine targets.

Furthermore, I wondered whether we could verify that Tc24 and other vaccine targets are indeed presented on MHC-I of *T. cruzi*-infected cells. Encouraging results were observed by Kurup *et al.*, who discovered that *T. cruzi* discards its flagella upon host cell invasion and that after this process the flagellar protein PAR4 becomes available for antigen processing and presentation on MHC-I and detection by specific CD8+ T cells (34). These findings suggest

that flagellar proteins might be among the earliest proteins to be recognized by CD8+ T cells, which might then be the case for Tc24 as well.

We used immunopeptidomics to identify which *T. cruzi* antigens have access to the MHC-I antigen presentation route of infected host cells. This technology to identify peptides presented on the MHC-I is predominantly used in the fields of cancer research and virology but has also been utilized for other infectious diseases, including parasitic NTDs (35). In the case of *T. cruzi*, this approach had not been used before and the use of immunopeptidomics is therefore novel for identifying vaccine targets for Chagas disease. As mentioned in **Chapter 5**, a series of experiments were optimized, allowing for the execution of immunopeptidomics experiments that resulted in the identification of 24 unique *T. cruzi* peptides, originating from 17 different *T. cruzi* proteins.

A significant advantage of immunopeptidomics is the ability to identify a wide selection of peptides derived from proteins described in proteome databases, avoiding the limitations of targeted searches, such as *in silico* prediction of peptides with MHC-I binding properties. Increased sensitivity in mass spectrometry makes it possible to analyze thousands of peptides presented by cells on their MHC complexes (36). This, however, requires the availability of a reference proteome for the species of interest. In the case of *T. cruzi*, the CL Brener strain is the reference proteome (37), and in our experiments the genetically related Tulahuen strain was used. Both the CL Brener and the Tulahuen strain are classified as DTU TcVI, making comparisons possible. However, to study parasitic strains that are genetically distant from the reference proteome of the species, can be a challenge. This is also the case for selecting the host cells, as a reference proteome of the species of the host cells are crucial to discriminate host self-peptides from the pathogen-derived peptides.

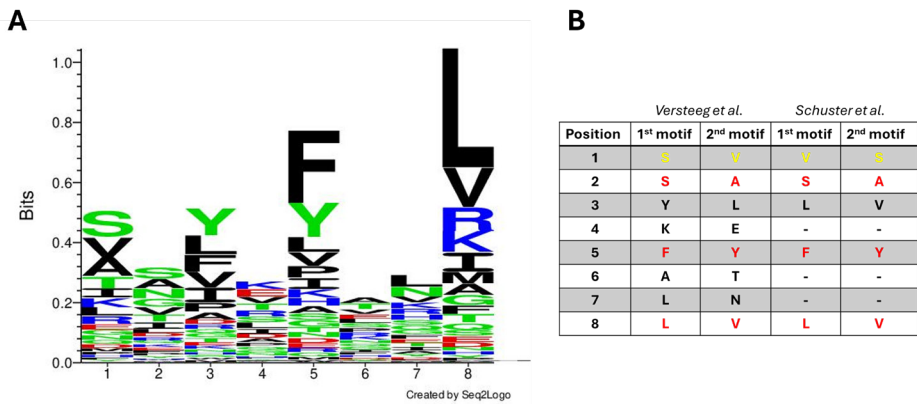
Altogether, identifying peptides that are presented on MHC-I molecules can give new insights on which proteins from *T. cruzi* are available for antigen presentation, and may be recognized by CD8+ T cells. This approach marks a significant advancement in vaccine research for Chagas disease.

6.3 INTERPRETING THE IMMUNOPEPTIDOME OF *T. CRUZI*-INFECTED CELLS

In **Chapter 5** the immunopeptidomics workflow was described to identify *T. cruzi* peptides presented on the MHC-I 48 hours post infection. From two duplicate experiments, 24 unique *T. cruzi* peptides were identified as well as hundreds of mouse self-peptides.

While the mouse self-peptides were not further addressed in **Chapter 5**, comparisons with the published literature were performed to validate our findings. After combining the self-peptide datasets from the duplicate *T. cruzi* - infected mouse MC57G fibroblasts

(background C57BL/6J) experiments, we identified the 8- and 9-mer peptides that had the highest confidence score. These peptides originated from proteins involved in antigen presentation, protein synthesis, and cellular transport, and included H-2 alpha chain, beta-2-microglobulin, ribosomal subunit proteins, actin, and dynein. When comparing these protein hits to the findings of Schuster *et al.*, where they analyzed the MHC-I immunopeptidome from healthy C57BL/6J mice for different tissues (38), we observed the same proteins in their lists of high-confidence MHC-I peptides. Furthermore, when the 8-mer mouse self-peptides from *T. cruzi*-infected fibroblasts were used to generate a binding motif plot, a very similar motif pattern to Schuster *et al.* for H2-Kb was observed, as shown in **Figure 4**. Overall, we observed that our self-peptide database followed similar patterns to previous established work, giving us additional confidence in the immunopeptidomics results and interpretation.



■ **Figure 4. Binding motif of self-peptides from *T. cruzi*-infected murine fibroblasts.** A) Binding motif prediction of 8-mer peptides, plotted using Seq2Logo (39). B) Comparison of the two highest scoring motifs for each position between our data and published data (38), sharing an identical order of the first two predicted motifs on positions 2, 3, 5, and 8. Additionally, on position 1 the two highest motifs were the same but switched. In red are the amino acids that are identical, in yellow are the ones that are identical but switched, and in black are the ones without any similarity. The “-” symbol means that the motif could not be determined.

6.3.1 Non-canonical peptides on MHC-I during *T. cruzi* infection

Typically, MHC-I presents 8-9-mer peptides, since these peptides fit best in the closed binding groove of the MHC complex. Interestingly, an increase in peptide size was observed when samples were infected with *T. cruzi*. Whereas the control experiment had 69% of all peptides between 8 and 15 amino acids (aa), both experiments where mouse fibroblasts were infected showed just 40% within this size range. Also, *T. cruzi* peptides did not display the typical 8-9-mer lengths associated with MHC-I peptide presentation but showed an atypical length averaging 11.3 aa. Similar observations have been made for other protozoan infections.

For instance, *T. gondii* infection has also been associated with larger parasitic peptides (average 14.6 aa) and host self-peptides (average 11.4 aa) compared to uninfected host cells (average 9.8 aa) (40). The average *T. gondii* peptide length was much longer than the expected 8-11-mer for HLA-A*02:01 (human MHC-I) evaluated. Also, immunopeptidomics studies on *Theileria parva*, a protozoan that causes East Coast fever in cattle, demonstrated peptides longer than 12 aa on BoLA-I (bovine MHC-I) (41). Therefore, the increase in length of peptides presented on MHC-I during infection is not unique to *T. cruzi* and has been observed for other protozoan infections.

These observations suggest that infection with *T. cruzi* modulates the antigen processing and presentation machinery, influencing the length of the presented peptides. A major factor involves the availability of peptides of different lengths for MHC binding (42). The increase in peptide length during infection could potentially be attributed to the switch from proteasome to immunoproteasome cleavage. This alternative proteasome has been found to generate peptides longer than 13 aa, which could explain the increase in peptide length during *T. cruzi* infection (43). Also, deficiencies in the transporter associated with antigen processing (TAP), which translocated peptides from the cytosol to the ER lumen for assembly with MHC-I, can result in the presentation of longer peptides (44). Therefore, TAP has been a target for immune evasion by viruses (35), but little is known about TAP during *T. cruzi* infection. Further research is needed to fully understand the mechanisms underlying peptide length modulation by *T. cruzi*, and how this could impact antigen processing and presentation of parasitic peptides to CD8⁺ T cells.

The presentation of longer peptides by MHC-I molecules and their potential to activate CD8⁺ T cells raises an important question. Can non-canonical peptides bind to MHC-I, and induce CD8⁺ T cell responses? Others have shown that longer peptides can fit in the groove by either adapting a zig-zag orientation, bulging out the middle of the groove, or extending out from the C- or N-terminus of the peptide (45). This has been observed in *T. gondii*-derived peptides with non-canonical lengths protruding through one end of the binding groove with their C-terminus (40). Other non-canonical peptides, including long, short, and glyco-peptides, have been shown to bind to MHC-I molecules and induce cellular responses (46). For example, this was observed in the case of a 13 aa peptide from the BZLF1 antigen of Epstein-Barr virus (EBV), as well as a 12-mer peptide from Cytomegalovirus (CMV) (47,48). For mouse H2-K^b and H2-D^b, peptide stabilization assays using random peptide libraries showed that peptides of 8-13-mers and 9-15-mers can be accepted, respectively (49). These observations suggest that non-canonical peptides, like the *T. cruzi* peptides identified in our immunopeptidomics experiments, can bind to MHC-I, and induce CTL responses.

In *T. gondii*, mass spec analysis revealed that some of these longer peptides bound with high affinity to HLA, while MHC-I binding prediction tools failed to predict binding. Similarly, when using the NetMHCpan 4.1 peptide affinity binding tool to predict binding affinity of the Tcj2-derived peptides identified by our immunopeptidomics experiments,

none of these peptides were predicted to bind with strong affinity to MHC-I (Supplementary data of **Chapter 5**) (50). A possible explanation for why the prediction tools do not align with these observations could be the way these tools work. The inaccuracy of these tools, like NetMHCpan, for predicting the binding of peptides derived from parasites like *T. cruzi* and *T. gondii* to MHC-I is likely due to the method in which these tools are trained to predict binding affinity. The bias in the training datasets to 9-mers and the underrepresentation of longer non-canonical peptides could therefore decrease binding prediction accuracy (51).

Importantly, vaccination strategies targeting Chagas disease should aim to induce CD8+ T cells that recognize (non-canonical) peptides presented by *T. cruzi*-infected cells. To investigate if mRNA candidate vaccines can induce the presentation of these peptides on MHC-I, one experiment could be to transfect cells *in vitro* with a mRNA construct encoding for a *T. cruzi* protein identified by immunopeptidomics, followed by performing immunopeptidomics on the transfected cells. This approach can confirm if the peptides presented to CD8+ T cells during vaccination are similar to peptides presented during infection. Overall, it is interesting for all vaccine candidates, including Tcj2 and Tc24, to test whether the vaccination strategy aligns with the actual immune response during *T. cruzi* infection.

6.3.2 Does a snapshot of the immunopeptidome provide the complete story?

The immunopeptidome of a cell is highly dynamic since the repertoire of peptides presented on the cell surface is constantly revised to reflect the actual protein composition of the cell at any given moment (52). The experiments conducted in **Chapter 5** only investigated the immunopeptidome at 48 hours post infection. A total of 17 (24 unique peptides) *T. cruzi* proteins were identified, and flagellar proteins like Tc24, and proteins from some of the large protein families from *T. cruzi* were absent. What could be the reasons behind this? Were certain proteins not presented at the chosen timepoints? To what extent do the immunopeptidomics findings tell the complete story of antigen presentation during *T. cruzi* infection?

As previous immunopeptidome studies on viruses have pointed out, the diversity and quantity of pathogen-specific peptides presented on host cells during infection are very dynamic. For instance, Hamza *et al.* showed that the majority of peptides from influenza A virus (IAV) could be detected between 6 to 9 hours after infection of human lung adenocarcinoma cells, peaking at 12 hours (53). However, major differences between individual peptides were observed, where some appeared immediately post-infection, while others took up to 9 hours to be detected. Also, when the kinetics of peptide-MHC-I presentation for peptides from Vaccinia virus (VACV, used for smallpox vaccine) infection were evaluated, unique kinetics of presentation were observed (54). Presentation of unique peptides peaked at very different times after infection, and some peptides were presented at 1000-fold higher compared to others, while this did not correlate with their predicted binding strength to MHC-I. These

studies using viruses demonstrate how the timepoint of immunopeptidome analysis could affect the identification of pathogenic peptides.

The timing of our immunopeptidome analysis of *T. cruzi*-infected cells may explain the absence of Tc24 peptides. Previous research showed that flagellar and subdominant proteins, like paraflagellar rod protein 4 (PAR4), are presented on MHC-I just hours after parasite invasion into host cells, whereas it took much longer for trans-sialidases to be presented (34). Considering the dynamics of peptide presentation on MHC-I, and the availability of *T. cruzi* proteins to the host's antigen processing and presentation machinery, flagellar proteins may be all presented before 48 hours post infection. Not much is known about the antigen presentation kinetics of *T. cruzi* peptides throughout infection. However, it would be very valuable to identify which *T. cruzi* proteins are presented early so that vaccine targets can be selected that can induce CD8+ T cells which can recognize and kill early infected cells before new parasites are produced.

Interestingly, also trans-sialidases, mucins, and MASPs were not detected, despite their general high expression profiles in *T. cruzi*. This raises the question of whether these proteins were not presented by our infected cells, or if this is related to the parasite itself. Since it has been shown that trans-sialidase-specific CD8+ T cells can recognize the same MC57G cell line used during our study, when infected with *T. cruzi* (34), it would be unlikely that there is an issue with the cell line. Another possible explanation could be that our parasite may have lost some virulence due to extensive passaging in just cells for an extended time. Trans-sialidases have been reported to be crucial for *T. cruzi* virulence (55), and passaging parasites in cells for extended times expressed lower levels of trans-sialidase and reduced virulence compared to parasites passaged in mic (56). Future research should involve occasionally passing *T. cruzi* strains in mice, so that loss of virulence is minimized. Moreover, another reason that proteins like trans-sialidase were not observed could be that trans-sialidases were not displayed on MHC-I at the time the peptides were isolated from the cells.

Notably, the immunopeptidomics-identified Kinetoplastid Membrane Protein 11 (KMP-11) is also evaluated as a vaccine target for Chagas disease (57,58), and its orthologue version as a vaccine target for *Leishmania* (59). In patients infected with *T. cruzi*, circulating CD8+ T cells were detected that recognized a unique peptide from KMP-11, supporting the hypothesis that KMP-11 peptides are presented on MHC-I during infection (60). The case for KMP-11 as a promising vaccine target is strengthened by our immunopeptidomics results, and should be further evaluated as a mRNA vaccine candidate.

6.3.3 Future outlook on the identification of Chagas disease vaccine targets by immunopeptidomics

Growing interest in immunopeptidomics by biotechnology companies, as well as by academic research labs, will continue to push the development of sample preparation,

instrumentation, and analysis of immunopeptidomics data (61,62). These developments will have a significant impact on vaccine development for parasitic and other diseases.

Exploring a range of different host cells for *T. cruzi* immunopeptidomics can reveal more about peptide presentation and kinetics. Besides murine MC57G fibroblasts, using other cell types would be of interest, since variations in each cell type's antigen processing and presentation machinery could result in the identification of different *T. cruzi* peptides, thereby expanding our protein list. Macrophages, for example, which are among the first cells to be invaded by *T. cruzi* when a host gets infected, play a protective role during *T. cruzi* infection (63). They can present phagocytized proteins as peptides on MHC-II, and in the presence of IFN- γ , exogenous antigens can be cross-presented on MHC-I, and would therefore be of interest for immunopeptidome analysis (64). Also, adipose tissue has been identified as a reservoir for *T. cruzi* during infection, therefore being an important cell target (65). Adipocytes can express both MHC-I and MHC-II and can activate CD8+ and CD4+ T cells, respectively. (66). Limited studies are described performing immunopeptidomics on adipose tissue and cells, but there are examples where this was successfully executed, for obesity studies for example (67). Furthermore, myocytes from both skeletal muscle and cardiac muscle would be very interesting to look at as well. Myocytes have been demonstrated to present antigens from *T. cruzi* on MHC-I (68,69). Cardiomyocytes play an important role in the development of Chronic chagasic cardiomyopathy (CCC) and understanding the antigens they present could be important in developing vaccines that assist CD8+ T cells in recognizing these infected cells during the chronic stage of the disease (70).

Beyond cell lines, conducting immunopeptidomics on complete tissues would provide valuable insights. This approach would give a broader representation of the immunopeptidome visible for T cells since peptides from multiple cell types will be analyzed. Scientists have already explored the MHC-I immunopeptidome of healthy tissues in mice and humans (35,38). For Chagas disease, it would be particularly relevant to analyze tissues where *T. cruzi* typically resides during infection. This should specifically include cardiac tissue, with a focus on comparing the immunopeptidome between acute and chronic stages of the infection.

6.4 THE NEXT STEPS FOR TCJ2 AND TC24 AS VACCINE TARGETS FOR CHAGAS DISEASE

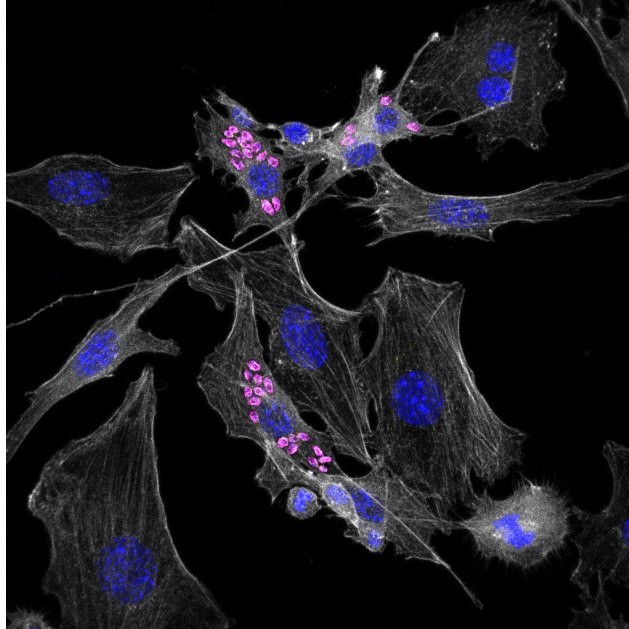
This thesis has expanded our understanding of the localization and expression kinetics of the vaccine target Tc24, and it has also identified Tcj2 as a new vaccine candidate for Chagas disease. How can this newly obtained knowledge be applied to vaccine development for Chagas disease, and which next steps and considerations are necessary?

6.4.1 Understanding the location and expression kinetics of Tcj2

Immunopeptidomics revealed in **Chapter 5** the presentation of Tcj2-derived peptides MHC-I molecules on the surface of *T. cruzi*-infected cells. Multiple peptides were identified, increasing the confidence that Tcj2 is presented by MHC-I of infected host cells. However, similar to the Tc24 vaccine target, it is important to understand the expression kinetics of Tcj2 to ensure its availability to the immune system. Furthermore, as mentioned earlier, expression of proteins by the parasite does not guarantee availability for MHC-I presentation. Many of the proteins in the living amastigotes are inaccessible to the MHC-I pathway of host cells, unless the parasite dies in the cytoplasm, or the parasite discards or secretes proteins. For Tcj2, the location is described to be predominantly in the cytoplasm of *T. cruzi*, serving as a co-chaperone of HSP70 located in the cytoplasm, mitochondria, and endoplasmic reticulum (71). The location of Tcj2 in the parasite makes it unlikely that it is available for the host's MHC-I pathway when parasites are alive unless Tcj2 is part of the discarded proteins when the flagella is shed. It would be possible that some Tcj2 proteins could be expelled during flagellar disposal, but since no flagellar proteins were identified by immunopeptidomics at 48-hours post infection, it is unlikely a significant source for MHC-I presentation. Alternatively, the parasite might secrete soluble Tcj2 or EVs containing Tcj2. This is supported by research that showed Tcj2 was present in EVs from both epimastigotes and tissue cell-culture-derived trypomastigotes, but EVs from amastigote stages were not analyzed (72). Thus, while the route of Tcj2 availability for MHC-I presentation is yet to be confirmed, it was determined that Tcj2 was presented on the MHC-I of fibroblasts and that it is a potential target for CD8+ T cells.

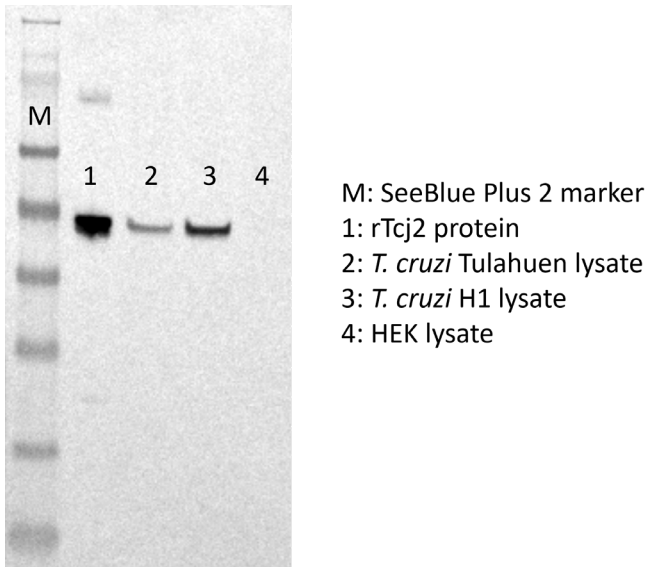
Moreover, additional research on the expression profile of Tcj2 revealed interesting observations that can help to understand the availability of Tcj2 to the MHC-I pathway. RNA-seq data from Díaz-Viraqué *et al.* showed that the transcript abundance of Tcj2 in trypomastigotes was triple that of amastigotes, which could indicate increased Tcj2 protein expression in the trypomastigote stages (73). Then, quantitative proteomics on tissue culture-derived trypomastigotes transforming into amastigotes *in vitro* (axenic amastigogenesis) revealed no distinct changes in Tcj2 protein levels between trypomastigotes and amastigotes at 30 min, 2 hours, and 9 hours after the start of amastigogenesis (74). Findings by Li and colleagues showed through RNA transcriptomics that Tcj2 was significantly more expressed at 12 and 24 hours post-infection compared to tissue culture-derived trypomastigotes, but not in amastigotes at earlier and later time points (75). Importantly, the RNA-seq data from Díaz-Viraqué does not describe a post-infection time point, so it could be that amastigotes were collected later than 24 hours, supporting the observations of Li *et al.* Overall, it could thus be that RNA transcription and protein expression of Tcj2 do not increase compared to trypomastigote levels until 12 hours after the start of amastigogenesis, followed by a decrease after 24 hours. Nevertheless, microscopy of *T. cruzi*-infected MC57G fibroblasts 72 hours post-infection revealed clear Tcj2 protein expression during the amastigote stages, indicating that despite a decrease in relative expression, a significant amount of Tcj2 protein is still expressed, potentially making it available for antigen processing and presentation soon after *T. cruzi*

invasion (**Figure 5**). Quantifying the Tcj2 protein content in intracellular amastigotes at different time points by mass spectrometry can further elucidate its availability.



■ **Figure 5. Expression of Tcj2 in *T. cruzi* amastigotes.** MC57G murine fibroblasts were infected with *T. cruzi*, Tulahuen strain. After 72 hours, extracellular parasites were washed off and cells were fixed and permeabilized, followed by Tcj2 detection using Tcj2 antisera from Tcj2 mRNA immunized mice. As a secondary antibody goat anti-mouse IgG AF488 was used (in magenta). Nuclei were stained with DAPI (in blue), and F-actin was stained using Phalloiden iFluor 647 (in white).

Besides studying the expression of Tcj2 in *T. cruzi* across different stages of host cell infection, it is crucial to inspect its expression across different *T. cruzi* strains (Distinct Typing Units, DTUs) to ensure that a vaccine candidate targets an antigen expressed by various circulating strains. Tcj2 expression was confirmed by western blot and microscopy for the Tulahuen stain (DTU TcVI) in **Chapter 5**, and we also observed expression by western blot for the H1 strain (DTU TcI) (**Figure 6**). Furthermore, transcriptomics evidence indicates expression of Tcj2 in the Y strain (DTU TcII) (75). Future research should explore the expression levels of Tcj2 in various strains to verify the availability of Tcj2 protein for antigen processing and presentation on MHC-I by host cells during infection. This approach will help in determining the viability of Tcj2 as a universal vaccine target against *T. cruzi*.



■ **Figure 6. Tcj2 is expressed by the *T. cruzi* Tulahuen and H1 strain.** An SDS-PAGE gel was run with rTcj2 protein, *T. cruzi* parasite lysate from Tulahuen strain and H1 strain, and lysate from human embryonic kidney 293 (HEK) cells. For each sample, 2 μ g of protein was loaded. After the transfer to western blot, Tcj2 was detected using pooled Tcj2 antisera from Tcj2 mRNA LNP immunized mice, followed by detection using a goat anti-mouse IgG alkaline phosphatase.

6.4.2 Designing Tcj2 and Tc24 as part of a multivalent mRNA vaccine

To make a vaccine against Chagas disease that is effective in complete elimination of *T. cruzi* parasites in the host, diversifying the number of antigens and epitopes to broaden the protection may be necessary, which can be achieved by targeting multiple *T. cruzi* antigens. While almost all vaccine targets have been evaluated as monovalent vaccine candidates, a few have been used to create multivalent vaccines. For instance, Tc24 has been encoded by a DNA vaccine together with cruzipain and Tc52 antigens, demonstrating improved protection against *T. cruzi* infection compared to their respective monovalent vaccine formulations (76). Enhanced protection from multivalent formulations have also been observed for the chimeric protein Traspain, consisting out of protein domains of the cruzipain and amastigote surface antigen 2 (ASP-2) antigens (77).

For Tcj2 and Tc24, certain key features of antigens have already been addressed, such as the expression kinetics of the antigens during trypomastigote and amastigote stages, as well as the genetic conservation of their protein sequences across different strains of *T. cruzi*. This initial knowledge of the vaccine targets supports the potential for a multivalent approach in vaccine development.

Additionally, the vaccine should ideally include antigens that harbor immunodominant and subdominant antigen and epitopes. Broadening the immune response by including subdominant antigens and epitopes contributes to host resistance, possibly enabling 100% parasite elimination (78). Importantly, antigens with subdominant profiles can be very good vaccine targets, often serving crucial functions for the parasite, showing minimal genetic variation among parasitic strains, and are proteins the parasite wants to hide by expressing other highly expressed proteins. For both Tcj2 and Tc24, in this thesis, no research was conducted to understand whether the antigens can be classified as immunodominant and subdominant, or whether they contain immunodominant and subdominant epitopes for the induction of antibodies or CTLs. However, in the case of Tc24, the fact that other flagellar proteins have been described as subdominant antigens and that Tc24 is not equally expressed throughout different parasitic stages in the host likely makes Tc24 a subdominant antigen for CTLs. In contrast, Tc24 seems to be more immunodominant for the humoral immune response, as *T. cruzi*-infected individuals show robust Tc24-specific antibody responses, and Tc24 is therefore pursued as an antigen target for serological testing (79,80). For Tcj2, the expression in all stages of the parasite, as well as the presentation of Tcj2-derived peptides on *T. cruzi*-infected cells, could contribute to a higher likelihood of it being an immunodominant antigen. To test these hypotheses, the recognition of Tcj2 by CTLs and by sera from *T. cruzi*-infected mice should be evaluated. For Tc24, this has already been done using samples from Chagas patients, showing that a low percentage of T cells from these patients responded to Tc24 stimulation, which supports its subdominant profile in the chronic phase of the disease (79).

Following the key features of effective antigen targets, and the knowledge available on Tc24 and Tcj2, what type of protection should both vaccine targets induce to effectively eliminate *T. cruzi*? For Tc24, the location of the protein strongly suggests that the induction of Tc24-specific antibodies may not be as important as inducing a cell-mediated immune response, consisting of CD4+ T helper cells and CD8+ CTLs. Induction of T helper cells may be achieved by subunit vaccine formulation with an adjuvant, similar to the Tc24-C4 recombinant protein with a TLR4 agonist. For the induction of CD8+ CTLs mRNA vaccines will be particularly suitable for inducing CD8+ T cells against Tc24, since mRNA-translated vaccine antigens, produced in the cytosol of cells, are directly available for MHC-I processing and presentation, whereas subunit vaccines are predominantly processed through the MHC-II route, activating CD4+ T cells and B cells. These CD8+ T cells can recognize and kill *T. cruzi*-infected host cells shortly after infection, potentially controlling the infection early and effectively. Recently, Tc24 mRNA formulated in lipid nanoparticles (LNPs) was tested as a therapeutic vaccine in mice, demonstrating a significant reduction in parasite burden in skeletal muscle, but not in heart tissue two weeks after vaccination. However, no improved outcomes were observed at 18 weeks after vaccination, suggesting the need for optimization (81). Other vaccination strategies, where Tc24 was given first as mRNA vaccine followed by Tc24 recombinant protein, so-called heterologous vaccine strategies, have also been investigated and showed increased induction of polyfunctional CD8+ T cells (82). For Tcj2, given the hypothesis that this antigen is expressed during both trypomastigote and amastigote stages, Tcj2-specific CD8+ T cells

could potentially recognize *T. cruzi*-infected cells at any stage of host cell infection. The mRNA platform also shows promise for inducing specific CD8+ T cells against Tcj2, as demonstrated in the immunogenicity studies described in **Chapter 5**. Future *in vivo* challenge studies are essential to confirm the efficacy of this approach in eliminating *T. cruzi* during infection.

In addition to testing Tcj2 and Tc24 and monovalent mRNA vaccines, both vaccine targets should be co-formulated in LNPs to be evaluated as a multivalent vaccine in mouse challenge models. As highlighted earlier in **Chapter 4**, co-formulating different mRNA constructs into LNPs is straightforward, as demonstrated by Chahal et al., who formulated six different mRNA constructs together (83). Furthermore, increasing the breadth of the immune response by combining different antigens is well-established, and has been done various times for subunit vaccines. Indeed, the immune system can handle simultaneous vaccinations, and is commonly done when kids are immunized with DTaP and MMR vaccines (84). However, the development of these multivalent subunit vaccines poses challenges, such as protein stability issues during co-formulation, stability issues with the production of chimeric proteins, or non-specific immune responses to linker structures used to couple proteins together (77). For mRNA vaccines, Tcj2 and Tc24 should be tested as a multivalent mRNA vaccine as a starting point. Additionally, an mRNA candidate vaccine should be designed that includes Tc24 and Tcj2 antigens, as well as immunodominant antigens such as trans-sialidases (TSA-1 and/or ASP-2) that are considered valuable for *T. cruzi* control (85). Since others have successfully combined up to 6 antigens in a multivalent mRNA vaccine, other promising *T. cruzi* vaccine targets, like KMP-11 and Tc52 could be considered as well (83).

6.4.3 Prophylactic and therapeutic vaccine considerations

For all vaccine targets currently under evaluation, a key question is whether to develop the candidate vaccine for prophylactic or therapeutic applications. For prophylactic applications, the induction of a strong Th1 response and specific CD8+ T cells is essential for the elimination of *T. cruzi*. mRNA vaccines are very effective in eliciting Th1 immune responses and CD8+ T cells, making them very suitable for prophylactic application. Tcj2 and Tc24 are both promising candidates for these types of cellular immune responses, hypothesized to be presented on MHC-I of infected cells and recognizable by CTLs. However, as discussed in **Chapter 1**, antibodies capable of opsonizing and complement-mediated lysis of extracellular parasites during acute infection are also highly effective. Therefore, it should be considered to add vaccine targets that can induce these antibodies, like cruzipain and Tc52.

For therapeutic vaccine strategies, it is hypothesized that a balanced Th1/Th2/Th17 (Type 1-3 immune profiles) response, as well as regulatory T cells producing IL-10, are important to prevent intensifying tissue inflammation and aggravating cardiac disease (86). mRNA vaccines typically do not achieve good Th2 and Th17 responses, and these types of responses are often not even detected (87,88). This is partly because mRNA-encoded proteins are generally presented on MHC-I, primarily activating CD8+ T cells. To elicit CD4+ helper T

cells, that can steer to Th1/Th2/Th17 responses, more frequent presentation on MHC-II is needed. This can be achieved by using signal sequences in the mRNA, such as GPI anchors or transmembrane sequences, which drive the presentation of the translated protein on the surface of transfected cells, allowing for increased MHC-II presentation (89). This strategy could be applied to Tcj2, Tc24, and other vaccine targets, and skewing of the responses towards Th1/Th2/Th17 can easily be verified by flow cytometry. Furthermore, activation of Toll-like receptors (TLRs) also plays a substantial role in steering the immune response. mRNA vaccines activate TLRs 7/8 and TLR 9, activating NF- κ B and the production of type I interferons, steering the response towards Th1, cytotoxic T cell responses, and IgG2a antibodies. However, TLR4 and TLR9 stimulation can lead to strong Th2 responses with IgG1 antibodies (90). The addition of specific TLR agonists in LNPs or in the vaccine formulation buffer can be tested to achieve the desired Th1/Th2/Th17 response. Furthermore, subunit vaccines are often formulated with TLR agonists and can steer the immune response effectively to Th1/Th17/Th17.

Additionally, heterologous vaccination strategies, where booster immunizations differ from prime immunizations in vaccine formulation and/or vaccine platform, might also be beneficial for prophylactic and therapeutic applications. Promising results for parasitic diseases have been observed in the case of malaria, Leishmania and also Chagas disease (91–93). Also, in the case of SARS-CoV-2, heterologous vaccine strategies have been associated with increased protection and more durable immune responses (94,95). However, the development of heterologous vaccine strategies can be labor-intensive, complicated and expensive due to the development of different vaccine products. Fortunately, for mRNA vaccines the development of a mRNA production pipeline is independent of the mRNA construct, so the majority of the investment to develop mRNA vaccines only has to be done once.

6.4.4 Avoiding mRNA vaccine-induced adverse effects that could exacerbate cardiac inflammation

Just like with every candidate vaccine or adjuvant, adverse effects due to toxicity and reactogenicity can occur that require mitigation. Potential mRNA vaccine toxicity concerns have been described (96). For example, certain ionizable lipids used in the LNP formulations were shown to act as adjuvants, activating the innate immune system and inducing the production of IL-6 or type I interferons (97,98). Strategies to minimize mRNA vaccine risks have been described, and ongoing research is trying to fill in additional knowledge gaps on toxicities of components used to develop mRNA vaccines (96).

Avoiding vaccine-induced cardiac inflammation is very important in the case of patients with CCC. A vaccine that targets *T. cruzi* antigens will induce immune activation in tissues where *T. cruzi* resides, so the goal is to induce a balanced Th1/Th2/Th3 response, avoiding excessive tissue damage. While there are no direct indications that mRNA vaccines can exacerbate cardiac inflammation in patients with CCC, studies should be done to address

mRNA vaccine safety in the context of existing cardiac inflammation, ensuring safe and effective application of therapeutic mRNA vaccines for Chagas disease (99).

To note, while data on COVID-19 mRNA vaccines BNT162b2 (Pfizer) and mRNA-1273 (Moderna) showed a minor increased risk for myocarditis and pericarditis (100), this risk appears to be related to the encoded vaccine antigen (SARS-CoV-2 spike protein) interacting with the host's cardiovascular system and to the mRNA vaccine platform (101).

6.4.5 Vaccine-linked chemotherapy using multivalent mRNA vaccines

For millions of people currently diagnosed with Chagas disease, the available antiparasitic drug treatments, benznidazole (BNZ) and nifurtimox, have limited success in the chronic phase and cause significant side effects. Vaccine-linked chemotherapy, where vaccinations are combined with antiparasitic drug regimens, is an attractive approach to reduce drug doses and decrease side effects as a treatment in the chronic stage of Chagas disease. When BNZ is used during vaccine-linked chemotherapy with a Tc24-C4 protein and TLR4 agonist adjuvant, a substantial dose reduction of BNZ still leads to a significant reduction in blood and cardiac parasite burdens during the acute stage of disease in mice (1), and in chronic infection improvements in cardiac function and structure were induced (102). Also, a vaccine targeting a fragment of *T. cruzi* trans-sialidase allowed for restoration of electrocardiographic (ECG) parameters when administered with BNZ as combination therapy in chronically infected mice, while vaccine or BNZ treatment alone did not achieve this (103). Furthermore, instead of using only one vaccine target, broadening the immune response by targeting different *T. cruzi* antigens using a multivalent vaccine, could lead to further reduction of parasite burdens, possibly even achieving elimination. For example, Dzul-Huchim *et al.* tested Tc24-C4 and TSA-1-C4 (trypomastigote surface antigen 1, a trans-sialidase) and TLR4 agonist as a multivalent subunit vaccine for vaccine-linked chemotherapy with BNZ, demonstrating protection from progression of cardiac fibrosis in chronically infected mice (104). This could potentially also lower the dose of BNZ to even less than four-fold. However, as mentioned earlier, vaccine formulations should be selected that can induce a balanced Th1/Th2/Th17 response.

6.5 OUTLOOK FOR A CHAGAS DISEASE VACCINE

While vaccine development for Tcj2 and Tc24 will continue and may potentially result in vaccine candidates capable of eliminating *T. cruzi* infection in animal models, what is the future outlook for Chagas disease vaccine development and the broader goal of solving Chagas disease?

6.5.1 Challenges for vaccine development

While the ongoing development of *T. cruzi* vaccines shows promise, there are still several challenges to address before licensure. The primary challenge is a lack of standard animal challenge models, leading to vaccine screening in different animal species, such as dogs, rats, non-human primates, and predominantly mice. Because of this diverse set of animal models, direct comparisons of immunogenicity and efficacy are challenging. Animals are also affected differently by *T. cruzi* infection, making it unclear how research outcomes translate to vaccine efficacy or pathogenesis in humans. An additional challenge is the use of various *T. cruzi* strains by different research groups, with virulence levels varying depending how the parasite cultures are maintained. Efforts are being made to develop more standardized *in vivo* models that address these issues, and harmonization solutions are being implemented to make it easier for research groups to share *T. cruzi* strains (105).

Another challenge that hampers vaccine development is the lack of effective serological methods and diagnostics that can detect *T. cruzi* in humans, especially in the chronic phase of the disease. Although existing diagnostic tests give satisfactory results in many cases, sensitivity levels vary based on the geographic origin of patients (106). As a result, there is no “gold standard” for diagnosis, and cases remain undetected due to discordant results, which is particularly an issue in North America (107,108) and Bolivia, where, for example, it is estimated that only 6% of the chronically infected patients are diagnosed (109). For vaccine development, this lack of tools to accurately diagnose *T. cruzi* infection is an issue. If a candidate vaccine comes to a point where its evaluation in a clinical trial is needed, assays are required to accurately monitor the status of the *T. cruzi* infection, e.g., parasitological cure. Fortunately, advancements in tools, such as high-density peptide arrays, now allow for the screening of millions of peptides, representing the complete *T. cruzi* proteome, and this might elucidate antigenic regions of *T. cruzi* proteins that can be used for future serological tools (107,110).

Moreover, for a Chagas disease vaccine that affects the poorest people in the world, the path through clinical trials and licensure is expensive, time-consuming, and challenging. Clinical evaluation typically happens in three phases, with phase III involving the largest and most costly human studies to assess vaccine efficacy. In the US it is estimated that a phase III vaccine study costs between 150 million and 1.5 billion dollars, although for Chagas disease an advanced clinical study would mostly likely happen (partially) outside the US (111). While the return on investment could be high, given that in the US alone \$1.2 billion is lost on Chagas disease annually (28), who would be interested in picking up the tab? Pharmaceutical companies are probably not interested since the target group is mostly impoverished people. A country where Chagas is endemic is unlikely to bear the costs either. Fortunately, the Drugs for Neglected Diseases initiative (DNDi) has demonstrated that by utilizing public relations and fundraising, clinical trials for Chagas disease can be fully funded (112). Furthermore, the design of a clinical trial to test a Chagas disease vaccine is not straightforward and poses difficult questions: Should a vaccine induce sterilizing immunity or only prevent or delay clinical

symptoms? And given that it takes years to develop clinical symptoms of Chagas disease, and only a subset of patients develop symptoms, what would a feasible vaccine clinical trial look like in terms of size and duration (113)? These questions need to be carefully addressed when designing a clinical trial to minimize the risk of potential failure.

6.5.2 What can be done for people with chronic chagasic cardiomyopathy?

When patients have progressed to CCC, their hearts have already sustained damage due to slowly developing, parasite-induced, fibrosis and inflammation. The primary aim of a therapeutic vaccine is clinical improvement or slowing the disease progression, by controlling cardiac inflammation and fibrosis, regardless of elimination of *T. cruzi* infection. In an ideal scenario, patients would clinically improve, and 100% parasitological cure is achieved, although that is currently impossible to measure in patients due to the lack of a suitable test for parasitological cure (112).

Currently, the primary aim of clinical improvement or slowing the disease progression is thought to be achieved through vaccine-linked chemotherapy. However, since this treatment is not yet available in the clinic, and the rTc24-C4 candidate vaccine is being prepared for evaluation in clinical trials, BNZ is currently still considered the best treatment for Chagas disease (114). Moreover, alternative strategies that combine vaccination and STAT inhibitors are explored, as transcription factors like STAT3 are believed to be involved in both fibrotic and inflammation pathways, and data suggests they play a crucial role in the pathogenesis of CCC (86). These strategies aim to prevent cardiac damage but will only benefit patients that have not yet developed severe clinical manifestations (115).

6.6 FUTURE OUTLOOK FOR MRNA VACCINE DEVELOPMENT FOR NEGLECTED TROPICAL DISEASES

The development and swift deployment of mRNA vaccines, as demonstrated during the COVID-19 pandemic, have marked a significant technological advancement in vaccinology. Moderna and Pfizer-BioNTech obtained emergency use authorization from the FDA with their COVID-19 mRNA vaccines mRNA-1273 and BNT162b2, respectively, within a year after the start of development (116). This showed how quickly mRNA vaccines now can be developed and tested in clinical trials if society considers this important. What are the current challenges with mRNA vaccine development? And could we develop mRNA vaccines for parasitic diseases causing human suffering in LMICs with the same priority?

In the last couple of years, mRNA vaccines, as well as mRNA-based therapeutics, have been studied and tested at a significantly increased amount, leading to an improved

production process and optimization of technologies. More resources are becoming available to make mRNA vaccines, and more scientists are becoming familiar with the platform.

6.6.1 Advancements in technology and manufacturing

Developments in the mRNA research and manufacturing field have resulted in several improvements. Advances in technology, like new cap analogs for mRNA capping, significantly improved the capping efficiency and translation efficiency of mRNA vaccines (117). Also advances in the formulation of LNPs are made to better direct the LNPs to target tissues other than the liver (118,119). Self-amplifying mRNA (saRNA) and circular mRNA also have lots of potential for dose reduction and extended translation to protein. These are all developments that can improve the efficacy of mRNA vaccines and bring down their costs. This is important for LMICs, since funding is always an issue. Furthermore, from a manufacturing efficiency standpoint, mRNA vaccines are a lot easier to make since cell-free systems can be used, excluding the use of bacteria, yeast, live infectious agents, or even eggs for vaccine production (120,121). Moreover, since manufacturing mRNA is unrelated to the encoded antigen, manufacturing sites could easily adapt to other vaccines for new pathogens, which enhances preparedness for emerging epidemics or seasonal vaccines (120). The technology allows for quick reprogramming to combat new diseases, a significant advantage for regions frequently hit by emerging infectious diseases. Moreover, costs can be saved for the storage and distribution of mRNA vaccines, when these vaccines are prepared and stored in areas where they are needed. Also, efforts are made to store mRNA LNPs refrigerated or even at room temperature, as this would further significantly improve treatment accessibility and transport (119). This would be a great benefit for tropical regions where cold-chain is unreliable or absent.

6.6.2 Ensuring a fair cost for mRNA vaccines for neglected tropical diseases

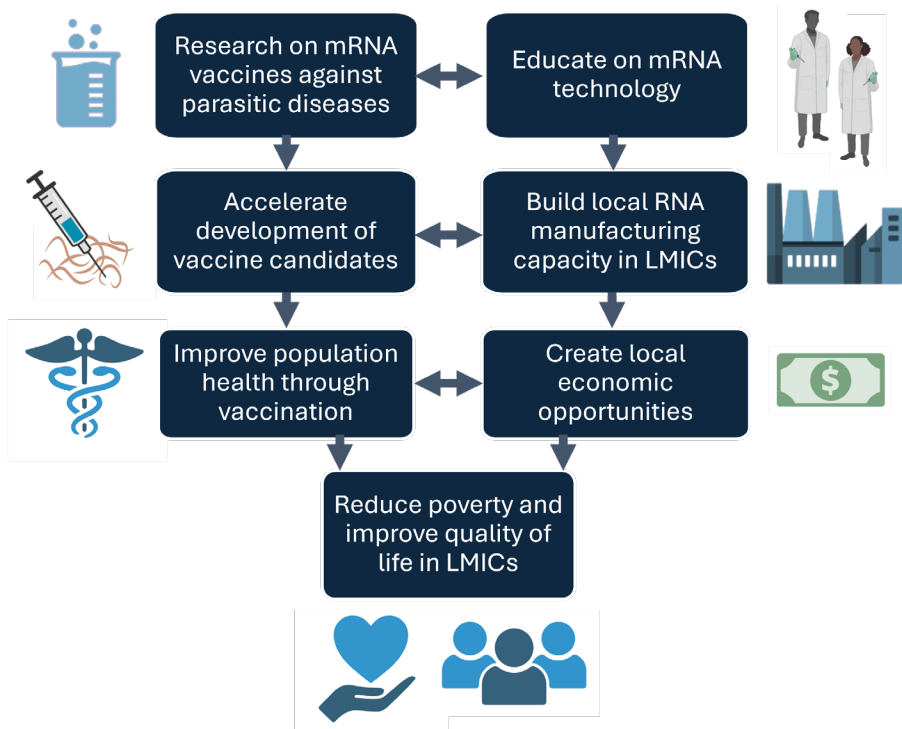
A very important aspect of the implementation of mRNA vaccines in LMICs is the costs associated with production and manufacturing. This is particularly crucial for LMICs, where financial constraints are significant. While initial costs for setting up mRNA production might be high, mRNA vaccine technology is expected to be more cost-effective in the future than older methods (122). Millipore Sigma estimated that at a yearly production volume of 10 million mRNA vaccine doses, the cost would be \$4-5 per dose (123). Of these costs, 80% is from materials, and while less expensive materials could be used, the best materials give the highest yield and efficiency, making the mRNA vaccines currently feasible (124). Materials including lipids for LNP formulations, modified nucleotides, and mRNA capping enzymes are currently covered by intellectual property (IP) rights, making their use expensive. The willingness of leading manufacturers to share their IP rights could reduce the cost of mRNA for LMICs significantly. Moderna has already shown openness to IP licensing without claiming infringement, setting an example for others to follow (125). Lowering the costs of making mRNA vaccines will make the accessibility and production of mRNA vaccines in LMICs a lot more likely.

Nonetheless, vaccines can still be too expensive for LMICs when prepared by companies in the western world. Pharmaceutical companies with an incentive for profit can increase the prices significantly, and LMICs should not rely on these companies. For instance, estimations of the net cost of manufacturing the COVID-19 vaccines range between \$0.54–0.98 a dose, and others estimated \$1.18–2.85, while Moderna and Pfizer charged between \$14.70 to \$23.50 per dose (126–128). Then in 2023, they asked \$120–130 per dose for the XBB.1.5 version of the Omicron mRNA vaccine booster (129). Note that most of the development cost for these vaccines was sponsored by public funding (130). Agreements between governments and pharmaceutical companies over vaccine prices are often unclear to the public and are made in secrecy, but the public should demand more clarity, allowing the verification of development and manufacturing costs, before and after taxpayer subsidies (126). Until then, no fair prices can be agreed upon and vaccines cannot be made more affordable, affecting especially LMICs (131). However, there is also much effort to make mRNA vaccines more affordable, as several biotechnology institutes are making investments to manufacture affordable cGMP-grade mRNA vaccines (132).

6.6.3 mRNA vaccine development by low and middle-income countries

Rather than developing vaccines for LMICs and deciding for them, it is essential to listen to and support these countries in developing vaccines for diseases prevalent in their regions. We should avoid the pattern seen during the COVID-19 pandemic, where expensive vaccines were developed in the Western world, prioritized for Western countries, and later found to be unaffordable for LMICs. (133). As depicted in **Figure 7**, the development of mRNA vaccines for (parasitic) infections may offer enhanced health and economic prospects, improving the quality of life in LMICs.

On a positive note, the World Health Organization (WHO) announced in June 2021 the initiation of technology transfer hubs (134). Through a center of excellence and training hub (mRNA vaccine technology hub) located at Afrigen, Cape Town, South Africa, recipients will receive support to build capacity to prepare for large-scale manufacturing and distribution of mRNA vaccines in LMICs. This is a promising initiative, which could help these countries develop their vaccines. The ability to produce vaccines locally in LMICs could dramatically improve access to life-saving vaccines and reduce dependence on international supply chains, which often prioritize higher-income markets. Additionally, investment costs of manufacturing facilities can be lower compared to the Western world due to lower real estate costs and construction costs (122). In 2022, Egypt, Kenya, Nigeria, Senegal, South Africa and Tunisia were announced as the first technology recipients to receive access to mRNA vaccine technology, knowledge to manufacture, and support in training scientists (135). Furthermore, the effort of making mRNA vaccine hubs is also being expanded to Latin America, where Argentina and Brazil have been receiving technology transfer training in mRNA vaccines (136).



■ **Figure 7.** A diagram illustrating the health and economic opportunities that mRNA vaccines can provide in LMICs.

6.7 CONCLUDING REMARKS

Throughout this thesis, the objective was to advance the creation and evaluation of vaccines against parasitic diseases. While the work was primarily focused on Chagas disease, it also contributed to a broader understanding of the challenges in developing vaccines for other parasitic NTDs. New approaches were implemented, existing hypotheses were re-evaluated, new knowledge on *T. cruzi* was acquired, and methodologies were employed to advance the development of vaccine targets against other parasitic diseases, such as *T. brucei* and *Leishmania spp.*

Given the current landscape, we are likely on the brink of a significant expansion in mRNA vaccines and therapeutics. This will impact the field of Chagas disease as well, with multivalent mRNA vaccines expected to show strong potential. Additionally, there is a hopeful outlook for LMICs to effectively tackle both current and future health challenges through the development and manufacturing of mRNA vaccines for parasitic NTDs.

6.8 REFERENCES

1. Jones K, Versteeg L, Damania A, Keegan B, Kendricks A, Pollet J, et al. Vaccine-linked chemotherapy improves benznidazole efficacy for acute Chagas disease. *Infect Immun*. 2018 Jan 8;|AI.00876-17.
2. Barry MA, Versteeg L, Wang Q, Pollet J, Zhan B, Gusovsky F, et al. A therapeutic vaccine prototype induces protective immunity and reduces cardiac fibrosis in a mouse model of chronic *Trypanosoma cruzi* infection. *PLoS Negl Trop Dis*. 2019 May 30;13(5):e0007413.
3. Cruz-Chan JV, Villanueva-Lizama LE, Versteeg L, Damania A, Villar MJ, González-López C, et al. Vaccine-linked chemotherapy induces IL-17 production and reduces cardiac pathology during acute *Trypanosoma cruzi* infection. *Sci Rep*. 2021 Feb 5;11(1):3222.
4. Martinez-Campos V, Martinez-Vega P, Ramirez-Sierra MJ, Rosado-Vallado M, Seid CA, Hudspeth EM, et al. Expression, purification, immunogenicity, and protective efficacy of a recombinant Tc24 antigen as a vaccine against *Trypanosoma cruzi* infection in mice. *Vaccine*. 2015 Aug 26;33(36):4505–12.
5. Filardy AA, Guimarães-Pinto K, Nunes MP, Zukeram K, Fliess L, Pereira L, et al. Human Kinetoplastid Protozoan Infections: Where Are We Going Next? *Front Immunol* [Internet]. 2018 Jul 25 [cited 2019 Aug 5];9. Available from: <https://www.ncbi.nlm.nih.gov/pmc/articles/PMC6069677/>
6. Xu X, Olson CL, Engman DM, Ames JB. NMR structure of the calflagin Tb24 flagellar calcium binding protein of *Trypanosoma brucei*. *Protein Sci Publ Protein Soc*. 2012 Dec;21(12):1942–7.
7. Eyford BA, Kaufman L, Salama-Alber O, Loveless B, Pope ME, Burke RD, et al. Characterization of Calflagin, a Flagellar Calcium-Binding Protein from *Trypanosoma congolense*. *PLoS Negl Trop Dis*. 2016 Apr 7;10(4):e0004510.
8. Godsel LM, Engman DM. Flagellar protein localization mediated by a calcium-myristoyl/palmitoyl switch mechanism. *EMBO J*. 1999 Apr 15;18(8):2057–65.
9. Pech-Canul Á de la C, Monteón V, Solís-Oviedo RL. A Brief View of the Surface Membrane Proteins from *Trypanosoma cruzi*. *J Parasitol Res*. 2017;2017:3751403.
10. Matos MN, Cazorla SI, Bivona AE, Morales C, Guzmán CA, Malchiodi EL. Tc52 Amino-Terminal-Domain DNA Carried by Attenuated *Salmonella enterica* Serovar Typhimurium Induces Protection against a *Trypanosoma cruzi* Lethal Challenge. *Infect Immun*. 2014 Oct;82(10):4265–75.
11. Garzón E, Borges MC, Cordeiro-da-Silva A, Nacife V, Meirelles M de N, Guilvard E, et al. *Trypanosoma cruzi* carrying a targeted deletion of a Tc52 protein-encoding allele elicits attenuated Chagas' disease in mice. *Immunol Lett*. 2003 Oct 9;89(1):67–80.
12. Cazorla SI, Frank FM, Becker PD, Arnaiz M, Mirkin GA, Corral RS, et al. Redirection of the Immune Response to the Functional Catalytic Domain of the Cystein Proteinase Cruzipain Improves Protective Immunity against *Trypanosoma cruzi* Infection. *J Infect Dis*. 2010 Jul 1;202(1):136–44.
13. Bivona AE, Alberti AS, Cerny N, Trinitario SN, Malchiodi EL. Chagas disease vaccine design: the search for an efficient *Trypanosoma cruzi* immune-mediated control. *Biochim Biophys Acta BBA - Mol Basis Dis*. 2020 May 1;1866(5):165658.
14. Bayer-Santos E, Aguilar-Bonavides C, Rodrigues SP, Cordero EM, Marques AF, Varela-Ramirez A, et al. Proteomic analysis of *Trypanosoma cruzi* secretome: characterization of two populations of extracellular vesicles and soluble proteins. *J Proteome Res*. 2013 Feb 1;12(2):883–97.
15. Caeiro LD, Alba-Soto CD, Rizzi M, Solana ME, Rodriguez G, Chidichimo AM, et al. The protein family TcTASV-C is a novel *Trypanosoma cruzi* virulence factor secreted in extracellular vesicles by trypomastigotes and highly expressed in bloodstream forms. *PLoS Negl Trop Dis*. 2018 May 4;12(5):e0006475.

16. de Pablos Torró LM, Retana Moreira L, Osuna A. Extracellular Vesicles in Chagas Disease: A New Passenger for an Old Disease. *Front Microbiol.* 2018 Jun 1;9:1190.
17. Bautista-López NL, Ndao M, Camargo FV, Nara T, Annoura T, Hardie DB, et al. Characterization and Diagnostic Application of *Trypanosoma cruzi* Trypomastigote Excreted-Secreted Antigens Shed in Extracellular Vesicles Released from Infected Mammalian Cells. *J Clin Microbiol.* 2017 Mar;55(3):744–58.
18. Marcilla A, Martin-Jaular L, Trelis M, Menezes-Neto A de, Osuna A, Bernal D, et al. Extracellular vesicles in parasitic diseases. *J Extracell Vesicles.* 2014 Jan 1;3(1):25040.
19. Cardoso MS, Reis-Cunha JL, Bartholomeu DC. Evasion of the Immune Response by *Trypanosoma cruzi* during Acute Infection. *Front Immunol* [Internet]. 2016 [cited 2018 Mar 22];6. Available from: <https://www.frontiersin.org/articles/10.3389/fimmu.2015.00659/full>
20. Toro Acevedo CA, Valente BM, Burle-Caldas GA, Galvão-Filho B, Santiago H da C, Esteves Arantes RM, et al. Down Modulation of Host Immune Response by Amino Acid Repeats Present in a *Trypanosoma cruzi* Ribosomal Antigen. *Front Microbiol* [Internet]. 2017 [cited 2020 Jun 28];8. Available from: <https://www.frontiersin.org/articles/10.3389/fmicb.2017.02188/full>
21. Bryan MA, Guyach SE, Norris KA. Specific Humoral Immunity versus Polyclonal B Cell Activation in *Trypanosoma cruzi* Infection of Susceptible and Resistant Mice. *PLoS Negl Trop Dis.* 2010 Jul 6;4(7):e733.
22. Tarleton RL. CD8+ T Cells in *Trypanosoma cruzi* Infection. *Semin Immunopathol.* 2015 May;37(3):233–8.
23. Low HP, Santos MAM, Wizel B, Tarleton RL. Amastigote Surface Proteins of *Trypanosoma cruzi* Are Targets for CD8+ CTL1. *J Immunol.* 1998 Feb 15;160(4):1817–23.
24. Garg N, Nunes MP, Tarleton RL. Delivery by *Trypanosoma cruzi* of proteins into the MHC class I antigen processing and presentation pathway. *J Immunol.* 1997 Apr 1;158(7):3293–302.
25. Zhang S, Zhang H, Zhao J. The role of CD4 T cell help for CD8 CTL activation. *Biochem Biophys Res Commun.* 2009 Jul 10;384(4):405–8.
26. Bingaman AW, Pearson TC, Larsen CP. The role of CD40L in T cell-dependent nitric oxide production by murine macrophages. *Transpl Immunol.* 2000 Nov 1;8(3):195–202.
27. Sánchez-Valdéz FJ, Padilla A, Wang W, Orr D, Tarleton RL. Spontaneous dormancy protects *Trypanosoma cruzi* during extended drug exposure. Soldati-Favre D, editor. *eLife.* 2018 Mar 26;7:e34039.
28. Dumonteil E, Bottazzi ME, Zhan B, Heffernan MJ, Jones K, Valenzuela JG, et al. Accelerating the development of a therapeutic vaccine for human Chagas disease: rationale and prospects. *Expert Rev Vaccines.* 2012 Sep 1;11(9):1043–55.
29. Netea MG, Van der Meer JWM, Suttmuller RP, Adema GJ, Kullberg BJ. From the Th1/Th2 Paradigm towards a Toll-Like Receptor/T-Helper Bias. *Antimicrob Agents Chemother.* 2005 Oct;49(10):3991–6.
30. Macaluso G, Grippi F, Di Bella S, Blanda V, Gucciardi F, Torina A, et al. A Review on the Immunological Response against *Trypanosoma cruzi*. *Pathogens.* 2023 Feb;12(2):282.
31. Elshal MF, McCoy JP. Multiplex Bead Array Assays: Performance Evaluation and Comparison of Sensitivity to ELISA. *Methods San Diego Calif.* 2006 Apr;38(4):317–23.
32. Reslova N, Michna V, Kasny M, Mikel P, Kralik P. xMAP Technology: Applications in Detection of Pathogens. *Front Microbiol* [Internet]. 2017 [cited 2023 Dec 24];8. Available from: <https://www.frontiersin.org/articles/10.3389/fmicb.2017.00055>

33. Zhang T, Aipire A, Li Y, Guo C, Li J. Antigen cross-presentation in dendritic cells: From bench to bedside. *Biomed Pharmacother*. 2023 Dec 1;168:115758.
34. Kurup SP, Tarleton RL. The Trypanosoma cruzi Flagellum Is Discarded via Asymmetric Cell Division following Invasion and Provides Early Targets for Protective CD8+ T Cells. *Cell Host Microbe*. 2014 Oct 8;16(4):439–49.
35. Shapiro IE, Bassani-Sternberg M. The impact of immunopeptidomics: From basic research to clinical implementation. *Semin Immunol*. 2023 Mar 1;66:101727.
36. Caron E, Kowalewski DJ, Koh CC, Sturm T, Schuster H, Aebersold R. Analysis of Major Histocompatibility Complex (MHC) Immunopeptidomes Using Mass Spectrometry. *Mol Cell Proteomics*. 2015 Dec 1;14(12):3105–17.
37. Trypanosoma cruzi (strain CL Brener) | Proteomes | UniProt [Internet]. [cited 2024 Jan 15]. Available from: <https://www.uniprot.org/proteomes/UP000002296>
38. Schuster H, Shao W, Weiss T, Pedrioli PGA, Roth P, Weller M, et al. A tissue-based draft map of the murine MHC class I immunopeptidome. *Sci Data*. 2018 Aug 7;5:180157.
39. Thomsen MCF, Nielsen M. Seq2Logo: a method for construction and visualization of amino acid binding motifs and sequence profiles including sequence weighting, pseudo counts and two-sided representation of amino acid enrichment and depletion. *Nucleic Acids Res*. 2012 Jul;40(Web Server issue):W281–7.
40. McMurtrey C, Trolle T, Sansom T, Remesh SG, Kaever T, Bardet W, et al. Toxoplasma gondii peptide ligands open the gate of the HLA class I binding groove. *Gilmore MS, editor. eLife*. 2016 Jan 29;5:e12556.
41. Connelley T, Nicastrì A, Sheldrake T, Vrettou C, Fisch A, Reynisson B, et al. Immunopeptidomic Analysis of BoLA-I and BoLA-DR Presented Peptides from Theileria parva Infected Cells. *Vaccines*. 2022 Nov;10(11):1907.
42. Trolle T, McMurtrey CP, Sidney J, Bardet W, Osborn SC, Kaever T, et al. The Length Distribution of Class I-Restricted T Cell Epitopes Is Determined by Both Peptide Supply and MHC Allele-Specific Binding Preference. *J Immunol*. 2016 Feb 15;196(4):1480–7.
43. Raule M, Cerruti F, Benaroudj N, Migotti R, Kikuchi J, Bachi A, et al. PA28 $\alpha\beta$ Reduces Size and Increases Hydrophilicity of 20S Immunoproteasome Peptide Products. *Chem Biol*. 2014 Apr 24;21(4):470–80.
44. Lorente E, Palomo C, Barnea E, Mir C, del Val M, Admon A, et al. Natural Spleen Cell Ligandome in Transporter Antigen Processing-Deficient Mice. *J Proteome Res*. 2019 Sep 6;18(9):3512–20.
45. Zajonc DM. Unconventional Peptide Presentation by Classical MHC Class I and Implications for T and NK Cell Activation. *Int J Mol Sci*. 2020 Oct 13;21(20):7561.
46. Lazoura E, Lodding J, Farrugia W, Day S, Ramsland PA, Apostolopoulos V. Non-canonical anchor motif peptides bound to MHC class I induce cellular responses. *Mol Immunol*. 2009 Mar;46(6):1171–8.
47. Green KJ, Miles JJ, Tellam J, van Zuylen WJM, Connolly G, Burrows SR. Potent T cell response to a class I-binding 13-mer viral epitope and the influence of HLA micropolymorphism in controlling epitope length. *Eur J Immunol*. 2004;34(9):2510–9.
48. Burrows JM, Bell MJ, Brennan R, Miles JJ, Khanna R, Burrows SR. Preferential binding of unusually long peptides to MHC class I and its influence on the selection of target peptides for T cell recognition. *Mol Immunol*. 2008 Mar 1;45(6):1818–24.
49. Stevens J, Wiesmüller KH, Walden P, Joly E. Peptide length preferences for rat and mouse MHC class I molecules using random peptide libraries. *Eur J Immunol*. 1998;28(4):1272–9.

50. Reynisson B, Alvarez B, Paul S, Peters B, Nielsen M. NetMHCpan-4.1 and NetMHCIpan-4.0: improved predictions of MHC antigen presentation by concurrent motif deconvolution and integration of MS MHC eluted ligand data. *Nucleic Acids Res.* 2020 Jul 2;48(W1):W449–54.
51. Atkins TK, Solanki A, Vasmatzis G, Cornette J, Riedel M. Evaluating NetMHCpan performance on non-European HLA alleles not present in training data. *Front Immunol* [Internet]. 2024 [cited 2024 Jan 27];14. Available from: <https://www.frontiersin.org/articles/10.3389/fimmu.2023.1288105>
52. Ternette N, Block PD, Sánchez-Bernabéu Á, Borthwick N, Pappalardo E, Abdul-Jawad S, et al. Early Kinetics of the HLA Class I-Associated Peptidome of MVA.HIVconsv-Infected Cells. *J Virol.* 2015 Mar 25;89(11):5760–71.
53. Hamza H, Ghosh M, Löffler MW, Rammensee HG, Planz O. Identification and Relative Abundance of Naturally Presented and Cross-reactive Influenza A virus MHC class I-restricted T Cell Epitopes. *Emerg Microbes Infect.* 2024;0(ja):2306959.
54. Croft NP, Smith SA, Wong YC, Tan CT, Dudek NL, Flesch IEA, et al. Kinetics of Antigen Expression and Epitope Presentation during Virus Infection. *PLOS Pathog.* 2013 Jan 31;9(1):e1003129.
55. de Castro Neto AL, da Silveira JF, Mortara RA. Comparative Analysis of Virulence Mechanisms of Trypanosomatids Pathogenic to Humans. *Front Cell Infect Microbiol.* 2021 Apr 16;11:669079.
56. San Francisco J, Astudillo C, Vega JL, Catalán A, Gutiérrez B, Araya JE, et al. Trypanosoma cruzi pathogenicity involves virulence factor expression and upregulation of bioenergetic and biosynthetic pathways. *Virulence.* 2022 Dec 31;13(1):1827–48.
57. Planelles L, Thomas MC, Alonso C, López MC. DNA Immunization with Trypanosoma cruzi HSP70 Fused to the KMP11 Protein Elicits a Cytotoxic and Humoral Immune Response against the Antigen and Leads to Protection. *Infect Immun.* 2001 Oct;69(10):6558–63.
58. Michel-Todó L, Reche PA, Bigey P, Pinazo MJ, Gascón J, Alonso-Padilla J. In silico Design of an Epitope-Based Vaccine Ensemble for Chagas Disease. *Front Immunol* [Internet]. 2019 [cited 2020 Apr 14];10. Available from: <https://www.frontiersin.org/articles/10.3389/fimmu.2019.02698/full>
59. de Mendonça SCF, Cysne-Finkelstein L, Matos DC de S. Kinetoplastid Membrane Protein-11 as a Vaccine Candidate and a Virulence Factor in Leishmania. *Front Immunol* [Internet]. 2015 [cited 2022 Aug 3];6. Available from: <https://www.frontiersin.org/articles/10.3389/fimmu.2015.00524>
60. Diez H, López MC, Del Carmen Thomas M, Guzmán F, Rosas F, Velazco V, et al. Evaluation of IFN- γ production by CD8+ T lymphocytes in response to the K1 peptide from KMP-11 protein in patients infected with Trypanosoma cruzi. *Parasite Immunol.* 2006 Mar;28(3):101–5.
61. Bouchie A, DeFrancesco L. Nature Biotechnology's academic spinouts of 2015. *Nat Biotechnol.* 2016 May;34(5):484–92.
62. Vizcaíno JA, Kubiniok P, Kovalchik KA, Ma Q, Duquette JD, Mongrain I, et al. The Human Immunopeptidome Project: A Roadmap to Predict and Treat Immune Diseases. *Mol Cell Proteomics MCP.* 2020 Jan;19(1):31–49.
63. Vellozo NS, Matos-Silva TC, Lopes MF. Immunopathogenesis in Trypanosoma cruzi infection: a role for suppressed macrophages and apoptotic cells. *Front Immunol* [Internet]. 2023 Aug 17 [cited 2024 Apr 26];14. Available from: <https://www.frontiersin.org/journals/immunology/articles/10.3389/fimmu.2023.1244071/full>
64. MARTÍN-OROZCO N, ISIBASI A, ORTIZ-NAVARRETE V. Macrophages present exogenous antigens by class I major histocompatibility complex molecules via a secretory pathway as a consequence of interferon- γ activation. *Immunology.* 2001 May;103(1):41–8.

65. Combs TP, Nagajyothi, Mukherjee S, de Almeida CJG, Jelicks LA, Schubert W, et al. The Adipocyte as an Important Target Cell for *Trypanosoma cruzi* Infection*. J Biol Chem. 2005 Jun 24;280(25):24085–94.
66. Song J, Deng T. The Adipocyte and Adaptive Immunity. Front Immunol [Internet]. 2020 Nov 27 [cited 2024 Apr 25];11. Available from: <https://www.frontiersin.org/journals/immunology/articles/10.3389/fimmu.2020.593058/full>
67. Chen X, Wang S, Huang Y, Zhao X, Jia X, Meng G, et al. Obesity Reshapes Visceral Fat-Derived MHC I Associated-Immunopeptidomes and Generates Antigenic Peptides to Drive CD8+ T Cell Responses. iScience. 2020 Mar 13;23(4):100977.
68. Pack AD, Tarleton RL. Cutting Edge: Augmenting Muscle MHC Expression Enhances Systemic Pathogen Control at the Expense of T Cell Exhaustion. J Immunol. 2020 Aug 1;205(3):573–8.
69. Seko Y, Tsuchimochi H, Nakamura T, Okumura K, Naito S, Imataka K, et al. Expression of major histocompatibility complex class I antigen in murine ventricular myocytes infected with Coxsackievirus B3. Circ Res. 1990 Aug;67(2):360–7.
70. Oliveira TGM, Venturini G, Alvim JM, Feijó LL, Dinardo CL, Sabino EC, et al. Different Transcriptomic Response to *T. cruzi* Infection in hiPSC-Derived Cardiomyocytes From Chagas Disease Patients With and Without Chronic Cardiomyopathy. Front Cell Infect Microbiol [Internet]. 2022 Jul 7 [cited 2024 Apr 26];12. Available from: <https://www.frontiersin.org/articles/10.3389/fcimb.2022.904747>
71. Edkins AL, Ludewig MH, Blatch GL. A *Trypanosoma cruzi* heat shock protein 40 is able to stimulate the adenosine triphosphate hydrolysis activity of heat shock protein 70 and can substitute for a yeast heat shock protein 40. Int J Biochem Cell Biol. 2004 Aug 1;36(8):1585–98.
72. Retana Moreira L, Prescilla-Ledezma A, Cornet-Gomez A, Linares F, Jódar-Reyes AB, Fernandez J, et al. Biophysical and Biochemical Comparison of Extracellular Vesicles Produced by Infective and Non-Infective Stages of *Trypanosoma cruzi*. Int J Mol Sci. 2021 Jan;22(10):5183.
73. Díaz-Viraqué F, Chiribao ML, Libisch MG, Robello C. Genome-wide chromatin interaction map for *Trypanosoma cruzi*. Nat Microbiol. 2023 Nov;8(11):2103–14.
74. Queiroz RML, Charneau S, Mandacaru SC, Schwämmle V, Lima BD, Roepstorff P, et al. Quantitative Proteomic and Phosphoproteomic Analysis of *Trypanosoma cruzi* Amastigogenesis *. Mol Cell Proteomics. 2014 Dec 1;13(12):3457–72.
75. Li Y, Shah-Simpson S, Okrah K, Belew AT, Choi J, Caradonna KL, et al. Transcriptome Remodeling in *Trypanosoma cruzi* and Human Cells during Intracellular Infection. PLOS Pathog. 2016 Apr 5;12(4):e1005511.
76. Cazorla SI, Matos MN, Cerny N, Ramirez C, Alberti AS, Bivona AE, et al. Oral Multicomponent DNA Vaccine Delivered by Attenuated Salmonella Elicited Immunoprotection Against American Trypanosomiasis. J Infect Dis. 2015 Mar 1;211(5):698–707.
77. Sanchez Alberti A, Bivona AE, Cerny N, Schulze K, Weißmann S, Ebensen T, et al. Engineered trivalent immunogen adjuvanted with a STING agonist confers protection against *Trypanosoma cruzi* infection. Npj Vaccines. 2017 Apr 10;2(1):1–12.
78. Dominguez MR, Silveira ELV, de Vasconcelos JRC, de Alencar BCG, Machado AV, Bruna-Romero O, et al. Subdominant/Cryptic CD8 T Cell Epitopes Contribute to Resistance against Experimental Infection with a Human Protozoan Parasite. PLoS ONE [Internet]. 2011 Jul 14 [cited 2019 Oct 25];6(7). Available from: <https://www.ncbi.nlm.nih.gov/pmc/articles/PMC3136500/>

79. Villanueva-Lizama LE, Cruz-Chan JV, Aguilar-Cetina A del C, Herrera-Sanchez LF, Rodriguez-Perez JM, Rosado-Vallado ME, et al. Trypanosoma cruzi vaccine candidate antigens Tc24 and TSA-1 recall memory immune response associated with HLA-A and -B supertypes in Chagasic chronic patients from Mexico. *PLoS Negl Trop Dis*. 2018 Jan 29;12(1):e0006240.
80. Mejia R, Verocai GG, Mosley IA, Zhan B, Vongthavaravat L, Busselman RE, et al. Evaluation of a novel Tc-24 recombinant antigen ELISA for serologic testing for Trypanosoma cruzi in dogs. *BioRxiv Prepr Serv Biol*. 2024 Feb 14;2024.02.12.579969.
81. Mancino C, Pollet J, Zinger A, Jones KM, Villar MJ, Leao AC, et al. Harnessing RNA Technology to Advance Therapeutic Vaccine Antigens against Chagas Disease. *ACS Appl Mater Interfaces* [Internet]. 2024 Mar 22 [cited 2024 Mar 25]; Available from: <https://doi.org/10.1021/acsami.3c18830>
82. Poveda C, Leão AC, Mancino C, Taraballi F, Chen YL, Adhikari R, et al. Heterologous mRNA-protein vaccination with Tc24 induces a robust cellular immune response against Trypanosoma cruzi, characterized by an increased level of polyfunctional CD8+ T-cells. *Curr Res Immunol*. 2023 Jan 1;4:100066.
83. Chahal JS, Khan OF, Cooper CL, McPartlan JS, Tsosie JK, Tilley LD, et al. Dendrimer-RNA nanoparticles generate protective immunity against lethal Ebola, H1N1 influenza, and Toxoplasma gondii challenges with a single dose. *Proc Natl Acad Sci*. 2016 Jul 19;113(29):E4133–42.
84. Skibinski DA, Baudner BC, Singh M, O'Hagan DT. Combination Vaccines. *J Glob Infect Dis*. 2011;3(1):63–72.
85. Rosenberg CS, Martin DL, Tarleton RL. CD8+ T cells specific for immunodominant trans-sialidase epitopes contribute to control of Trypanosoma cruzi infection but are not required for resistance. *J Immunol Baltim Md 1950*. 2010 Jul 1;185(1):560–8.
86. Jones KM, Poveda C, Versteeg L, Bottazzi ME, Hotez PJ. Preclinical advances and the immunophysiology of a new therapeutic Chagas disease vaccine. *Expert Rev Vaccines*. 2022 Jun 23;0(0):1–19.
87. Corbett KS, Flynn B, Foulds KE, Francica JR, Boyoglu-Barnum S, Werner AP, et al. Evaluation of the mRNA-1273 Vaccine against SARS-CoV-2 in Nonhuman Primates. *N Engl J Med*. 2020 Oct 15;383(16):1544–55.
88. Echaide M, Labiano I, Delgado M, Fernández de Lascoiti A, Ochoa P, Garnica M, et al. Immune Profiling Uncovers Memory T-Cell Responses with a Th17 Signature in Cancer Patients with Previous SARS-CoV-2 Infection Followed by mRNA Vaccination. *Cancers*. 2022 Jan;14(18):4464.
89. Scaria PV, Roth N, Schwendt K, Muratova OV, Alani N, Lambert LE, et al. mRNA vaccines expressing malaria transmission-blocking antigens Pfs25 and Pfs230D1 induce a functional immune response. *NPJ Vaccines*. 2024 Jan 6;9:9.
90. Muslimov A, Tereshchenko V, Shevyrev D, Rogova A, Lepik K, Reshetnikov V, et al. The Dual Role of the Innate Immune System in the Effectiveness of mRNA Therapeutics. *Int J Mol Sci*. 2023 Jan;24(19):14820.
91. de Camargo TM, de Freitas EO, Gimenez AM, Lima LC, de Almeida Caramico K, Françoço KS, et al. Prime-boost vaccination with recombinant protein and adenovirus-vector expressing Plasmodium vivax circumsporozoite protein (CSP) partially protects mice against Pb/Pv sporozoite challenge. *Sci Rep*. 2018 Jan 18;8(1):1118.
92. Duthie MS, Van Hoeven N, MacMillen Z, Picone A, Mohamath R, Erasmus J, et al. Heterologous Immunization With Defined RNA and Subunit Vaccines Enhances T Cell Responses That Protect Against Leishmania donovani. *Front Immunol*. 2018;9:2420.

93. Sanchez-Alberti A, Bivona AE, Matos MN, Cerny N, Schulze K, Weißmann S, et al. Mucosal Heterologous Prime/Boost Vaccination Induces Polyfunctional Systemic Immunity, Improving Protection Against *Trypanosoma cruzi*. *Front Immunol* [Internet]. 2020 [cited 2023 Jun 20];11. Available from: <https://www.frontiersin.org/articles/10.3389/fimmu.2020.00128>
94. Andersson NW, Thieson EM, Baum U, Pihlström N, Starrfelt J, Faksová K, et al. Comparative effectiveness of heterologous third dose vaccine schedules against severe covid-19 during omicron predominance in Nordic countries: population based cohort analyses. *BMJ*. 2023 Jul 24;382:e074325.
95. Tan CS, Collier A ris Y, Yu J, Liu J, Chandrashekar A, McMahan K, et al. Durability of Heterologous and Homologous COVID-19 Vaccine Boosts. *JAMA Netw Open*. 2022 Aug 10;5(8):e2226335.
96. Bitounis D, Jacquinet E, Rogers MA, Amiji MM. Strategies to reduce the risks of mRNA drug and vaccine toxicity. *Nat Rev Drug Discov*. 2024 Apr;23(4):281–300.
97. Alameh MG, Tombácz I, Bettini E, Lederer K, Sittplangkoon C, Wilmore JR, et al. Lipid nanoparticles enhance the efficacy of mRNA and protein subunit vaccines by inducing robust T follicular helper cell and humoral responses. *Immunity*. 2021 Dec 14;54(12):2877–2892.e7.
98. Li C, Lee A, Grigoryan L, Arunachalam PS, Scott MKD, Trisal M, et al. Mechanisms of innate and adaptive immunity to the Pfizer-BioNTech BNT162b2 vaccine. *Nat Immunol*. 2022 Apr;23(4):543–55.
99. Chen JH, Ikwuanusi IA, Bommu VJL, Patel V, Aujla H, Kaushik V, et al. COVID-19 Vaccine-Related Myocarditis: A Descriptive Study of 40 Case Reports. *Cureus*. 14(1):e21740.
100. Faksova K, Walsh D, Jiang Y, Griffin J, Phillips A, Gentile A, et al. COVID-19 vaccines and adverse events of special interest: A multinational Global Vaccine Data Network (GVDN) cohort study of 99 million vaccinated individuals. *Vaccine*. 2024 Apr 2;42(9):2200–11.
101. Bellavite P, Ferraresi A, Isidoro C. Immune Response and Molecular Mechanisms of Cardiovascular Adverse Effects of Spike Proteins from SARS-CoV-2 and mRNA Vaccines. *Biomedicines*. 2023 Feb;11(2):451.
102. Jones KM, Mangin EN, Reynolds CL, Villanueva LE, Cruz JV, Versteeg L, et al. Vaccine-linked chemotherapy improves cardiac structure and function in a mouse model of chronic Chagas disease. *Front Cell Infect Microbiol*. 2023 Feb 9;13:1106315.
103. Prochetto E, Bontempi I, Rodeles L, Cabrera G, Vicco M, Cacik P, et al. Assessment of a combined treatment with a therapeutic vaccine and benznidazole for the *Trypanosoma cruzi* chronic infection. *Acta Trop*. 2022 May;229:106334.
104. Dzul-Huchim VM, Ramirez-Sierra MJ, Martinez-Vega PP, Rosado-Vallado ME, Arana-Argaez VE, Ortega-Lopez J, et al. Vaccine-linked chemotherapy with a low dose of benznidazole plus a bivalent recombinant protein vaccine prevents the development of cardiac fibrosis caused by *Trypanosoma cruzi* in chronically-infected BALB/c mice. *PLoS Negl Trop Dis*. 2022 Sep 12;16(9):e0010258.
105. Chatelain E, Scandale I. Animal models of Chagas disease and their translational value to drug development. *Expert Opin Drug Discov*. 2020 Dec 1;15(12):1381–402.
106. Ponce C, Ponce E, Vinelli E, Montoya A, de Aguilar V, Gonzalez A, et al. Validation of a Rapid and Reliable Test for Diagnosis of Chagas' Disease by Detection of *Trypanosoma cruzi*-Specific Antibodies in Blood of Donors and Patients in Central America. *J Clin Microbiol*. 2005 Oct;43(10):5065–8.
107. Ricci AD, Bracco L, Salas-Sarduy E, Ramsey JM, Nolan MS, Lynn MK, et al. The *Trypanosoma cruzi* Antigen and Epitope Atlas: antibody specificities in Chagas disease patients across the Americas. *Nat Commun*. 2023 Apr 3;14(1):1850.
108. Guzmán-Gómez D, López-Monteon A, de la Soledad Lagunes-Castro M, Álvarez-Martínez C, Hernández-Lutzon MJ, Dumonteil E, et al. Highly discordant serology against *Trypanosoma cruzi* in central Veracruz, Mexico: role of the antigen used for diagnostic. *Parasit Vectors*. 2015 Sep 17;8:466.

109. López R, García A, Aruni JJC, Balboa V, Rodríguez A, Erkosar B, et al. Comparative evaluation of lateral flow assays to diagnose chronic *Trypanosoma cruzi* infection in Bolivia. *PLoS Negl Trop Dis*. 2024 Mar 4;18(3):e0012016.
110. Majeau A, Dumonteil E, Herrera C. Identification of highly conserved *Trypanosoma cruzi* antigens for the development of a universal serological diagnostic assay. *Emerg Microbes Infect*. 2024 Dec;13(1):2315964.
111. Black S. The costs and effectiveness of large Phase III pre-licensure vaccine clinical trials. *Expert Rev Vaccines*. 2015 Dec 2;14(12):1543–8.
112. Tarleton RL. Avoiding Clinical Trial Failures in Neglected Tropical Diseases: The Example of Chagas Disease. *Clin Infect Dis*. 2023 Apr 15;76(8):1516–20.
113. Camargo EP, Gazzinelli RT, Morel CM, Precioso AR. Why do we still have not a vaccine against Chagas disease? *Mem Inst Oswaldo Cruz*. 2022 May 9;117:e200314.
114. Gonzaga BM de S, Ferreira RR, Coelho LL, Carvalho ACC, Garzoni LR, Araujo-Jorge TC. Clinical trials for Chagas disease: etiological and pathophysiological treatment. *Front Microbiol* [Internet]. 2023 [cited 2023 Dec 29];14. Available from: <https://www.frontiersin.org/articles/10.3389/fmicb.2023.1295017>
115. Hoffman KA, Villar MJ, Poveda C, Bottazzi ME, Hotez PJ, Tweardy DJ, et al. Signal Transducer and Activator of Transcription-3 Modulation of Cardiac Pathology in Chronic Chagasic Cardiomyopathy. *Front Cell Infect Microbiol*. 2021 Aug 24;11:708325.
116. Geall AJ, Kis Z, Ulmer JB. Vaccines on demand, part II: future reality. *Expert Opin Drug Discov*. 2023 Feb 1;18(2):119–27.
117. Shanmugasundaram M, Senthilvelan A, Kore AR. Recent Advances in Modified Cap Analogs: Synthesis, Biochemical Properties, and mRNA Based Vaccines. *Chem Rec N Y N*. 2022 Aug;22(8):e202200005.
118. Chen J, Ye Z, Huang C, Qiu M, Song D, Li Y, et al. Lipid nanoparticle-mediated lymph node–targeting delivery of mRNA cancer vaccine elicits robust CD8+ T cell response. *Proc Natl Acad Sci*. 2022 Aug 23;119(34):e2207841119.
119. Youssef M, Hitti C, Puppín Chaves Fulber J, Kamen AA. Enabling mRNA Therapeutics: Current Landscape and Challenges in Manufacturing. *Biomolecules*. 2023 Oct 9;13(10):1497.
120. Rauch S, Jasny E, Schmidt KE, Petsch B. New Vaccine Technologies to Combat Outbreak Situations. *Front Immunol*. 2018;9:1963.
121. Brisse M, Vrba SM, Kirk N, Liang Y, Ly H. Emerging Concepts and Technologies in Vaccine Development. *Front Immunol*. 2020;11:583077.
122. Kis Z, Shattock R, Shah N, Kontoravdi C. Emerging Technologies for Low-Cost, Rapid Vaccine Manufacture. *Biotechnol J*. 2019 Jan;14(1):e1800376.
123. Cheng J, Dalin J, Peterson C, Delor V. Cost Modeling Vaccine Manufacturing: Estimate Production Costs for mRNA and other Vaccine Modalities [Internet]. [cited 2023 Nov 25]. Available from: Making COVID-19 mRNA vaccines accessible
124. Kis Z, Kontoravdi C, Shattock R, Shah N. Resources, Production Scales and Time Required for Producing RNA Vaccines for the Global Pandemic Demand. *Vaccines*. 2020 Dec 23;9(1):3.
125. Niazi SK. Making COVID-19 mRNA vaccines accessible: challenges resolved. *Expert Rev Vaccines*. 2022 Sep 2;21(9):1163–76.
126. Light DW, Lexchin J. The costs of coronavirus vaccines and their pricing. *J R Soc Med*. 2021 Nov 1;114(11):502–4.

127. Clendinen C, Zhang Y, Warburton RN, Light DW. Manufacturing costs of HPV vaccines for developing countries. *Vaccine*. 2016 Nov 21;34(48):5984–9.
128. Kis Z, Rizvi Z. Public Citizen. 2021 [cited 2023 Nov 25]. How to Make Enough Vaccine for the World in One Year. Available from: <https://www.citizen.org/article/how-to-make-enough-vaccine-for-the-world-in-one-year/>
129. COVID vaccine manufacturers set list price between \$120-\$130 per dose. Reuters [Internet]. 2023 Sep 12 [cited 2023 Nov 25]; Available from: <https://www.reuters.com/business/healthcare-pharmaceuticals/covid-vaccine-manufacturers-set-list-price-between-120-130-per-dose-2023-09-12/>
130. Dyer O. Covid-19: Countries are learning what others paid for vaccines. *BMJ*. 2021 Jan 29;372:n281.
131. Arguedas-Ramírez G. A Call to Action Against Persistent Lack of Transparency in Vaccine Pricing Practices During the COVID-19 Pandemic. *Ann Glob Health*. 2022;88(1):87.
132. Hunting the ‘perfect protein’ for malaria mRNA vaccine | Gavi, the Vaccine Alliance [Internet]. [cited 2023 Nov 26]. Available from: <https://www.gavi.org/vaccineswork/hunting-perfect-protein-malaria-mrna-vaccine>
133. Pidiyar V, Kumraj G, Ahmed K, Ahmed S, Shah S, Majumder P, et al. COVID-19 management landscape: A need for an affordable platform to manufacture safe and efficacious biotherapeutics and prophylactics for the developing countries. *Vaccine*. 2022 Aug 26;40(36):5302–12.
134. The mRNA vaccine technology transfer hub [Internet]. [cited 2023 Nov 26]. Available from: <https://www.who.int/initiatives/the-mrna-vaccine-technology-transfer-hub>
135. Africa Renewal [Internet]. 2022 [cited 2024 Apr 21]. WHO announces first technology recipients of mRNA vaccine hub with strong support from African and European partners. Available from: <https://www.un.org/africarenewal/magazine/who-announces-first-technology-recipients-mrna-vaccine-hub-strong-support-african-and>
136. Latin American manufacturers complete first training in mRNA technology in bid to improve regional vaccine production - PAHO/WHO | Pan American Health Organization [Internet]. [cited 2023 Nov 26]. Available from: <https://www.paho.org/en/news/24-3-2022-latin-american-manufacturers-complete-first-training-mrna-technology-bid-improve>



SUMMARIES

SUMMARY IN ENGLISH

Historically, infectious diseases have caused immense suffering, but vaccines have greatly reduced their impact. However, effective vaccines against Neglected Tropical Diseases (NTDs) are still lacking, and these diseases continue to be a major burden in low- and middle-income countries (LMICs). Many NTDs are caused by parasites, and vaccine development against these has been challenging due to the complexity of parasites and their complex interactions with the host. Chagas disease is a NTD caused by infection with the protozoan parasite *Trypanosoma cruzi*, affecting 6 to 7 million people worldwide, resulting in 10,000 – 50,000 deaths annually. The predominant transmission route of Chagas disease is by the kissing bug (*Triatominae*). The disease has an acute and chronic stage of disease, with 30-40% of the chronically infected persons developing cardiac, digestive, or neurological symptoms. Current antiparasitic drugs are only partially effective and have severe side effects. A vaccine for Chagas disease could either enhance the existing immune response to reduce the parasite burden and prevent or delay the onset of clinical manifestations like chronic chagasic cardiomyopathy (CCC) or serve as a preventative vaccine for uninfected individuals.

In this thesis, the overall goal was to advance the development and evaluation of effective vaccine candidates against Chagas disease. Throughout the chapters, different objectives were aimed to achieve this goal. To start, **Chapter 1** introduced the challenges in vaccine development for parasitic diseases. After the introduction of Chagas disease and its etiological agent *T. cruzi*, the current advancements of Chagas disease vaccines are summarized, followed by a description of the proposed properties of an effective vaccine candidate for Chagas disease. Finally, the messenger RNA (mRNA) vaccine platform is introduced as a promising platform for Chagas disease vaccines.

In **Chapter 2** the objective was to improve existing techniques to assess vaccine-induced immune responses. Luminex is a valuable tool in immunology and vaccine research to perform multiplex cytokine analysis, but its use has been limited due to constraints like sample volume requirements and high reagent costs. Therefore, DropArray technology was evaluated to mitigate these constraints. While minimal changes were applied to the workflow of Luminex, the application of the Droparray technology reduced the sample and reagent volumes by up to 80%, greatly decreasing the cost of the assays. Furthermore, the results demonstrated that the DropArray technology was similar or superior in terms of assay sensitivity, precision, and accuracy. The overall improvements achieved by implementing DropArray makes Luminex analysis more feasible and affordable for vaccine research.

The *T. cruzi* antigen Tc24 is a promising vaccine target for Chagas disease and is currently prepared as a subunit candidate vaccine for a phase I clinical trial. Since Tc24-induced immune protection was not fully understood, it was aimed to advance knowledge on this vaccine target. As described in **Chapter 3**, monoclonal antibodies (mAbs) against Tc24-C4 were developed and characterized. Using these mAbs, it was shown that Tc24 is not exposed

on the surface of *T. cruzi* trypomastigotes, making a direct role of Tc24-specific antibodies in the protection against *T. cruzi* infection very unlikely). In addition, it was demonstrated that Tc24 is differentially expressed during the parasite's lifecycle. These findings provided insights on the mechanisms of protection employed by the Tc24 vaccine.

While subunit vaccines, like the recombinant Tc24-C4 vaccine candidate, are generally good in inducing CD4+ T helper cells and humoral immunity, they are typically less effective in the induction of CD8+ cytotoxic T cells (CTLs). Importantly, CTLs play a key role in elimination of *T. cruzi*-infected cells, hence the objective to investigate alternative vaccine platforms. Therefore, in **Chapter 4** a literature review is given on the potential of mRNA vaccines as a novel vaccine platform for Chagas disease, as well as for other parasitic diseases that affect people in LMICs. This chapter described the mRNA vaccine platform's great potential for the development of more effective vaccines for parasitic diseases. They can induce strong cellular immunity, including CD8+ T cells, their relatively easy development and manufacturing procedures, fast and scalable production processes, as well as the possibility for multi-valent vaccine formulations. It was concluded that mRNA vaccines could be particularly advantageous for Chagas disease.

Following the identification of the mRNA platform to induce strong CD8+ T cells responses, it was aimed to identify *T. cruzi* vaccine targets that can be targeted by CD8+ T cells. In **Chapter 5**, studies were done to understand which *T. cruzi* proteins are available for antigen processing and presentation on MHC-I by *T. cruzi*-infected cells. Here, a previously unexplored method for identifying vaccine targets for CD8+ cytotoxic T cells (CTLs) for Chagas disease was presented. By analyzing the immunopeptidome of *T. cruzi*-infected cells, 24 unique *T. cruzi* peptides presented on MHC-I were identified, of which six peptides were derived from Tcj2, a heat-shock protein from the DnaJ family. After Tcj2 was selected as vaccine target, *in vitro* production and evaluation of a Tcj2 mRNA construct was performed, followed by administration of Tcj2 mRNA lipid nanoparticles (LNPs) to mice in a prime/boost regimen. The results from the immunogenicity study showed a robust memory cytotoxic CD8+ T cell response along with a Th1-skewed humoral antibody response. Splenocytes from these immunized mice also showed protective properties against infection in an *in vitro* co-culture with *T. cruzi*-infected cells. This research not only demonstrated the feasibility of using mRNA vaccine technology to combat parasitic diseases, exemplified by Chagas disease, but also suggests wider applicability to other tropical diseases, as described in **Chapter 4**.

Finally, in **Chapter 6**, a comprehensive summary of the results is presented, along with a discussion of the findings in a broader context, including the opportunities and limitations of the research. For the Tc24 vaccine target, the findings of the location and expression of Tc24 in the parasite were used to hypothesize how Tc24 becomes available to the immune system during *T. cruzi* infection. The discussion then elaborates on the current hypothesized mechanisms of vaccine-induced protection in the context of prophylactic and therapeutic vaccination, emphasizing the role of the cell-mediated immune response.

Furthermore, this chapter also highlights the advancement of cutting-edge techniques and implementation of new methodologies for vaccine research, including DropArray for Luminex cytokine analysis, and immunopeptidomics for vaccine target identification. The immunopeptidome of *T. cruzi*-infected cells was further discussed, and future directions for immunopeptidomics experiments were provided. For the immunopeptidomics-identified Tcj2 vaccine target, the availability for MHC-I presentation was discussed, as well as the antigen's expression kinetics between different *T. cruzi* stages and different *T. cruzi* strains. Moreover, the discussion addresses design considerations for multivalent mRNA vaccines, including the combination of Tcj2 and Tc24, tailored for both prophylactic and therapeutic applications. The specific needs for vaccine candidates aimed at individuals with chronic chagasic cardiomyopathy (CCC) are considered.

This thesis offers an outlook on the future development of Chagas disease vaccines and outlines strategic next steps for advancing mRNA vaccines for parasitic diseases in LMICs.

SAMENVATTING IN HET NEDERLANDS

Historisch gezien hebben infectieziekten enorm veel leed veroorzaakt, maar vaccins hebben veel van dit leed kunnen voorkomen. Desondanks hun succes, ontbreken er effectieve vaccins tegen vele tropische ziekten. Deze ziekten, vaak benoemd in de Engelse vakliteratuur als “Neglected Tropical Diseases” (NTD’s), blijven daardoor een grote last voor de bevolking van lage- en middeninkomenslanden. Veel NTD’s worden veroorzaakt door parasieten. De ontwikkeling van vaccins tegen deze ziekten is erg moeilijk door de complexiteit van de parasieten en hun ingewikkelde interacties met de gastheer. De ziekte van Chagas is een NTD veroorzaakt door infectie met de protozoaire parasiet *Trypanosoma cruzi*, die 6 tot 7 miljoen mensen wereldwijd treft en jaarlijks tussen de 10.000 en 50.000 sterfgevallen veroorzaakt. *T. cruzi* wordt vooral overgebracht door de beet van een soort kever (*Triatominae*), ook wel de “kissing bug” genoemd. De ziekte van Chagas kent een acute en een chronische fase, waarbij 30-40% van de chronisch geïnfecteerde personen hart-, spijsverterings- of neurologische symptomen ontwikkelt. De huidige anti-parasitaire medicijnen zijn slechts gedeeltelijk effectief en kunnen ernstige bijwerkingen geven. Een preventief vaccin tegen de ziekte van Chagas moet de kans om met de parasiet geïnfecteerd te raken sterk verminderen. Een vaccin zou ook therapeutisch toegepast kunnen worden bij patiënten die al geïnfecteerd zijn. Door het versterken van de afweer tegen de parasiet kan deze beter door het immuunsysteem onder controle gehouden worden, waardoor symptomen als chronische cardiomyopathie (CCC) voorkomen of uitgesteld kunnen worden.

Het in dit proefschrift beschreven onderzoek had als doel om vooruitgang te boeken met de ontwikkeling en evaluatie van vaccins tegen de ziekte van Chagas. De algemene introductie in **Hoofdstuk 1** bespreekt de uitdagingen die bij de ontwikkeling van vaccins voor parasitaire ziekten komen kijken. Na een bespreking van de ziekte van Chagas en de parasiet *T. cruzi*, worden de huidige vorderingen van vaccins tegen de ziekte van Chagas samengevat, gevolgd door een beschrijving van de eigenschappen die een effectief Chagas vaccin zou moeten hebben. Tot slot wordt het potentieel van het messenger RNA (mRNA) vaccinplatform besproken voor vaccins tegen de ziekte van Chagas.

In **Hoofdstuk 2** was het doel om bestaande technieken voor het analyseren van vaccin-geïnduceerde afweerreacties te verbeteren. Luminex is een waardevolle techniek voor immunologisch en vaccinonderzoek, waarmee meerdere biomarkers van het immuunsysteem (zoals cytokines) gelijktijdig getest kunnen worden. Het gebruik is echter beperkt door de relatief grote hoeveelheid staal die nodig is en de hoge kosten van de techniek. De DropArray-technologie werd geëvalueerd als methode om deze bezwaren te ondervangen. Met minimale veranderingen in het Luminex protocol kon door toepassing van de DropArray-technologie de kosten per analyse aanzienlijk verlaagd worden. Bovendien toonden de resultaten aan dat de DropArray-technologie vergelijkbaar of zelfs hogere assaygevoeligheid en nauwkeurigheid had. De implementatie van DropArray zullen Luminex-analysen voor vaccinonderzoek beter uitvoerbaar en betaalbaarder maken.

Het *T. cruzi*-antigeen Tc24 is een veelbelovend vaccin doelwit voor de ziekte van Chagas en zal als een subunit-vaccin kandidaat in een fase 1 klinische studie getest gaan worden. Aangezien het mechanisme van de door Tc24-geïnduceerde bescherming tegen Chagas nog niet was bewezen, was het doel om kennis over het Tc24 antigeen te vergroten. In **Hoofdstuk 3** wordt beschreven hoe monoklonale antistoffen (mAbs) tegen Tc24-C4 werden ontwikkeld en gekarakteriseerd. Met behulp van deze mAbs werd vervolgens aangetoond dat Tc24 niet op het oppervlak van *T. cruzi* trypomastigoten aanwezig is, waardoor een directe rol van Tc24-specifieke antistoffen bij de bescherming tegen *T. cruzi*-infectie zeer onwaarschijnlijk is. Bovendien werd aangetoond dat Tc24 differentieel tot expressie wordt gebracht tijdens de levenscyclus van de parasiet. Deze bevindingen geven meer inzicht in de beschermingsmechanismen die aan het Tc24-vaccin ten grondslag liggen.

Hoewel subunitvaccins, zoals het recombinante Tc24-C4-vaccin kandidaat, over het algemeen goed zijn in het induceren van CD4+ T-helpercellen en het opwekken van antistoffen, zijn ze doorgaans minder effectief in het induceren van CD8+ cytotoxische T-cellen (CTLs). Belangrijk is dat CTLs een sleutelrol spelen in de eliminatie van *T. cruzi*-geïnfecteerde cellen, vandaar het doel om alternatieve vaccinplatformen te onderzoeken. Daarom wordt in **Hoofdstuk 4** een literatuurstudie gegeven over het potentieel van mRNA-vaccins als een nieuw vaccinplatform voor de ziekte van Chagas en andere parasitaire ziekten die mensen in lage- en middeninkomenslanden treffen. Dit hoofdstuk beschrijft het enorme potentieel van het mRNA-vaccinplatform voor de ontwikkeling van effectievere vaccins voor parasitaire ziekten. Messenger RNA-vaccins kunnen sterke cellulaire immuniteit induceren, inclusief CD8+ T-cellen, ze kunnen relatief eenvoudig ontwikkeld en geproduceerd worden, de productieprocessen zijn snel en goed op te schalen, en ze bieden goede mogelijkheden voor multivalente vaccinformaties. De conclusie van deze literatuurstudie was dat mRNA-vaccins bijzonder aantrekkelijk zijn voor het ontwikkelen van vaccins tegen de ziekte van Chagas.

Na de identificatie van het mRNA-platform om sterke CD8+ T-celresponsen te induceren, was het doel om *T. cruzi*-vaccin doelwitten te identificeren die door CD8+ T-cellen kunnen worden herkend. In **Hoofdstuk 5** werden experimenten uitgevoerd om te begrijpen welke *T. cruzi*-eiwitten beschikbaar zijn voor antigeenverwerking en presentatie op MHC-I door *T. cruzi*-geïnfecteerde cellen, wat een voorwaarde is om een geïnfecteerde cel door CD8+ T-cellen kunnen herkennen. Hiervoor werd een methode gebruikt, genaamd immunopeptidomics, die in het Chagas vaccinveld nog niet eerder gebruikt was. Door het “immunopeptidome” van *T. cruzi*-geïnfecteerde cellen te analyseren, werden er 24 unieke *T. cruzi*-peptiden geïdentificeerd die op MHC-I aan het immuunsysteem gepresenteerd worden. Van deze peptiden waren er zes afkomstig van Tcj2, een heat-shock eiwit uit de DnaJ-familie. Nadat Tcj2 was geselecteerd als vaccin doelwit, werd de *in vitro* productie en evaluatie van een Tcj2 mRNA construct uitgevoerd, gevolgd door het vaccineren van muizen met Tcj2 mRNA lipid nanoparticles (LNPs) in een prime/boost-regime. Dit mRNA-vaccin induceerde een robuuste T-celrespons van “memory”-cytotoxische CD8+ en een Th1-gemedieerde Tcj2-specifieke antistofrespons. Verder bleken miltcellen (waarin veel T cellen zitten) van deze geïmmuniseerde muizen, in

een *in vitro* co-cultuur met *T. cruzi*-geïnfecteerde cellen, de replicatie van *T. cruzi* parasieten te vertragen. Dit onderzoek laat zien dat mRNA-vaccintechnologie potentie heeft voor de ziekte van Chagas en suggereert ook een bredere toepasbaarheid voor andere tropische parasitaire ziekten, zoals beschreven in **Hoofdstuk 4**.

In **Hoofdstuk 6**, wordt tot slot een uitgebreide samenvatting van de resultaten gegeven en worden de bevindingen uit dit onderzoek in een breder perspectief geplaatst, inclusief de mogelijkheden en beperkingen van het onderzoek. Voor het subunit Tc24-vaccin werden de bevindingen met betrekking tot de locatie en expressie van Tc24 in de parasiet gebruikt om een hypothese te formuleren hoe Tc24 tijdens *T. cruzi*-infectie beschikbaar is voor het immuunsysteem. In de discussie wordt vervolgens dieper ingegaan op hypothesen van het Tc24-vaccin geïnduceerde bescherming in de context van profylactische en therapeutische vaccinatie, met de nadruk op de rol van de celgedieerde immuunrespons.

Verder wordt in dit hoofdstuk ook het belang besproken van geavanceerde technieken, waaronder DropArray voor Luminex cytokine-analyse en immuno-peptidomics voor identificeren van vaccin doelwitten, voor vaccinonderzoek aan parasitaire aandoeningen. Voor het door middel van immuno-peptidomics-geïdentificeerde Tcj2-vaccin doelwit werd de beschikbaarheid van Tcj2 voor MHC-I presentatie besproken, evenals de expressiekinetiek van het antigeen tussen verschillende fasen gedurende een *T. cruzi*-infectie en bij verschillende *T. cruzi* stammen. Verder wordt de ontwikkeling van multivalente mRNA-vaccins besproken, inclusief het combineren van Tcj2 en Tc24 voor zowel profylactische als therapeutische toepassingen. De specifieke vereisten voor een Chagas vaccin voor patiënten met chronische *T. cruzi*-geïnduceerde cardiomyopathie (CCC) worden ook bediscussieerd.

Dit proefschrift biedt zicht op de toekomstige ontwikkeling van vaccins tegen de ziekte van Chagas en schetst een strategie voor het bevorderen van mRNA-vaccins voor andere parasitaire ziekten in lage- en middeninkomenlanden.



APPENDICES

ABOUT THE AUTHOR



Leroy Versteeg was born on November 2nd 1988, in the city Purmerend in the Netherlands. He attended elementary school “De KlimOp”, after which he started the preparatory scientific education (VWO) study track at high school “Jan van Egmond”. Inspired by his grandfather, Leroy always had an interest and fascination for animals and plants, which made him ultimately decide to enroll in the BSc Biology at Wageningen University in 2007. During his studies he selected the Human and Animal Health Biology specialization, he performed a six-month internship at the Nematology department under the supervision of Dr. Geert Smant and Dr. Ruud Wilbers, focusing on immunomodulation of dendritic cells by venom allergen-like proteins (VAPs) from helminths. After graduating the BSc, Leroy continued with the MSc Health and Disease Biology at Wageningen University in 2011, attending immunology- and cell biology-related courses, including the courses Immuno-technology, Cell Biology and Advanced Imaging Technologies, and Molecular Regulation of Health and Disease. He performed his MSc thesis at the Cell Biology and Immunology Group under the supervision of Dr. Edwin Tijhaar, developing molecular tools for cytokine research for veterinary applications. For the MSc internship, Leroy travelled for seven months to Houston, Texas to work at the Texas Children’s Hospital Center for Vaccine Development. There, he worked on the development of microparticle vaccines against neglected tropical diseases under the supervision of Dr. Michael Heffernan. After the internship ended, Leroy graduated his MSc, and then got hired at the Texas Children’s Hospital Center for Vaccine Development as a Research Assistant to work on the Analytical Development and Quality Control unit in 2013. There he evaluated the long-term stability of Hookworm vaccine candidates, and he performed accelerated stability studies on preclinical vaccine candidates. After a year and a half, Leroy moved to the Preclinical – Immunology unit, where he studied the immunological response against candidate vaccines for Chikungunya, Ascariasis, Trichuriasis and Chagas disease.

In 2019, Leroy joined the Cell Biology and Immunology Group of Wageningen University as an external PhD candidate under the supervision of Dr. Huub Savelkoul and Dr. Edwin Tijhaar, while executing his research at the Texas Children’s Hospital Center for Vaccine Development under supervision of Dr. Maria Elena Bottazzi and Dr. Jeroen Pollet. His PhD project was part of the larger goal to advance the development of a vaccine against Chagas disease. Currently, Leroy continues to work at the Texas Children’s Hospital Center for Vaccine Development on projects that were started during his PhD project, such as mRNA vaccines and immunopeptidomics.

Since Leroy started at the Texas Children’s Hospital Center for Vaccine Development, he has published 31 peer-reviewed manuscripts, including six as the first author. As of September 2024, these publications have been cited by the scientific community more than 800 times.

LIST OF SELECTED PUBLICATIONS

Leroy Versteeg and Jeroen Pollet. “mRNA Vaccines for Malaria and Parasitic Pathogens.” *Trends in mRNA Vaccine Research*.

Book chapter in press

Leroy Versteeg, Rakesh Adhikari, Gonteria Robinson, Jungsoon Lee, Junfei Wei, Brian Keegan, William K. Russell, Cristina Poveda, Maria Jose Villar, Kathryn Jones, Maria Elena Bottazzi, Peter Hotez, Edwin Tijhaar, Jeroen Pollet. “Immunoepitomic MHC-I Profiling and Immunogenicity Testing Identifies Tc2 as a New Chagas Disease mRNA Vaccine Candidate.”

Manuscript under review at PLOS Pathogens

Mancino, Chiara, Jeroen Pollet, Assaf Zinger, Kathryn M. Jones, Maria José Villar, Ana Carolina Leao, Rakesh Adhikari, **Leroy Versteeg**, et al. “Harnessing RNA Technology to Advance Therapeutic Vaccine Antigens against Chagas Disease.” *ACS Applied Materials & Interfaces*, March 22, 2024. <https://doi.org/10.1021/acsami.3c18830>.

Jones, Kathryn M., Elise N. Mangin, Corey L. Reynolds, Liliana E. Villanueva, Julio Vladimir Cruz, **Leroy Versteeg**, Brian Keegan, et al. “Vaccine-Linked Chemotherapy Improves Cardiac Structure and Function in a Mouse Model of Chronic Chagas Disease.” *Frontiers in Cellular and Infection Microbiology* 13 (February 9, 2023): 1106315. <https://doi.org/10.3389/fcimb.2023.1106315>.

Poveda, Cristina, Ana Carolina Leão, Chiara Mancino, Francesca Taraballi, Yi-Lin Chen, Rakesh Adhikari, Maria Jose Villar, Rahki Kundu, Duc M. Nguyen, **Leroy Versteeg**, et al. “Heterologous mRNA-Protein Vaccination with Tc24 Induces a Robust Cellular Immune Response against Trypanosoma Cruzi, Characterized by an Increased Level of Polyfunctional CD8+ T-Cells.” *Current Research in Immunology* 4 (January 1, 2023): 100066. <https://doi.org/10.1016/j.crimmu.2023.100066>.

Jones, Kathryn M., Cristina Poveda, **Leroy Versteeg**, Maria Elena Bottazzi, and Peter J. Hotez. “Preclinical Advances and the Immunophysiology of a New Therapeutic Chagas Disease Vaccine.” *Expert Review of Vaccines* 0, no. 0 (June 23, 2022): 1–19. <https://doi.org/10.1080/14760584.2022.2093721>.

Versteeg, Leroy, Rakesh Adhikari, Cristina Poveda, Maria Jose Villar-Mondragon, Kathryn M. Jones, Peter J. Hotez, Maria Elena Bottazzi, Edwin Tijhaar, and Jeroen Pollet. “Location and Expression Kinetics of Tc24 in Different Life Stages of Trypanosoma Cruzi.” *PLOS Neglected Tropical Diseases* 15, no. 9 (September 3, 2021): e0009689. <https://doi.org/10.1371/journal.pntd.0009689>.

Cruz-Chan, Julio V., Liliana E. Villanueva-Lizama, **Leroy Versteeg**, Ashish Damania, Maria José Villar, Cristina González-López, Brian Keegan, et al. “Vaccine-Linked Chemotherapy Induces IL-17 Production and Reduces Cardiac Pathology during Acute Trypanosoma Cruzi Infection.” *Scientific Reports* 11, no. 1 (February 5, 2021): 3222. <https://doi.org/10.1038/s41598-021-82930-w>.

Villanueva-Lizama, Liliana E., Julio V. Cruz-Chan, **Leroy Versteeg**, Christian F. Teh-Poot, Kristyn Hoffman, April Kendrick, Brian Keegan, et al. “TLR4 Agonist Protects against Trypanosoma Cruzi Acute Lethal Infection by Decreasing Cardiac Parasite Burdens.” *Parasite Immunology* 42, no. 10 (October 2020): e12769. <https://doi.org/10.1111/pim.12769>.

Versteeg, Leroy, Mashal M. Almutairi, Peter J. Hotez, and Jeroen Pollet. “Enlisting the mRNA Vaccine Platform to Combat Parasitic Infections.” *Vaccines* 7, no. 4 (December 2019): 122. <https://doi.org/10.3390/vaccines7040122>.

Barry, Meagan A., **Leroy Versteeg**, Qian Wang, Jeroen Pollet, Bin Zhan, Fabian Gusovsky, Maria Elena Bottazzi, Peter J. Hotez, and Kathryn M. Jones. “A Therapeutic Vaccine Prototype Induces Protective Immunity and Reduces Cardiac Fibrosis in a Mouse Model of Chronic Trypanosoma Cruzi Infection.” *PLOS Neglected Tropical Diseases* 13, no. 5 (May 30, 2019): e0007413. <https://doi.org/10.1371/journal.pntd.0007413>.

- Gunter, Sarah M., **Leroy Versteeg**, Kathryn M. Jones, Brian P. Keegan, Ulrich Strych, Maria Elena Bottazzi, Peter J. Hotez, and Eric L. Brown. "Covalent Vaccination with *Trypanosoma Cruzi* Tc24 Induces Catalytic Antibody Production." *Parasite Immunology* 40, no. 11 (November 2018): e12585. <https://doi.org/10.1111/pim.12585>.
- Jones, Kathryn, **Leroy Versteeg**, Ashish Damania, Brian Keegan, April Kendricks, Jeroen Pollet, Julio Vladimir Cruz-Chan, Fabian Gusovsky, Peter J. Hotez, and Maria Elena Bottazzi. "Vaccine-Linked Chemotherapy Improves Benznidazole Efficacy for Acute Chagas Disease." *Infection and Immunity*, January 8, 2018, IAI.00876-17. <https://doi.org/10.1128/IAI.00876-17>.
- Versteeg, Leroy**, Xavier Le Guezennec, Bin Zhan, Zhuyun Liu, Minilik Angagaw, Janice D. Woodhouse, Subhabrata Biswas, and Coreen M. Beaumier. "Transferring Luminex® Cytokine Assays to a Wall-Less Plate Technology: Validation and Comparison Study with Plasma and Cell Culture Supernatants." *Journal of Immunological Methods* 440, no. Supplement C (January 1, 2017): 74–82. <https://doi.org/10.1016/j.jim.2016.11.003>.
- Seid, Christopher A., Kathryn M. Jones, Jeroen Pollet, Brian Keegan, Elissa Hudspeth, Molly Hammond, Junfei Wei, Patrick M. McAtee, **Leroy Versteeg**, et al. "Cysteine Mutagenesis Improves the Production without Abrogating Antigenicity of a Recombinant Protein Vaccine Candidate for Human Chagas Disease." *Human Vaccines & Immunotherapeutics* 13, no. 3 (October 13, 2016): 621–33. <https://doi.org/10.1080/21645515.2016.1242540>.

ACKNOWLEDGEMENTS

My PhD journey has been incredibly enriching, teaching me about focus, personal development, and my own interests. It would not have been possible without the support of colleagues, family, and friends. I would like to express my gratitude to a select group of the people that have been instrumental throughout this journey.

First, I would like to acknowledge my promotor and co-promotor at Wageningen University. Dear **Huub Savelkoul**, thank you for the opportunity to do this PhD thesis at the Cell Biology and Immunology department, and serving as my promotor. Your enthusiasm for my PhD topic and immunology in general is inspiring. Dear **Edwin Tijhaar**, working with you during my MSc thesis in 2012 was one of the most enjoyable periods of my studies at Wageningen. You are very knowledgeable, very social, and you always have a positive approach on things. When I reached out in 2019 about the possibility of a PhD project in Wageningen, I was very happy to hear you thought I could perform it under your supervision. I always enjoyed our monthly and later bi-weekly meetings, which were rich in brainstorming, creative problem-solving, and sharing personal life news and interests. Your strong immunology background helped me understand the mechanisms of vaccine-induced immunity a lot better. I thank you for all the help and supervision, and I hope we continue to work together in a collaborative fashion.

I would also like to thank my promotor and co-promotor at the Texas Children's Hospital Center for Vaccine Development (TCH-CVD). Dear **Maria Elena Bottazzi**, thank you so much for providing the opportunity to conduct the PhD research in the labs of TCH-CVD, providing financial support and opportunities. You have encouraged me to investigate whether I could do this PhD in Europe while working in the lab. Despite your busy schedule, you always make time to help me refine presentations and simplify complex stories to the general public, a great talent from which I continue to learn. I deeply appreciate all your support over the years, the time and effort you've invested in me, and that you care for me to develop myself. I hope we will continue to work together on neglected tropical diseases in the future. Dear **Jeroen Pollet**, from the moment I joined the lab we had a good connection, and a friendship developed quickly after. Running Texas Independence Relay races, participating in soccer and volleyball teams, canoe trips, pool parties and happy hours are some highlights of this. You have been the biggest help in the PhD, and our discussions, insights, and shared ideas have been incredibly beneficial. Your eye for detail, your drive for innovation, and your ability to prepare compelling presentations and manuscripts are skills I learn from every day. I hope that I continue to learn from you and that we stay good friends in the future.

Dear **Peter Hotez**, I want to thank you for encouraging me to explore a PhD project in Europe. I also appreciate the time you took during the multiple occasions where Layal and I would meet you for career advice in your office, I very much appreciate this act of mentorship as it has been invaluable.

Additionally, I want to thank a bunch of colleagues at the TCH-CVD who have supported my PhD work in various ways. Thank you, **Brian Keegan** for helping with animal work and making sure there is a chili cook-off every year. **Rakesh Adhikari**, thank you for your assistance with experiments, particularly when growing 30 or more *T. cruzi*-infected culture flasks. Thank you, **Maria Jose Villar** assisting with growing *T. cruzi* parasites and writing positive little messages on Post-its. **Cristina Poveda**, I appreciate your support with large experiments and your flow cytometry panel designs for the Cytex Aurora. The successful production and purification of recombinant proteins could not have been achieved without the help of **Zhuyun Liu, Junfei Wei** and **Nelufa Islam**. Also, many thanks to **Kay Razavi** and **Diane Nino** for managing material orders and shipping samples to collaborators. **Ulrich Strych** and **Nate Wolf**, I am grateful for your constructive feedback, manuscript proofreading, and editing. **Kathryn Jones**, thank you for always sharing your extensive knowledge on Chagas disease and your unlimited supply of bacon jam. Rani Thimmiraju, I always enjoyed your delicious home-cooked Indian snacks you share so frequently. **Alex Kneubehl**, I appreciate you joining the late Chipotle and Piata dinners in the Texas Medical Center that provided a much-needed break during long days. And **Athos Silva de Oliveira**, thank you for making sure we do not forget about stopping by Valhalla at Rice University for a “Ziegenstar” beer every now and then. I would also like to thank everybody else at the TCH-CVD for your help and making it such a pleasant work environment.

Special thanks to **Jungsoon Lee** for our small social gatherings, lunches and quick coffee breaks where we enjoyed cookies and chocolates. Your feedback on my PhD work, and brainstorming sessions on recombinant protein and monoclonal antibody production, have been immensely helpful. I deeply appreciate your technical guidance.

During my PhD, I had the privilege of working with interns **Lauren Graham, Gonteria (Junje) Robinson**, and **Isha Thapar**. Thank you very much for your assistance with ELISAs, Tcj2 fermentations, and mRNA transfections.

Outside the lab I received additional help from colleagues and friends. I am particularly grateful to the Flow Cytometry and Cell Sorting Core, and especially to **Joel Sederstrom**, for all your help and guidance on flow cytometry. Joel, I remember at the conference in Prague, Czech Republic, you gave me some heartfelt advice on pursuing a PhD, and how I really needed to consider this opportunity. I greatly valued this conversation, as well as all the other insightful conversations we had in Prague and in your office in Houston over the years. **Alex Carisey**, when I wanted to learn about more about confocal microscopy, you put a lot of effort and time in teaching me how to use the Leica microscope. I felt privileged learning from you and seeing how skilled and dedicated you are in your work. **Amal El-Mabhough**, thank you for taking the time to meet during and outside of work hours, teaching me the tricks of imaging flow cytometry. **Melvin Lye**, I am grateful for your career advice and the opportunities you provided to share my research and connect with others in the biotechnology field.

I am also very grateful for my paranympths **Bas Pels** and **Neima Briggs**. Bas, we are friends since we were five years old, and to this date we are still best friends. Even when I moved 9000 km away, you still took the effort to visit me multiple times to keep our friendship strong. Neima, we met at the TCH-CVD and from day one it was fun, pranks and laughter. We became housemates, brewing beer at home and conducting vaccine research at work. It is awesome to have a good friend who also works in the same field of research.

Importantly, I would like to thank my parents, all my family and extended family for love and support throughout the years, all the times you have visited me and Loyal in Houston, and all the times that you have sent stroopwafels, drop and pepernoten by mail to feed me (all that glucose fueled my brain to do PhD brainstorming). I have always felt very fortunate to have you in my life.

When workdays were long and stressful, I could always rely on social activities with friends. To my buddies from Houston and other places in the US, beer brew partners, friends from the Netherlands, Jaarclub Chaac comrades, you have all supported me directly or indirectly in some way, thank you for that.

Above all, I would like to thank my partner in crime. Dear **Loyal**, you are the only one who has truly witnessed and understood the immense time I invested in this PhD. You must have heard me say “I am coming home late tonight” probably a thousand times. All that time you supported me a 100%, and I am very grateful for that. You taught me to keep pushing myself and not get too comfortable, I know I need this reminder every now and then. You evolved from an amazing girlfriend into a wonderful wife, and recently to an incredible mother to our son **Axel**. I am excited about our future together and look forward to enjoying life with our growing family. I love you!

Leroy Versteeg

Colophon:

The research described in this thesis was financially supported by the Carlos Slim Foundation, the Merck Research Laboratories, the Robert J. and Helen C. Kleberg Foundation, the Southern Star Medical Research Institute, and by intramural funds from Texas Children's Hospital Center for Vaccine Development at Baylor College of Medicine.

Financial support from Wageningen University and for printing this thesis is gratefully acknowledged.

Front cover image shows a mouse cardiac fibroblast infected with dozens of *T. cruzi* parasites. This image has won the 2023 FASEB BioArt Award and the 2021 ASM-TMC Microworld image contest. Back cover image shows additional cells infected with *T. cruzi*. Images were acquired using a confocal microscope by Leroy Versteeg.

Provided by thesis specialist Ridderprint, ridderprint.nl

Printing: Ridderprint

Layout and design: Indah Hijmans, persoonlijkproefschrift.nl

Cover design: Indah Hijmans

